THE EFFECT OF AGE AND SEX ON CHEMOTHERAPY-INDUCED CACHEXIA AND BRANCHED-CHAIN AMINO ACID METABOLISM

STEPHEN MORA

A DISSERTATION SUBMITTED TO THE FACULTY OF GRADUATE STUDIES IN PARTIAL FULFILLMENT OF THE REQUIREMENTS FOR THE DEGREE OF DOCTOR OF PHILOSOPHY

GRADUATE PROGRAM IN KINESIOLOGY AND HEALTH SCIENCES
YORK UNIVERSITY
TORONTO, ONTARIO

2024

Abstract

Cachexia remains one of the most complex and challenging aspects in cancer care. The impact of cachexia on body wasting, particularly on the depletion of muscle mass, significantly impairs patient's energy, strength and quality of life. Tumour-related factors and poor nutritional status are associated with cachexia development. Additionally, while effective in combatting cancer, chemotherapy causes appetite loss, fatigue, altered metabolism and decreased physical activity, all contributing to muscle tissue breakdown and cachexia. Decades of research into investigating interventions to mitigate the effects of cachexia have been unsuccessful. Even the use of nutritional supplements like the branched-chain amino acids (BCAA) in reversing cachexia remains limited and inconsistent. However, researchers typically prioritize tumour BCAA metabolism and overlook these amino acids in the skeletal muscle. In addition, studies investigating chemotherapy-induced cachexia frequently utilize young male animals and the effects of chemotherapy on the abundance and activity of enzymes involved in BCAA metabolism have not extensively been compared across the sexes, nor studied in aged animal tissues. Understanding the alterations in skeletal muscle BCAA metabolism and availability following chemotherapy, especially across different sex and age groups, may help provide a better understanding of why certain interventions are ineffective in treating cachexia and may present findings that more accurately represent clinical diversity. Therefore, the objective of this dissertation is to examine the effect of age and sex on the mechanisms and severity of chemotherapy-induced cachexia, with a focus on BCAA availability, metabolism and transporter expression in young and aged animals.

Briefly, I showed that preventing the degradation of LAT1, a transporter protein crucial for BCAA uptake into skeletal muscle, counteracted the effects of chemotherapy-induced damage on myotubes. Further, *in-vivo*, I showed sex-dependent differences in the susceptibility

of young and aged animals to chemotherapy-induced cachexia. I also show that altered BCAA availability and metabolism following chemotherapy may contribute to muscle wasting in a sex- and age-dependent manner. Findings from this dissertation suggest that interventions regulating muscle amino acid transporters may represent a promising strategy to treat cachexia. These findings underscore the need for age- and sex-specific responses when developing interventions that can manage cachexia.

Acknowledgements

First and foremost, I'd like to thank Dr. Adegoke. You have been an incredible mentor, guiding me through a significant 7 year journey from my Masters to my PhD. I believe the bond we have formed is truly special and I will cherish this unforgettable lab experience forever. Without you, this process would not have been possible and I will be forever grateful.

To my past and present lab mates, I am grateful for the invaluable lessons I have learned from all of you. From the late night troubleshooting experiments that never really seemed to work out, to the celebratory breakthrough of a successful experimental result, you have made this lab experience nothing short of an outstanding experience.

To my parents and brothers, no one could match the unconditional love you have shown for me over my Graduate student years. It is impossible to put into words or express how much you have done for me.

Lastly (and of course not least), to my girlfriend Karen. You have been through it all with me, the milestones, the setbacks and you have never left my side. I can't wait for what our future holds.

Table of Contents

List of Tables

Chapter 2

Chapter 7

List of Figures

Chapter 2

Chapter 4

Chapter 5

Chapter 6

List of Abbreviations

4E-BP1	eIF4e-binding protein-1
5-FU	5-Fluorouracil
AA	Amino acids
ACE	Angiotensin-converting enzyme
AKT	Protein kinase B (PKB)
AMPK	AMP-activated protein kinase
AMP	Adenosine monophosphate
aPKC	Atypical protein kinase C
AS160	AKT substrate of 160 kDa
ATG13	Autophagy-related protein 13
ATP	Adenosine triphosphate
BCAA	Branched-chain amino acid
BCAT1	Branched-chain amino transferase 1
BCAT2	Branched-chain amino transferase 2
BCKA	Branched-chain keto acid
BCKDH	Branched-chain alpha-keto acid dehydrogenase complex (referred as BCKD)
BDK	Branched-chain α-keto acid dehydrogenase complex kinase
BMP	Bone Morphogenetic Proteins
BNIP3	BCL2/adenovirus E1B 19 kDa protein-interacting protein 3
BW	Body Weight
CO_2	Carbon Dioxide
C26	Colon 26 Adenocarcinoma
CPT-11	Irinotecan Hydrochloride
CSA	Cross Sectional Area
D0	Day 0
ddH_2O	Double Distilled Water
DFBS	Dialyzed fetal bovine serum
DM	Differentiation Medium
DMB	1,2-diamino-4,5- methylenedioxybenzene
E3 Protein	E3 ubiquitin ligases
EDL	Extensor Digitorum Longus
eIF2β	Eukaryotic translation initiation factor 2 subunit 2
eIF4E	Eukaryotic translation initiation factor-4E
eIF4F	Eukaryotic translation initiation factor-4F
eIF4G	Eukaryotic translation initiation factor-4G
FBS	Fetal Bovine Serum
FBW	Final Body Weight
FdUMP	5-fluoro-2'-deoxyuridine-5'-monophosphate
FdUTP	5-fluorodeoxyuridine-5'-triphosphate
FoxO	Forkhead box-O
FUTP	5-fluorouridine-5'triphosphate
GH	Growth Hormone
GLUT4	Glucose transporter type 4
GM	Growth Medium
GSK3β	Glycogen synthase kinase 3 Beta

HMB	β-Hydroxy-β-Methylbutyrate
IGF-1	Insulin-like growth factor-1
IGF-2	Insulin-like growth factor-2
IL-1	Interleukin-1
IL-6	Interleukin-6
IRS-1	Insulin receptor substrate-1
KIC	2-keto-isocaproate/4-methyl-2- oxopentanoic acid
KIV	2-keto-isovalerate/3-methyl-2-oxobutanoic acid
KLF15	Krueppel-like factor 15
KMV	α-keto-β-methylvaleric acid/3-methyl-2-oxopentanoate
LAT1	L-type amino acid transporter 1
LC3I	Microtubule-associated proteins 1A/1B light chain 3B
LEU	Leucovorin
LLC	Lewis Lung Carcinoma
MAFbx	F-box only protein 32
MAPK	Mitogen activated protein kinase
MHC-1	Myosin heavy chain-1
MPB	Muscle protein breakdown
MPS	Muscle protein synthesis
mTOR	Mammalian target of rapamycin
mTORC1	Mammalian target of rapamycin complex-1
MUNE	Motor Unit Number Estimation
MuRF-1	Muscle ring finger protein-1
NAD	Nicotinamide adenine dinucleotide
NADH	Nicotinamide Adenine Dinucleotide Hydrogen
NF-KB	Nuclear factor kappa-light-chain-enhancer of activated B cells
NSCLC	Non-small cell lung carcinoma
OPA	Phthalaldehyde
PAT1	Proton-assisted amino acid transport 1
PDAC	Pancreatic ductal adenocarcinoma
PDK1	3-Phosphoinositide-dependent kinase 1
PIP3	phosphatidylinositol (3,4,5)-trisphosphate
PP2CM	Protein phosphatase 2Cm
PTEN	Phosphatase and tensin homolog deleted on chromosome 10
REDD1	Regulated in Development and DNA Damage Response 1
Rex	Resistance exercise
Rheb	Ras homolog enriched in brain
ROS:	Reactive oxygen species
Ser/S	Serine
SNAT1	Sodium-dependent neutral amino acid transporter 1
SNAT2	Sodium-dependent neutral amino acid transporter 2
S6/rpS6	Ribosomal protein S6
S6K1	p70 ribosomal protein S6 kinase 1
T1DM	Type 1 diabetes mellitus
T2DM	Type 2 diabetes mellitus
TBC1D1	TBC1 domain family member 1

TCA	Trichloroacetic acid
TGF-β	Transforming growth factor beta
thr	Threonine
TNF-α	Tumour necrosis factor alpha
TSC1	Tuberous sclerosis 1 protein
TSC2	Tuberous sclerosis 2 protein
ULK-1	Unc-51-like kinase 1
UPP	Ubiquitin proteasome pathway

Chapter 1 General Introduction

Age (1) and sex (2) are significant risk factors for cancer, a leading cause of death in Canada (3). Cachexia, a debilitating consequence of cancer that affects 80% of patients (4), is a multifactorial and complex body and muscle wasting syndrome that impacts various aspects of health and overall well-being. Chemotherapy, while instrumental in being an effective anti-cancer treatment (5), can lead to several negative side effects, one of which is being a major contributor to cachexia sustainment (6–8). Cachexia is also associated with the onset of systemic inflammation (9), insulin resistance (10), increases in energy expenditure (11), negative protein/energy balance (12), appetite loss (13), anorexia (14), fatigue (15), and reduced muscle strength (16). Most profoundly, cancer- and chemotherapy-induced cachexia is associated with exacerbated skeletal muscle depletion (6, 8, 17, 18), leading to diminished quality of life, lower survival rates (19) and higher rates of mortality (20) in patients. Importantly, there are currently no successful and specific approved therapies that solely target cachexia. Therefore, exploring interventions to mitigate the negative effects of chemotherapy on skeletal muscle loss is vital in order to better manage this condition, as skeletal muscle mass is a determinant of chemotherapy dose (21), effectiveness (22), toxicity and treatment failure (23).

Muscle protein synthesis is regulated through activation of the mammalian/mechanistic target of rapamycin complex 1 (mTORC1). First, stimulation by insulin and/or insulin-like growth factor 1 (IGF-1) activates the insulin receptor substrate-1 (IRS-1)/phosphatidylinositol-3 kinase (PI3K)/protein kinase B (AKT) pathway which allows RHEB, an mTORC1 activator, to stay GTP loaded (24, 25). Second, mTORC1 sensing of the BCAAs (BCAA: leucine, isoleucine and valine) is required for full activation. After being transported into the skeletal muscle via L-type amino acid transporter 1 (LAT1) (26), the BCAAs activate key components in the sestrins/gator/RAG/ragulator pathway, leading to the translocation of mTORC1 to the lysosomal

membrane where RHEB is localized (27). Activated mTORC1 phosphorylates several downstream targets, such as ribosomal protein S6 kinase (S6K1) and eukaryotic mRNA translation initiation factor 4E-binding protein 1 (4E-BP1), leading to an increase in translation initiation (28), ribosomal biogenesis (29), protein synthesis (25) and an inhibition of protein breakdown (30). However, these anabolic pathways described are downregulated in cachexia (18, 31), while activation of catabolic pathways that increase protein breakdown, such as the autophagy/lysosomal and ubiquitin proteasome pathway (UPP) are upregulated (32), leading to skeletal muscle wasting.

The BCAAs are mainly metabolized in the skeletal muscle and liver, but can serve several intermediary roles in other tissues, such as the brain and adipose (33). The BCAAs are first transaminated by branched-chain aminotransferase 2 (BCAT2) forming glutamate and the branched-chain α-keto acids (BCKA): 2-keto-isocaproate/4-methyl-2-oxopentanoic acid (KIC) from leucine, α-keto-β-methylvaleric acid/3-methyl-2-oxopentanoate (KMV) from isoleucine, and 2-keto-isovalerate/3-methyl-2-oxobutanoic acid (KIV) from valine. The BCKAs are then oxidatively decarboxylated by the branched-chain α-keto acid dehydrogenase complex (BCKDH, referred hereon as BCKD), producing their corresponding acyl CoA derivates: isovaleryl-CoA from KIC, 2-methylbutyryl-CoA from KMV, and isobutyryl-CoA from KIV (33), which ultimately go on to fuel several metabolic pathways, such as the TCA cycle (33).

Since the roles of the BCAAs, especially leucine, in the stimulation of skeletal muscle protein synthesis have been well documented (34, 35), they serve as promising candidates to address skeletal muscle loss in cachexia. However, since reversing the complex nature of cachexia extends far beyond just the promotion of protein synthesis, clinical studies examining the effectiveness of the BCAAs in cachexia are limited and yield mixed results (36–39). These

inconsistencies may in part be due to altered metabolism of skeletal muscle BCAAs following chemotherapy, a factor often overlooked and minimally investigated, as previous studies have prioritized tumour BCAA metabolism (40–42). It is also important to consider that much of the research documenting the effects of chemotherapy-induced cachexia are conducted in animal models, often focusing on young males (6, 8, 18, 43). Although these studies have provided valuable insights into the mechanisms of cachexia, these findings perhaps do not accurately represent the whole clinical picture. Especially when you consider age and sex differences in factors that may affect key outcome measures in cachexia, such as cancer incidence (44), cancer type (45), chemotherapy responses (46) and BCAA intake (47), concentrations (48) and metabolism (49). Therefore, the overall goal of this dissertation is to examine the effect of age and sex on mechanisms and severity of chemotherapy-induced cachexia, with a focus on BCAA availability, metabolism and transporter expression in young and aged animals.

Chapter 2 Literature Review

2.1 Skeletal Muscle

Skeletal muscle makes up ~40% of total body weight (50) and is a contributor to energy expenditure (51) and protein metabolism (52). It provides support for locomotion, posture, balance and movement (53). Skeletal muscle plays a vital role in glucose homeostasis (54, 55) and glycogen synthesis (56), while also being a major reservoir for amino acids (AA) (57) and a site for fatty acid metabolism (58). The preservation of skeletal muscle mass is linked to better health outcomes, lessened mortality risk (59) and a higher quality of life (60). However, adverse side effects such as fatigue (61) and weakness (62) are commonly experienced in individuals during muscle mass depletion, often contributing to the worsening of chronic metabolic disorders such as obesity (63), diabetes (55, 64) and cardiovascular disease (65).

2.1.1 Aging and Skeletal Muscle

Sarcopenia is defined as the age-related decrease in skeletal muscle mass, strength and functionality (66), with recent work suggesting that muscle decreases by ~3-8% per decade after the age of 30, with progressive worsening after the age of 60 (67). Sarcopenia significantly contributes to frailty and increased vulnerability to stressors, leading to increased mortality and morbidity in all individuals (68). Briefly, sarcopenia is due to many factors that extend way beyond mere physical changes: 1) anabolic resistance in response to key factors, such as nutrition (69) and exercise (70); 2) physical inactivity (71); 3) elevated production of pro-inflammatory cytokines (72) and reactive oxygen species (ROS) (73); 4) impaired AA induction and propagation of protein synthesis signalling (74, 75).

2.1.2 Sex and Skeletal Muscle

Sex differences in the skeletal muscle have been studied for decades. Briefly, males on

average have greater muscle mass than females (76), with the majority of these differences being observed in the upper body (77). These differences are related to greater satellite cell content and proliferative capacity in males (78, 79). Satellite cells, which are myogenic progenitor stem cells, play crucial roles in muscle regeneration (80). For fibre type, females have a greater distribution of type 1 (slow twitch) fibres (81, 82), corresponding to a greater reliance on oxidative metabolism (83), whereas males have a greater muscle distribution of type II (fast-twitch) muscle fibres (81, 82).

In terms of disease pathology, women are more susceptible to muscle loss from disuse atrophy, as this disease targets more oxidative fibres (84, 85). However, males are more susceptible to inflammatory-based pathologies, as glycolytic fibres are more at risk in these diseases (86). In aging, total muscle mass loss is greater in men, although women have lower overall muscle mass (87).

2.2 Skeletal Muscle Anabolism

Skeletal muscle is one of the most dynamic plastic tissues in the human body. To ensure functionality, it possesses the ability to undergo adaptive changes in response to stimuli (53). In response to anabolic stimuli, such as growth factors (88), anabolic hormones (89, 90), nutrition (91) and resistance exercise (92), skeletal muscle undergoes protein synthesis whereby mass is either maintained or increased. The focus of this section (2.2 – 2.4) will be identifying anabolic factors and their respective signalling pathways that maintain skeletal muscle mass.

2.2.1 Skeletal Muscle Anabolism – Anabolic Hormones

Insulin (93), testosterone (94) and estrogen (95) will be the focus of this section due to their importance in age and sex. However, other hormones (not discussed) also have roles in skeletal muscle anabolism. Briefly, growth hormone, known to have synergistic effects with

testosterone, controls skeletal muscle growth (96) and deficiencies in this hormone are associated with decreases in skeletal muscle mass (97, 98), size (99), strength (97, 98) and anti-insulin effects (100). In addition, progesterone, another sex hormone, increases muscle protein synthesis and mass (101, 102), as it positively affects mitochondrial efficiency (103, 104).

2.2.1.1 Anabolic Hormones – Insulin

During hyperglycemia, insulin is released from the pancreas and facilitates the uptake of glucose into multiple tissues, notably skeletal muscle. Additionally, some AAs, such as leucine and glutamine can also stimulate pancreatic insulin release (105). When glucose enters the skeletal muscle, it can be used as energy for muscle contraction, stored as glycogen (in excess), or be used as primary fuel for protein synthesis (54). Insulin plays a pivotal role in stimulating skeletal muscle anabolism (106, 107) and protein synthesis (108) by triggering two important responses: 1) Insulin facilitates the uptake of AAs into skeletal muscle (109), providing essential building blocks for protein synthesis; 2) Insulin decreases muscle protein breakdown (110–113), thus increasing muscle mass.

2.2.1.2 Anabolic Hormones – Testosterone

Testosterone is produced in the testicles in men and the ovaries in females. This hormone exerts its effects by binding to intracellular androgen receptors present in skeletal muscle, forming a complex that travels to the nucleus, interacts with DNA and increases transcription of genes associated with hypertrophy, such as insulin-like growth factor-1 (IGF-1) (114). Testosterone promotes muscle hypertrophy by triggering many responses: 1) Increases intramuscular AA uptake (115), providing essential building blocks to enhance skeletal muscle protein synthesis (116); 2) Inhibits protein breakdown (117), thus increasing muscle mass.

2.2.1.3 Anabolic Hormones – Estrogen

Estrogen is produced in the testicles in men and the ovaries in females. It is responsible for the development of physical and sexual characteristics in females, as well as regulating reproduction, bone density and metabolism in both sexes (118). Estrogen exists in multiple forms: estrone, made after menopause; estradiol, the most potent form made during reproductive years; estriol, made during pregnancy. Mechanistically, estrogen binds to the estrogen receptor α in skeletal muscle to exert its effects and is important for maintenance of skeletal muscle mass (119, 120). The hypertrophic effects of estrogen are supported by *in-vitro* work, whereby estrogen enhances myoblast differentiation (121) and increases IGF-1 in satellite cells (122).

2.2.2 Skeletal Muscle Anabolism – Nutrition and Exercise

Without exercise, protein intake alone stimulates skeletal muscle protein synthesis in young (123), old (124) and obese individuals (125). Resistance exercise, without protein supplementation, also increases skeletal muscle protein synthesis in young males (126), females (92) and untrained individuals (127). Combined with resistance exercise, whey protein intake stimulates greater protein synthesis in young (128, 129) and trained individuals (130–132) compared to either protein or exercise alone. Casein (133, 134) and soy (135–137) protein intake also increases net protein synthesis following resistance exercise, but not to the same magnitude as whey. Carbohydrates have minimal effects on protein synthesis following exercise (138).

2.2.3 Skeletal Muscle Anabolism – Branched-Chain Amino Acids (BCAA)

There are a total of 20 primary AAs that serve as building blocks for proteins. Nine are classified as essential AAs, meaning they must be obtained through diet as the body cannot synthesize these. The remaining 11 are non-essential AAs that can be produced by the body on its own (139). Although some AAs, such as arginine can stimulate protein synthesis (140), the BCAAs (leucine, isoleucine and valine) have garnered specific attention and will be the main

focus of this dissertation as they are both substrates and stimulators (141–143) of protein synthesis in skeletal muscle. They are also important energy sources during exercise (144), suppress proteolysis (57), regulate body weight (145) and promote glucose transport (146, 147), cholesterol synthesis (148) and muscle recovery (149, 150). However, among these benefits, previous reports have linked insulin resistance (151) and type 2 diabetes mellitus (T2DM) (152) with sustained elevations in circulating BCAAs.

2.2.3.1 Amino Acid Transport into Skeletal Muscle

The BCAAs cannot readily diffuse across lipid or plasma membranes. Therefore, they are transported into skeletal muscle through the L-type amino acid transporter 1 (LAT1), transcribed by the SLC7A5 gene. LAT1 also transports histidine, methionine, phenylalanine, tyrosine, tryptophan and glutamine (153). Multiple other LAT isoforms exist in skeletal muscle that transport AAs, such as LAT2 and LAT4 (154–156). However, LAT1 is the most highly expressed skeletal muscle transporter (157). LAT1 is also present in the liver, bone marrow, placenta, testis and brain (158). Other AA transporters in the skeletal muscle and the respective AAs they transport are as follows: 1) sodium-dependent neutral amino acid transporter 1 (SNAT1), transporting alanine, serine and glutamine; 2) sodium-dependent neutral amino acid transporter 2 (SNAT2), transporting glycine, proline, alanine, serine, cysteine, glutamine, asparagine, histidine, methionine; 3) proton-assisted amino acid transport 1 (PAT1), transporting proline, glycine and alanine (153).

AA transport takes place through a sequence of events: 1) AAs bind to an opened exposed site on the *cis* (outside) membrane surface; 2) the transporter goes through a conformational change whereby the AA-bound site becomes exposed to the *trans* (inside) membrane surface; 3) the AA is released into skeletal muscle as the transporter returns to its

normal conformation (159). The influx of BCAAs into skeletal muscle through LAT1 is dependent on the removal of glutamine and other ions such as Na^+, H^+, K^+, and/or Cl^- out of the skeletal muscle. Therefore, LAT1 requires a glutamine gradient which is generated by the SNAT transporters (159).

2.2.3.2 BCAA Catabolism in Skeletal Muscle

A simplified schematic of BCAA catabolism in skeletal muscle is shown in Figure 2.1. A more complex diagram can be reviewed (33). Mediated by branched-chain aminotransferase (BCAT2), the BCAAs are first transaminated, yielding the branched-chain α-keto acids (BCKA) and glutamate. The BCKAs are 2-keto-isocaproate/4-methyl-2- oxopentanoic acid (KIC) (from leucine), α-keto-β-methylvaleric acid/3-methyl-2-oxopentanoate (KMV) (from isoleucine) and 2-

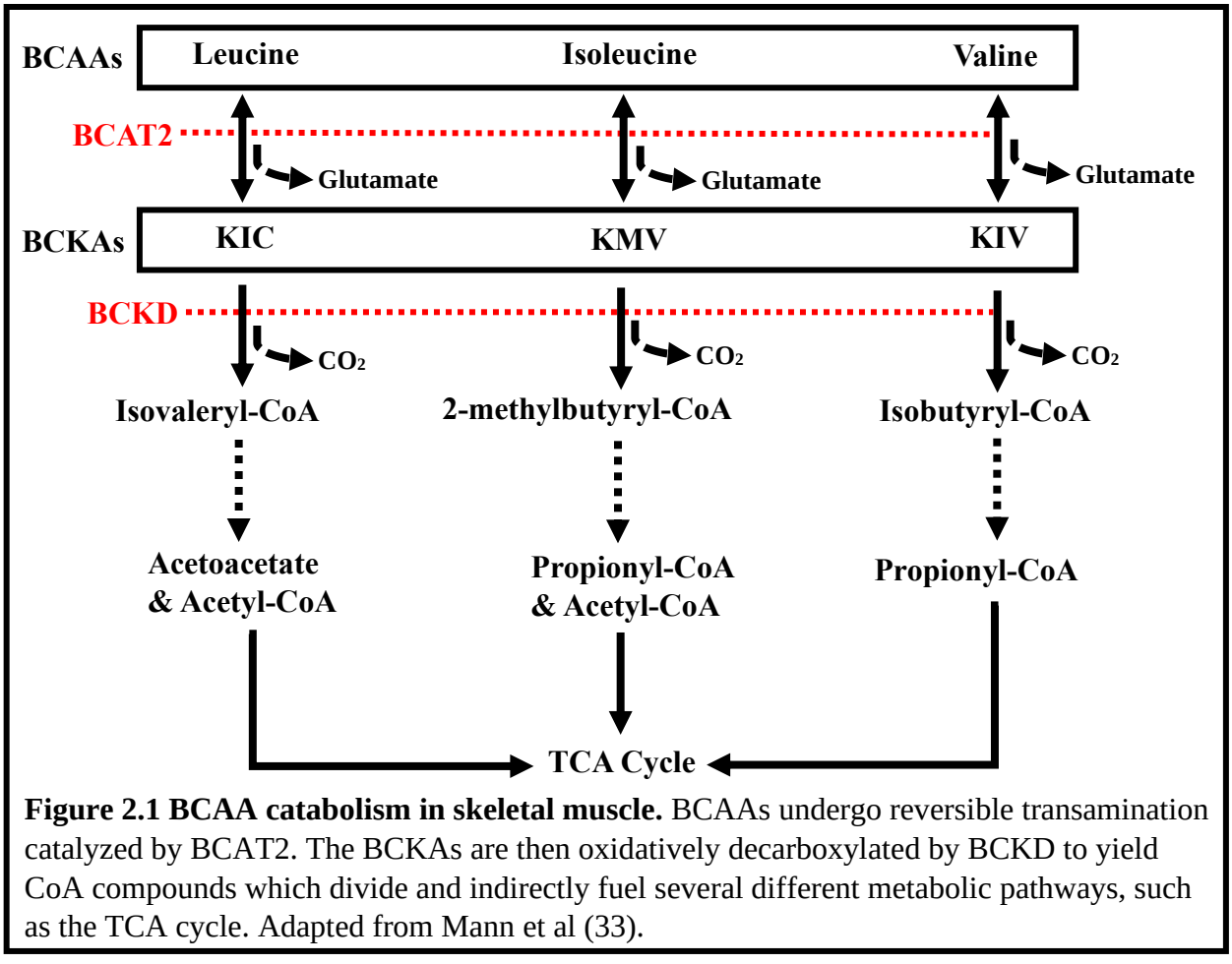

Figure 2.1 BCAA catabolism in skeletal muscle. BCAAs undergo reversible transamination catalyzed by BCAT2. The BCKAs are then oxidatively decarboxylated by BCKD to yield CoA compounds which divide and indirectly fuel several different metabolic pathways, such as the TCA cycle. Adapted from Mann et al (33).

keto-isovalerate/3-methyl-2-oxobutanoic acid (KIV) (from valine).

In this first step, BCAT2 removes and transfers the amino group from the BCAAs onto α-ketoglutarate producing glutamate. This step in BCAA catabolism is reversible, whereby BCAT2 can remove and transfer the amino group from glutamate back to the BCKAs, re-forming the BCAAs. In the BCAT2 reaction, the active form of vitamin B6, pyridoxal 5′-phosphate (PLP), serves as a coenzyme by binding to the amino group of the BCAAs, producing their respective keto acids and the pyridoxamine 5′-phosphate (PMP)-bound form of the enzyme. PMP then facilitates the transfer of the amino group to α-ketoglutarate, producing glutamate and restoring the BCAT-PLP conformation (160). There are two isoforms of BCAT: cytosolic BCAT (BCAT1) and mitochondrial BCAT (BCAT2). BCAT1 is only found in the brain, ovary and placenta. However, BCAT2 is known to be more widespread, found in the skeletal muscle, kidney, cortex, heart, subcutaneous adipose tissue, stomach, colon and liver (161). BCAT2 will be the main focus in this dissertation, as both the abundance and activity of the mitochondrial isoform is highest in the skeletal muscle (162). Since the liver has low levels of BCAT2 (163), the transamination reaction by BCAT2 takes place in the skeletal muscle. The resulting keto acids then travel to the liver for further oxidation by the branched-chain α-keto acid dehydrogenase complex (BCKD), as this enzyme's levels are higher in the rodent liver (164).

In the second step, the BCKAs are oxidatively decarboxylated by BCKD, producing their corresponding acyl CoA derivates (isovaleryl-CoA from KIC, 2-methylbutyryl-CoA from KMV, and isobutyryl-CoA from KIV). The acyl-CoA derivatives are then all metabolized along separate pathways, yielding acetoacetate and acetyl-CoA (from leucine), propionyl-CoA and acetyl-CoA (from isoleucine) and propionyl-CoA (from valine), all of which serve to fuel several metabolic pathways, such as the TCA cycle (33). In addition, KIC can be converted into beta-

hydroxy-beta-methylbutyrate (HMB) (165), an enzyme reported to stimulate muscle protein synthesis (166) and suppress proteolysis (167). The distribution of BCKDs activity (mU/g) is tissue dependent in humans, for example: liver, 4.2±0.41; skeletal muscle, 1.3±0.3; adipose tissue 1.1±0.1 (162).

The BCKD complex is made up of three subunits: heterodimeric branched-chain α-keto acid decarboxylase (E1), dihyrolipoyl transacyclase (E2) and homodimeric dihydrolipoyl dehydrogenase (E3). During oxidative decarboxylation by BCKD, the process begins through E1 decarboxylation of the keto acids, yielding branched-chain acyl intermediates and CO_2. The respective BCKA is then transferred to the core of the E2 subunit by the lipoyl domain, where it attaches to coenzyme A and produces branched-chain acyl-CoA ester. In this process, dihydrolipoic acid is produced through lipoate reduction. Lastly, the E3 subunit reoxidizes dihydrolipoic acid (using NAD+), yielding NADH and lipoate (168). A simplified diagram of the subunits involved in the BCKD reaction is shown in Figure 2.2.

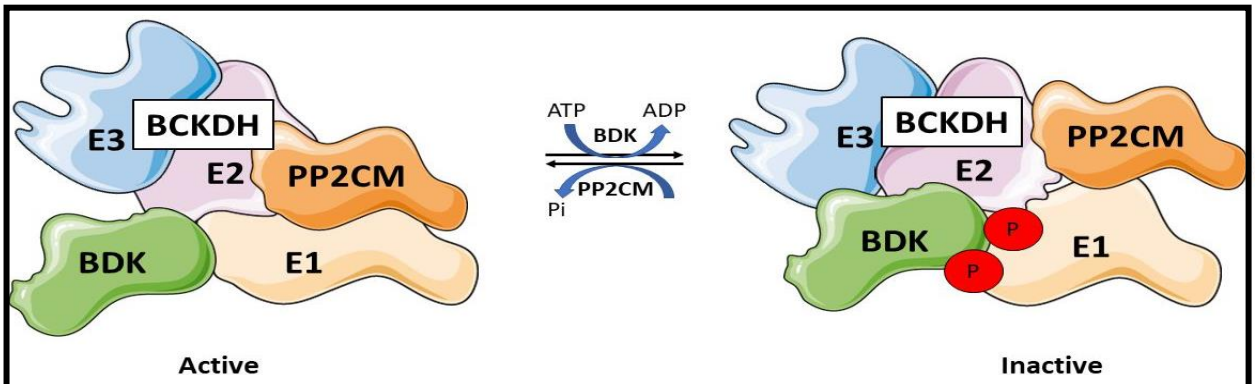

Figure 2.2 Regulation of BCKDH. BCKDH (referred as BCKD) is regulated by a kinase, branched-chain ketoacid dehydrogenase kinase (BDK), and a phosphatase, protein phosphatase 2Cm (PP2Cm), both in which interact with the E1 subunit. In the inactive form (right), BDK phosphorylates BCKD at ser293 and 303. In the active form (left), PP2CM dephosphorylates BCKD. Adapted from Mann et al (33).

Since the BCKD reaction is irreversible and the rate-limiting step in BCAA metabolism, the activity of this enzyme is regulated by a kinase and phosphatase (169). Expression of the

BCKD kinase (BDK) is high in the skeletal muscle and is responsible for phosphorylating the E1 subunit of BCKD on ser293 and ser303 resulting in inactivation (170) of the BCKD complex. In contrast, expression of protein phosphatase 2Cm (PP2CM) is low in the skeletal muscle and is responsible for dephosphorylating the BCKD complex, leading to its reactivation (171). The differences in expression of these enzymes in the skeletal muscle explains, in part, why activity of the BCKD complex is low in the skeletal muscle (172).

2.3 Mechanisms of Skeletal Muscle Anabolism

Pathways related to insulin receptor substrate-1(IRS-1)/phosphatidylinositol-3 kinase (PI3K)/protein kinase B (AKT) pathway, mammalian/mechanistic target of rapamycin complex 1 (mTORC1), β-catenin/c-Myc signalling (173) and the bone morphogenetic protein (BMP) axis (174) are all positive regulators of skeletal muscle mass. To remain within the scope of this dissertation, IGF-1/PI3K/AKT and mTORC1 will be discussed, as the BCAAs primarily target mTORC1 to stimulate skeletal muscle protein synthesis (34, 175).

2.3.1 IRS-1/PI3K/AKT

Binding of insulin or IGF-1 to its cognate receptors activates insulin receptor substrate (IRS). IRS activates the PI3K family generating phosphatidylinositol-3, 4, 5- trisphosphate (PIP3) from PIP2. PIP3 signals through phosphatase and tensin homolog deleted on chromosome 10 (PTEN) to activate phosphoinositide-dependent kinase 1 (PDK1), which then phosphorylates AKT on thr308 (176). AKT increases skeletal muscle cross-sectional area and individual muscle fibres by indirectly activating the mTORC1 pathway (177). The IGF-1/PI3K/AKT pathway also inhibits pathways related to protein breakdown (178). AKT phosphorylates (ser253) and inactivates forkhead box O (FOXO), a family of transcription factors that stimulate E3 ligases F-box only protein 32 (MAFbx/Atrogin-1) and TRIM63 (MURF1) in the skeletal muscle (179).

AKT also phosphorylates glycogen synthase kinase β (GSK3β) on ser9 relieving the inhibition on eukaryotic translation initiation factor 2 subunit B (eIF2B), a translation initiation factor for protein synthesis in skeletal muscle (180). Further, IGF-1/AKT inhibits the effects of myostatin, a member of the transforming growth factor-β (TGF-β) family that is a negative regulator of skeletal muscle mass (181). Activation of AKT is also required for glucose uptake in skeletal muscle (182–184). In response to insulin, AKT phosphorylates AKT substrate of 160 kDa (AS160) on thr642 and its homolog TBC1 domain family 1 (TBC1D1) on thr596 (185). Phosphorylation of these substrates results in the translocation of glucose transporter type 4 (GLUT4) from the cytoplasm to the outer plasma membrane promoting glucose uptake (186). These signalling pathways are simplified in figure 2.3.

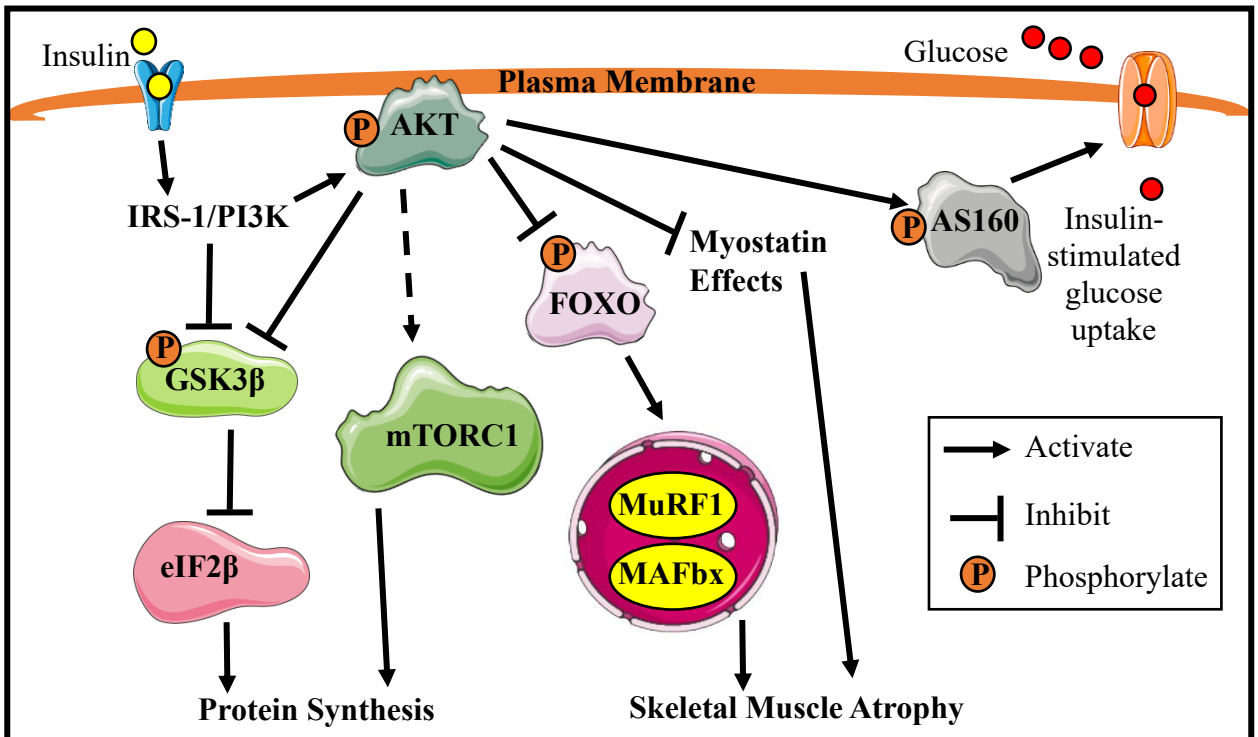

Figure 2.3 The effects of activated AKT in skeletal muscle. Via insulin activation of the IRS-1/PI3K pathway, AKT indirectly activates mTORC1 and inhibits GSK3β leading to protein synthesis. AKT also reduces skeletal muscle atrophy by inhibiting the effects of myostatin and decreasing nuclear translocation of MuRF1 and MAFbx via FOXO phosphorylation. Lastly, AKT phosphorylates AS160, leading to the translocation of GLUT4 to the plasma membrane and an increase in insulin-stimulated glucose uptake.

2.3.2 mTORC1

As mentioned (section 2.3.1), PDK1 phosphorylates AKT on thr308 leading to its activation (176). However, phosphorylation on ser473 by mTORC2 is required for full AKT activation. AKT indirectly activates mTORC1 by phosphorylating the Tuberous Sclerosis Complex 2 (TSC2) and Tuberous Sclerosis Complex 1 (TSC1) on ser939 and thr1462, relieving the inhibitory effect of the TSC2 complex on mTORC1 (187).

The mTORC1 complex can also be activated via BCAA sensing through the sestrins/gator/Rags/ragulator pathway. The Rags regulate mTORC1 activity by recruiting mTORC1 to the lysosomal membrane, where RHEB GTPase, an mTORC1 activator, is located. During BCAA availability, specifically leucine (the most studied), leucyl-tRNA synthetase migrates to the lysosome to facilitate proper RAG GTPase nucleotide loading, thus stimulating mTORC1 activity. However, the Rags are inhibited by GATOR1, which in turn is inhibited by GATOR2. Sestrin2, a leucine sensor, is upstream and inhibits GATOR2. However, in the presence of the BCAAs, sestrin2 is inhibited, leading to the eventual downstream translocation and activation of mTORC1 at the lysosome (27).

Once activated, mTORC1 phosphorylates multiple substrates, such as ribosomal protein S6 kinase (S6K1) and eukaryotic translation initiation factor 4E-binding protein 1 (4E-BP1). Once phosphorylated on thr389, S6K1 phosphorylates ribosomal protein S6 (S6), eukaryotic translation initiation factor 4B (eIF4B), eukaryotic translation elongation factor 2 kinase (eEF2K) and programmed cell death protein 4 (PDCD4) (188, 189). Once 4E-BP1 is phosphorylated on thr37/46 by mTORC1, 4E-BP1 dissociates from eukaryotic translation initiation factor-4E (eIF4E) (190). mTORC1 also inhibits the Unc-51 Like Autophagy Activating Kinase 1/Autophagy-related protein 13 (ULK-1/ATG13) complex (191), highlighting the

importance of mTORC1 in not only increasing protein synthesis, but also inhibiting protein breakdown. mTORC1 upstream and downstream signalling is shown in Figure 2.4.

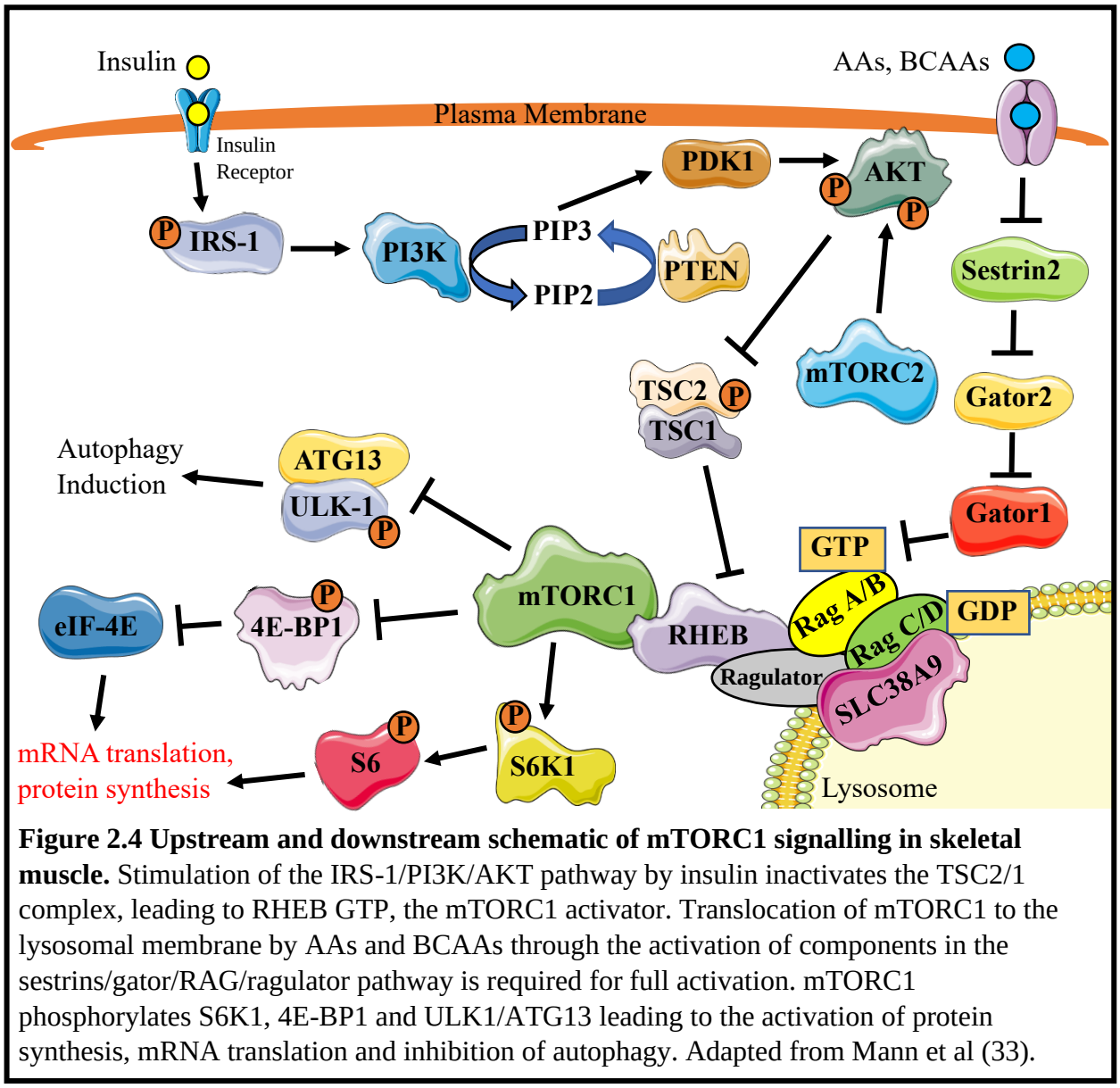

Figure 2.4 Upstream and downstream schematic of mTORC1 signalling in skeletal muscle. Stimulation of the IRS-1/PI3K/AKT pathway by insulin inactivates the TSC2/1 complex, leading to RHEB GTP, the mTORC1 activator. Translocation of mTORC1 to the lysosomal membrane by AAs and BCAAs through the activation of components in the sestrins/gator/RAG/ragulator pathway is required for full activation. mTORC1 phosphorylates S6K1, 4E-BP1 and ULK1/ATG13 leading to the activation of protein synthesis, mRNA translation and inhibition of autophagy. Adapted from Mann et al (33).

2.4 Skeletal Muscle Catabolism

In response to catabolic stimuli, such as poor nutritional status (192), muscle disuse (193), disease/illness (63–65) and cachexia (194), skeletal muscle undergoes protein breakdown, whereby mass is decreased. The following section will briefly address malnutrition, inflammation and insulin resistance as they pertain to skeletal muscle catabolism, but to remain

within the scope of this dissertation, the bulk of this section will address cachexia.

2.4.1 Skeletal Muscle Catabolism – Malnutrition

Malnutrition, resulting from lack or inadequate caloric intake can lead to a range of health issues such as alterations in body composition, physical mobility, quality of life and mental function across all populations (195, 196). Lack of essential nutrients can also cause loss of muscle mass and strength, due to factors related to reduced hemodynamics (197), decreased mitochondrial capacity (198), insulin resistance (199) and anabolic resistance (200).

2.4.2 Skeletal Muscle Catabolism – Inflammation

Inflammation is the body's defense mechanism against pathogens, damaged cells or illness/disease (201). In response to certain stressors, such as resistance exercise, the immune response is necessary for repair and maintenance of skeletal muscle (202) and is deemed vital to health (203). However, low-grade chronic inflammation can pathologically alter skeletal muscle function and metabolism.

2.4.3 Skeletal Muscle Catabolism – Insulin Resistance

Insulin resistance is a metabolic problem in which the normal biological response to insulin is impaired. Typically, the hormonal action of insulin results in the removal of glucose from the blood into target tissues such as the skeletal muscle, liver and adipose tissue (204). However, in insulin resistance, impairments in glucose disposal and transport can lead to a compensatory increase in beta-cell insulin production (205). Overtime, target tissues become resistant to the repeated compensatory increase in insulin, leading to insulin resistance. Metabolic consequences of insulin resistance include hyperglycemia, hypertension, and elevated inflammatory markers (205) and if left untreated, can eventually develop into T2DM (206).

Hyperactivation of mTORC1 has been linked to insulin resistance (207). Over activation

of mTORC1 either by growth factors (208) or BCAAs (209), potentiates a negative feedback loop, whereby S6K1 phosphorylates IRS on serine residues. Since IRS is only activated when phosphorylated on tyrosine residues, the PI3K/AKT pathway is not activated and GLUT4 does not translocate to the plasma membrane to uptake glucose and relieve hyperglycemia (207).

Insulin resistance has also been linked to alterations in skeletal muscle BCAA metabolism. In obese type 2 diabetic mice, PP2CM was unchanged in skeletal muscle, however, increased p-BCKD and protein expression of BDK, resulting in decreased BCKD activity and increased plasma BCAAs and BCKAs were found in these mice (210). In obese mice, another mouse model of insulin resistance, skeletal muscle mRNA and protein expression of BCAT2 and BCKD were unchanged (211). However, in the liver and adipose tissue, these catabolic enzymes were decreased (211, 212). In obese patients, elevated serum BCAA levels are associated with higher body-mass index and insulin resistance (213).

2.4.4 Skeletal Muscle Catabolism – Cachexia

Cachexia is a complex, multifactorial body and muscle wasting syndrome. Cachexia is diagnosed in individuals who have lost more than 5% of total body weight in 12-months or less while being diagnosed with a chronic condition (214). Chronic conditions such as kidney disease, congestive heart failure and cancer account for the greatest prevalence of cachexia diagnoses. However, cancer is the leader in disease-associated cachexia, as it is estimated that over 80% of all cancer patients will experience symptoms of cachexia. Cachexia is associated with uncontrollable and unvoluntary weight loss with detrimental decreases in muscle mass, function and strength (16). Metabolically, loss of appetite (13), fatigue (15), aggravated skeletal muscle catabolism (6, 8, 17, 18), systemic inflammation (9) and increases in energy expenditure (11) are all observed in cachexia. Clinically, cachexia decreases quality of life (19) and treatment

outcomes (22), while increasing morbidity and mortality in patients (20).

Cachexia induces skeletal muscle wasting through a prolonged and exacerbated negative protein balance that leads to extreme skeletal muscle proteolysis. Protein synthesis is also decreased in cachexia (18), but the increase in protein breakdown far outweighs the loss of protein synthesis. I will limit the discussion on cachexia to cancer (215) and chemotherapy (216) with respect to age- and sex-related differences in muscle maintenance. Factors such as the BCAAs (33), inflammation (9) and insulin resistance (10) will also be discussed as they pertain to cancer and chemotherapy.

2.5 Cancer

Cancer is a leading cause of death worldwide. There are greater then 10 million cases diagnosed annually and 1 in 2 Canadians will develop cancer in their lifetime. Genetics (217), environmental factors (218) and lifestyle (219) are all risk factors for this disease. However, age (1) and sex (2) are two of the most significant risk factors for cancer diagnosis. Briefly, cancer is characterized by uncontrollable and mutated cell growth with metastatic potential (220). Among others, although often dependent on cancer diagnosis and type, newly developed lumps, bloody urine, unexplained difficulties in food intake or swallowing and extreme weight loss are all common symptoms of cancer (221). Lung, breast, prostate and colon are the most commonly diagnosed cancers and have a significant impact on psychological and economic stress to patients, caregivers and families (222).

2.5.1 Age and Cancer

Cancer is considered to be an age-related disease, as incidence and diagnosis of the majority of cancer cases increases with age (1). For example, many invasive cancers begin to rise in individuals starting at the age of 45 and peak at 70 (223). However, due to better screening

technology today, this age of cancer diagnosis is beginning to decline.

The increase in cancer with age can be due to the fact that older individuals are subject to carcinogenic factors such as environmental agents (e.g. smoking) (224), occupational exposures (225) and ultraviolet radiation (226) for longer. In addition, hallmark factors of cancer diagnosis, such as genomic instability and epigenetic alterations (227) are increased in aging (228).

2.5.2 Sex and Cancer

Sex is a significant risk factor for cancers (45). In men, cancers of the prostate, lung and colon are most often diagnosed, while breast, lung and colon are most often diagnosed in females (45). However, cancer incidence is ~20% higher in men (229). For example, incidence of colon cancer is higher in males (230). Bladder cancer and leukemia are more often diagnosed in males (231), while females have a higher incidence of thyroid cancer (232). Males are also reported to have greater mortality from cancer compared to women (45), especially in the United States, where mortality rate was also about ~40% higher in men (229). In general, lung, colon and stomach cancers account for the majority of cancer deaths, with all these cancers showing higher mortality in men. Cancer death from bladder, liver and esophagus also all showed higher mortality in men (45), in addition to melanoma, where men had a 34% greater risk of death (233), whereas females (compared to males) have higher mortality for breast cancer (45, 234).

Differences in cancer incidence and mortality between the sexes can be due to differences in genetic composition. For example, men have a higher incidence of bladder cancer due to a protective role played by a genetic polymorphism of sulfotransferase 1A1 in women (232, 235). Sex differences in other genetic polymorphisms have also been shown to increase the incidence of certain cancers in men, such as acute leukemia (236) and lymphoma (237).

Sex hormones also play a prominent role in cancer incidence between the sexes. Higher

levels of serum testosterone lead to increased risk of prostate cancer in older men (238). Lower levels of estrogen in males leads to an increased risk of leukemia as estrogen plays a protective role in this cancer (239). However, in females, where estrogen levels are potentially elevated, there is an increased risk of thyroid (240) and breast cancer (241) development.

2.5.3 Cancer Cachexia – Aging

According to the Jackson laboratory, 3-month, 10-month and 18-month-old mice are equivalent to 20, 38 and 56-year-old humans, respectively (242). However, due to factors such as cost, supply and historical data compatibility (243), very few studies investigate cancer or chemotherapy-associated cachexia in aged mice. Physiologically (among others), changes in the mouse microbiome (244), liver enzymes (245), blood flow (243) and disease susceptibility (246) with age further support the use of younger animals. Although age is rarely compared within the same study, it is possible to compare the magnitude of differences across different studies. However, due to inter-study differences such as cancer type, treatment length and animal strain, variability in body and muscle weight loss differs.

Certain tumour models are used to induce body and skeletal muscle wasting, making them viable options to study cancer cachexia, as cachexia accompanies growth of these tumours in xenograft models. AH-130 Yoshida hepatoma (247–252), C26 adenocarcinoma (6, 7, 18, 252–258), Walker-256 (259–263) and Lewis Lung carcinoma (LLC) (264–273) are animal tumour models of the liver, colon, breast and liver, respectively. The majority of the studies outlined here are conducted in mice aged between 3 and 24-weeks of age, which according to the Jackson lab equates to a 20 or 30-year-old human. Therefore, this explains why there are not vast differences in body or muscle weight in these studies. Three-week-old mice inoculated with walker-256 cancer cells showed ~20% loss of body weight (263) , while human melanoma

caused a 20% decrease in body weight in five-week-old mice (274, 275). AH130 Yoshida cells led to an average loss of 15% in skeletal muscle weights of five-week-old mice (247). In 6-week-old mice, LLC led to only a 10% loss of body weight, but a 40% decrease in skeletal muscle weight (268). Using mice between the age of 6-8-weeks of age, C26 inoculation resulted in a 10% (276), 13% (18), 15% (253), 20% (7, 277, 278), 23% (279), and 30% (6, 280) loss of body weight. Loss of skeletal muscle weights of either the TA, gastrocnemius or quadricep also ranged from ~20-50% in these studies. In 12-week-old rats, walker 256 tumour inoculation caused less then 10% loss of body weight (281, 282), while LLC caused ~20% loss of body weight and ~25% loss of muscle weights (265). LLC was also seen to cause ~5% loss of body weight in 20-week-old mice (264) and ~20% loss of body weight in 28-week-old mice (269).

In patients with lung cancer (average age of 66), a recent review (283) highlighted that patients show a loss of skeletal muscle mass of between 3 and 10% following 3-10 months of chemotherapy (46, 284–287). In 111 advanced gastric cancer patients (average age of 65), skeletal muscle (11.3%), body mass index (3.2%) and body weight (3.5%) were all decreased within 4 weeks of chemotherapy treatment initiation. This study also found that females lost more skeletal muscle (2.7%) and body weight (1.3%) compared to males (288). Other studies in gastric cancers also showed losses in skeletal muscle (6.1%; >5%) following chemotherapy (289, 290). In 94 pancreatic cancer patients (>70 age) receiving chemotherapy, skeletal muscle loss was >10% over the course of their treatment (291). Another study in pancreatic cancer also showed ~6% loss in skeletal muscle (292), while skeletal muscle index was also seen to be decreased by ~18% (293). In all these studies, the loss of body and skeletal muscle weight negatively affected survival and treatment outcomes in all patients.

2.5.4 Cancer Cachexia – Sex

In a recent 2023 study, sex differences in the onset of C26-induced cancer cachexia were investigated in male and female mice after 25 days of tumour inoculation. Male mice experienced worsened outcomes for body weight, muscle mass, torque force, protein synthesis and mitochondrial dynamics. Similarities between the sexes were found for fat loss and increased proteolytic markers. Findings from this study suggest preservations in muscle quality displayed by females during early onset of cancer cachexia (294).

These results in animals are confirmed in humans, as cancer cachexia-related outcomes are worsened in males. For example, in lung (295), colorectal (296, 297) and pancreatic (298) cancer cachexia, clinical outcomes (such as muscle depletion), tumour phenotype, survival, cardiac muscle loss and inflammatory responses are all more severe in male cancer patients. Mechanistically, these findings may be due to the effects of cancer cachexia on glycolytic fibres (86, 299), the fibre type that has greater distribution in males (82). In various other cancers, reductions in grip strength (300), cancer-related fatigue (301) and overall survival (302) were also all worse in males. This is highlighted by the fact that the inability of males to produce sufficient testosterone (hypogonadism), often accompanies cachexia (303). Moreover, as mentioned, females may be more protected against inflammatory-based pathologies such as cancer cachexia, as estrogen can blunt liver IL-6 secretion (304). In summary, as outlined in a review by Zhong et al (305), cachexia prevalence, and loss of weight, grip strength, muscle mass, myofiber area, type 2 muscle fibres and mitochondrial function are all more severe in male cancer patients, whereas females experience greater atrophy of type 1 muscle fibres.

2.5.5 BCAA Levels and Metabolism in Cancer

The metabolism of the BCAAs is altered in some cancers. During the first step of BCAA catabolism, BCAT2 transamination generates glutamate, which in turn is metabolized to

glutamine via glutamine synthetase. Interestingly, there is an increased requirement for glutamine in cancer cells (306), an AA that can drive the TCA cycle and activate ATP production in the mitochondria. In addition, some tumour cells also use the BCAAs as alternative fuel to drive cellular proliferative capacity and tumour formation (307). In addition, the expression of MYC, a family of transcription factors involved in BCAA catabolism, is also upregulated in over 70% of cancers (308). Mechanistically, MYC upregulates LAT1 and BCAT1 expression, while increasing glucose and glutamine uptake (309). These changes drive the BCAAs and energy into tumours, further supporting growth. The direct effects of folfiri on MYC expression remain to be elucidated, but overexpression of the MYC family of transcription factors have been reported to initiate chemoresistance (310).

In hepatocellular carcinoma, Ericksen et al found that BCAT2 mRNA was increased, while protein expression and enzymatic activity of BCKD were decreased. In addition, serum concentrations of the BCAAs were lower, but significantly increased in liver tumours (40), highlighting a potential mechanism whereby BCKAs are unable to undergo further oxidation and are therefore re-aminated back into the BCAAs. High BCAA concentrations can drive hyperactivation of mTORC1, a mechanism linked to liver tumour progression (311–313).

In breast cancer patients, serum BCAA levels are significantly increased compared to healthy controls. BCAA levels were also found to be increased in breast cancer tissue. The mRNA expression of BCAT1/2 and BCKD were also increased in breast cancer tissue, leading to increased substrates for the TCA cycle and enhanced growth of breast cancer cells. However, lentiviral knockdown of BCAT1 not only repressed breast cancer cell growth, but also reduced colony number (41). A prospective analysis by Zeleznik et al, found that serum BCAA levels were associated with higher breast cancer risk in postmenopausal women compared to their

premenopausal counterparts (314). In addition, Lecuyer et al found that higher plasma levels of valine were associated with elevated breast cancer risk (315).

Elevated serum BCAA levels are observed in mice inoculated with pancreatic ductal adenocarcinoma (PDAC) cells (316). Interestingly, PDAC tumours display decreased BCAA uptake (317), while PDAC cells exhibit increased BCAA uptake (318). In addition, elevated plasma BCAA levels are associated with future pancreatic cancer risk (316), and tumour progression in PDAC patients (319). In both mouse models and human PDAC, BCAT2 is significantly elevated, while BCKD activity is decreased (317). Consistent with this, during cell proliferation, the BCAAs can be used by PDAC tumours as a source of carbon for fatty acid synthesis (318). However, tissue-specific pancreatic knockout of BCAT2 slows pancreatic neoplasia (320). In tandem, inhibition of BCKD also reduced proliferation and colony formation, stressing the importance of BCAT2 and BCKD enzymes in PDAC growth and progression (321). These changes are summarized in Table 1.

Table 1 The effect of cancer on serum, tumour and BCAA catabolic enzyme levels

Cancer Type	Serum BCAA Levels	Tumour BCAA Levels	Effect on BCAA Enzymes
Liver	Decreased	Increased	BCAT2 mRNA increased and BCKD enzymatic activity decreased
Breast	Increased	Increased	BCAT1/2 and BCKD mRNA increased
Pancreas	Increased	Decreased	BCAT2 protein upregulated and BCKD protein decreased
Lung	Increased	Increased	BCAT2 elevated and BCKD elevated

In patients suffering from non-small cell lung carcinoma (NSCLC), serum (322), and tumour (317) BCAA levels are increased. In tandem, LAT1 was increased in these tumours. Both BCAT2 and BCKD were also found to be elevated in lung tumours. BCAT was found to be essential for NSCLC growth, as BCAT null NSCLC cells failed to form tumours (317).

In studies utilizing other cancer models, such as Yoshida AH-130 hepatoma, observed

increases in skeletal muscle leucine oxidation were found (323), while animals inoculated with Walker-256 tumours showed enhanced BCAA dehydrogenase activity (324). In some cancers, such as lymphoma and sarcoma, where minimal weight loss was observed, plasma AA levels were similar to controls. However, in esophageal cancer patients who experienced ~20% decreases in body weight, total serum AAs were markedly reduced compared to controls (325). However, BCAT1 seems to be the main culprit, as BCAT1 drives cell proliferation and tumour formation. In addition, BCAT1 overexpression accelerates tumour growth in multiple cancers (326–329). Therefore, adjuvant therapy combined with the inhibition of BCAT1 shows promise in cancer treatment.

2.5.5.1 BCAA and AA Treatment in Cancer Cachexia

Considering their anabolic effects, the BCAAs have the potential to act as nutritional aids in certain muscle wasting syndromes like cancer cachexia. Many studies have investigated the potential for leucine to reduce the loss of body weight and muscle mass in cachexia, as this is the most common BCAA attributed to the enhancement of protein synthesis (142).

In mice inoculated with the MAC16 colon tumour, valine and leucine together suppressed body weight loss and inhibited tumour growth, by increasing protein synthesis through phosphorylation of mTORC1, S6K1 and 4E-BP1 (330). In C26 tumour bearing mice, 8g of leucine supplementation counteracted muscle-mass loss, but had no effect on E3 ligase expression (331). However, glycine treatment decreased E3 ligase protein expression (332), while glutamine has also been shown to preserve body weight (333) and reduce tumour growth (334) in C26 tumour bearers. In another study of C26 tumour bearing mice, a nutritional diet of high protein and fish oil also significantly reduced carcass, muscle and fat loss, while improving muscle performance and total daily activity (276). In Walker-256 tumour bearing animals,

leucine supplementation improved muscle gastrocnemius strength, while leading to a maintenance of body weight and muscle mass (335). In this same tumour model, animals supplemented with leucine also exhibited smaller reductions in carcass mass and muscle myosin (336). Mechanistically, leucine supplementation in the gastrocnemius elevated protein synthesis and significantly reduced 20S and 19S ubiquitin proteasome subunits (337), while also inducing a shift from glycolytic towards oxidative phosphorylation and enhanced mitochondrial density in walker-256 tumour bearing animals (338). HMB, the metabolite of leucine, also attenuated body weight and muscle loss in tumours (261, 339–341). It should be mentioned that in the majority of these studies, although the BCAAs provided beneficial effects on the attenuation of muscle loss, the cachexia phenotype was not fully reversed and survival was not increased in these animals.

In hepatocellular carcinoma patients undergoing chemotherapy, BCAA supplementation, either through long term administration or a late evening snack, had no significant effects on skeletal muscle mass and fat free mass (38, 39). However, BCAAs have been seen to improve protein kinetics and albumin synthesis in malnourished cancer cachectic patients (342, 343). In other patients, oral administration of the BCAAs following liver resection improved body weight and red blood cell count, but tumour recurrence and survival rate was not benefitted (344). In gastrointestinal tumour patients, an isolated BCAA diet was not associated with increases in skeletal muscle index (345), while a high protein diet, including the BCAAs, did not promote better muscle function (346). Other studies, using a mixture of HMB, arginine and glutamine yield mixed results, as one study showed a significant increase in lean mass (347), while others showed minimal beneficial effects on muscle mass maintenance (348, 349). Other nutritional interventions that have been studied in cachexia are shown (Table 2).

Table 2 Nutritional interventions and their effects on attenuating cachexia

Nutritional Intervention	Tumour (Host)	Effect	Ref
Fish Oil	Pancreatic (Human)	Increased weight gain and dietary intake. Decreased serum IL-6, cortisol and proteolysis inducing factor	(350) (351)
Fish Oil	Walker-256 (Rat)	Increased body weight and food intake	(263)
High Protein and Fish Oil	C26 (Mice)	Increased muscle contraction, reduced systemic inflammation, muscle loss and physical performance loss	(352) (276)
Iron Supplementation	C26 (Mice)	Prevented decreases in grip strength, body weight, muscle mass and increased mitochondrial function	(353)
Niacin	C26 (Mice)	Increased muscle weights and protein synthesis, while, improving mitochondrial function	(354)
Carnitine	C26 (Mice)	Increased dietary intake and gastrocnemius weight, downregulated inflammatory cytokines, proteasome and MuRF1	(355) (356)
Coix Seed Oil	LLC (Mice)	Prevented body weight loss and systemic inflammation, while decreasing MuRF1	(357)
Fucoidan	Bladder (Mice)	Reduced the loss of body weight and muscle atrophy, while decreasing pro-inflammatory cytokine production	(358)
Creatine	Walker-256 (Rat)	Attentuated body weight loss, decreased tumour size and decreased MuRF1/Atrogin-1	(359)

2.5.6 Cancer and Inflammation

Elevated inflammatory cytokine levels are the most prominent feature of cancer cachexia (360). Tumour-necrosis factor-alpha (TNF-α) (361, 362), interleukin-1 (IL-1) (360, 363), and interleukin-6 (IL-6) (364, 365) are the most common inflammatory cytokines produced by the tumours of cancer patients. These cytokines can readily cross the blood-brain barrier and suppress appetite (366, 367). In addition, these cytokines act directly on skeletal muscle and promote protein degradation by increasing E3 ubiquitin ligase expression (361, 362, 368, 369) and activating the ubiquitin proteasome. However, inhibiting these cytokines does not always slow cachexia progression or increase food intake (369, 370), highlighting the complex interplay of multiple factors in cachexia.

2.5.7 Cancer and Insulin Resistance

Cancer induces the loss of skeletal muscle mass (6, 7, 253), the major glucose reservoir in the human body. Theoretically, this could lead to hyperglycemia and a compensatory response to increase beta-cell insulin production. Cancer also increases pro-inflammatory cytokines (361, 362) and ROS (371–373), two factors known to induce insulin resistance (374–376). Cancer also decreases serum insulin (377, 378), serum glucose (378) and glucose availability to healthy tissues as glucose is the favourable energy source for tumours (379).

2.6 Chemotherapy and Cachexia

Chemotherapy is the one of the most common forms of cancer treatment (380). Generally, chemotherapy acts by attacking and damaging the DNA of rapidly dividing cells, such as those from tumours. However, chemotherapy is not specific to just tumours and therefore causes severe side effects such as hair loss, appetite loss, nausea and vomiting (381). Different chemotherapy drugs are used dependent on the cancer diagnosis. A few examples are provided. Cisplatin, a platinum containing compound, is used in the treatment of cervical, head, neck and lung cancers (382). Carboplatin, another platinum containing compound, is also used in the treatment of cervical cancer (383). Irinotecan hydrochloride (CPT-11) is used in the treatment of colorectal cancer (384). 5-fluorouracil (5FU) is used in the treatment of colon, breast, head and neck cancers (385, 386). However, chemotherapy drugs can be combined, as combinatory cocktails can reduce drug toxicity and resistance, while increasing bioavailability of drugs (387, 388). Different chemotherapeutics can also significantly affect the organs. Conventional chemotherapeutic drugs that are effective anti-cancer agents cause toxicity in the kidney (389, 390), liver (391, 392), spleen (393, 394) heart (395, 396) and other dividing cells.

CPT-11 is an inhibitor of DNA topoisomerase-1, a critical enzyme involved in DNA

replication and transcription, as it makes single strand cuts in DNA (397). Following administration, via carboxylesterase, CPT-11 is converted into its active form SN-38 in the liver. SN-38 is then excreted from the liver in the bile and absorbed into the intestine (398), where the potent topoisomerase inhibition of this compound makes CPT-11 a primary treatment for colon cancer (398, 399). Barriers to CPT-11 treatment include neutropenia (low white blood cell count) (400), debilitating diarrhea (401) and intestinal mucositis (inflammation of the mucosa) (402).

5FU is a pyrimidine analog that is transported into cells either by non-facilitated diffusion or facilitated nucleobase transport (403). Since 5FU by itself is inactive, this compound undergoes a myriad of intracellular changes until it is converted into one of three active forms: 5-fluoro-2'-deoxyuridine-5'-monophosphate (FdUMP), 5-fluorodeoxyuridine-5'-triphosphate (FdUTP), 5-fluorouridine-5'triphosphate (FUTP). In these active forms, 5FU is a potent inhibitor of DNA synthesis, DNA function, RNA synthesis and mRNA translation (404, 405). Intracellularly, FdUMP (the most studied) binds to and inhibits thymidylate synthase, an enzyme critical for DNA synthesis (405). However, major barriers exists in the use of 5FU as an anti-cancer treatment: 1) Treatment with 5FU leads to increases in catabolic enzymes responsible for the breakdown of FdUMP, FdUTP and FUTP (406); 2) 5FU treatment augments compensatory increases in protein content and synthesis of thymidylate synthase (407, 408), leading to greater dosage requirements and possible toxicity from 5FU; 3) 5FU is rapidly excreted from the body following administration, again leading to greater dosage requirements.

Leucovorin (folinic acid) is a reduced form of folate, and was originally used as a treatment for folate deficiency in individuals treated with methotrexate (409), a common drug used to treat certain cancers (e.g. leukemia). However, it was discovered that intracellularly, leucovorin can bind to FdUMP (an active form of 5FU), leading to greater binding of the

FdUMP-leucovorin complex to thymidylate synthase (410) and greater bio-availability of the 5FU, as the FdUMP-leucovorin complex takes longer to be excreted (405).

Taken together, the combination of CPT-11, 5FU and leucovorin make up folfiri, a combinatory drug cocktail used in the treatment of colorectal cancer (411). Previous reports have found greater cytotoxic action and significantly higher response rates when 5FU and leucovorin are combined (412, 413). In addition, since colon cancer is one of the top diagnosed cancers in both men and women and colon cancer diagnosis rates increase with age, we chose this chemotherapy cocktail as a viable option to study age and sex differences following treatment.

In myotubes, cisplatin induces myotube atrophy via impairment of AKT signalling and increases in proteasomal activity (414). Treatment with ghrelin rescues cisplatin-induced myotube atrophy via down regulation of pathways associated with inflammation and myostatin (265). Doxorubicin also induces myotube atrophy via increased expression of MuRF1 and ROS, while decreasing protein synthesis, myosin and mitochondrial content. However, electrical stimulation was able to reverse doxorubicin-induced mitochondrial content loss, but did not affect ROS levels (415). Another chemotherapy drug, carboplatin, often used to treat ovarian cancer, also reduces myotube diameter, protein synthesis and markers of mTORC1 activity in C2C12 myotubes. In these myotubes, knockout of Regulated in Development and DNA Damage Response 1 (REDD1), a stress response protein, reversed all these effects (416). Chemotherapy drug cocktails have also been seen to induce myotube atrophy, associated with significant loss of myosin content, protein synthesis and mitochondrial abundance (417). However, activin receptor 2B (a myostatin inhibitor), has been seen to rescue decreases in myotube diameter and AKT in C2C12 myotubes treated with folfiri (8).

The effects of chemotherapy have also been studied on myofiber type. Doxorubicin

treatment in rats decreases fiber cross sectional area of both the slow twitch soleus and fast twitch EDL muscles (418). Cisplatin treatment also decreased myofiber diameter of the quadricep and hindlimb fast twitch muscles (17). Combinatory chemotherapy drug cocktails such as folfiri and folfox have also been shown to decrease the myofiber size of glycolytic type II fibres, specifically the gastrocnemius and tibialis anterior (6, 18). Another study in mice, using a combination of cyclophosphamide, doxorubicin and 5FU also caused atrophy of the type II muscle fibers of the tibialis anterior (419). In breast and colon cancer patients, chemotherapy reduced force development, suggesting greater effects on type II fibers (420). Another study in breast cancer patients treated with cyclophosphamide, doxorubicin or trastuzumab also decreased myosin heavy chain-related type II muscle fibers (421).

Side effects of common chemotherapy drugs is highlighted in Table 3.

2.6.1 Chemotherapy-induced Cachexia – Aging

In 7-week-old mice, cisplatin treatment led to ~15% decreases in body and skeletal muscle weights (253). In 8-week-old mice, folfiri or folfox led to ~15-20% decreases in body and skeletal muscle weights (6, 8, 18). Doxorubicin treatment in 8-week-old mice led to ~15% decreases in body weight, but greater then 25% decreases in the cross-sectional areas of the soleus and EDL (418). In 9-week-old mice, cisplatin caused ~15% and 30% decreases in body and skeletal muscle weights respectively (17), while doxorubicin only led to ~10-15% decreases in body and skeletal muscle weights (422). In 10-week-old rats, doxorubicin led to a modest 2% decrease in body weight and ~3% decrease in EDL (423). However, in 14-week-old rats, doxorubicin led to a significant change in body weight and ~25% decrease in EDL CSA (424).

One study, by Huot et al investigated the effects of cisplatin-induced cachexia in young and old mice. In young mice, cisplatin induced ~13% decrease in gastrocnemius weight, ~6%

decrease in muscle force and ~52% decrease in motor unit estimation (MUNE). In old mice, cisplatin induced ~25% decrease in gastrocnemius, ~19% decrease in muscle force and ~72% decrease in MUNE, highlighting exacerbation of cachexia in older mice. Older mice were also more susceptible to the loss of mitochondrial proteins following cisplatin treatment (425).

In humans, several different chemotherapeutic agents have induced skeletal muscle atrophy and/or loss in aging patients diagnosed with (among others) gastrointestinal cancer (426, 427), liver cancer (285, 428), pancreatic cancer (429, 430) and esophageal cancer (431, 432).

2.6.2 Chemotherapy-induced Cachexia – Sex

In young mice treated with cisplatin, no sex differences were observed for the loss of muscle force, but males experienced greater gastrocnemius (5%) and MUNE (2%) loss. In the same study, older female mice experienced a 5% greater gastrocnemius muscle loss, but males experienced greater loss of muscle weakness (3%) and MUNE (425).

Compared to males, females have a 34% increased risk of developing severe adverse drug reactions from chemotherapy (433). These adverse drug reactions differ between chemotherapeutic agents: 5FU causes stomatitis (inflamed mouth), leukopenia (low white blood cell count) and alopecia (hair loss) (434); paclitaxel causes myocardial infarction and lesion revascularization (434); oxaliplatin causes leukopenia, neutropenia and stomatitis (435). Other common adverse events are cardiovascular complications, sleep disturbances, mood changes, musculoskeletal loss, skin lesions and gastrointestinal difficulties (433). Females are also significantly more likely to be hospitalized due to these adverse events (434). One main cause of this phenomenon is that the majority of clinical trials are conducted in men. Therefore, the majority of the findings from these trials are generalized to women and their maximum tolerated dose is often lower, compared to the dose they receive from treatment (436–438).

The increased incidence of adverse reactions in females is also due to pharmacokinetic differences between the sexes. During treatment, elevated blood concentrations for the majority of FDA approved chemotherapy drugs were found in women (434). In addition, women have lower elimination and drug clearance rates (2, 434, 439) for almost all chemotherapeutic agents including, but not limited to paclitaxel (440), 5FU (441) and doxorubicin (442) compared to men. Elevated blood concentration and lower elimination rates may be due to higher plasma volume, organ perfusion and body fat in women (443). Since these chemotherapy drugs often bind to erythrocytes to be removed from circulation, lower hematocrit levels in females may also account for these differences (444). However, one study found men to experience more cases of thrombocytopenia (low platelet count) compared to women (435). Kidney function is important for elimination of drugs and chemicals from the circulation. Specifically, renal clearance, blood flow, glomerular filtration rate and passive diffusion are all greater in men (445, 446).

In women, these pharmacokinetics lead to higher drug plasma levels and more extensive rates of toxicity incidence compared to men (447). Due to the greater tissue toxicity in females, chemotherapy dose and therefore treatment effectiveness is decreased overtime as women have significantly higher rates of neuropathic pain (439), cognitive dysfunction (448), nausea and vomiting, especially from chemotherapeutic agents cisplatin (449) and oxaliplatin (435).

2.6.3 BCAA Levels and Metabolism following Chemotherapy

Very few studies have investigated the effect of chemotherapy on BCAA metabolism and availability in the skeletal muscle. The main reason for this is because the majority of studies focus on BCAA availability and their metabolism in tumours of cancer patients and overlook how the skeletal muscle and surrounding tissues/organs are affected. In a study by Fabris et al, they investigated AA concentrations in the plasma, interstitial space and gastrocnemius muscle

of rats for 8 days following a single 1.5mg/kg dose of doxorubicin. Plasma concentrations of total, essential and BCAAs were all increased up to 8 days following the doxorubicin injection. Similar elevations of the AAs were found in the interstitial space up to 6 days post treatment, but returned to normal levels at day 8. Interestingly, BCAA levels were significantly elevated in the gastrocnemius and remained elevated up to 8 days following the doxorubicin dose (450). In another study, mice treated with folfiri for 6-weeks were found to have elevated levels of BCAAs in the plasma, but no change in the skeletal muscle compared to vehicle. Compared to cancer, folfiri-treated animals had increased plasma BCAA concentrations, but similar skeletal muscle concentrations (6). The discrepancies between the two studies could be due to factors such as animal type, treatment time, muscle examined and chemotherapy type. A third study by Barreto et al, found that folfiri treatment in mice led to a drastic downregulation of several enzymes involved in AA metabolism, but this study was not explicit in which or how many of the enzymes were affected (18).

2.6.4 The Effect of Chemotherapy on Inflammation and Insulin Resistance

Current research suggests chemotherapy is associated with pro-inflammatory cytokine levels, as anti-cancer agents activate Nuclear factor kappa-light-chain-enhancer of activated B cells (NF-KB) (451). NF-KB is a stress response gene that promotes production of IL-1, IL-6 and TNF-α (452). Cancer patients receiving chemotherapy also show increased inflammatory cytokine content (453, 454).

Similar to the effects of cancer-induced insulin resistance, chemotherapy similarly decreases skeletal muscle mass (6, 8, 17), increases pro-inflammatory cytokines (455–457) and increases ROS production (458, 459). Chemotherapy also increases hyperglycemia (460), decreases insulin sensitivity and decreases glucose uptake (417, 424).

2.6.5 Chemotherapy and Sex Hormones

In cancer patients receiving chemotherapy, studies have shown low levels of testosterone (461–463), suggestive of hypogonadism in cancer patients (303). However, levels of testosterone return to normal levels following the cessation of chemotherapy treatment (464). In rats, chemotherapy has also been seen to inhibit the testosterone synthesis pathway (465).

Chemotherapy also decreases estradiol levels in breast cancer patients (466, 467) and mice (468), whereby chemotherapy can decrease the ovarian follicle pool size (469, 470). Estrogen has also been seen to increase efficacy of chemotherapy treatment in breast cancer cells (471). However, long term chemotherapy treatment can induce ovarian failure or premature menopause (472, 473).

2.6.6 Cancer and Chemotherapy-induced Mitochondrial Damage

Mitochondria play a pivotal role in skeletal muscle health, as they are essential contributors to whole-body energy expenditure. Their primary role is to oxidize nutrients in order to generate ATP molecules that serve multiple high energy demanding processes (474). Mitochondria also play vital roles in muscle contraction (475), glucose metabolism/insulin sensitivity (476), exercise adaptation (477) and thermogenesis (478). These roles highlight the importance of mitochondria in the maintenance of skeletal muscle homeostasis.

During cancer cachexia, DNA encoding multiple subunits of the mitochondrial complexes are downregulated (479–481), suggesting decreased mitochondrial functioning. However, the effects of cancer cachexia on mitochondrial biogenesis are inconsistent, as some studies have reported upregulation (482, 483), with other studies showing downregulation (480). One study comparing cancer cachectic patients to their weight-stable counterparts, found that mitochondrial fission was increased, consistent with higher autophagy-related proteins and

apoptosis (484). Ultimately, any decline or alteration in mitochondrial functioning in cancer cachexia leads to elevated ROS production, potentially driving cancer cachexia (485).

In skeletal muscle, chemotherapeutic agents such as doxorubicin, enhance ROS production (486), increase mitophagy (487) and negatively regulate calcium homeostasis (488). In breast cancer patients, doxorubicin decreases mitochondrial content and peroxisome proliferator-activated receptor-gamma coactivator (PGC-1alpha) expression (489). In mice, folfiri administration significantly decreased mitochondria number, size and genes in the skeletal muscle (8). Folfiri has also been reported to decrease mitochondrial fusion proteins and to alter oxidative phosphorylation in the TCA cycle (18). Folfox is also documented as a negative regulator of mitochondrial content and mitophagy (490).

2.7 Mechanisms of Skeletal Muscle Catabolism

Mechanisms related to autophagy (491), ubiquitin proteasome pathway (UPP)(492), myostatin (493) and calcium calpains (494) are all negative regulators of skeletal muscle mass. To remain within the scope of this dissertation, autophagy and UPP will be discussed, as these are the two catabolic pathways severely upregulated in cachexia (32, 495).

2.7.1 UPP

The majority of protein degradation in mammalian skeletal muscle is regulated by the UPP (496). In preparation for proteins to be degraded, substrates are conjugated by multiple units of ubiquitin through a cascade of events. First, ubiquitin proteins are activated by E1 enzymes using ATP. The ubiquitin molecule is then transferred from E1 to E2, a ubiquitin carrying molecule. E3 ligases then bind to both E2 and the protein substrate, activating the transfer of ubiquitin from E2 onto the protein substrate that is set for degradation. Polyubiquitination occurs and the ready to degrade protein is docked to the 26S proteasome for degradation (497), a crucial

protein complex involved in the final steps of the UPP (498).

In humans, there are over 650 ubiquitin ligases (499), however, only a few have been identified as muscle specific: atrogin-1 (also known as MAFbx) and MuRF1 (32). Specifically, atrogin-1 promotes the degradation of muscle transcription factor MyoD (500) and activator of protein synthesis eIF3f (501). MuRF1 interacts and targets structural proteins such as troponin, myosin heavy chain, actin and desmin (502–504). In many animals models, atrogin-1 and MuRF1 have been deemed necessary for muscle atrophy (505). For example, mice are resistant to denervation-induced muscle atrophy when they lack atrogin-1 and MuRF1 (32). In addition, atrogin-1 knockdown prevents fasting-induced muscle atrophy (506), while MuRF1 knockdown prevents dexamethasone-induced muscle atrophy (507).

2.7.1.1 UPP in Cachexia

In cancer cachexia, mRNA expression of 26S proteasomal subunits are elevated in skeletal muscle (508, 509), suggesting increased proteasomal activity. In C26 tumour-bearing animals, multiple studies have shown either increases in subunits and activity of the proteasome (508) or elevations in the skeletal muscle E3 ubiquitin ligases atrogin-1 and MuRF1 (253, 510). Similarly, in melanoma tumour-bearing mice, MuRF1 gene expression was increased. (511). In cancer patients suffering weight loss, increases in subunits, activity and genes from the UPP are all increased (512–514).

In-vitro, multiple studies have shown upregulation of the E3 ligases MuRF1 and Atrogin-1 following cisplatin treatment (17, 414). In addition, doxorubicin (515) and oxaliplatin (516) have shown similar effects. However, another study using folfox and folfiri found no changes in E3 ligase protein expression or proteasome activity (8). However a chemotherapy cocktail of cisplatin, 5FU and leucovorin increased ubiquitinated proteins in myotubes (417). Differences

may be explained by chemotherapeutic agent, cell line and timing of treatment.

2.7.2 Autophagy

Autophagy is a highly regulated protein and cellular recycling process. Microautophagy, macroautophagy and chaperone mediated autophagy (CMA) are the three primary forms of autophagy, all of which transport substrates, such as harmful products from mitochondria energy production, towards the lysosome for autophagy. Highlighted in a review by Bonaldo et al (497), the three types of autophagy are described as: Microautophagy is the simple engulfing of small cytoplasmic portions into the lysosome; During macroautophagy, beclin-1 signals towards ULK1 to initiate autophagosome formation, a process facilitated by the conversion of microtubule-associated proteins 1A/1B light chain 3B (LC3I) to LC3II. Tagged cargo ready for recycling is then brought to the autophagosome by P62 and degraded by the lysosome (517, 518); In CMA, chaperones recognize exposed amino acid sequences of damaged proteins and deliver them to the lysosome. Mitochondria can also undergo autophagy, a process known as mitophagy (519). Although autophagy is vital for the maintenance and survival of cells (520), progression of certain pathologies such as cancer and diabetes have been linked to dysregulated autophagic machinery (520, 521).

2.7.2.1 Autophagy in Cachexia

In cancer cachexia, elevations in Beclin-1 (autophagy induction) and LC3II levels (autophagosome formation) were found in patients (522). C26 tumour-bearing animals also show significantly elevated p62 levels, suggestive of overloading autophagic flux in skeletal muscle (523). Lung (524) and esophageal (525) cancer cachectic patients also show muscle wasting due to autophagic dysregulation.

In-vitro studies have investigated autophagy related markers following chemotherapy.

Specifically, BNIP3, as well as beclin-1 and LC3BII have all been observed to be upregulated following chemotherapy treatment (414, 417). In addition, since chemotherapy is a well-characterized inhibitor of upstream and downstream mTORC1 signalling in skeletal muscle (17, 18, 417), mTORC1 would not be able to inhibit ULK-1-mediated increases in autophagy (30).

2.8 Current Treatments

There are currently no effective or approved therapies to combat cancer cachexia. Some studies have proposed that treatment of cachexia relies heavily on treating the tumour itself (526). However, research has heavily focused on different pharmacological, nutritional and targeted therapies in an attempt to attenuate cachexia.

In rats, treatment with β-blockers (heart medication) preserved body, lean and adipose tissue weight in liver cancer (527). In mice, angiotensin-converting enzyme (ACE) inhibitors (another type of heart medication) also reduced the loss of muscle mass by inhibiting TNF-α production in colon cancer (528). Erythropoietin treatment has also proven successful in relieving body and muscle weight loss in cachectic mice, through a mechanism related to reduced IL-6 production (529–531).

In humans, megestrol acetate treatment increases appetite and caloric intake in cachectic patients (532–536). Progestogens (steroid hormones) (537) and corticosteroids (anti-inflammatories) (538) have also shown positive effects on the stimulation of appetite in cachexia. However, side effects such as insulin resistance and protein breakdown limit their long-term use (539). Ghrelin has been shown to improve body weight and lean mass, while stimulating food intake during cancer cachexia (540, 541). COX-2 inhibitor treatments have also led to weight gain, increased BMI and improvements in quality of life (542). Treatment with the omega-3-fatty acids have also been shown to improve body weight and stimulate appetite by decreasing pro-

inflammatory cytokine content (539, 543, 544). Other treatments, such as bortezomib (545), cannabinoids (546, 547) and insulin (548) have very minimal effects on reversing the loss of tissue mass in patients.

2.9 Age and Sex Differences

2.9.1 Anabolic Hormones and Nutrition

2.9.1.1 Insulin

Aging is associated with some changes in insulin dynamics following hyperglycemic challenges, but basal circulating levels of insulin remain similar between young and old individuals (549). However, in the context of aging, pancreatic insulin secretion (550) and insulin sensitivity (551) are both decreased in older individuals. Sedentary lifestyles and weight gain, two factors commonly seen in aging, can exacerbate these declines in insulin dynamics, contributing to a higher risk of developing diabetes.

For sex, hormonal differences contribute to variations in insulin dynamics, but circulating insulin levels do not differ between the sexes (552). However, females exhibit greater insulin secretion (553) and are more insulin sensitive (554, 555) compared to men.

2.9.1.2 Testosterone

Testosterone increases skeletal muscle mass and strength in healthy young and old individuals (556–560). However, in aging, decreases in free testosterone and hypogonadism are both associated with increased risks of falls, functional disabilities and lower muscle mass (561, 562). Sarcopenia is linked to decreased testosterone in men (563), but this effect is unclear in women, as testosterone does not decrease independently of estrogen (564). In the aging male, testosterone decreases at about 1-2% every year after the age of 50 (565), but the decrease in female testosterone with aging is controversial and unclear, as women show small steady

increases in testosterone after the age of 70 (566).

Male plasma testosterone concentrations are 10-35nmol/L, while females are 0.5-2.4nmol/L. Higher concentrations in males compared to females (567) is due to the fact that primary production of testosterone is in the testicles, while females produce limited amounts in the ovaries and adrenal glands (568). This disparity in circulating testosterone levels between the sexes likely contributes to the observed differences in various physiological aspects, such as muscle mass/strength (569), fat distribution (570) and bone density (571). However, no sex differences are observed in androgen receptor content or sensitivity in the skeletal muscle (572, 573). In addition, only testosterone supplementation in males shows promise in attenuating muscle loss in spinal cord injury (574) and elevated glucocorticoid conditions (575).

2.9.1.3 Estrogen

With aging, decreases in circulating estrogen levels are observed, irrespective of sex (576). Around menopause, estrogen loss leads to dysfunction in muscle mass and strength (577, 578). Due to age-related decreases in estrogen, the protective effects of this hormone on bone mineral density (579), muscle repair (580), oxidative damage (581, 582) and mitochondrial oxidative enzymes (583, 584) are all suggestive to be reduced in the aging female. However, whether these losses in relation to estrogen also occur in the aging male remains to be elucidated.

Compared to females, there is less available research on the effects of estrogen in males (585). Healthy young female plasma concentrations are between 30-400pg/mL, compared to 10-50pg/mL in males. However, these levels are known to fluctuate severely in females dependent on their estrous stage (586). Interestingly, estrogen supplementation rescued disuse atrophy in male (587), but not female (588) rats, whereas only females show maintenance of mitochondrial efficiency with estrogen (589).

2.9.1.4 Nutrition and Exercise

Compared to young, older individuals have significantly decreased nutrient intake of energy, protein, alcohol, water, sodium and fibre (590). Other nutrient deficiencies in vitamin B12, vitamin D, iron and calcium are also common (591). Reduced appetite and food intake likely accounts for these changes as circulating levels and production of ghrelin (hunger hormone) decrease (592) and cholecystokinin (satiety hormone) production increases (593) in aging. Moreover, older populations face barriers such as poor health, pain, fatigue and a lack of willpower (594) that may hinder their involvement in resistance exercise.

Compared to women, men tend to have greater total energy intake, protein intake and sodium intake (590). Men also have greater absolute intakes of all the macronutrients, while women were more likely to exceed recommendations for total fat and sugar (595). In addition, men are more likely to resistance or strength train compared to women (596).

2.9.2 BCAAs

2.9.2.1 Concentrations

Compared to young, total AAs, essential AAs, non-essential AAs and BCAAs are all decreased in the skeletal muscle of older individuals. The only AAs that were increased with aging were cysteine and citrulline (590), however, citrulline is not one of the 20 primary AAs.

Since men have higher muscle mass than women, men typically have higher skeletal muscle BCAA levels (47). Higher plasma BCAAs were also more likely to be found in individuals who were males (597). Higher concentrations of essential AAs and other small AAs were also found to be higher in males (590).

2.9.2.2 Transport

Although expression of these AA transporters are regulated by amino acid ingestion in

both young (598) and elderly (599) individuals, sex differences in amino acid transporter expression have not been reported. Basal expression of these amino acid transporters in skeletal muscle are similar between young and old individuals. However, these studies report inconsistent results, as one study found an increase in AA transporter expression following resistance exercise in old individuals (600), while another study did not (601).

2.9.2.3 Catabolism

Minimal studies have investigated sex differences in BCAA metabolism. Following endurance exercise, males show higher rates of leucine oxidation compared to females (602), suggesting that males tend to oxidize more AAs for energy, while females oxidize more fats. Another study found that estrogen can activate BDK, thereby inhibiting the BCKD complex and decreasing BCAA metabolism (603, 604).

2.9.3 Skeletal Muscle Anabolism

2.9.3.1 mTORC1

Compared to young, basal phosphorylation of mTORC1 and S6K1 are higher in older subjects, with no changes observed for muscle fractional synthetic rate (605). However, following a bout of resistance exercise, phosphorylation of S6 (ser240/244) and activation of transcription factor 4 is higher in younger individuals (606), suggesting that exercise-induced increases in protein synthesis are either delayed (607) or blunted (608) in older populations.

Current research suggests there are no sex differences in mTORC1 signalling/activation following food consumption (609) or resistance exercise (610, 611).

2.9.4 Skeletal Muscle Catabolism

2.9.4.1 Malnutrition

In aging, malnutrition is linked to chronic illness, hospitalizations, dementia, depression

and socioeconomic status (612). Malnutrition is not limited to older populations, but is more frequent with higher age, especially when you consider the effects that malnourishment can have on clinical outcomes, disease recovery, trauma and surgery (613, 614). Following malnutrition, older populations show a greater loss of body composition (615), slower recovery (616) and a greater risk of geriatric syndrome development (e.g. dementia, depression, delirium) (617).

Current literature reveals that males are more likely to be malnourished in their early years, but with age, this disadvantage lessens (618–620).

2.9.4.2 Inflammation

Older populations have higher basal levels of inflammation, linking these signals to reduced regenerative responses (621) and lower muscle mass and strength (202). A key pro-inflammatory cytokine elevated in aging is TNF-α (622), which leads to physical decline (623) and decreases in force-generating capacity (624). Other inflammatory factors increased in aging include IL-6 and IL-1 (625). Aging-induced increases in pro-inflammatory cytokines is also associated with metabolic dysfunction (626), weakened anabolic signalling (627), elevated muscle protein catabolism (628) and reductions in oxidative metabolism (629).

Current research suggests females may be protected against inflammatory-induced muscle wasting diseases (630), as males are observed to have greater muscle mass loss and side effects in these conditions (296, 297). These findings can be explained by sex hormone abundance, as estrogen can blunt atrophy by inhibiting liver secretion of IL-6 (304). In addition, less cachectic symptoms are experienced by cycling females compared to their acyclic counterparts (631).

2.9.4.3 Insulin Resistance

In aging, there is an increased risk for both type 2 diabetes (632) and insulin resistance

(633). In addition, the prevalence of impairments in glucose tolerance increases with age (634). Mechanistically, compared to their younger counterparts, greater risk of insulin resistance in older populations is a consequence of decreased skeletal muscle glucose transporter 4 (635), lower insulin-stimulated AKT activity (636) and impaired insulin signalling/sensitivity (637).

Sex differences have also been reported, with men showing greater prevalence and development of insulin resistance compared to women (638). Lower adiponectin levels (639) and higher visceral and hepatic adipose tissue levels (640) contribute to greater prevalence in men. In addition, estrogen can improve glucose uptake in skeletal muscle (641) and reduce liver glucose production (642). However, after menopause, the incidence of insulin resistance is similar between men and women (643), further highlighting the protective effects of estrogen in young females.

2.9.5 Mitochondria

Highlighted by multiple reviews (644–646), aging is associated with significant alterations in mitochondrial dynamics. In aging, mitochondria are characterized by decreased oxidative capacity, oxidative phosphorylation, ATP production, antioxidant defenses and mitochondrial biogenesis and fusion. Further, aging is associated with increased mutations to mitochondrial DNA, ROS generation and oxidative damage. Therefore, it should come as no surprise that the loss of mitochondrial content is associated with early onset sarcopenia, resulting in loss of muscle mass and function (647).

Compared to males, females have greater mitochondrial content (648–650), oxygen affinity (651), transcription factors (652) and activity (649, 650, 653). In addition, estrogen, helps maintain mitochondrial biogenesis (654). These findings suggest that mitochondrial quality is greater in females relative to males. Other studies have found similarities between the sexes

for maximal mitochondrial respiration rates and abundance of ADP transporter proteins. However, females display lower mitochondrial ADP sensitivity and create less ATP during muscle atrophy (652, 655, 656).

2.9.6 Skeletal Muscle Catabolism

2.9.6.1 UPP

Proteasome activity declines in aging skeletal muscle (657). This decline is related to decreases (658), replacement (659) or disassembly (660) of proteasomal subunits. However, E3 ligases MuRF1 and Atrogin-1 are markedly increased in aging tibialis anterior muscle (661). Perturbations in protein homeostasis and proteostasis have been linked to the proteasome and the onset of neurogenerative diseases such as Alzheimers (662).

Current research suggests that basal UPP activity is greater in males, a finding likely mediated by estrogen signalling (663, 664).

2.9.6.2 Autophagy

Reduced autophagy has been reported in aging (665). Although specific autophagy regulators such as beclin-1 were upregulated, decreases in autophagosome formation, observed through reduced LC3BII levels, suggests reduced autophagic machinery in aging (666). Therefore, in aging, insufficient autophagy is found, either due to a build up of ready-to-degrade cargo (causing cellular damage in itself) or diminished autophagic flux (665).

Current research suggests that protein expression of autophagy initiation proteins are greater in females, leading to greater autophagy-related protein degradation compared to males (667, 668).

Table 3 Common chemotherapeutic agents, their affecting organs and side effects

Chemotherapy Agent / Drug	Cancers Treated	Side Effects
Carboplatin	Ovary, Lung, Head, Neck, Esophagus, Bladder, Cervical	Nausea, Vomiting, Anemia, Hair Loss, Fatigue
Cisplatin	Testicle, Ovary, Head, Neck, Lung, Esophagus	Nausea, Vomiting, Anemia, Kidney toxicity
Doxorubicin	Breast, Ovarian, Bladder, Stomach	Nausea, Vomiting, Anemia, Hair loss
Irinotecan (CPT-11)	Colon, Lung	Diarrhea, Fever, Cramping, Nausea, Vomiting, Anemia, Neutropenia, Mucositis
Oxaliplatin	Intestine, Pancreas, Stomach	Neuropathy, Nausea, Vomiting, Diarrhea, Anemia, Fatigue, Appetite Loss, Stomatitis, Neutropenia
5-Fluorouracil	Breast, Colon, Pancreas, Skin, Stomach, Rectal, Head, Neck	Diarrhea, Nausea, Anemia, Hair loss, Taste changes, Appetite Loss, Stomatitis, Neutropenia
Paclitaxel	Bone, Lung, Ovary, Breast	Anemia, Hair loss, Joint pain, Neuropathy, Diarrhea, Mouth sores
Methotrexate	Blood, Breast	Dizziness, Drowsiness, Hair loss, Headaches, Decreased Appetite

(References, PMID: 37397557, 30186799, 35158895)

Chapter 3 Overview, Rationale, Objective and Hypotheses

3.1 Dissertation Overview

The overall goal of this dissertation is to examine the effect of age and sex on mechanisms and severity of chemotherapy-induced cachexia, with a focus on BCAA availability, metabolism and transporter expression in young and aged animals.

3.2 Dissertation Rationale

Cancer incidence varies with sex and is more common with advancing age. However, previous research investigating chemotherapy-induced cachexia focuses primarily on young male animals. Clinically, these studies provide a limited understanding of cachexia across different demographics, as older age and sex can affect various aspect of cancer care. In addition, the branched-chain amino acids (BCAA), which present as promising targets to treat cachexia, have yielded inconsistent and minimal results in humans, a finding that may in part be due to altered skeletal muscle BCAA availability and metabolism following chemotherapy, a topic rarely studied. Better understanding of the mechanisms associated with chemotherapy-induced damage on skeletal muscle and BCAA metabolism may help in the development of interventions that attenuate muscle wasting and enhance overall quality of life in cancer patients.

3.3 Study Objectives

The objective of Chapter 4 is to investigate the effect of a chemotherapy drug cocktail on BCAA concentrations, transporter expression and metabolism in myotubes. Examining whether maintaining BCAA concentrations could attenuate myotube atrophy was also investigated.

The objective of Chapter 5 is to evaluate sex differences in cachexia outcomes and BCAA metabolism/availability in young mice following chemotherapy.

The objective of Chapter 6 is to evaluate sex differences in cachexia outcomes and

BCAA metabolism/availability in aged mice following chemotherapy.

3.4 Hypotheses

1. Chemotherapy is a potent inducer of skeletal muscle atrophy (8). In addition, the BCAAs are potent stimulators of skeletal muscle protein synthesis (27). I hypothesize that chemotherapy-induced atrophy is associated with decreases in transporter expression, metabolism and concentrations of the BCAAs in myotubes (Chap. 4).
2. LAT1 is the most abundant BCAA transporter in skeletal muscle and been linked with myotube anabolism, via mechanisms additional to AA transport (157). I hypothesize that increasing LAT1 expression will help maintain myotube BCAA levels and attenuate measures of myotube atrophy following chemotherapy (Chap. 4).
3. Males have greater skeletal muscle mass and BCAA concentrations (48). In addition, estrogen decreases BCAA breakdown in skeletal muscle of females (603). Chemotherapy will induce greater catabolism and loss of the BCAAs in male skeletal muscle and that this change would be associated with more severe cachexia (Chap. 5).
4. Estrogen has protective roles against insulin resistance (641), therefore males will experience worsened insulin tolerance following chemotherapy in young mice (Chap. 5).
5. Cachexia prevalence is greater in male cancer patients receiving chemotherapy (305). I hypothesize that aged male mice will experience greater reductions in body and muscle weight, corresponding to more severe decreases in skeletal muscle BCAA concentrations and their metabolism following chemotherapy (Chap. 6).
6. Estrogen has protective roles against insulin resistance (641). Since this hormone decreases substantially during aging in females (576), I hypothesize that insulin tolerance will not differ following chemotherapy in male and female aged mice (Chap. 6).

Chapter 4

MAINTENANCE OF THE BRANCHED-CHAIN AMINO ACID TRANSPORTER LAT1 COUNTERACTS MYOTUBE ATROPHY FOLLOWING CHEMOTHERAPY

Stephen Mora[1] , Olasunkanmi A.J. Adegoke[1]

Muscle Health Research Centre, School of Kinesiology and Health Science, York University, Toronto, ON, M3J 1P3

Corresponding Author: Dr. Olasunkanmi A.J. Adegoke

Muscle Health Research Centre, School of Kinesiology and Health Science, York University, Toronto, ON, Canada. Tel: 416-7362100 Ext 20887. Fax: 416-736- 5774. Email: oadegoke@yorku.ca

Keywords: Cachexia, Chemotherapy, Protein Synthesis, BCAA Metabolism, LAT1

Figures: 7

*A version of this has been published in *American Journal of Physiology – Cell Physiology**

Citation: Mora S, Adegoke OAJ. Maintenance of the branched-chain amino acid transporter LAT1 counteracts myotube atrophy following chemotherapy. Am J Physiol Cell Physiol. 2024 Mar 1;326(3):C866-C879.

Chapter Summary

Preventing cachexia is a critical issue in muscle wasting conditions. Although the branched-chain amino acids (BCAA) have anabolic roles in skeletal muscle, they have minimal beneficial effects on treating cachexia. The diminished effects of the BCAAs may be related to altered metabolism from chemotherapy, the most common form of cancer treatment. Since this topic is minimally studied, the purpose of this study was to investigate the effects of chemotherapy on BCAA concentrations, transporter expression and their metabolism. L6 myotubes were treated with vehicle (DMSO) or a common chemotherapy drug cocktail, folfiri (a mixture of CPT-11 (20μg/mL), leucovorin (10μg/mL), and 5-fluorouracil (5-FU, 50μg/mL)) for 24-48h. Following chemotherapy, myotube diameter (43%), myofibrillar protein content (50%) and the mTORC1 substrate $S6K1^{thr389}$ (80%) were all decreased. BCAA concentrations (52%) and expression of their transporter, LAT1 (67%) also exhibited decreases following drug treatment. Increased BCAT2 transaminase expression, but decreased PP2CM (54%) and increased phosphorylation of $BCKD^{ser293}$ (98%), corresponding with decreased BCKD enzyme activity (23%) were found following chemotherapy. Time course analyses showed that the loss of BCAA concentrations was preceded by decreases in LAT1 and BCKD activity. In drug-treated myotubes, BCAA supplementation was successful in restoring intracellular myotube BCAAs, but did not counteract atrophy. However, siRNA knockdown of NEdd4 in chemotherapy-treated myotubes counteracted the loss of LAT1, BCAA concentrations, anabolic signalling, protein synthesis and myofibrillar proteins. Our findings suggest that interventions regulating muscle amino acid transporters might represent a promising strategy to treat cachexia.

Introduction

Cancer cachexia is a devastating body and skeletal muscle wasting syndrome that contributes to poor prognosis (669), treatment outcomes (22) and reduced quality of life (19). In addition to poor nutritional status and tumour-related factors, chemotherapy is also a major contributor to the loss of skeletal muscle mass in cachexia (6–8, 18). With no available cure, development of therapeutic strategies to mitigate the loss of skeletal muscle mass in cachexia is vital in order to better manage this condition.

The branched-chain amino acids (BCAA: leucine, isoleucine and valine) regulate body weight (145), activate skeletal muscle protein synthesis (143) and have been studied in the context of muscle wasting conditions for decades (670). However, nutritional support/treatment with the BCAAs shows minimal effects on fully reversing cachexia (36–39), a finding that may be related to altered metabolism of these amino acids.

The BCAAs are transported into skeletal muscle via the L-type amino acid transporter 1 (LAT1) (26) and activate skeletal muscle protein synthesis (34), a process regulated by the mammalian/mechanistic target of rapamycin complex 1 (mTORC1). In addition to upstream activation by the insulin receptor substrate-1(IRS-1)/phosphatidylinositol-3 kinase (PI3K)/protein kinase B (AKT) pathway (25), the BCAAs also activate components in the sestrins/gator/RAG/ragulator pathway, translocating mTORC1 to the lysosomal membrane where the mTORC1 activator RHEB, is localized. Activated mTORC1 positively regulates mRNA translation initiation (28) and ribosomal biogenesis (29), while also inhibiting protein breakdown (30). In cachexia, anabolic pathways, such as mTOR and insulin-like growth factor1-AKT are downregulated (18, 31), while catabolic pathways, mainly the autophagy/lysosomal and ubiquitin proteasome pathway (UPP) are upregulated (32, 495).

During BCAA metabolism, the BCAAs are first transaminated by branched-chain aminotransferase (BCAT2) forming glutamate and the branched-chain α-keto acids (BCKA): 2-keto-isocaproate/4-methyl-2-oxopentanoic acid (KIC) from leucine, α-keto-β-methylvaleric acid/3-methyl-2-oxopentanoate (KMV) from isoleucine, and 2-keto-isovalerate/3-methyl-2-oxobutanoic acid (KIV) from valine. The BCKAs are then oxidatively decarboxylated by the branched-chain α-keto acid dehydrogenase complex (BCKD), producing their corresponding acyl CoA derivates: isovaleryl-CoA from KIC, 2-methylbutyryl-CoA from KMV, and isobutyryl-CoA from KIV, which fuel several metabolic pathways such as the TCA cycle (33).

In tumours, BCAT1/2 and BCKD are increased, leading to sustained BCAA catabolism and elevations in substrates that support tumour cell growth (40–42). However, in these tumour-inoculated animals, skeletal muscle BCAA metabolism is often overlooked. Since any alterations in skeletal muscle BCAA concentrations and their transporters may help to rationalize the diminished effectiveness of the BCAAs in treating cachexia, we present data on the effects of chemotherapy on BCAA metabolism in skeletal muscle myotubes. We then investigated whether increasing BCAA concentrations either through supplementation or by genetically manipulating the abundance of the BCAA transporter LAT1 would rescue chemotherapy-induced myotube atrophy. We hypothesized that chemotherapy, a main cause of cachexia, would decrease skeletal muscle BCAA concentrations and alter BCAA metabolism, and that interventions that maintain myotube amino acid concentrations would attenuate chemotherapy-induced myotube damage.

Materials and Methods

Reagents

Growth media (GM) was made by supplementing AMEM (Wisent Inc, #310-010-CL) with 10% fetal bovine serum (Gibco, #12483-020) and 1% antibiotic-antimycotic (Gibco, #15240-062). Differentiation medium (DM) was made by supplementing AMEM with 1% antibiotic-antimycotic and 2% horse serum (Gibco, #26050-088). Opti-MEM, reduced serum media was purchased from Gibco (#31985-062). Phosphate buffered saline (PBS) (#311-010-CL) and trypsin (#325-043-CL) were purchased from Wisent Inc. Protease inhibitor (#P8340), phosphatase inhibitor (#P5726), dimethyl sulfoxide (DMSO) (#D5879-100mL), O-phthalaldehyde (OPA) (#P1378), TCA (#196057) and chemotherapeutic agents CPT-11 (#l1406), 5-FU (#F6627-1G) and leucovorin (#F7878-500MG) were purchased from Sigma Aldrich (St. Louis, MO). Radioactive ^{14}C-L-valine (#NEC291EU050UC) was purchased from Perkin Elmer. Dithiothreitol (DTT) was purchased from Research Organics (#2190D-A101X). Triton X-100 was purchased from MP Biomedicals, LLC (#M2528).

Cell Culture and Chemotherapy Treatment

L6 skeletal muscle myoblasts (American Type Culture Collection) were thawed from -80°C, cultured in GM and incubated at 37°C and 5% CO_2. Cells were passed daily at 70-80% confluency to avoid clustering and contact inhibition. On experiment start dates, cells were counted and seeded into either 6-well ($2x10^5$) or 12-well ($1x10^5$) plates. Once cells reached 80-90% confluency, cells were shifted into DM (Day 0). The horse serum in DM, which has less proliferative factors compared to that of FBS, slows down the proliferation of myoblasts, providing the ability for myotubes to differentiate rather than proliferate (671). Fresh DM was replenished every 24 – 48h until Day 4 or 5 when experiments were performed on myotubes.

Myotubes were used to model skeletal muscle *in-vitro*, as skeletal muscle fibres are composed of myoblasts that fuse together and form multi-nucleated myotubes. Stock solutions for each chemotherapy drug were made (See Appendix A). On day 4 or 5 depending on experiment, myotubes were treated with either vehicle (1.4µL/mL DMSO) or a chemotherapy drug cocktail, folfiri (CPT-11 (20µg/mL), leucovorin (10µg/mL), and 5-FU (50µg/mL)) for 24 – 48h. Since CPT-11 and 5-FU were dissolved in DMSO, this reagent was chosen as the suitable vehicle for these experiments.

For BCAA supplementation experiments, myotubes were grown until day 4 of differentiation and were then treated with chemotherapy in DM, combined with 400µM of each of the BCAAs for 24h. After 24h, 1mL of media was collected and myotubes were re-supplemented with an additional 200uM of each of the BCAAs for the remaining 24h. Media was collected again (1mL) after 48h. All myotubes were then harvested for western blotting and HPLC analyses.

siRNA Gene Silencing

On day 3 of differentiation, myotubes were transfected with 10µM of NEdd4 (Sigma Aldrich, #NM_001008300) or scrambled (Sigma Aldrich, #SIC001) siRNA oligonucleotides with lipofectamine RNAiMAX (Thermo Fisher, #100014472) according to manufacturer's instructions. Lipofectamine, NEdd4 siRNA and scrambled siRNA were all diluted in Opti-MEM medium. Diluted siRNAs were then mixed with diluted lipofectamine reagent (1:1 ratio) and incubated for 5 min at room temperature. Two-hundred and fifty µL of the siRNA-lipid complex was added to each well of the 6-well plate, containing 1mL of antibiotic free DM. Twenty-four h after transfection, 1mL of DM was added to each well. Thirty hours following transfection, myotubes were treated for 48h with chemotherapy and harvested for western blotting and high

pressure liquid chromatography (HPLC) analyses. Full procedure is in Appendix B.

Western Blotting

After 24 and 48h of treatment, myotubes were washed in PBS and lysed (final concentration diluted in ddH_2O: 1mM ethylenediaminetetraacetic acid (EDTA), 2% sodium dodecyl sulfate (SDS), 25mM Tris-HCl pH 7.5, 10 µL/mL protease inhibitor cocktail, 10 µL/mL phosphatase inhibitor cocktail, 1mM DTT). Following lysing, the pierce Bicinchoninic acid (BCA) protein assay method (Thermo Fisher #23225) was used to determine protein concentrations. Approximately 25µg of protein extracts were then heated (80°C, 5min), vortexed, electrophoresed in 10 or 15% SDS-page gels and transferred onto polyvinylidene difluoride (PVDF, 0.2µM, BIO-RAD) membranes overnight at 4°C. The following day, ponceauS (Sigma Aldrich, #81460) staining (15min, room temperature) was used to confirm quality of transfer. Membranes were then incubated in a milk solution (5% skim milk powder in TBST for 1h, room temperature) to block non-specific antigen binding. Each membrane was then washed (3X5min in Tris-Buffered Saline + Tween 20 (TBST)) followed by overnight incubation at 4°C in primary antibody of choice:

Primary Antibody	Dilution	Company	Secondary
MHC-1	1:500	Development Hybridoma #MF 20 – s	Mouse
Tropomyosin	1:400	Development Hybridoma #CH1 – s	Mouse
Troponin	1:400	Development Hybridoma #JLT12 – s	Mouse
p-FoxO3a^{ser253}	1:1000	Cell Signalling #9466	Rabbit
p-AKT^{ser473}	1:2000	Cell Signalling #4060	Rabbit
p-S6$^{ser235/236}$	1:1000	Cell Signalling #4858	Rabbit
p-S6K1^{thr389}	1:1000	Cell Signalling #9234	Rabbit
SNAT1	1:1000	Cell Signalling #36057	Rabbit
p-BCKD^{ser293}	1:1000	Cell Signalling #40368	Rabbit
BCKD	1:1000	Cell Signalling #90198	Rabbit
NEdd4	1:1000	Cell Signalling #4013	Rabbit
AKT	1:1000	Cell Signalling #4691	Rabbit
S6K1	1:1000	Cell Signalling #9202	Rabbit

S6	1:1000	Cell Signalling #2317	Mouse
BCAT2	1:1000	Protein Tech #16417-1-AP	Rabbit
LAT1	1:500	Invitrogen #PA5-50485	Rabbit
MuRF1	1:1000	Protein Tech #55456-1-AP	Rabbit
PP2CM	1:1000	Protein Tech #14573-1-AP	Rabbit
BDK	1:1000	Invitrogen #PA5-31455	Rabbit
γ-tubulin	1:10000	Sigma Aldrich #T6557	Mouse

After overnight incubation, primary antibodies were stored, and membranes were washed (3X5min in TBST) and incubated in anti-rabbit (Cell Signalling) or anti-mouse (Cell Signalling) secondary antibody conjugated to HRP at a 1:10000 dilution for 3h. Following, membranes were washed (3X5min in TBST) and HRP chemical luminescent substrate (BioRad, #1705060S) was applied to each membrane for signal visualization by the BioRad ChemiDoc XRS+. Images were quantified using image lab software v7 (Bio-Rad).

Protein Synthesis (SuNSET Analysis)

After 48h of treatment, myotubes were starved (complete serum free media absent of any amino acids, US Biological, #R8999-03) for 24h to avoid nutrient uptake variability for protein synthesis in myotubes. After the 24h starvation, myotubes were treated with 1µM of puromycin (Sigma Aldrich, #P8833) dissolved in DM for 30 minutes. Myotubes were then lysed (as described above for western blotting) and immunoblotted against an anti-puromycin antibody (EMD Millipore, #MABE343), corrected to their respective ponceauS staining.

For SuNSET analysis in NEdd4-depleted myotubes treated with chemotherapy, following transfection, cells were treated with chemotherapy drugs for 36h. The remaining 12h of chemotherapy treatment took place in starvation media, prior to puromycin treatment and lysing.

HPLC (Amino Acid Concentrations)

After 24 and 48h of treatment, myotubes were washed (in PBS) and harvested in 250µL of 10% TCA. Cell lysates were then centrifuged (2.3g for 15 min, 4°C). Sample amino acids, in the supernatant (following centrifugation), were then diluted: 1 (sample): 2 (potassium borate

buffer): 1 (0.1N hydrochloric acid): 8 (HPLC grade water). Diluted samples were pre-column derivatized in OPA (ratio of 1:1) and samples were then injected into a YMC-Triart C18 column (C18, 1.9µm, 75 x 3.0mm; YMC America, Allentown, PA, USA) fitted onto an ultra HPLC system (Nexera X2, Shimadzu, Kyoto, Japan) connected to a fluorescence detector (Shimadzu, Kyoto, Japan; excitation: 340 nm; emission: 455 nm). Mobile phase A (20mM potassium phosphate buffer (pH 6.5)) and Mobile phase B (45% acetonitrile, 40% methanol, 15% HPLC grade water) formed a gradient solution and the amino acids were eluted at a flow rate of 0.8mL/min. A gradient made up of 5%-100% mobile phase B was run over 21 minutes. Amino acid standard curves were used to calculate amino acid concentrations and all samples were normalized to total protein. Full procedure can be found in Appendix C.

Immunofluorescence Microscopy

Myotubes were grown in 12-well plates on top of cover slips (Fisher Scientific, #092815-9). Twenty-four and 48h following chemotherapy treatment, myotubes on cover slips were fixed (4% paraformaldehyde in PBS for 10 min, room temperature, 1mL/well), permeabilized (0.03% Triton X-100 in PBS for 5 min, room temperature, 1mL/well), blocked (10% horse serum in PBS for 1h, 37°C, 400µL/well) and incubated overnight in primary antibody (2.5µg/mL of MHC-1 in 1% Bovine Serum Albumin (BSA) in PBS, 4°C, 500µL/well). After overnight incubation, all cover slips were washed (3X5min in PBS, room temperature), exposed to secondary antibody (Texas Red anti-mouse IgG secondary antibody (1:100 with 1% BSA in PBS) for 2h, room temperature, 500µL/well), stained for nuclei (4′,6-diamidino-2-phenylindole (DAPI)) and mounted on cover slides. All cover slips were imaged using the EVOS FL Auto microscope (Life technologies) and the EVOS FL Auto program was used to maintain acquisition (light and brightness) settings for each slide. Blinding took place during microscopy to avoid any treatment

bias. ImageJ was used to quantify all images by measuring the diameter of myotubes (in μm). See full procedure in Appendix D**.**

BCKD Activity Assay

At 24 and 48h following drug treatment, myotubes were incubated in ^{14}C-L-valine and the resultant CO_2 given off via BCKDs decarboxylation activity was collected on 2M NaOH soaked filter paper wicks. Valine was used as KIV, the keto acid of valine, is the preferred substrate for BCKD (33). The radiolabelled bicarbonate (formed by CO_2 mixing with NaOH on each wick) was inserted into scintillation vials (Perkin-Elmer, #6008118), containing scintillation fluid (Ecoscint A, National Diagnostics, #LS-273). Each vial containing a wick was subject to scintillation counting. To calculate BCKD activity, we divided each CPM by the amount of counts that is equal to 1μmol of the BCKD enzyme activity and corrected for total protein. See full procedure in Appendix E.

Statistical Analyses

Quantified immunoblot bands were adjusted to their corresponding gamma tubulin (loading control) values. Gamma tubulin was used as loading control as we noticed no significant effects of chemotherapy on it's abundance. All graphs were drawn and statistical analyses were performed using GraphPad prism 9 software. For figures 1 – 3, a two-way analysis of variance (ANOVA) with a tukey's post-hoc test was used to analyze vehicle and drug treatment differences at the 24 and 48h time points. For figures 4 – 6, a one-way ANOVA was used to analyze vehicle and drug treatment differences. Significance was determined $p < 0.05$. P-values were considered a trend when they were equal to or less than 0.1. All results were expressed as ±SEM of at least 3 independent experiments (biological replicates), with each independent experiment conducted with at least three technical replicates.

Results

A chemotherapy drug cocktail induces myotube atrophy, decreases protein synthesis and increases protein breakdown

Immunofluorescence detection of MHC-1 staining following chemotherapy revealed reduced myotube diameter (–43%), but no effect on nuclei (Figure 4.1A – C). Myotube atrophy coincided with decreases in the abundance of myofibrillar proteins at 48h: MHC-1 (–48%), troponin (–52%) and tropomyosin (–47%) (Figure 4.1D – G). Chemotherapy also decreased the phosphorylation of AKT^{ser473} (–56%), $S6^{ser235/236}$ (–68%) and its kinase, $S6K1^{thr389}$ at 48h (–80%), with no changes in total protein levels (Figure 4.1H – L). Protein synthesis, observed through the SUnSET analysis, was also decreased 24 and 48h following chemotherapy (Figure 4.1M). At 48h, phosphorylation of p-$FoxO3a^{ser253}$ was also decreased (–85%), coinciding with a treatment-induced increase in MuRF1 following chemotherapy (+100%; Figure 4.1N – P).

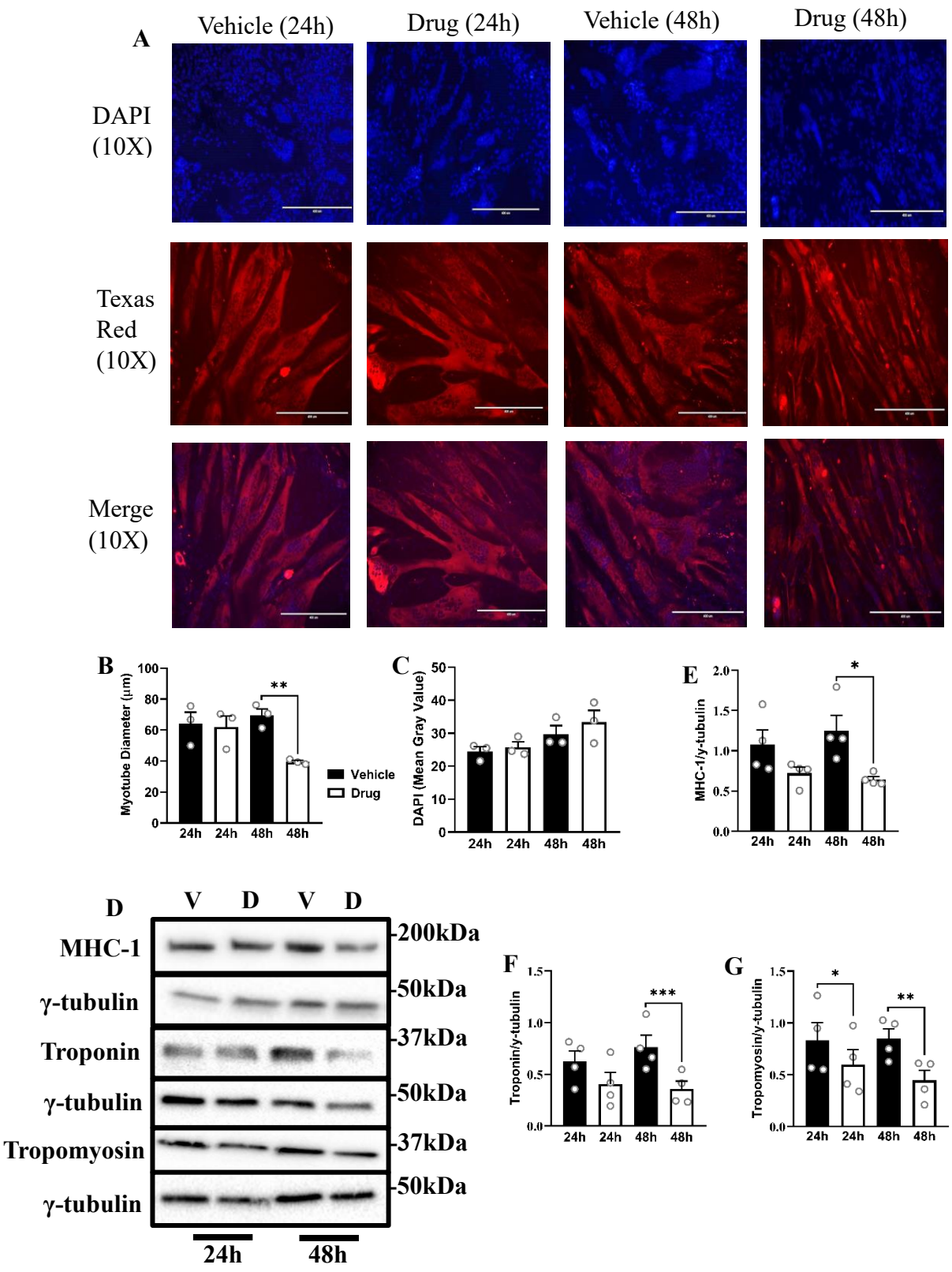
A
Vehicle (24h)
Drug (24h)
Vehicle (48h)
Drug (48h)
DAPI (10X)
Texas Red (10X)
Merge (10X)
B
Myotube Diameter (μm)
Vehicle
Drug
24h
24h
48h
48h
C
DAPI (Mean Gray Value)
E
MHC-1/γ-tubulin
D
V
D
V
D
MHC-1
γ-tubulin
Troponin
γ-tubulin
Tropomyosin
γ-tubulin
200kDa
50kDa
37kDa
50kDa
37kDa
50kDa
24h
48h
F
Troponin/γ-tubulin
G
Tropomyosin/γ-tubulin

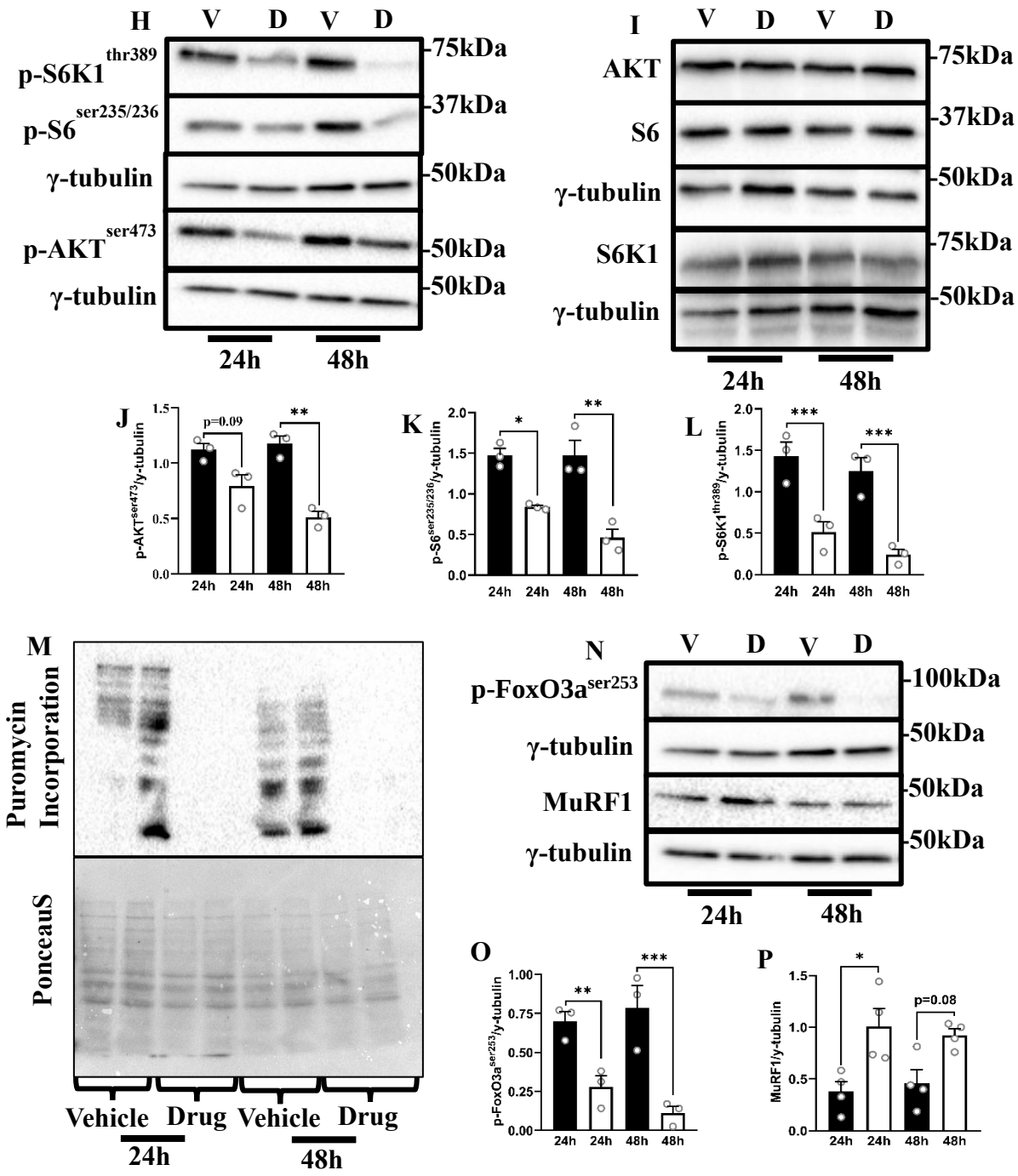

Figure 4.1 A chemotherapy drug cocktail induces myotube atrophy, decreases protein synthesis and increases protein breakdown. Myotubes were treated with differentiation medium in combination with either a chemotherapy drug cocktail (20µg/mL CPT11, 50µg/mL 5-Fluorouracil and 10µg/mL Leucovorin) or vehicle (DMSO) for 24 and 48h. **A:** Immunofluorescence detection of MHC-1 and nuclei DAPI staining (Bar, 400µM). Quantification of myotube diameter **(B)** and nuclei **(C)**. Immunoblotting **(D)** and quantified data for MHC-1 **(E)**, troponin **(F)**, tropomyosin **(G)**, as well as phosphorylated AKT^{ser473} **(H, J)**, S6$^{ser235/236}$ **(H, K)** and S6K1^{thr389} **(H, L)** and their total levels **(I)**. Protein synthesis was measured via SUnSET analysis

(M). Immunoblotting **(N)** and quantified data for phosphorylated p-FoxO3a^{ser253}**(O)** and MuRF1 **(P)**. Data are mean ± SEM, n = 3-4 independent experiments, with at least three technical replicates per experiment, *p < 0.05, **p < 0.01, ***p < 0.001. MHC-1, myosin heavy chain-1; DAPI, 4′,6-diamidino- 2- phenylindole; V, Vehicle; D, Drug; h, hours; p, phosphorylated; DMSO, dimethyl sulfoxide.

Chemotherapy decreases BCAA concentrations and their transporter expression

At 48h of treatment, chemotherapy tended to reduce myotube intracellular concentrations of leucine (–48%, p=0.08), isoleucine (–56%, p=0.07) and valine (–56%, p=0.06), but significantly reduced total BCAAs (–52%; Figure 4.2A – D). Valine concentration also tended (p=0.09) to be lower at 24h. No effects on alanine (Figure 4.2E) and serine (Figure 4.2F) were observed, but at 48h, there were decreases in the concentrations of arginine (–65%), and trends for phenylalanine (–59%, p=0.08) and glutamate (–46%, p=0.1; Figure 4.2G – I). Chemotherapy drugs also reduced the expression of amino acid transporters SNAT1 (–63%) and the BCAA transporter LAT1 at 24 (–38%) and 48h (–67%) following treatment initiation (Figure 4.2J – L).

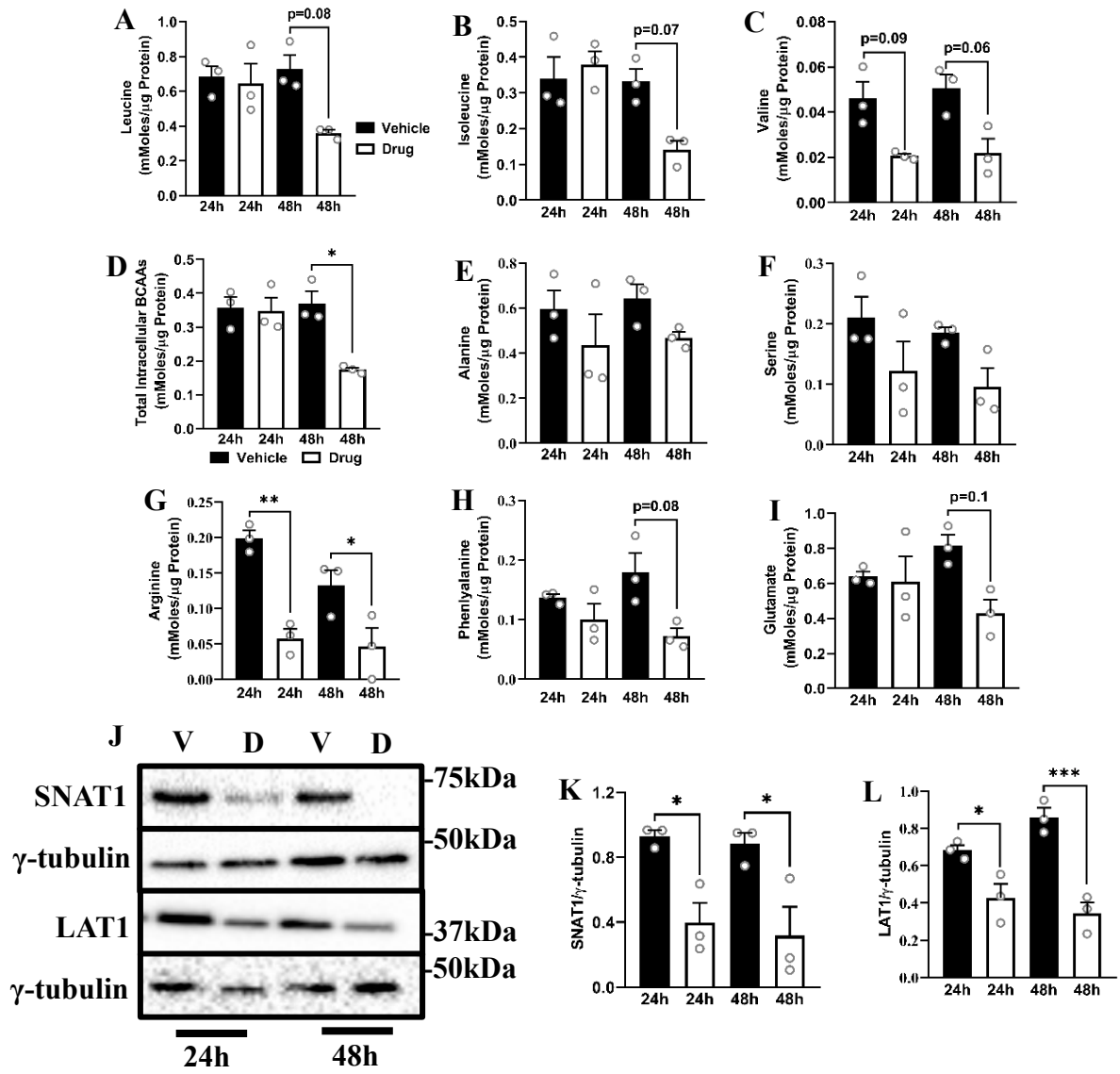

Figure 4.2 Chemotherapy decreases BCAA concentrations and their transporter expression. Myotube were treated with chemotherapy drugs as described in Figure 1. Samples were harvested and myotube concentrations of leucine **(A)**, isoleucine **(B)**, valine **(C)**, total BCAAs **(D)**, alanine **(E)**, serine **(F)**, arginine **(G)**, phenylalanine **(H)** and glutamate **(I)** were measured by HPLC. Immunoblots **(J)** and quantified data for SNAT1 **(K)** and LAT1 **(L)**. Data are mean ± SEM, n = 3 independent experiments, with at least three technical replicates per experiment, *p < 0.05, **p < 0.01, ***p < 0.001. HPLC, high-pressure liquid chromatography; V, Vehicle; D, Drug; BCAAs, branched-chain amino acids.

A chemotherapy drug cocktail reduces BCAA catabolism

Decreases in amino acid levels, especially the BCAA, intrigued us to explore BCAA catabolism. BCAT2 was significantly increased in drug-treated myotubes (Figure 4.3A, B). Total protein expression of BCKD and BDK were unchanged (Figure 4.3A, C, D), but the level of PP2CM was reduced at 48h (–54%; Figure 4.3A, E). At 48h, the inhibitory phosphorylation of BCKD^{ser293} was increased (+98%) following chemotherapy (Figure 4.3A, F). This change, along with the reduced level of PP2CM, likely contributed to the observed reduction (–23%) in BCKD enzyme activity at 48h (Figure 4.3G).

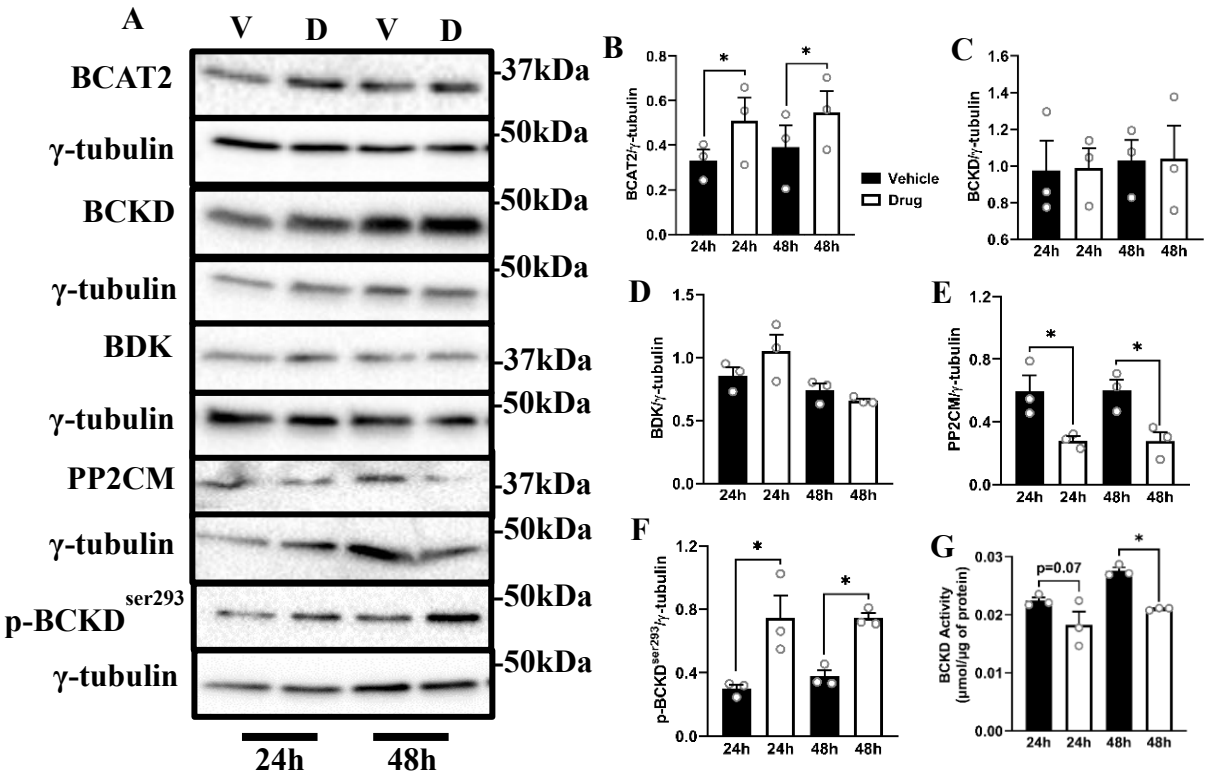

Figure 4.3 A chemotherapy drug cocktail reduces BCAA catabolism. Myotubes were treated with chemotherapy drugs as described in Figure 1. Samples were harvested and immunoblots **(A)** and quantified data for BCAT2 **(B)**, BCKD **(C)**, BDK **(D),** PP2CM **(E)** and p-BCKD^{ser293} **(F)** are shown. BCKD activity was measured from the release of $^{14}CO_2$ from ^{14}C labelled valine **(G)**. Data are mean ± SEM, n = 3 independent experiments, with at least three technical replicates per experiment, *p < 0.05. h, hours; V, Vehicle; D, Drug.

Decreases in LAT1 and BCKD activity precede BCAA loss following chemotherapy

Decreased LAT1 and BCAA concentrations could explain the reductions in BCAA catabolism. Therefore, we ran a time course experiment to address these changes. Chemotherapy decreased SNAT1 (–57%) and LAT1 (–76%) transporter expression starting at 18h (Figure 4.4A, B). However, the enzyme activity of BCKD did not start to decrease (–28%) until the 24h time point (Figure 4.4C). In addition, as a later response, leucine (Figure 4.4D) and isoleucine (Figure 4.4E) had a delayed decrease, being noticeable at 48h.

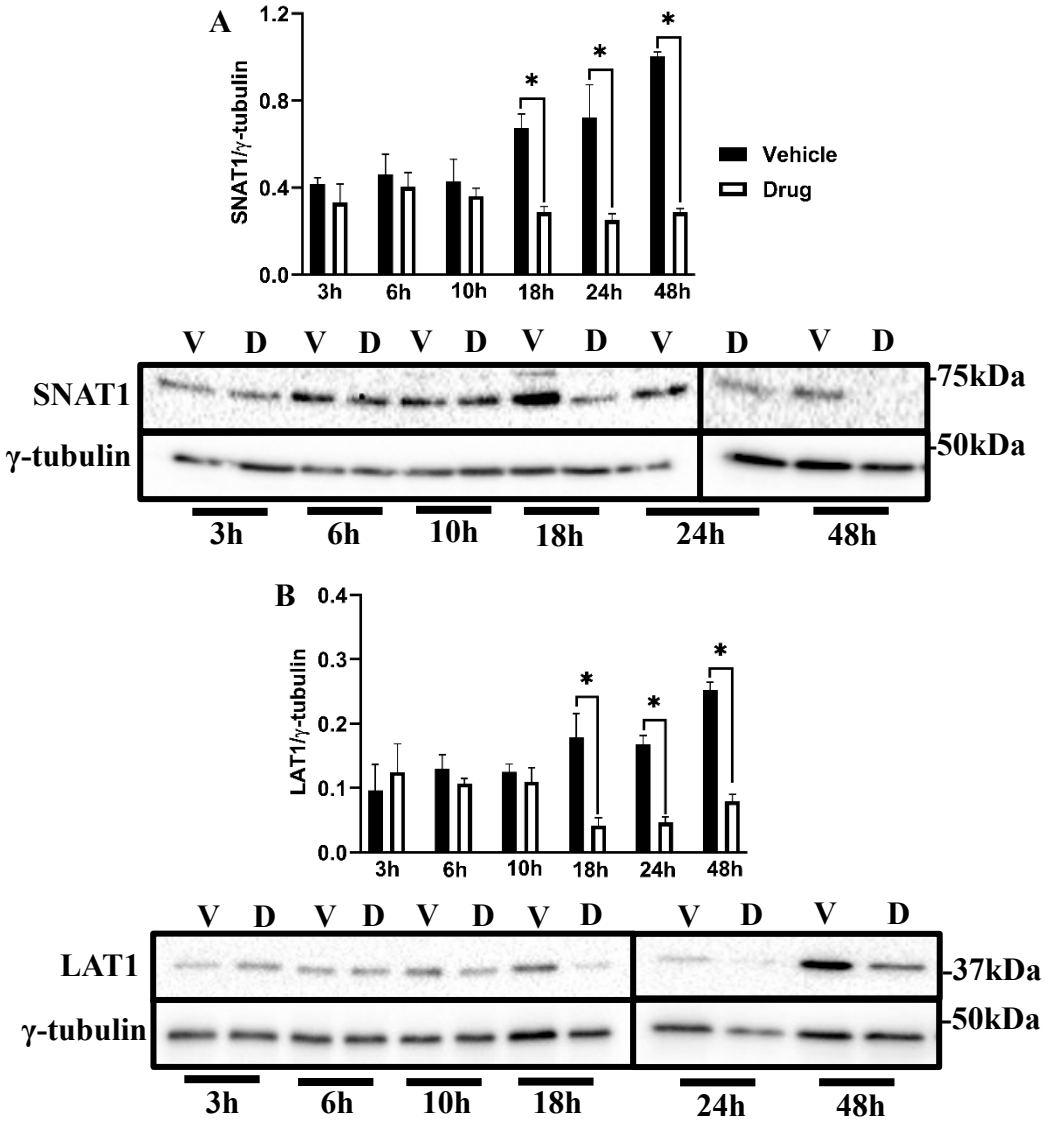

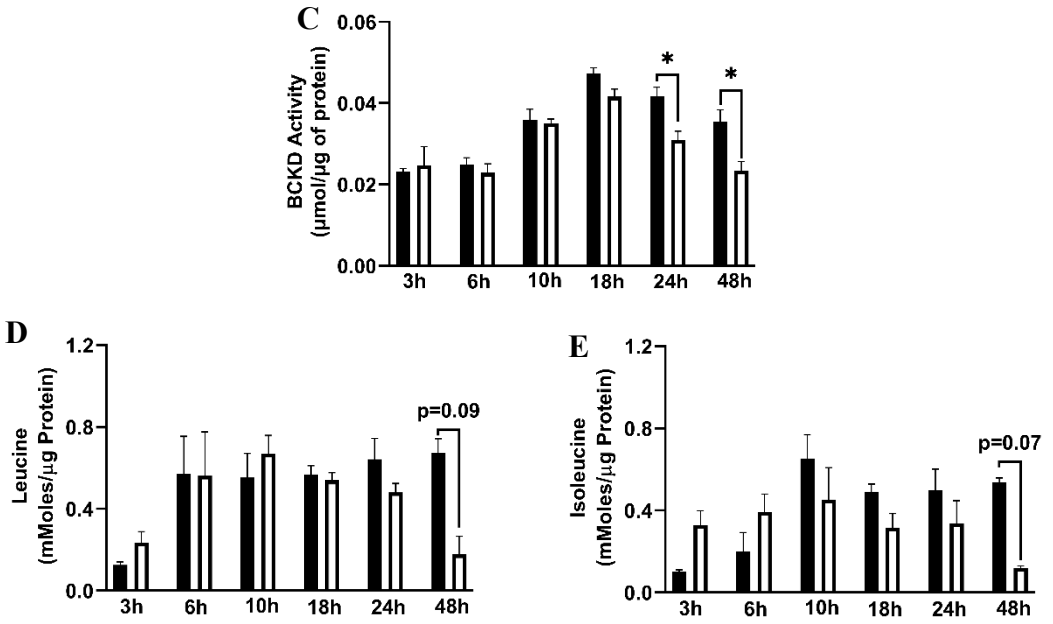

Figure 4.4 Decreases in LAT1 and BCKD activity precede BCAA loss following chemotherapy. Myotubes were treated as in Figure 1, but were harvested at 3, 6, 10, 18, 24 and 48h following the start of treatment. Immunoblots and quantified data for SNAT1 **(A)** and LAT1 **(B)**. BCKD activity **(C)** and concentrations of leucine **(D)** and isoleucine (**E)** following chemotherapy. Data are mean ± SEM, n = 3 independent experiments, with at least three technical replicates per experiment, *p < 0.05. h, hours; V, Vehicle; D, Drug.

BCAA supplementation increases myotube BCAA concentrations, but does not rescue myotube amino acid concentrations or myofibrillar protein abundance

The pattern of changes our time course revealed, made us to hypothesize that the maintenance of BCAA concentrations may help reduce atrophy following chemotherapy. Supplementation with BCAAs led to increases in their media content at 24h (Figure 4.5A – C) and returned their myotube concentrations back to their control levels, especially for leucine and isoleucine (Figure 4.5D – F), but had no effect on increasing amino acid levels or expression of their transporters (Figure 4.5G – N). In addition, increasing BCAA concentrations in drug- treated myotubes did not rescue mTORC1 signalling (Figure 4.5O – Q) or myofibrillar protein abundance (Figure 4.5R – T).

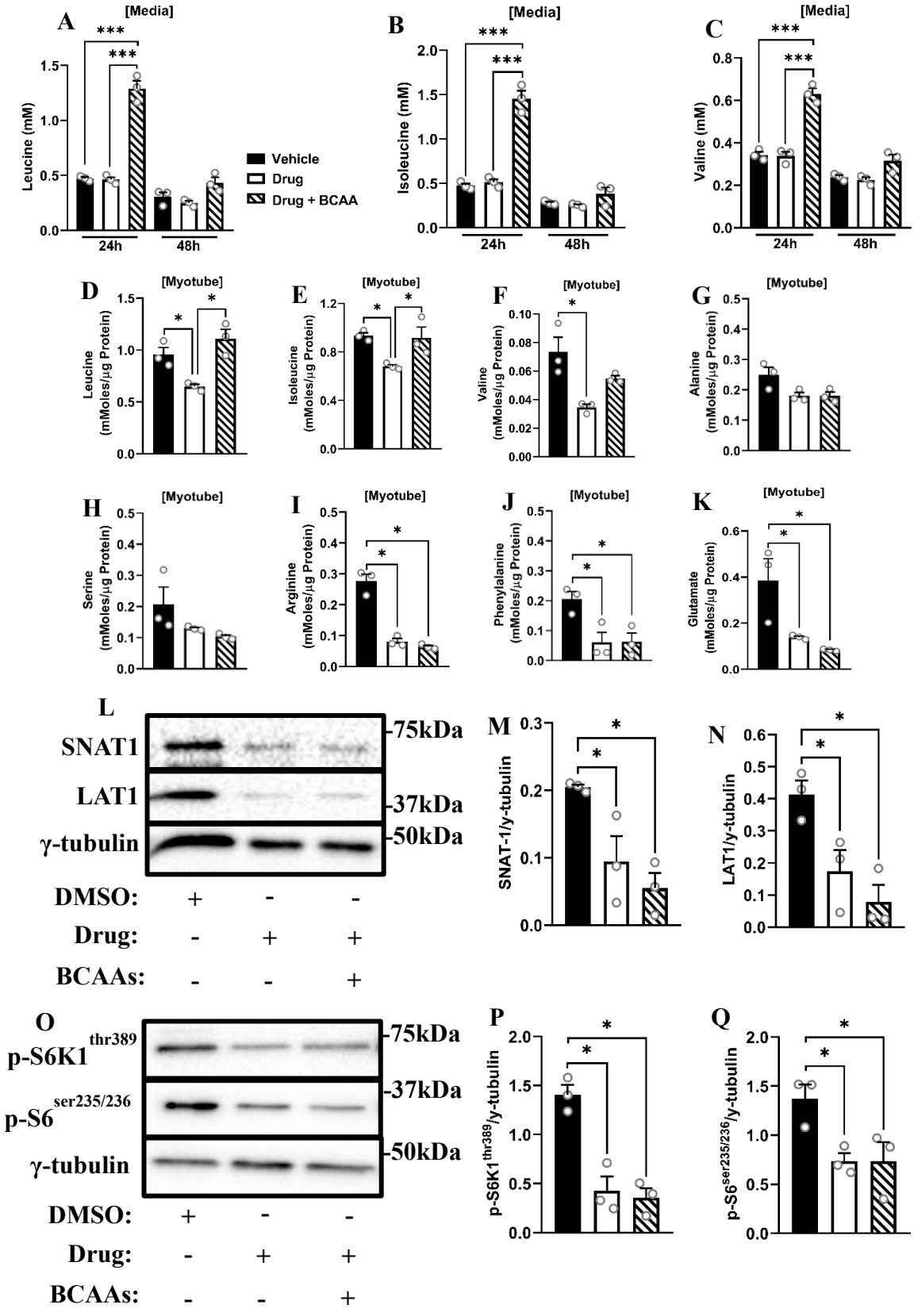
A
[Media]
Leucine (mM)
Vehicle
Drug
Drug + BCAA
24h
48h
B
[Media]
Isoleucine (mM)
C
[Media]
Valine (mM)
D
[Myotube]
Leucine (mMoles/μg Protein)
E
[Myotube]
Isoleucine (mMoles/μg Protein)
F
[Myotube]
Valine (mMoles/μg Protein)
G
[Myotube]
Alanine (mMoles/μg Protein)
H
[Myotube]
Serine (mMoles/μg Protein)
I
[Myotube]
Arginine (mMoles/μg Protein)
J
[Myotube]
Phenylalanine (mMoles/μg Protein)
K
[Myotube]
Glutamate (mMoles/μg Protein)
L
SNAT1
LAT1
γ-tubulin
75kDa
37kDa
50kDa
DMSO:
Drug:
BCAAs:
M
SNAT-1/γ-tubulin
N
LAT1/γ-tubulin
O
p-S6K1 thr389
p-S6 ser235/236
γ-tubulin
75kDa
37kDa
50kDa
DMSO:
Drug:
BCAAs:
P
p-S6K1 thr389/γ-tubulin
Q
p-S6 ser235/236/γ-tubulin

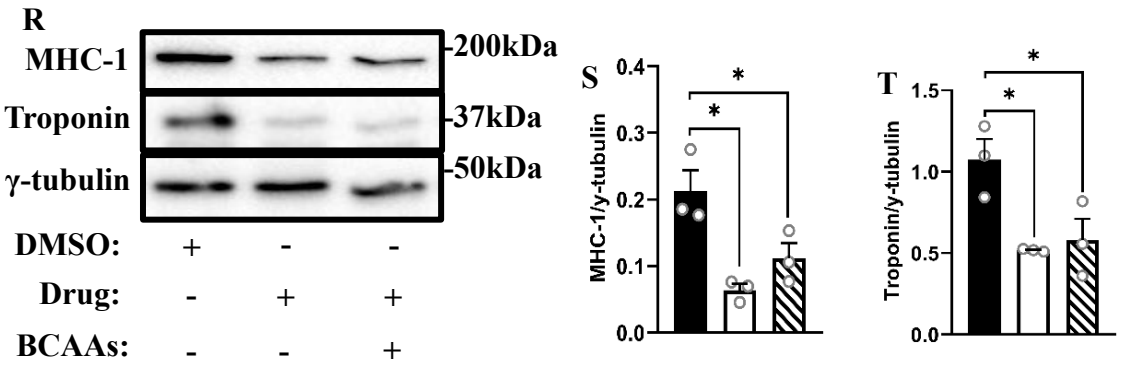

Figure 4.5 BCAA supplementation increases myotube BCAA concentrations, but does not rescue myotube amino acid concentrations or myofibrillar protein abundance. Myotubes were treated as in Figure 1, but a separate group of myotubes were treated with chemotherapy and supplemented with 400μM of the BCAAs for 24h, followed by treatment with 200μM of the BCAAs for the remaining 24h. Media concentrations of leucine **(A)**, isoleucine **(B)** and valine **(C)**, as well myotube intracellular levels of leucine **(D)**, isoleucine **(E)**, valine **(F)**, alanine **(G)**, serine **(H)**, arginine **(I)**, phenylalanine **(J)** and glutamate **(K)** were measured by HPLC. Immunoblots **(L, O, R)** and quantified data for SNAT1 **(M)**, LAT1 **(N)**, p-S6K1^{thr389} **(P)**, p-S6$^{ser235/236}$ **(Q)**, MHC-1 **(S)** and troponin **(T)** are shown. Data are mean ± SEM, n = 3 independent experiments, with at least three technical replicates per experiment, *p < 0.05, ***p < 0.001. BCAAs, branched-chain amino acids; HPLC, high-pressure liquid chromatography; h, hours; DMSO, dimethyl sulfoxide.

Prevention of LAT1 degradation counteracts myofibrillar protein abundance and BCAA loss following chemotherapy

NEdd4 is the ubiquitin protein ligase responsible for the ubiquitination of LAT1, targeting it for degradation. Therefore, we examined whether loss of NEdd4 would ameliorate the decreases in LAT1 and BCAA concentrations. We used siRNA to deplete NEdd4 (Figure 4.6A, B) and found a resulting increase in LAT1 (Figure 4.6A, C). In NEdd4 depleted myotubes treated with chemotherapy, BCAA concentrations (Figure 4.6D – F), mainly leucine and isoleucine were returned to their control levels, but the effects of chemotherapy on arginine, phenylalanine, glutamate and SNAT1 were not rescued following NEdd4 depletion (Figure 4.6G – M). Anabolic signaling (Figure 4.6N – P), protein synthesis (Figure 4.6Q), ubiquitinated proteins (Figure 4.6R, S) and myofibrillar protein content (Figure 4.6T – W) were all restored.

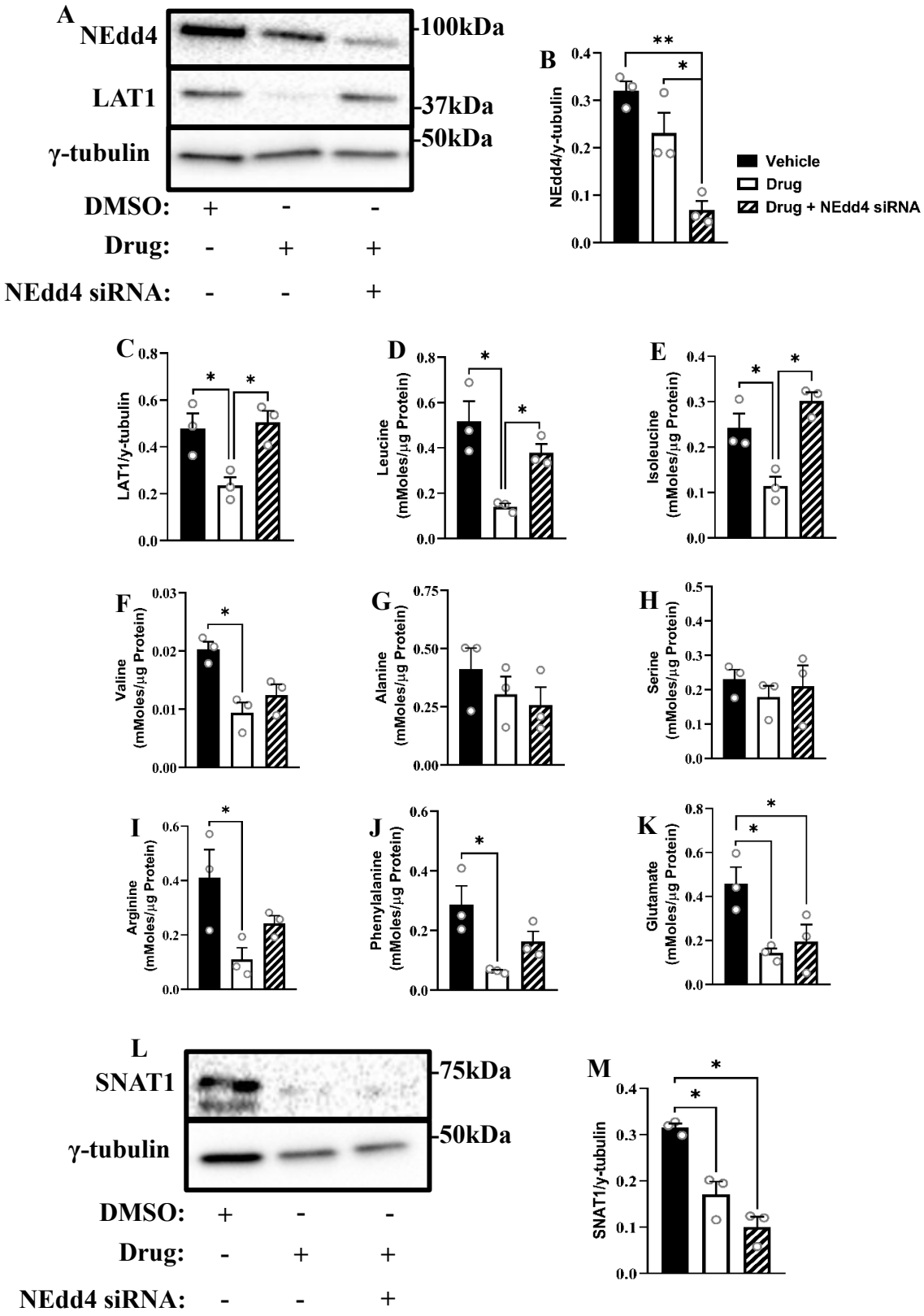
A
NEdd4
LAT1
γ-tubulin
100kDa
37kDa
50kDa
DMSO: + - -
Drug: - + +
NEdd4 siRNA: - - +
B
NEdd4/γ-tubulin
Vehicle
Drug
Drug + NEdd4 siRNA
C
LAT1/γ-tubulin
D
Leucine (mMoles/μg Protein)
E
Isoleucine (mMoles/μg Protein)
F
Valine (mMoles/μg Protein)
G
Alanine (mMoles/μg Protein)
H
Serine (mMoles/μg Protein)
I
Arginine (mMoles/μg Protein)
J
Phenylalanine (mMoles/μg Protein)
K
Glutamate (mMoles/μg Protein)
L
SNAT1
γ-tubulin
75kDa
50kDa
DMSO: + - -
Drug: - + +
NEdd4 siRNA: - - +
M
SNAT1/γ-tubulin

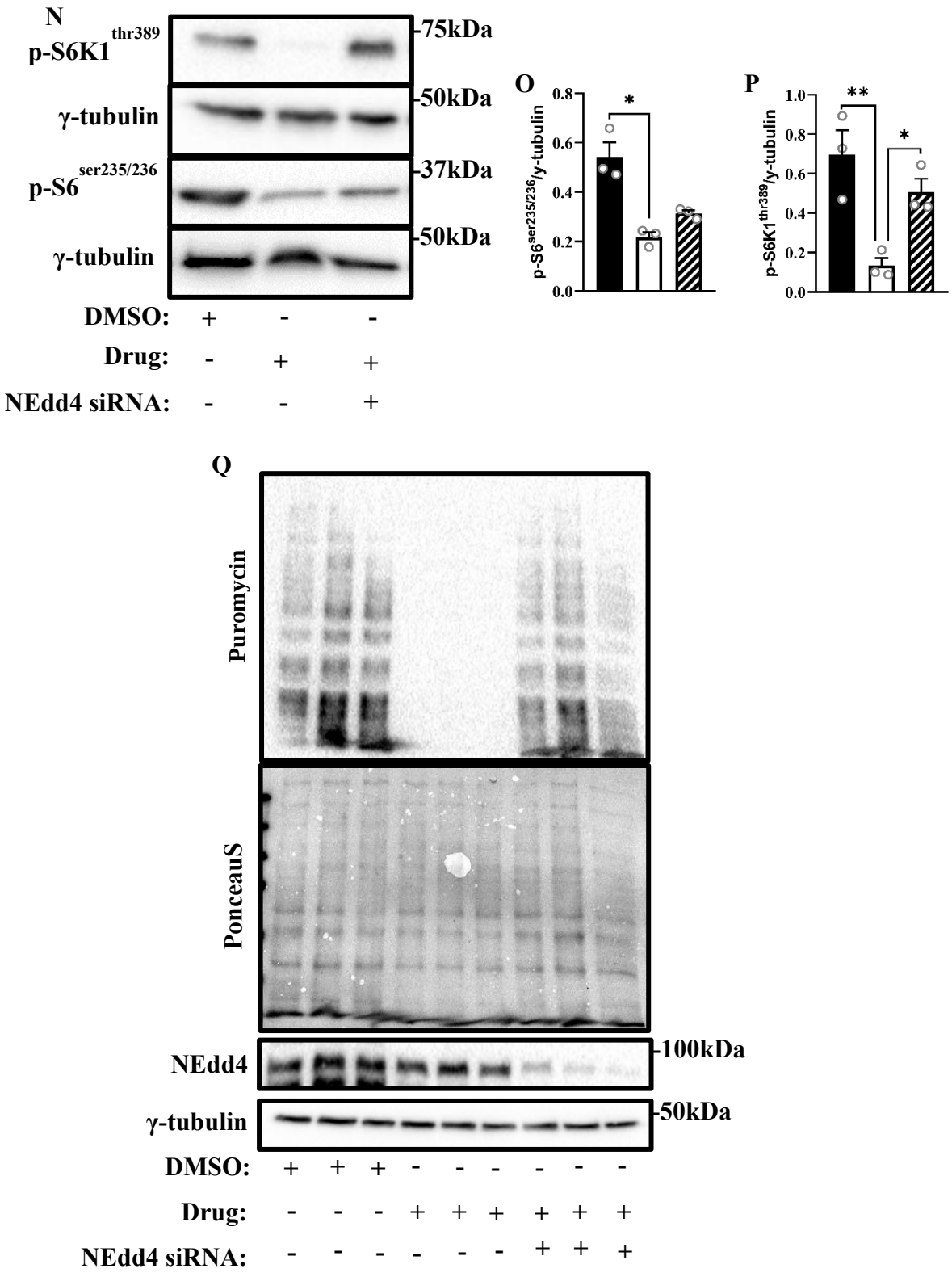
N
p-S6K1 thr389
γ-tubulin
p-S6 ser235/236
γ-tubulin
75kDa
50kDa
37kDa
50kDa
DMSO: + - -
Drug: - + +
NEdd4 siRNA: - - +
O
p-S6 ser235/236/γ-tubulin
0.0
0.2
0.4
0.6
0.8
*
P
p-S6K1 thr389/γ-tubulin
0.0
0.2
0.4
0.6
0.8
1.0
**
*
Q
Puromycin
PonceauS
NEdd4
γ-tubulin
100kDa
50kDa
DMSO: + + + - - - - - -
Drug: - - - + + + + + +
NEdd4 siRNA: - - - - - - + + +

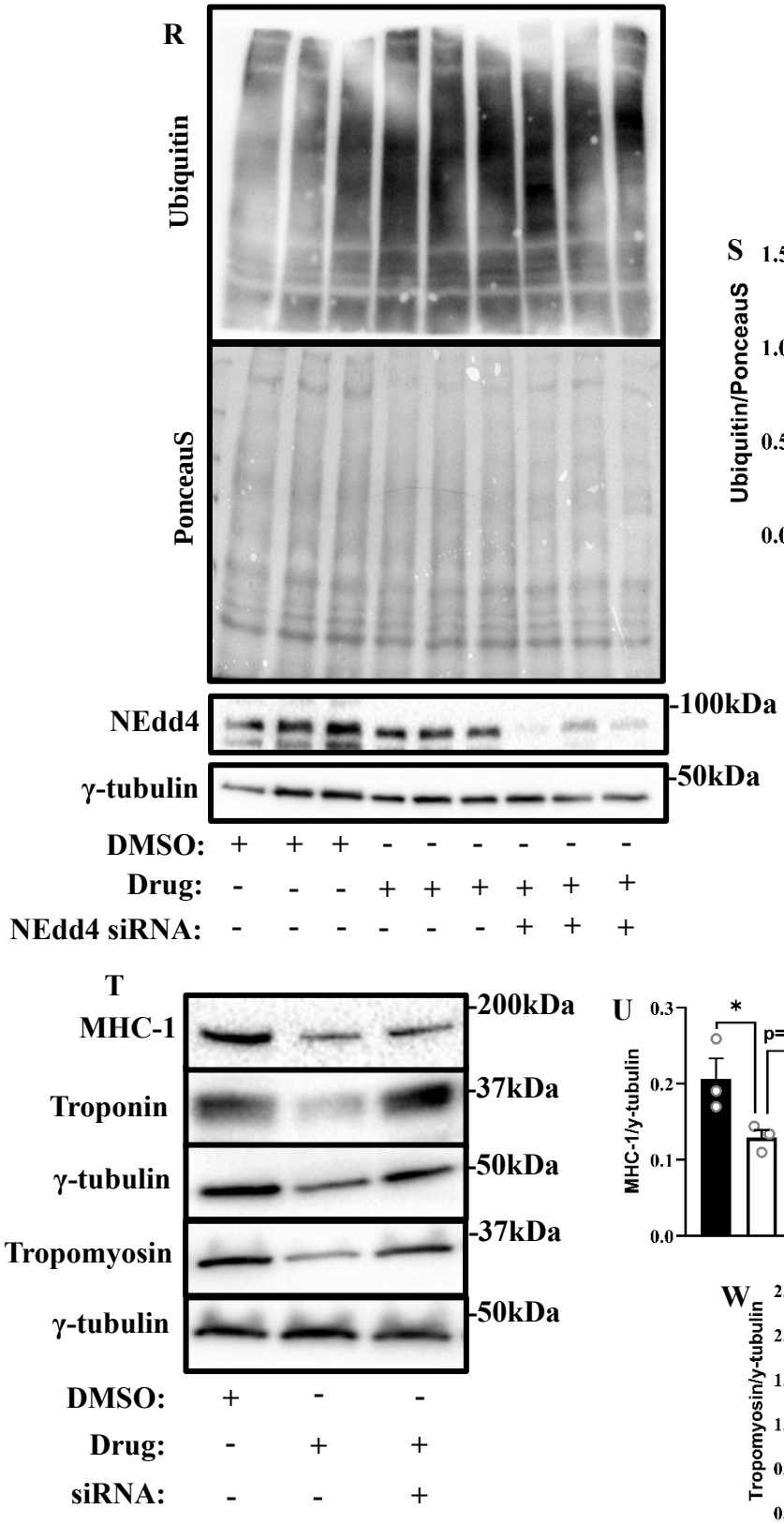
R
Ubiquitin
PonceauS
NEdd4
γ-tubulin
-100kDa
-50kDa
DMSO: + + + - - - - - -
Drug: - - - + + + + + +
NEdd4 siRNA: - - - - - - + + +
S
Ubiquitin/PonceauS
1.5
1.0
0.5
0.0
***
**
T
MHC-1
Troponin
γ-tubulin
Tropomyosin
γ-tubulin
-200kDa
-37kDa
-50kDa
-37kDa
-50kDa
DMSO: + - -
Drug: - + +
siRNA: - - +
U
MHC-1/γ-tubulin
0.3
0.2
0.1
0.0
*
p=0.1
V
Troponin/γ-tubulin
0.8
0.6
0.4
0.2
0.0
*
*
W
Tropomyosin/γ-tubulin
2.5
2.0
1.5
1.0
0.5
0.0
**
**

Figure 4.6 Prevention of LAT1 degradation counteracts myotube atrophy and BCAA loss following chemotherapy. L6 myotubes were treated with control or NEdd4 siRNA oligonucleotides for 24h, followed by treatment with the chemotherapy drug cocktail for an additional 48h. Immunoblots **(A)** and quantified data for NEdd4 **(B)** and LAT1 **(C)** in myotubes from the different treatment groups. Concentrations of leucine **(D)**, isoleucine **(E)**, valine **(F)**, alanine **(G)**, serine **(H)**, arginine **(I)**, phenylalanine **(J)** and glutamate **(K)** were measured via HPLC. Immunoblots **(L, N)** and quantified data for SNAT1 **(M)**, p-S6$^{ser235/236}$ **(O)** and p-S6K1^{thr389} **(P)**. Protein synthesis was measured via SUnSET analysis **(Q)**. Immunoblots **(R, T)** and quantified data for ubiquitinated proteins **(S)**, MHC-1 **(U)**, troponin **(V)** and tropomyosin **(W)**. Data are mean ± SEM, n = 3 independent experiments, with at least three technical replicates per experiment, *p < 0.05, **p < 0.01, ***p < 0.001. h, hours; HPLC, high-pressure liquid chromatography; DMSO, dimethyl sulfoxide.

BCAAs are positively correlated with myotube diameter, LAT1 and BCKD activity

BCAA concentrations showed positive correlations with myotube diameter (Figure 4.7A), BCKD activity (Figure 4.7B), protein expression of LAT1 (Figure 4.7C), MHC-1 (Figure 4.7D) and troponin (Figure 4.7E). We found positive correlations between LAT1 and myotube diameter (Figure 4.7F), MHC-1 expression (Figure 4.7G) and troponin expression (Figure 4.7H). A positive correlation was found between BCKD activity and myotube diameter (Figure 4.7I).

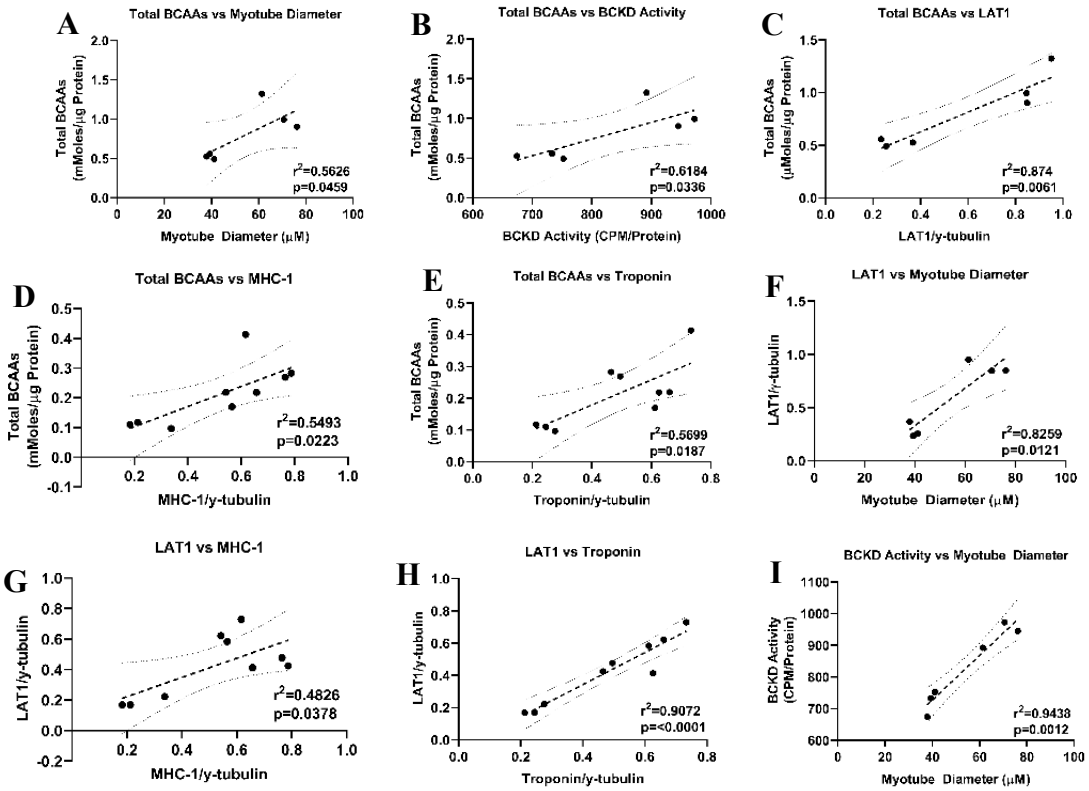

Figure 4.7. BCAA levels are positively correlated with myotube diameter, LAT1 and BCKD activity. Correlations between total intracellular BCAAs and myotube diameter **(A)**, BCKD activity **(B)**, protein expression of LAT1 **(C)**, MHC-1 **(D)**, and troponin **(E)**. Correlations between LAT1 and myotube diameter **(F)**, MHC-1 **(G)**, and troponin **(H)**. BCKD activity and myotube diameter correlation **(I)**. Data were analyzed using linear regression and 95% confidence intervals are denoted. BCAAs, branched-chain amino acids; MHC-1, myosin heavy chain-1.

Discussion

We show that administration of chemotherapeutic agents to skeletal muscle myotubes causes atrophy and decreases in BCAA concentrations, as well as reduced expression of the amino acid transporters LAT1 and SNAT1. These changes occurred in parallel to altered expression of key enzymes involved in BCAA catabolism, leading to decreased BCKD activity, the rate-limiting enzyme in BCAA metabolism. Importantly, we showed that maintaining LAT1 attenuates the loss of BCAAs, myofibrillar proteins, protein synthesis and anabolic signalling following chemotherapy.

The effects of the chemotherapy drug cocktail on decreasing myotube diameter and myofibrillar content were expected, as previous studies have reported similar findings (415–417). However, the fact that myotube diameter was not affected until 48h, but anabolic signalling and protein synthesis were decreased as early as 24h, suggests, as least in part, that the loss of anabolic processes may precede myotube atrophy. In terms of protein synthesis, we were surprised to see no effect of the chemotherapy drugs on total levels of AKT, S6K1 and S6, especially since we saw next to zero puromycin incorporation in drug-treated myotubes. However, this finding is similar to a previous study whereby severely decreased protein synthesis following chemotherapy treatment in myotubes also had no effect on total protein levels (416).

Studies investigating the effects of the BCAAs often focus on the anabolic properties of these amino acids, as anabolism is their primary role (34). However, the BCAAs serve a number of other roles in the body such as: yielding keto acids (33), beta-hydroxy-beta-methylbutyrate (HMB, from leucine) (672) and glutamine (673). Therefore, altered metabolism of the BCAAs following chemotherapy, a topic that has received very little attention in the skeletal muscle, may help explain the inability for these amino acids to successfully reverse cachexia.

A main finding of our work is that BCAA supplementation in chemotherapy-treated myotubes restored intracellular BCAA levels, but did not rescue atrophy. Of note, although we supplemented the media with 400μM of BCAAs, these increases do not match what we saw intracellularly, as not all the BCAAs that we supplemented are going to be absorbed. In addition, the y-axis units are different as intracellular BCAA levels are expressed as a fraction of total protein, while plasma is expressed as μM in the media. The inability for BCAAs to rescue atrophy is in line with inefficacy of BCAA/protein supplementation to fully reverse cachexia (38, 39). However, the fact that supplementation with the BCAAs did not attenuate LAT1 expression, but were still able to increase intracellular BCAAs, suggests that maybe the activity of LAT1 is a rate limiting step in the transport of BCAAs into the cell. It is also possible that other kinases, such as general control nonderepressible 2, which plays a role in inhibiting global protein synthesis during amino acid deficiency (674), may also play a role in decreased protein synthesis during chemotherapy, however, we did not investigate this phenomenon. Since a previous overexpression of LAT1 was unable to increase intracellular AA concentrations (675), we used RNAi to deplete NEdd4, the ubiquitin protein ligase that targets LAT1 for proteasomal degradation (676). However, the fact that increasing LAT1 (which only transports select amino acids), was more effective in attenuating myotube atrophy compared to simply the addition of BCAAs, underlies the significance of the BCAAs and LAT1 in myotube anabolism. In further support of this point, the transport rate and expression of LAT1 can be controlled by intracellular amino acids, as intracellular (compared to extracellular) amino acids having a higher affinity for LAT1 (154, 677). We also showed strong and significant positive correlations between LAT1, myotube diameter and BCAA concentrations. Thus, LAT1 may play roles in myotube anabolism by mechanisms additional to facilitating the transport of its cognate amino acids (678, 679).

BCAT2 is responsible for removing the amino group from the BCAAs, forming glutamate and the BCKAs (33). We observed higher BCAT2 expression and lower glutamate concentrations in drug-treated myotubes, suggesting that BCAT2 is removing and transferring the amino group from glutamate back to the BCKAs, attempting to regenerate the BCAAs. Inhibited BCKD and reductions in this enzyme's activity further support our finding, as the BCKAs cannot undergo further decarboxylation. Therefore, our findings on the effects of chemotherapy on BCAA catabolism suggest a compensatory mechanism, whereby the BCKAs build up and give BCAT2 a chance to replenish the BCAA pool.

Ordinarily, reductions in protein synthesis and increases in protein breakdown would result in increased intracellular BCAAs and amino acids, however we saw decreases. For the BCAAs, these amino acids cannot be made in the skeletal muscle, therefore, there decreases can be explained by decreased transport. We found no differences for alanine, serine or phenylalanine, therefore, we provide reasoning as to why arginine and glutamate were decreased. Since glutamate can be metabolized into glutamine in the skeletal muscle and increase antioxidant capacity (680), a decrease in this amino acid suggests a reduction in the ability for myotubes to handle reactive oxygen species generated from chemotherapy (425). Decreased arginine concentrations could be related to the fact that arginine can be converted to glucose and catabolized to produce energy during chemotherapy (681)(682), therefore, reductions in intracellular arginine levels may worsen glucose homeostasis following chemotherapy.

Aside from just BCAA concentrations, it is also important to consider other factors that may be playing a role in chemotherapy-induced myotube atrophy and changes in BCAA catabolism that we observed. For example, chemotherapy reduces peroxisome proliferator-activated receptor-gamma coactivator (PGC-1α) in skeletal muscle (425), a transcriptional

activator that can increase BCAT2 and BCKD (683). Krueppel-like factor 15 (KLF15) has also been seen to increase BCAT2 and reduce BCAA concentrations under BCAA-starved conditions (684), however the direct effects of chemotherapy on KLF15 have not been reported. Chemotherapy has also been seen to increase myostatin expression, a factor involved in negative regulation of muscle mass (265). Inhibition of myostatin prevented chemotherapy-induced myotube atrophy, but the effects of myostatin on BCAA metabolism were not reported (8).

A main limitation of our current study is that although NEdd4 depletion resulted in an increase in LAT1 with a concomitant increase in BCAA intracellular levels, we can not rule out the contributions of the other substrates of NEdd4 to the observed benefits of NEdd4 depletion on protein synthesis. Therefore, other substrates that are ubiquitinated by NEdd4, such as phosphatase and tensin homolog (PTEN), AKT and RNA polymerase 2 (685) may also cause the observed benefits that we observed on protein synthesis. PTEN and AKT are two important substrates involved in the propagation of insulin signalling that leads to the activation of mTORC1. Less ubiquitination and breakdown of these substrates suggests hyperactivation of mTORC1, which could account for the increased protein synthesis. In addition, less degradation of RNA polymerase 2, an indispensable kinase involved in DNA transcription (686), also supports more protein synthesis. Another limitation is that we cannot fully rule out is that some of our findings may be related to the effect of chemotherapy on myoblasts, especially since myoblasts are known to express LAT1 (687). Therefore, we ensured that our myotubes were fully differentiated prior to treatment and blotted for proteins such as MHC-1, troponin and tropomyosin that only appear in myotubes. Since this is an *in-vitro* model, we are unable to investigate the contributions of other tissues, including adipose tissue and liver to the altered BCAA catabolism. Therefore, *in-vivo* studies investigating the effects of cancer and

chemotherapy on similar measures as in our study are warranted. Nonetheless, by using a clinically relevant chemotherapy cocktail (216), this *in-vitro* model allows us to explore the direct mechanistic effects of chemotherapy on skeletal muscle cell atrophy and amino acid metabolism. Lastly, in some cases, double bands (for example SNAT1 in figure 4.5/4.6 and NEdd4 in 4.6) are seen in blotting, but only for scrambled conditions. We are not sure why this phenomenon occurred, but may due to off target background binding of the antibodies.

In this study, we demonstrated profound negative effects of chemotherapy on the concentrations, metabolism and transporter expression of the BCAAs in myotubes. However, using RNA interference against NEdd4 to prevent the decline in LAT1 expression rescued the atrophy phenotype, including improvements in anabolic signalling, protein synthesis and myofibrillar protein abundance. While these findings suggest that interventions that preserve LAT1 have therapeutic potential in cancer cachexia, they would need to be replicated in pre-clinical models and LAT1 manipulation would need to be done in tissue- (skeletal muscle) specific manner because whole body increases in LAT1 expression might have undesirable consequences in other tissues, especially in cancer cells (26).

Author Contributions

SM and OAJA designed the experiments. SM performed the experiments. SM analyzed the samples and drafted the initial version of the manuscript. OAJA reviewed and edited the manuscript. Both SM and OAJA approve the final version of the manuscript.

Conflict of Interest

The authors declare no conflict of interest.

Acknowledgements

This study was funded by grants from the Natural Science and Engineering Research Council of Canada (NSERC) and from the Faculty of Health, York University, Toronto Canada to OAJA. Thank you to the Muscle Health Research Centre at York University for use of the HPLC and to Dr. Paluzzi for the use of their imaging systems.

Funding

Work is supported by funds from the Natural Science and Engineering Research Council of Canada by the Faculty of Health, York University.

Chapter 5

SEX DIFFERENCES IN CACHEXIA AND BRANCHED-CHAIN AMINO ACID METABOLISM FOLLOWING CHEMOTHERAPY IN YOUNG ANIMALS

Stephen Mora[1], Gagandeep Mann Olasunkanmi A.J. Adegoke[1]

Muscle Health Research Centre, School of Kinesiology and Health Science, York University, Toronto, ON, M3J 1P3

Corresponding Author: Dr. Olasunkanmi A.J. Adegoke

Muscle Health Research Centre, School of Kinesiology and Health Science, York University, Toronto, ON, Canada. Tel: 416-7362100 Ext 20887. Fax: 416-736- 5774. Email: oadegoke@yorku.ca

Keywords: Cachexia, Chemotherapy, Protein Synthesis, BCAA Metabolism, Sex

Figures: 6

*A version of this has been accepted in *Physiological Reports* – Currently in Press*

Chapter Summary

Cachexia is a body wasting syndrome that affects 25-80% of cancer patients. Chemotherapy is reported as a major contributor to cachexia, but studies investigate mainly male animals. Although the branched-chain amino acids (BCAA: leucine, isoleucine and valine) have anabolic roles in skeletal muscle, BCAA nutritional support does not fully reverse cachexia and this may be related to their altered metabolism during chemotherapy. Our study examines sex differences in cachexia outcomes and BCAA metabolism following chemotherapy. Ten-12-week-old CD2F1 male and female mice were treated with either the chemotherapy drug cocktail folfiri (50mg/kg 5-FU, 90mg/kg Leucovorin and 24mg/kg CPT-11) (drug) or vehicle (10% DMSO in saline) for 6-weeks. Insulin tolerance tests were conducted during treatment and BCAA levels and their metabolism were measured in plasma and tissues. In both sexes, body weight, skeletal muscle weight and anabolic signalling were reduced following chemotherapy. Worsened outcomes for body weight (male: –15%, female: –25%, $p < 0.05$) , gastrocnemius weight (male: –17%, female: –23%, $p < 0.05$) and p-S6K1^{thr389} (male: –36%, female: –61%, $p < 0.05$) were found in female drug-treated mice. While only male drug-treated animals showed elevated plasma BCAAs, the drug cocktail reduced BCAA concentrations in the skeletal muscle of both sexes; this reduction was more severe in males (male: –70%, female: –33%, $p < 0.05$). LAT1, the BCAA transporter, was also reduced following drug treatment in both sexes, a reduction that was more severe in females (male: –40%, female: –50%, $p < 0.05$). Minimal differences were found for key enzymes involved in BCAA metabolism following chemotherapy. However, the activity of the BCKD enzyme was decreased following chemotherapy in both sexes. In the liver, BCAA concentrations and their transporter were both increased regardless of sex. Lastly, positive correlations were observed between muscle weight and LAT1 ($r^2=0.39$ $p=0.0008$) and BCKD activity ($r^2=0.34$,

p=0015). Our study demonstrates sex- and tissue-specific differences following chemotherapy-induced cachexia in mice. We suggest that sex needs to be a major consideration when developing interventions that can correct/manage cachexia, as altered availability and metabolism of the BCAAs may contribute to muscle wasting dependent on sex.

Introduction

Affecting 20-80% of cancer patients dependent on cancer stage and type is cachexia, a devastating body and skeletal muscle wasting syndrome (688). Systemic inflammation, insulin resistance, increases in energy expenditure, negative protein/energy balance, appetite loss, anorexia and fatigue are all experienced in cachexia (62). Chemotherapy is also major contributor to skeletal muscle loss and cachexia (6–8).

During cachexia, autophagy/lysosomal and the ubiquitin proteasome pathway (UPP), two of the main pathways implicated in skeletal muscle protein breakdown (32), are severely upregulated leading to muscle wasting (495). Muscle protein synthesis is regulated by the mammalian/mechanistic target of rapamycin complex 1 (mTORC1). Upstream, mTORC1 is activated through the insulin receptor substrate-1(IRS-1)/phosphatidylinositol-3 kinase (PI3K)/protein kinase B (AKT) pathway which allows RHEB, an mTORC1 activator, to stay GTP loaded. mTORC1 sensing of amino acids (AA) and especially the branched-chain amino acids (BCAA: leucine, isoleucine, and valine) is also required for full activation (25). Activation of components in the sestrins/gator/RAG/ragulator pathway by AAs and BCAAs leads to the translocation of mTORC1 to the lysosomal membrane where RHEB is localized (27). Once activated, mTORC1 phosphorylates several downstream targets, such as ribosomal protein S6 kinase beta-1 (S6K1) and eukaryotic translation initiation factor 4E-binding protein 1 (4E-BP1) leading to protein synthesis (25). Due to this, the BCAAs are potent stimulators of skeletal muscle protein synthesis and represent a promising target to treat cachexia, as the BCAAs have shown some positive effects on reversing cancer-induced cachexia (36, 337). However, nutritional interventions using the BCAAs to mitigate cachexia have yielded minimal and inconsistent benefits (38, 39).

Apart from activating protein synthesis, the BCAAs can also be metabolized in the

skeletal muscle and other organs/tissues, including the liver and adipose tissue. Branched-chain aminotransferase (BCAT2) reversibly transaminates the BCAAs into their respective branched-chain α-keto acids (BCKA) and glutamate. The branched-chain α-keto acid dehydrogenase complex (BCKD) then oxidatively decarboxylates the BCKAs producing their corresponding acylCoA derivates: isovaleryl-CoA from KIC, 2-methylbutyryl-CoA from KMV, and isobutyryl-CoA from KIV (33). Although it is known that enzymes involved in the metabolism of these BCAAs are increased in some cancers (40, 41), the impact of cancer and/or chemotherapy on the metabolism of the BCAAs in skeletal muscle is rarely studied. Therefore, exploring BCAA metabolism in the skeletal muscle following chemotherapy may provide a rationale to help explain the inability for BCAAs to successfully treat cachexia.

Although sex is a major risk factor for cancer, many of the previous studies on chemotherapy-induced cachexia are conducted in male animals (6, 8, 18). However, there is evidence for sex differences in BCAA metabolism. Compared to females, males have higher concentrations of the BCAAs (48) and greater leucine oxidation after endurance exercise (49). Further, estrogen has been shown to decrease BCKD activity, but this study only investigated female animals (603). Here, we hypothesized that chemotherapy would induce greater catabolism of BCAAs in tissues of male mice, and that this change would be associated with more severe cachexia.

Materials and Methods

Ethics Statement

All animal experiments were approved by the York University Animal Care Committee in accordance with the recommendations of the Canadian Council on Animal Care and the requirements of the Government of Ontario's Animal Research Act (1980).

Reagents

Protease inhibitor (#P8340), phosphatase inhibitor (#P5726), dimethyl sulfoxide (DMSO) (#D5879-100ML), O-phthalaldehyde (OPA) (#P1378), puromycin (#P8833), leupeptin (#L2884), CoA (#C4282), NAD+ (#N0632), thiamine (#T1270) and our chemotherapy drugs, CPT-11 (#I1406), 5-FU (#F6627) and leucovorin (#F7878) were purchased from Sigma Aldrich (St. Louis, MO). Insulin was purchased from Shoppers Drugmart (Humulin R, #DIN00586714). Radioactive ^{14}C-L-valine (#NEC291EU050UC) was purchased from Perkin Elmer, DTT from Research Organics (#2190D-A101X), FBS from Gibco (#12483-020), Triton X-100 from MP Biomedicals (#M2528) and HEPES from BioShop (#HEP001). PBS was purchased from Wisent (#311-010-CL).

Animals

Fourteen male and 14 female 8-week-old CD2F1 mice were purchased from Charles River Laboratories and Envigo. Mice were acclimatized, housed in the vivarium and given free access to food and water until 10-weeks of age. For females, estrous tracking occurred 1-week prior to the beginning of treatment and experiments were conducted during di-estrous. Tracking was completed by following a step-by-step procedure outlined in Appendix F and outlined by Byers et al (689). Mice were separated into four groups: male vehicle, male drug, female vehicle, female drug (n=7 for all groups). Mice were administered intraperitoneally (i.p) either the chemotherapy drug cocktail folfiri (50mg/kg 5-FU, 90mg/kg Leucovorin and 24mg/kg CPT-11)

(drug) or vehicle (10% DMSO in saline) for 6-weeks. Dosing calculations are shown in Appendix A. Our drug dosages were taken from a previous study (18). Animal body weight and food consumption were recorded daily. An example of our daily logs is shown in Appendix G. At the end of the study, animals were euthanized via cervical dislocation. Following sacrifice, several skeletal muscles and other tissues were collected, weighed, flash-frozen and stored at -80°C until further analysis.

Insulin Tolerance Testing

At both 3 and 6 weeks of treatment, insulin tolerance tests (ITT) were performed in all animals. After fasting for 6 hours, insulin (0.75units/kg) was administered via subcutaneous injection and blood glucose concentrations were collected on glucose strips (Alpha TRAK, #71681) using a glucometer (AlphaTRAK Blood Glucose Monitoring System, #71675-01) from the saphenous vein at 0, 5, 15, 30 and 120 minutes. Following each ITT, mice were rehydrated with a 750µL intraperitoneal injection of saline.

BCKD Activity Assay

Frozen gastrocnemius muscles or livers were crushed in liquid nitrogen and homogenized (Bio-Gen PRO200 Homogenizer) in 250µL of ice-cold buffer 1 (30mM KPI, 3mM EDTA, 5mM DTT, 1mM valine, 3% FBS, 5% Triton X-100, 1µm leupeptin). The resulting sample was centrifuged (10minutes at 10,000g, 4°C) and 50uL of the supernatant was added to 300uL of buffer 2 (50mM HEPES, 30mM KPI, 0.4mM CoA, 3mM NAD+, 5% FBS, 2mM Thiamine, 2mM magnesium chloride and 7.8µM [^{14}C]valine). Valine was used as KIV, the keto acid of valine, is the preferred substrate for BCKD (33). This reaction took place in a 1.5mL eppendorf tube containing a raised 2M NAOH CO_2 wick trap. Each eppendorf tube was capped and sealed tight using tape, before being place in a non-shaking incubator at 37°C for 30minutes. The

radiolabeled $^{14}CO_2$ contained in the wick trap was counted in a liquid scintillation counter. To calculate BCKD activity, we divided each CPM by the amount of counts that is equal to 1µmol of the BCKD enzyme activity and corrected for total protein. A more detailed procedure is shown in Appendix H.

Western Blotting

Approximately 30-200mg of gastrocnemius muscle or liver tissue was weighed out and homogenized in 7X complete buffer: 20mM HEPES, 2mM EGTA, 50mM NaF, 100mM KCI, 0.2mM EDTA, 50mM B-Glycerospahte. This buffer was completed with protease inhibitor (10µL/mL), phosphatase inhibitor (10µL/mL), sodium vanadate (2.5µL/mL), DTT (1µL/mL) and benzamidine (5µL/mL). Homogenized samples were then centrifuged (1000g for 3 minutes, 4°C), and the resulting supernatant was centrifuged again (10000g for 30minutes, 4°C). Protein concentration was determined using the Pierce BCA Protein Assay Kit (Thermo Scientific #23225). Approximately 25µg of protein was then loaded and electrophoreses in 10 or 15% SDS-page gels. Gels were transferred overnight onto PVDF (0.2µM, BIO-RAD) membranes and quality of transfer was measured via ponceauS staining. Membranes were then incubated in milk to block non-specific antigen binding. Each membrane then underwent a 3x5 minute wash in TBST followed by overnight incubation at 4°C in the primary antibody of interest:

Primary Antibody	Dilution	Company	Secondary
MHC-1	1:500	Development Hybridoma #MF 20 – s	Mouse
Tropomyosin	1:400	Development Hybridoma #CH1 – s	Mouse
Troponin	1:400	Development Hybridoma #JLT12 – s	Mouse
p-FoxO3a^{ser253}	1:1000	Cell Signalling #9466	Rabbit
p-AKT^{ser473}	1:2000	Cell Signalling #4060	Rabbit
p-S6$^{ser235/236}$	1:1000	Cell Signalling #4858	Rabbit
p-S6K1^{thr389}	1:1000	Cell Signalling #9234	Rabbit
SNAT1	1:1000	Cell Signalling #36057	Rabbit
p-BCKD^{ser293}	1:1000	Cell Signalling #40368	Rabbit
BCKD	1:1000	Cell Signalling #90198	Rabbit

p-4E-BP1$^{thr37/46}$	1:1000	Cell Signalling #2855	Rabbit
AKT	1:1000	Cell Signalling #4691	Rabbit
S6K1	1:1000	Cell Signalling #9202	Rabbit
S6	1:1000	Cell Signalling #2317	Mouse
4E-BP1	1:1000	Cell Signalling #9644	Rabbit
BCAT2	1:1000	Protein Tech #16417-1-AP	Rabbit
LAT1	1:500	Invitrogen #PA5-50485	Rabbit
MuRF1	1:1000	Protein Tech #55456-1-AP	Rabbit
BDK	1:1000	Invitrogen #PA5-31455	Rabbit
γ-tubulin	1:10000	Sigma Aldrich #T6557	Mouse

The following day, membranes were washed 3x5 minutes in TBST and incubated in either anti rabbit (Cell Signalling) or mouse (Cell Signalling) secondary antibodies for 3h. Membranes were washed again 3x5 minutes in TBST and HRP chemical luminescent was applied to each membrane and BioRad ChemiDoc XRS+ was used for signal visualization. Images were quantified using image lab software v7 (Bio-Rad).

High Pressure Liquid Chromatography

During sample preparation of skeletal muscle and liver (see section *"Western Blotting"*), free amino acids were collected from the supernatant following the centrifugation step (10000g for 30 minutes). Free amino acids (also from plasma) were diluted in a ratio of 1 (sample): 2 (potassium borate buffer): 1 (0.1N hydrochloric acid): 8 (HPLC grade water). Diluted samples from skeletal muscle, liver and plasma were pre-column derivatized in a ratio of 1 (sample): 1 (OPA, 29.28mM). Samples were then injected into a YMC-Triart C18 column (C18, 1.9µm, 75 x 3.0mm; YMC America, Allentown, PA, USA) fitted onto an ultra HPLC system (Nexera X2, Shimadzu, Kyoto, Japan) connected to a fluorescence detector (Shimadzu, Kyoto, Japan; excitation: 340nm; emission: 455nm). A gradient solution derived from 20mM potassium phosphate buffer (pH 6.5) (Mobile phase A) and a solution made from HPLC grade water (15%), acetonitrile (45%) and methanol (40%) (Mobile phase B) at a flow rate of 0.8mL/min was used to elude the amino acids. A gradient made up of 5%-100% mobile phase B was run over 21

mins. Amino acid standard curves were used to help calculate amino acid concentrations and all samples from muscle and liver were normalized to total protein. Full procedure can be found in Appendix C.

Protein Synthesis (SUnSET Analysis)

Mice were starved for 3h to control for any nutrient uptake effects on protein synthesis. Thirty minutes prior to euthanasia, mice were intraperitoneally injected with 0.040μmol/g bodyweight of puromycin in saline. Skeletal muscle samples were then immunoblotted against an anti-puromycin antibody (EMD Millipore, #MABE343) and corrected to their respective ponceauS staining.

Statistical Analyses

All immunoblot analyses were quantified and adjusted to their corresponding γ-tubulin values. Gamma tubulin was used as loading control as we noticed no significant effects of chemotherapy on it's abundance. In some cases, double bands are noticed in gamma tubulin blots. This is because when the membranes were previously blotted against anti-BCKD or p-BCKD^{ser293} antibodies before blotting with anti-gamma tubulin antibodies, the signals from BCKD or p-BCKD^{ser293} could still be seen. All graphs were drawn using Graph pad prism version 9. Since male and female mice came from separate vendors, statistical comparison using a two-way ANOVA was viewed as inappropriate. Instead, unpaired t-tests were used to measure treatment differences within each sex (identified as an *). We then calculated percentage change due to treatment (within each sex) and used an unpaired t-test to compare whether percentage change in one sex was different from percentage change in another sex (identified as an #). For our ITT data, within sex, a two-way-ANOVA was used to measure blood glucose differences following chemotherapy across all time points followed by area under the curve (AUC) analysis.

Significance was determined when p-value < 0.05. P-values were considered a trend when they were equal to or less than 0.1. Results were expressed as standard error of the mean (SEM).

Results

Drug-treated female mice have worsened outcomes for body and skeletal muscle weight following chemotherapy

Following 6 weeks of chemotherapy, both male (~15%) and female (~25%) drug-treated mice lost body weight compared to controls (Figure 5.1A). Body weight loss at each time point relative to control can be found in Appendix I. At week 6, drug-treated females lost more weight compared to males (Figure 5.1B). We found no difference in food intake following chemotherapy in both sexes (Figure 5.1C). The loss of body weight in drug-treated animals was consistent with a significant decrease in the skeletal muscle mass of the gastrocnemius (Figure 5.1D), tibialis anterior (Figure 5.1E) and quadriceps (Figure 5.1F), but not the EDL (Figure 5.1G) or soleus (Figure 5.1H). The loss of gastrocnemius muscle mass in females was more severe compared to drug-treated males (Figure 5.1D). We found minimal effects of drug treatment on the adipose tissue (Figure 5.1I), kidney (Figure 5.1J) and heart (Figure 5.1K), but both sexes showed a significant increase in spleen weight (Figure 5.1L), while only drug-treated females showed an increase in liver weight compared to female controls (Figure 5.1M). Protein expression of skeletal muscle contractile proteins myosin heavy chain-1 (Figure 5.1N, O), troponin (Figure 5.1N, P) and tropomyosin (Figure 5.1N, Q) were decreased in both sexes.

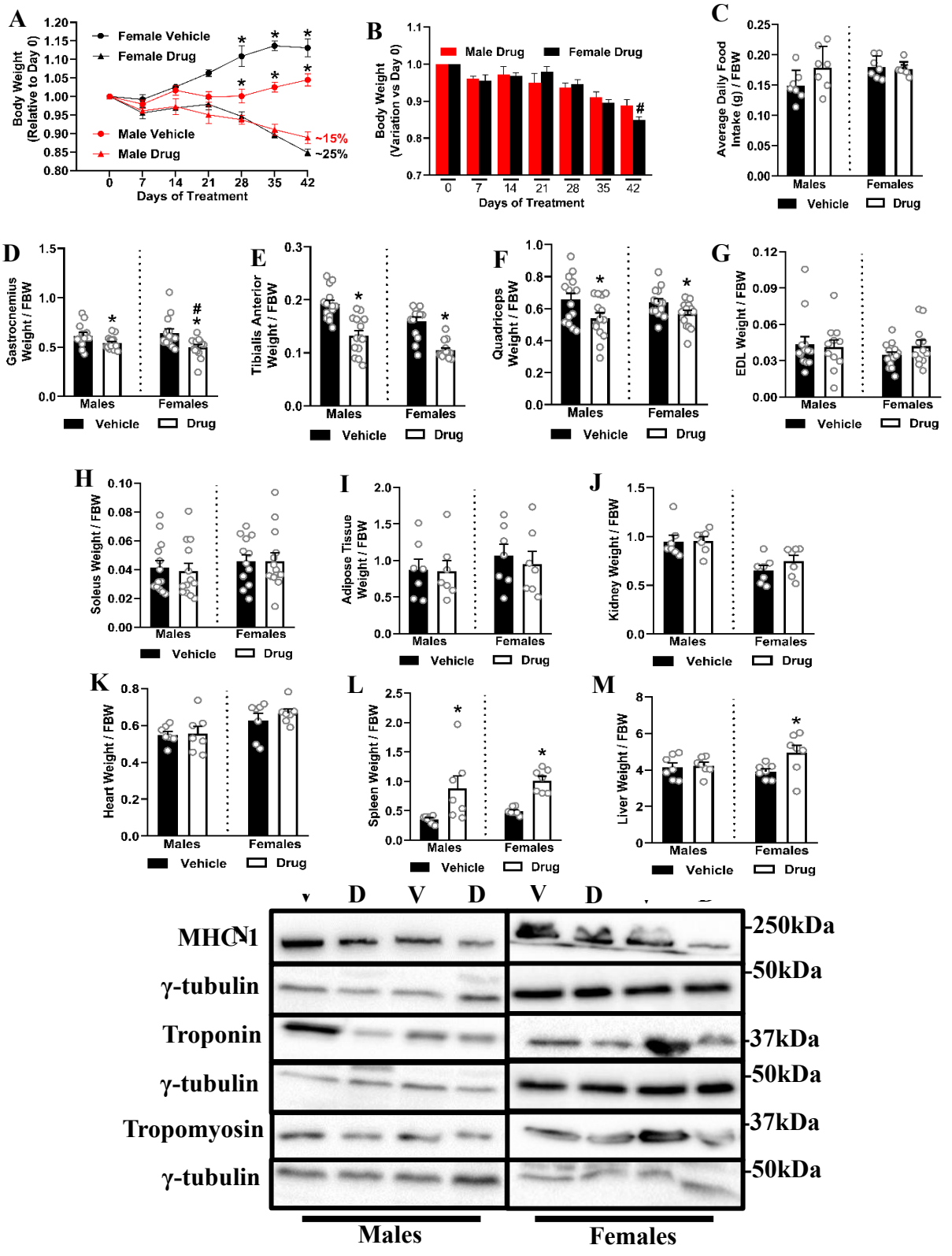
A
Body Weight (Relative to Day 0)
Female Vehicle
Female Drug
Male Vehicle
Male Drug
~15%
~25%
Days of Treatment
B
Body Weight (Variation vs Day 0)
Male Drug
Female Drug
Days of Treatment
C
Average Daily Food Intake (g) / FBW
Males
Females
Vehicle
Drug
D
Gastrocnemius Weight / FBW
E
Tibialis Anterior Weight / FBW
F
Quadriceps Weight / FBW
G
EDL Weight / FBW
H
Soleus Weight / FBW
I
Adipose Tissue Weight / FBW
J
Kidney Weight / FBW
K
Heart Weight / FBW
L
Spleen Weight / FBW
M
Liver Weight / FBW
D V D V D
MHCN1
γ-tubulin
Troponin
γ-tubulin
Tropomyosin
γ-tubulin
250kDa
50kDa
37kDa
50kDa
37kDa
50kDa
Males
Females

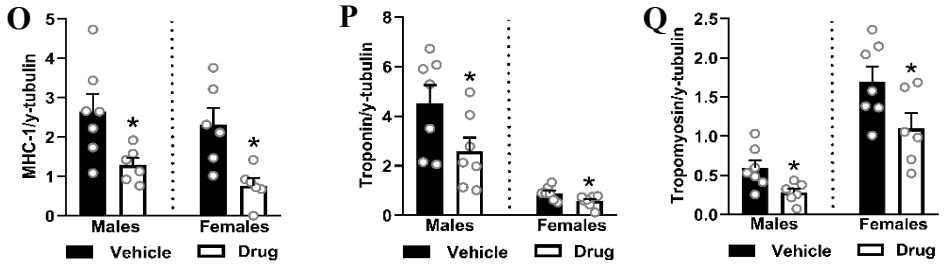

Figure 5.1 Drug-treated female mice have worsened outcomes for body and skeletal muscle weight following chemotherapy. Male and female 10-12-week-old CD2F1 mice were treated with either vehicle (10% DMSO in saline) or a chemotherapy drug cocktail (Drug: 50mg/kg 5-FLU, 90mg/kg Leucovorin, 24mg/kg CPT11) for 6 weeks. Body weight **(A, B)** and food intake **(C)** were recorded daily for 6 weeks. Weights of the skeletal muscles: gastrocnemius **(D)**, tibialis anterior **(E)**, quadriceps **(F)**, EDL **(G)** and soleus **(H)**, as well as the organs: adipose tissue **(I)**, kidney **(J),** heart **(K),** spleen **(L)** and liver **(M).** Weights were normalized to FBW. Immunoblotting and quantified data for muscle contractile proteins: MHC-1 **(N, O)**, troponin **(N, P)** and tropomyosin **(N, Q)** are shown. Data are mean ± SEM; n = 6-7 animals per group; * $p < 0.05$ for within sex drug vs vehicle, # $p < 0.05$ for whether percentage change in one sex is different from the other sex. V, Vehicle; D, Drug; DMSO, dimethyl sulfoxide; FBW, final body weight.

Chemotherapy causes insulin resistance in both sexes, but female-drug treated mice experience worsened outcomes for anabolic and catabolic signalling

We conducted ITT during week 3 and 6 of treatment. At week 3 of treatment (Figure 5.2A-C), male (Figure 5.2A), but not female (Figure 5.2B) drug-treated mice showed impaired insulin tolerance, corresponding with a trend toward higher blood glucose AUC (Figure 5.2C). However, at week 6 of treatment (Figure 5.2D – F), both male (Figure 5.2D) and female (Figure 5.2E) drug-treated mice showed impaired insulin tolerance, with greater impairment in males (Figure 5.2F). We measured and found decreases in the phosphorylation of AKT^{ser473}, $S6K1^{thr389}$, $S6^{ser235/236}$ and $4E\text{-}BP1^{thr37/46}$ in the skeletal muscle (Figure 5.2G – K) compared to controls. Consistent with gastrocnemius muscle weight data, the decreased phosphorylation of $S6K1^{thr389}$ in drug-treated females was more severe in the gastrocnemius (Figure 5.2G, I). No differences for total proteins were found (Figure 5.2L). Protein synthesis (SUnSET analysis) was also decreased following drug treatment in the gastrocnemius of both sexes (Figure 5.2M, N). For catabolic signalling, only drug-

treated female mice showed significant decreases in p-FoxO3a^{ser253} (Figure 5.2O, P), consistent with a treatment-induced increase in MuRF1 expression (Figure 5.2O, Q) and ubiquitin in the gastrocnemius (Figure 5.2R, S).

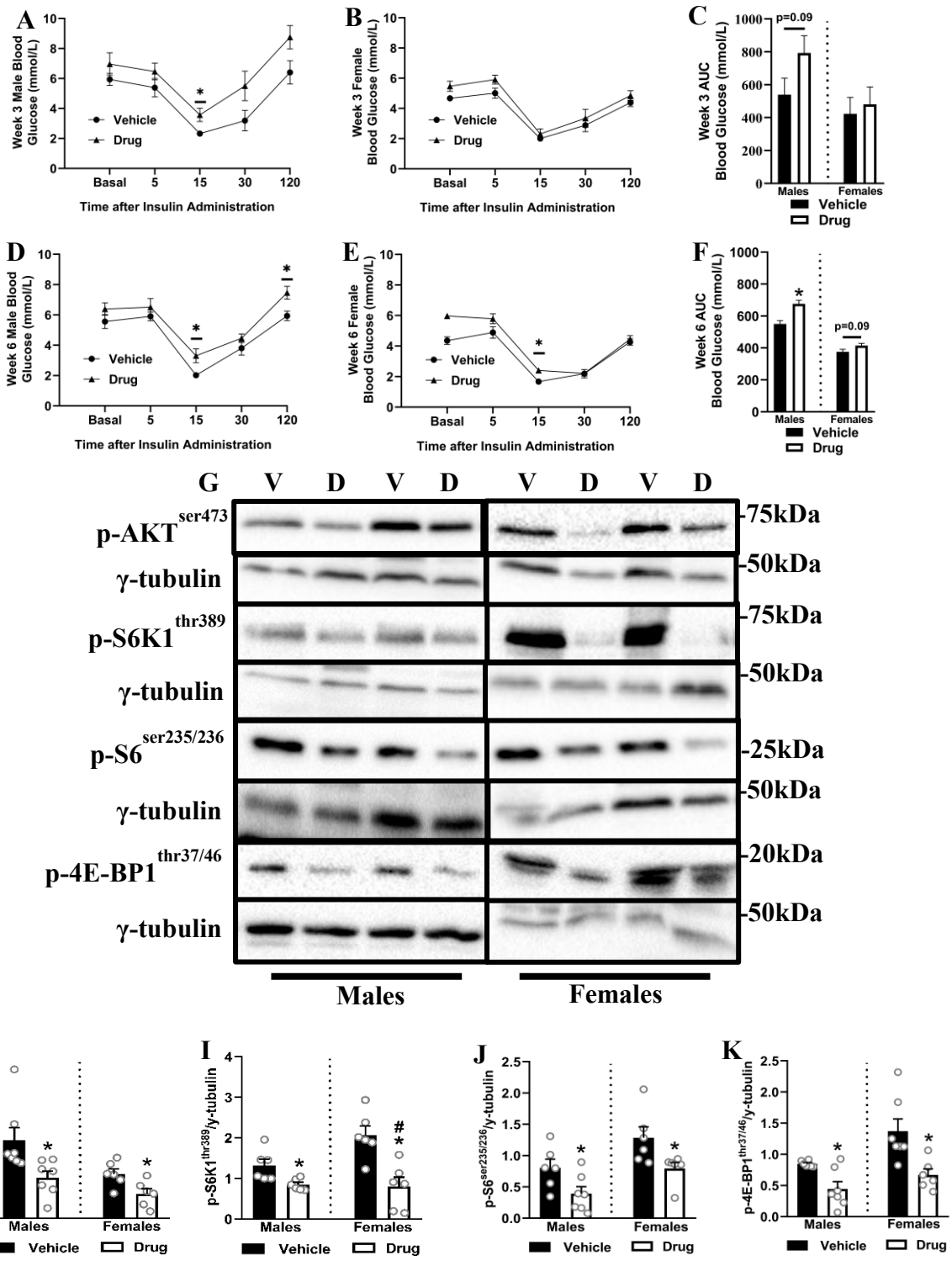

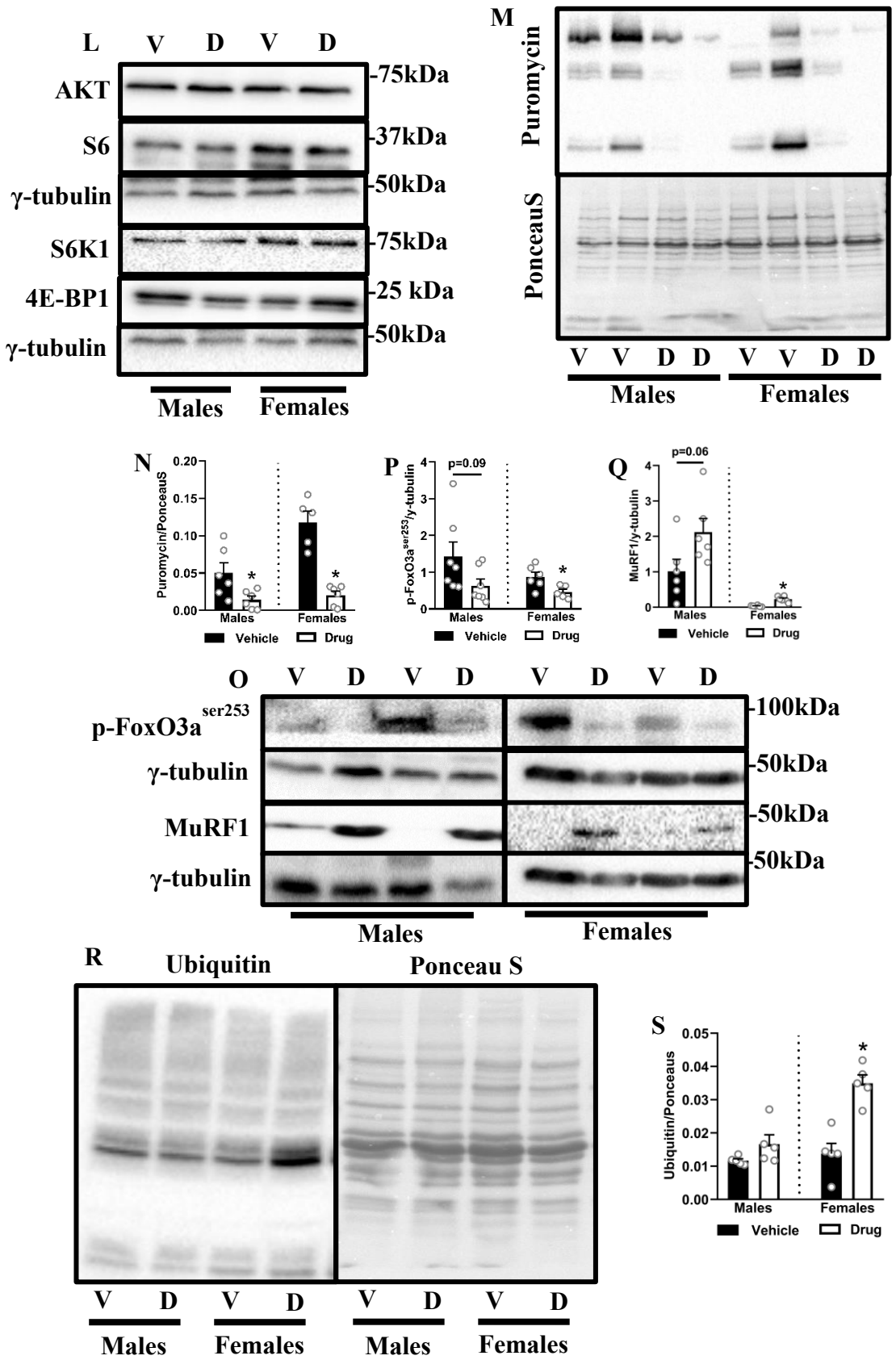
L
V D V D
AKT
S6
γ-tubulin
S6K1
4E-BP1
γ-tubulin
75kDa
37kDa
50kDa
75kDa
25 kDa
50kDa
Males
Females
M
Puromycin
PonceauS
V V D D V V D D
Males
Females
N
Puromycin/PonceauS
Males
Females
Vehicle
Drug
P
p=0.09
p-FoxO3a ser253/γ-tubulin
Males
Females
Vehicle
Drug
Q
p=0.06
MuRF1/γ-tubulin
Males
Females
Vehicle
Drug
O
V D V D V D V D
p-FoxO3a ser253
γ-tubulin
MuRF1
γ-tubulin
100kDa
50kDa
50kDa
50kDa
Males
Females
R
Ubiquitin
Ponceau S
V D V D V D V D
Males
Females
Males
Females
S
Ubiquitin/Ponceaus
Males
Females
Vehicle
Drug

Figure 5.2 Chemotherapy causes insulin resistance in both sexes, but female-drug treated mice experience worsened outcomes for anabolic and catabolic signalling. During week 3 **(A-C)** and 6 **(D-F)** of treatment, male and female mice were starved for 6h and underwent ITT. Immunoblotting and quantified data for the phosphorylation of AKT^{ser473} **(G, H)**, $S6K1^{thr389}$ **(G, I)**, $S6^{ser235/236}$ **(G, J)**, $4E\text{-}BP1^{thr37/46}$ **(G, K)** and total proteins **(L)**. Thirty minutes prior to euthanization, mice were injected with 0.040µmol/g bodyweight of puromycin, immunoblotted against an anti-puromycin antibody and corrected to their respective ponceauS stain **(M, N)**. Immunoblotting and quantified data for $p\text{-}FoxO3a^{ser253}$ **(O, P)**, MuRF1 **(O, Q)** and ubiquinated proteins **(R, S)** are shown. Data are mean ± SEM; n = 5-7 animals per group; * $p < 0.05$ for within sex drug vs vehicle, # $p < 0.05$ for whether percentage change in one sex is different from the other sex. All measures were made in the skeletal muscle. V, Vehicle; D, Drug; p, phosphorylated; h, hours; ITT, insulin tolerance test; AUC, area under the curve.

Following chemotherapy, the reduction in skeletal muscle BCAA concentrations is more severe in males

Due to decreased expression of their transporters, we next examined BCAA concentrations in the gastrocnemius. Concentrations of leucine (Figure 5.3A), isoleucine (Figure 5.3B), valine (Figure 5.3C) and total BCAAs (Figure 5.3D) were all significantly decreased in drug-treated animals. The decreases were more severe in males compared to females. Aside from arginine (Figure 5.3E), males (Figure 5.3F, H) and females (Figure 5.3G, H) showed minimal differences for concentrations of other amino acids measured. Both sexes showed significant decreases in amino acid transporter expression of SNAT1 (Figure 5.3I, J) and LAT1 (Figure 5.3I, K), with females showing a more severe decrease in LAT1.

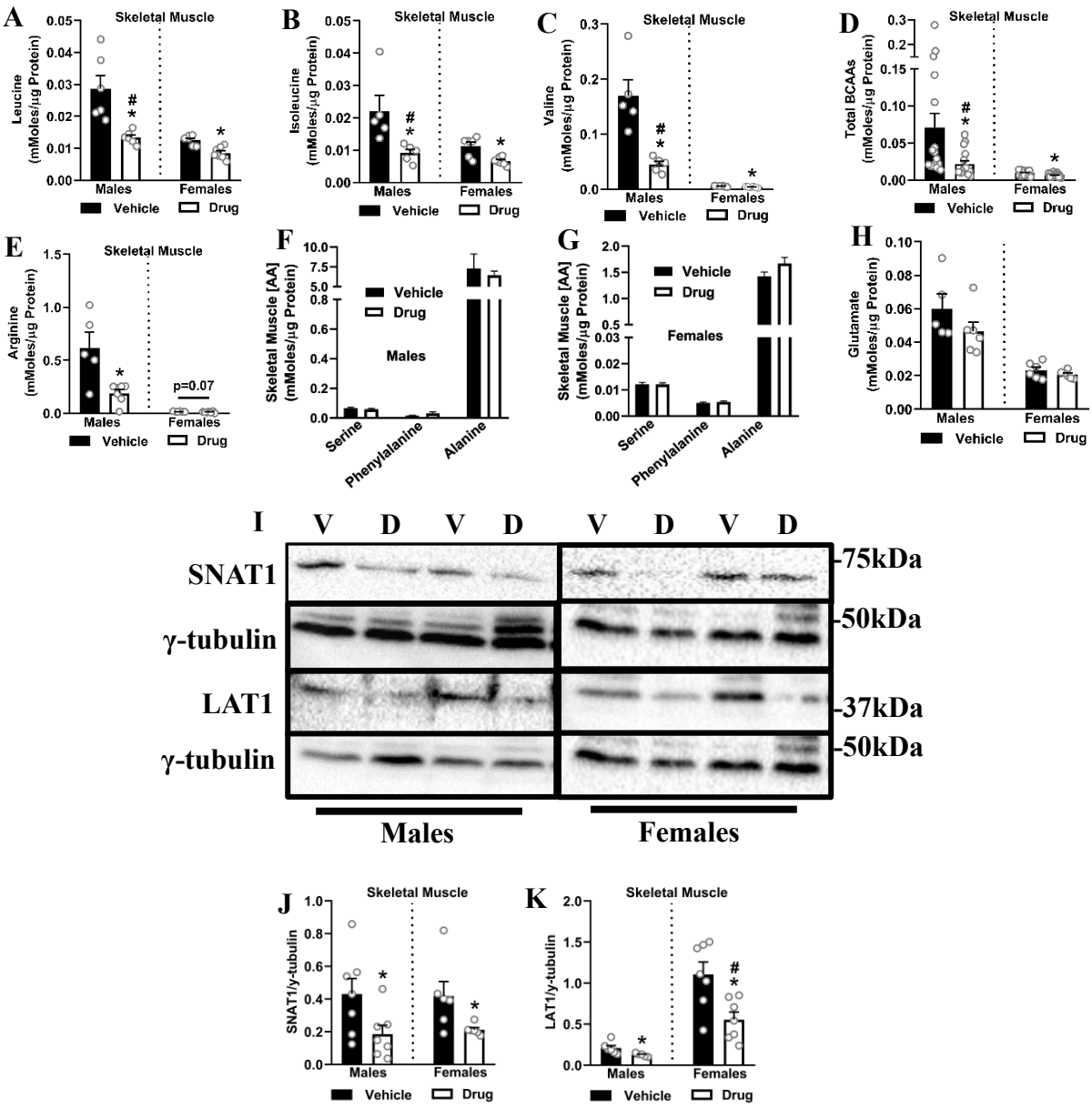

Figure 5.3 Following chemotherapy, the reduction in skeletal muscle BCAA concentrations is more severe in males. Concentrations of leucine **(A)**, isoleucine **(B)**, valine **(C)**, total BCAAs **(D)**, arginine **(E)**, other amino acids **(F, G)** and glutamate **(H)** in the gastrocnemius were measured by HPLC. Immunoblotting **(I)** and quantified data for SNAT1 **(J)** and LAT1 **(K)** are shown. Data are mean ± SEM; n = 5-7 animals per group; * $p < 0.05$ for within sex drug vs vehicle, # $p < 0.05$ for whether percentage change in one sex is different from the other sex. V, Vehicle; D, Drug; h, hours; BCAAs, branched-chain amino acids; HPLC, high-pressure liquid chromatography; p, phosphorylated.

Skeletal muscle BCAA metabolism is decreased following chemotherapy in both sexes

Since changes in BCAA catabolism could explain changes in their concentrations, we

measured key enzymes involved in their catabolism. BCAT2 and BDK were unchanged following drug treatment in both sexes (Figure 5.4A, B, D). Protein expression of BCKD was unchanged in males, but drug-treated female animals showed significant decreases in BCKD compared to controls (Figure 5.4A, C). However, p-BCKD^{ser293} was significantly increased in both sexes (Figure 5.4A, E), corresponding with decreased activity of this kinase following chemotherapy (Figure 5.4F).

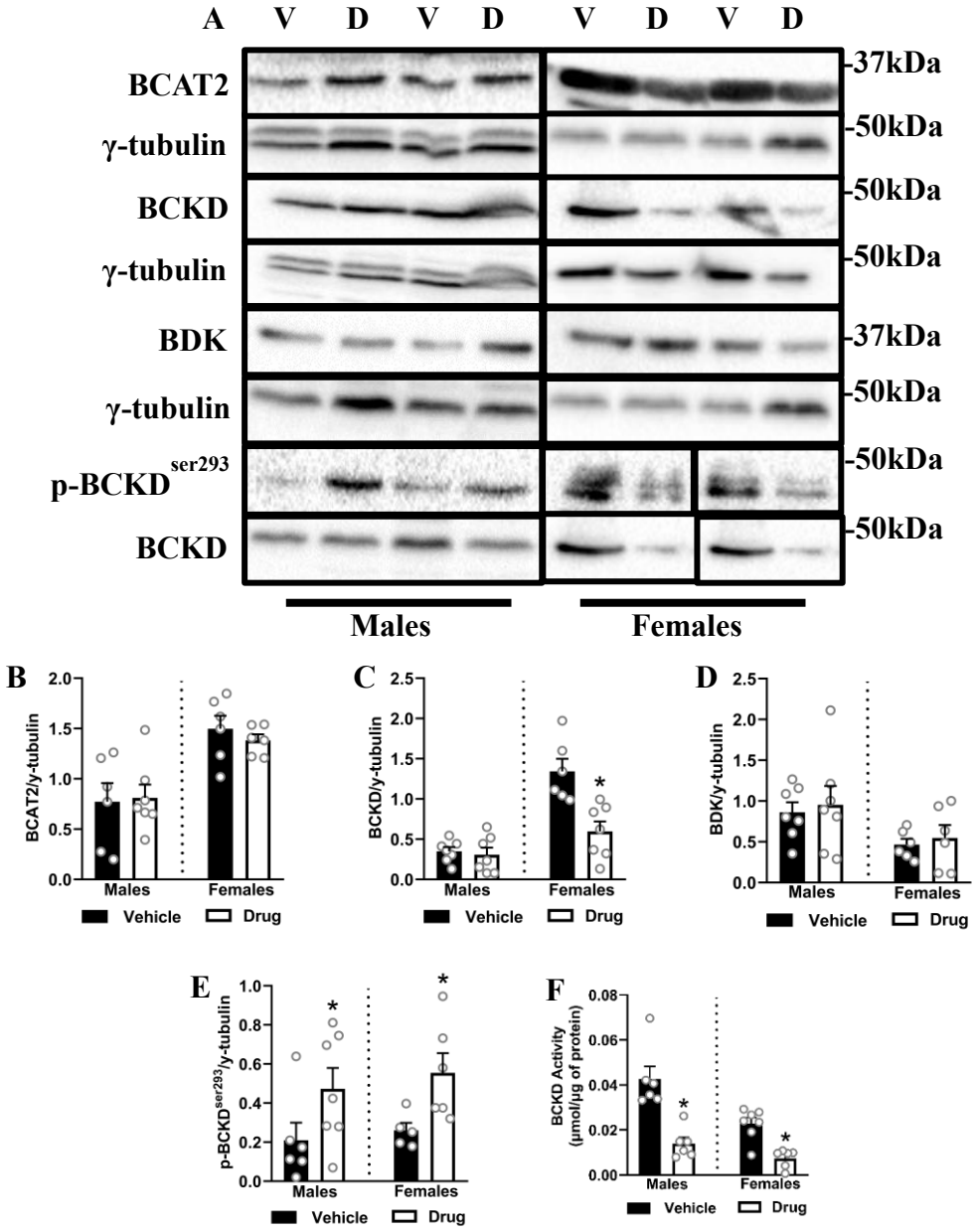

Figure 5.4 Skeletal muscle BCAA metabolism is decreased following chemotherapy in both sexes. Immunoblotting **(A)** and quantified data for BCAT2 **(B)**, BCKD **(C)**, BDK **(D)** and phosphorylated $BCKD^{ser293}$ **(E)** are shown. BCKD activity was measured from the release of $^{14}CO_2$ (BCKD's decarboxylation) from ^{14}C labelled valine **(F)**. Data are mean ± SEM; n = 5-7 animals per group; * $p < 0.05$ for within sex drug vs vehicle. V, Vehicle; D, Drug; p, phosphorylated.

Chemotherapy treatment leads to elevated concentrations of liver BCAAs in both sexes, but only males show elevated plasma BCAAs

Drug-treated males, but not females showed elevated plasma concentrations of leucine (Figure 5.5A), valine (Figure 5.5C) and total BCAAs (Figure 5.5D), but not isoleucine (Figure 5.5B). The livers of drug-treated animals showed elevated concentrations of leucine (Figure 5.5E), valine (Figure 5.5G), and total BCAAs (Figure 5.5H), but not isoleucine (Figure 5.5F) for both sexes. LAT1 expression was also increased in the liver from both sexes (Figure 5.5I, J). Protein expression of liver BCKD (Figure 5.5K, L) and BDK (Figure 5.5K, M) were unchanged following drug treatment in both sexes. However, the inhibitory phosphorylation of $BCKD^{ser293}$ was higher following drug treatment (Figure 5.5K, N), corresponding with decreased activity of BCKD in the liver (Figure 5.5O).

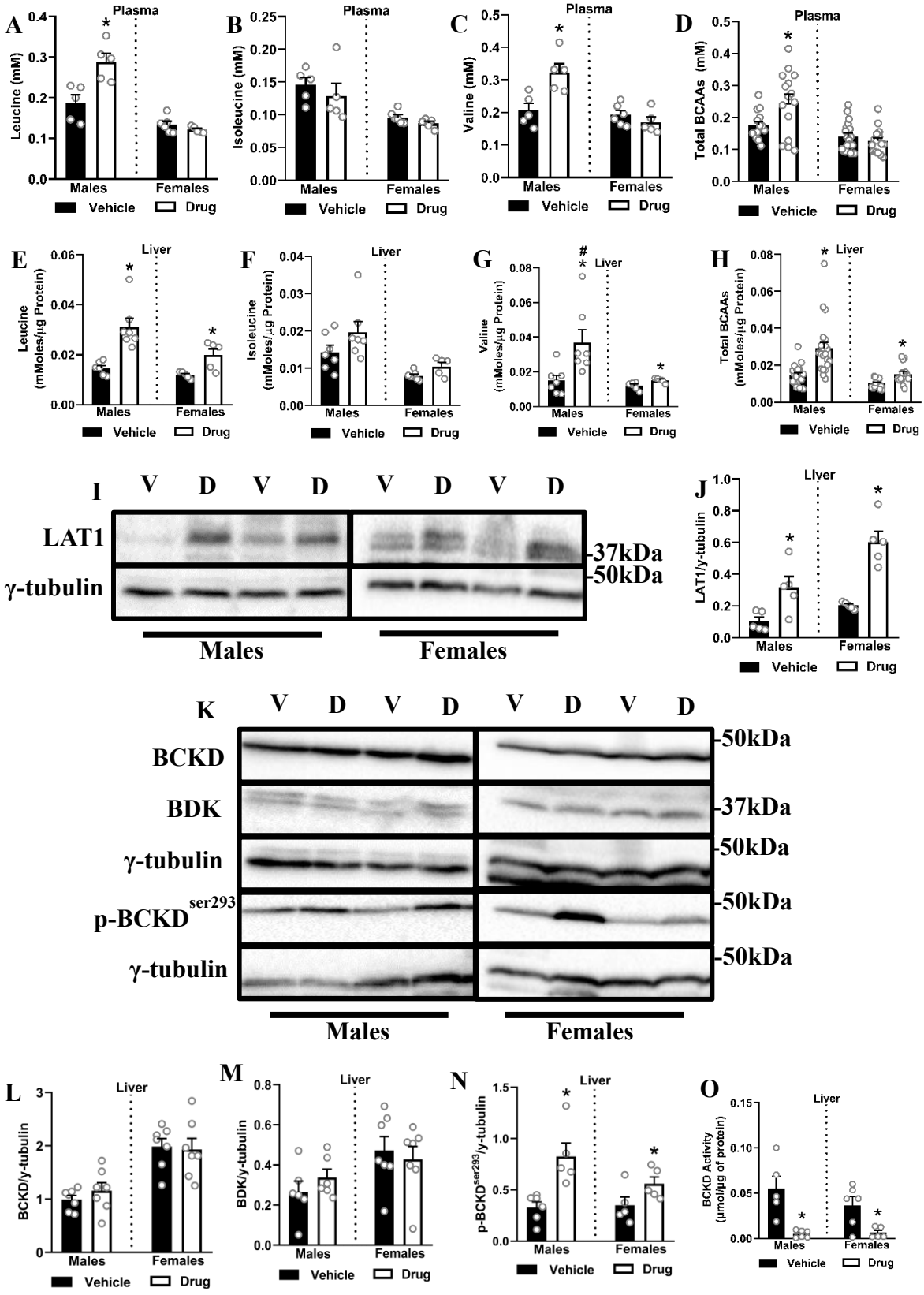
A
Plasma
Leucine (mM)
Males
Females
Vehicle
Drug
B
Plasma
Isoleucine (mM)
C
Plasma
Valine (mM)
D
Plasma
Total BCAAs (mM)
E
Liver
Leucine (mMoles/µg Protein)
F
Liver
Isoleucine (mMoles/µg Protein)
G
Liver
Valine (mMoles/µg Protein)
H
Liver
Total BCAAs (mMoles/µg Protein)
I
V D V D V D V D
LAT1
γ-tubulin
37kDa
50kDa
Males
Females
J
Liver
LAT1/γ-tubulin
K
V D V D V D V D
BCKD
BDK
γ-tubulin
p-BCKD ser293
γ-tubulin
50kDa
37kDa
50kDa
50kDa
50kDa
Males
Females
L
Liver
BCKD/γ-tubulin
M
Liver
BDK/γ-tubulin
N
Liver
p-BCKD ser293/γ-tubulin
O
Liver
BCKD Activity (µmol/µg of protein)

Figure 5.5 Chemotherapy treatment leads to elevated concentrations of liver BCAAs in both sexes, but only males show elevated plasma BCAAs. Plasma leucine **(A)**, isoleucine **(B)**, valine **(C)** and total BCAAs **(D)**, as well as liver leucine **(E)**, isoleucine **(F)**, valine **(G)** and total BCAAs **(H)** were measured via HPLC. Immunoblotting and quantified data for LAT1 **(I, J)**, BCKD **(K, L)**, BDK **(K, M)** and p-BCKD^{ser293} **(K, N)**. BCKD activity in the liver **(O)**. Data are mean ± SEM; n = 5-7 animals per group; * $p < 0.05$ for within sex drug vs vehicle, # $p < 0.05$ for whether percentage change in one sex is different from the other sex. V, Vehicle; D, Drug; BCAAs, branched-chain amino acids; p, phosphorylated; HPLC, high-pressure liquid chromatography.

The BCAAs are positively correlated with gastrocnemius muscle weight, LAT1 transporter expression and BCKD activity

Total BCAAs showed significant positive correlations with gastrocnemius muscle weight (Figure 5.6A), protein expression of their transporter LAT1 (Figure 5.6B) and BCKD activity (Figure 5.6C). Lastly, positive correlations were observed between gastrocnemius muscle weight and LAT1 (Figure 5.6D) and BCKD activity (Figure 5.6E).

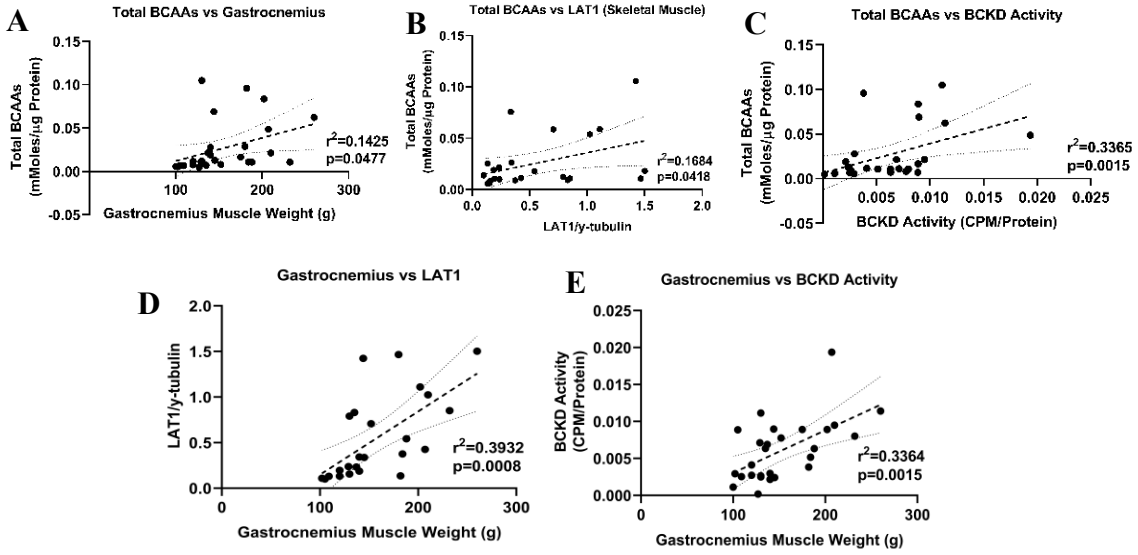

Figure 5.6 The BCAAs are positively correlated with gastrocnemius muscle weight, LAT1 transporter expression and BCKD activity. Correlations between the BCAAs and gastrocnemius muscle weight **(A)**, skeletal muscle LAT1 transporter expression **(B)** and skeletal muscle BCKD activity **(C)**. Relationship between gastrocnemius muscle weight and LAT1 **(D)** and BCKD activity **(E)** are also shown. Data were analyzed using linear regression and 95% confidence intervals are denoted. BCAAs, branched-chain amino acids**.**

Discussion

We report, to our knowledge for the first time, sex differences in BCAA availability and metabolism following administration of anti-cancer drugs to mice. Body and gastrocnemius muscle weight loss in females was more severe compared to males, consistent with a greater loss of anabolic signalling and increases in catabolic signalling. However, drug-treated males were observed to have more severe decreases in skeletal muscle BCAA concentrations and impaired insulin tolerance compared to females. In opposition to BCAA concentrations, the suppression of LAT1, the canonical BCAA transporter, was more severe in females. Findings from this study highlight sex-and tissue-specific alterations to muscle BCAA metabolism and suggest that sex may determine the magnitude of skeletal muscle loss during chemotherapy.

In our study, food intake was not affected by chemotherapy. Although this may seem surprising, findings on food intake are similar to past studies (8). In addition, since we corrected food intake for final body weight, our food intake data provides a better indication of food intake, rather than a result mediated by an overall change in body weight. Nonetheless, at the forefront of cachectic studies today, is the need for nutritional interventions that successfully treat cachexia. In this study, we focus on the BCAAs, substrates that have shown to increase skeletal muscle anabolism (34), but have little effect on increasing survival during cachexia (36, 337). We believe that our data presented here and in our *in-vitro* work (Chapter 4, Study 1), demonstrate that inability for nutritional interventions to rescue cachexia may be due to blunted substrate delivery to skeletal muscle.

We have previously shown that myotubes treated with a chemotherapy drug cocktail exhibit decreases in myotube diameter, myofibrillar protein content and anabolic signalling (417). In this study, drug-treated female mice lost more body and gastrocnemius muscle weights

compared to males. This is an important finding, given that skeletal muscle mass is a determinant of chemotherapy dose and treatment effectiveness (21). In healthy subjects, males have greater muscle mass than females (77) and higher levels of testosterone, the prominent anabolic hormone that enhances muscle mass in a dose dependent manner (690). In addition, females have lower blood elimination and drug clearance (2, 439) for chemotherapy agents, supporting a more catabolic environment in females. Therefore, females may experience more side effects and decreased chemotherapy effectiveness compared to males. Since chemotherapy can also decrease fat mass (691), we were surprised to see no significant effect of chemotherapy on the adipose tissue weight in both sexes, especially since females have a greater fat mass compared to males (692). However, it is important to note that cachexia can occur with or without the loss of adipose tissue and since these animals are relatively young in age, it is possible they do not have large fat storage, compared to the fat storage seen in aging (693). We also did not measure muscle force here, but since previous studies in mice (8) and humans (694, 695) have found decreases in muscle force/strength following chemotherapy, we can reasonably suggest that muscle weakness may be associated with the muscle atrophy we observed.

As insulin resistance is a feature of cachexia (696), we conducted ITTs on our animals to determine whether sex differences may be related to sex-dependent altered insulin sensitivity. We have also shown previously in myotubes, that chemotherapy leads to decreased insulin-stimulated glucose uptake and substrate availability of glucose (417). Our finding of worsened insulin sensitivity only in males is likely related to hormonal differences between the sexes, as estrogen has protective effects against insulin resistance in females (697). Therefore, repeating these experiments in female animals that are aged past the point to when they are no longer cycling and producing estrogen may produce different results.

Contrary to current literature whereby minimal sex differences exist in mTORC1 signalling and protein synthesis (610), we found that in healthy mice administered chemotherapy, drug-treated female animals were more susceptible to decreases in mTORC1 signalling, observed through a more severe loss of p-S6K1^{thr389} compared to males. We also found drug-treated female mice had increased MuRF1 protein expression, a finding not seen in males. This is contrary to previous literature, whereby males have greater ubiquitin proteasome activity compared to females (664). However, we only measured protein expression of an E3 ligase associated with the proteasome, not proteasome activity per se. We suggest that chemotherapy administration in healthy mice alters sex differences related to protein turnover. Therefore, the more severe loss of gastrocnemius muscle weight in drug-treated female mice, is related to a more severe loss in p-S6K1^{thr389} and increase in MuRF1. We also observed increases in ubiquitinated proteins only in females, which is also supportive of a more catabolic environment. However, a build up of ubiquitinated proteins does not always translate to greater protein breakdown, as ubiquitinated proteins are degraded rather quickly (698) and differences may be related to the fact that the proteasome may be degrading proteins faster then what we can detect. Therefore, using proteasome inhibitors such as MG132 may provide a more accurate picture of poly ubiquitinated proteins following chemotherapy.

Since all twenty amino acids are required for protein synthesis in skeletal muscle (27, 34), we believe a main finding of this work is the profound sex differences in tissue and circulating BCAA levels. Males have higher concentrations of skeletal muscle BCAAs (48). Therefore, higher BCAA concentrations may present a protective effect against chemotherapy-induced cachexia in males, an observation that may partially explain the more severe loss of gastrocnemius muscle weight in females. Nonetheless, in both sexes, we present novel findings

whereby chemotherapy decreases BCAA concentrations, an effect that is more severe in males. This finding could simply be due to the greater BCAA pools found in males, giving these animals more to lose. However, during skeletal muscle substrate deficits, males tend to oxidize more amino acids for energy, while females tend to oxidize more fats (699). Therefore, following chemotherapy, males, but not females, may generate more energy from amino acids within their skeletal muscle to support protein synthesis and abrogate some of the loss of muscle mass from chemotherapy. Since insulin is typically required for skeletal muscle BCAA uptake into skeletal muscle (700), males may also be more susceptible to reduced concentrations of BCAAs in their skeletal muscle, as they showed greater insulin intolerance compared to females. Decreased concentrations of BCAAs in both sexes is associated with decreased expression of their transporter LAT1, an effect that is more severe in females. The greater loss of LAT1 in females may be explained by the fact that LAT1 can function as a bi-directional transporter (701), helping to limit the loss of BCAAs and other amino acids in females, especially given that females lost more muscle, had greater S6K1 suppression, higher MuRF1 expression and greater ubiquination of proteins, all consistent with a more catabolic environment in females.

Decreased BCAA concentrations in the skeletal muscle following chemotherapy may also be related to altered metabolism of these amino acids. We believe that the decreased BCKD activity in the skeletal muscle of both sexes following chemotherapy is a compensatory mechanism to reduce further oxidation in an attempt to try and preserve the BCAA pool.

Lastly, we were interested in alternate fates of the BCAAs. Male, but not female elevations in the plasma BCAAs can be partially explained by multiple factors: 1) Since males had decreased skeletal muscle BCAA concentrations and rely on oxidation of amino acids during substrate deficits, the transport of BCAAs through the plasma towards the skeletal muscle may

be increased; 2) Our drug-treated male mice were insulin resistant and previous reports have associated circulating plasma BCAAs levels and insulin resistance (702); 3) A previous review has outlined that dysregulation of BCAA metabolism in the gut microbiome can result in elevated plasma BCAAs (703), an interesting finding as chemotherapy may cause changes in gut microbiome (704). However, we did not measure gut microbiome in this study.

Our liver data indicates that accelerated efflux of the BCAAs from the skeletal muscle are travelling towards the liver. In the liver, amino acids such as alanine and glutamine can be converted into glucose, by gluconeogenesis (705). Therefore, it is likely that the increase in liver BCAAs is a compensatory mechanism in an attempt to not only remove excess BCAAs from the plasma, but to also generate glucose, following chemotherapy where there are substrate deficits.

A limitation of this study is that for our ITT data, because mice were starved prior to the commencement of ITT, data on glucose levels during the ITT could be confounded by chemotherapy-induced changes in baseline glucose levels. Another limitation is that chemotherapy drugs are not typically given to healthy individuals. However, we have used clinically relevant chemotherapy drugs (216) to probe sex differences in metabolic responses, especially BCAA catabolism, to these drugs. The fact that elevations in liver BCAA concentrations (40, 41) are seen in many cancers is consistent with observations made in this study, and suggest that the changes we observed will likely be heightened when tumour implantation is combined with chemotherapy, a subject that our lab is interested in.

In conclusion, compared to male animals, drug-treated female animals experienced worsened outcomes for body weight, gastrocnemius weight and p-S6K1^{thr389} signalling. On the other hand, male drug-treated animals were more insulin resistant and experienced more severe decreases in skeletal muscle BCAA concentrations. The positive correlations that we observed

between LAT1, BCKD activity and muscle weight suggest that disruption of BCAA metabolism may play a role in cachexia and that interventions that can correct this disruption may help in the management of this condition.

Author Contributions

SM and OAJA designed the experiments. SM performed all body weight, food intake and chemotherapy dosing measurements, dosing and calculations. SM performed euthanasia and tissue weight measurements, while GM dissected all tissues. All western blotting was performed by SM. For ITT, SM performed insulin calculations and injections, saphenous vein blood gathering onto glucose strips and insertion into glucometer, while GM recorded blood glucose values. For HPLC, SM formulated buffers and diluted and loaded all standards/samples, while GM made standards, inserted column and set machine parameters. SM analyzed the samples and drafted the initial version of the manuscript. OAJA reviewed and edited the manuscript. SM, GM and OAJA approve the final version of the manuscript.

Conflict of Interest

The authors declare no conflict of interest.

Acknowledgements

This study was funded by grants from the Natural Science and Engineering Research Council of Canada (NSERC) and from the Faculty of Health, York University, Toronto Canada to OAJA. Thank you to the Muscle Health Research Centre at York University for use of the HPLC and to Dr. Paluzzi for use of their imaging systems.

Funding

Work is supported by funds from the Natural Science and Engineering Research Council of Canada by the Faculty of Health, York University.

Chapter 6

SEX-RELATED DIFFERENCES IN CACHEXIA OUTCOMES AND BRANCHED-CHAIN AMINO ACID METABOLISM FOLLOWING CHEMOTHERAPY IN AGED ANIMALS

Stephen Mora[1], Gagandeep Mann, Olasunkanmi A.J. Adegoke[1]

Muscle Health Research Centre, School of Kinesiology and Health Science, York University, Toronto, ON, M3J 1P3

Corresponding Author: Dr. Olasunkanmi A.J. Adegoke

Muscle Health Research Centre, School of Kinesiology and Health Science, York University, Toronto, ON, Canada. Tel: 416-7362100 Ext 20887. Fax: 416-736- 5774. Email: oadegoke@yorku.ca

Keywords: Cachexia, Chemotherapy, Protein Synthesis, BCAA Metabolism, Sex, Aging

Figures: 7

A version of this is being prepared to be submitted to PLOS ONE

Chapter Summary

Age is the most significant risk factor for cancer, but models of cachexia often study young male animals. The branched-chain amino acids (BCAA: leucine, isoleucine, and valine) are critical anabolic stimulators in skeletal muscle. However, altered metabolism of these amino acids may account for their diminished effectiveness in fully reversing cachexia. Therefore, we present data on sex-related differences in cachexia outcomes and BCAA metabolism following chemotherapy in aged animals. Mice aged 18±2 months of age were treated with either the chemotherapy drug cocktail folfiri (50mg/kg 5-fluorouracil (5FU), 90mg/kg Leucovorin and 24mg/kg CPT11) (drug) or vehicle (10% DMSO in saline) for 6-weeks. The metabolism and concentrations of the BCAAs were measured in plasma and tissues. In both sexes, chemotherapy reduced body weight, skeletal muscle weight, myofibrillar protein content, anabolic signalling and protein synthesis. Drug-treated male animals showed worsened outcomes for body weight, gastrocnemius muscle weight and ubiquitination of proteins. Following chemotherapy, only drug-treated males showed decreases in skeletal muscle BCAAs, but both sexes exhibited reduced expression of their transporter, LAT1. Minimal differences were found for the enzymes involved in skeletal muscle BCAA metabolism. However, only drug-treated males showed reduced skeletal muscle p-BCKD^{ser293}, corresponding with increased activity of this enzyme. Only drug-treated males showed elevated plasma BCAAs, while minimal sex differences were found for liver BCAA concentrations following chemotherapy. Due to sex-related differences in cachexia and BCAA metabolism, data from our study suggests that aged male animals are more susceptible to the damaging effects of chemotherapy.

Introduction

Cachexia is a complex metabolic muscle wasting syndrome that affects the majority of hospitalized cancer patients receiving chemotherapy (62, 706). The preservation of muscle mass during chemotherapy represents an important therapeutic intervention to increase disease-free survival (707). However, *in-vivo* models that study cancer- and/or chemotherapy-induced cachexia investigate mainly young male animals (6, 8, 18), even though age (1) and sex (2) are two of the most significant risk factors for cancer.

The branched-chain amino acids (BCAA: leucine, isoleucine and valine) are transported into the skeletal muscle by the L-type amino acid transporter 1 (LAT1) and are transaminated by branched-chain aminotransferase 2 (BCAT2) into their respective branched-chain α-ketoacids (BCKA): 2-keto-isocaproate/4-methyl-2-oxopentanoic acid (KIC) from leucine, α-keto-β-methylvaleric acid/3-methyl-2-oxopentanoate (KMV) from isoleucine, and 2-keto-isovalerate/3-methyl-2-oxobutanoic acid (KIV) from valine (33). The BCKAs are then transported mainly towards the liver, where they are oxidatively decarboxylated by the branched-chain α-keto acid dehydrogenase complex (BCKD), an enzyme that is predominantly found in the liver (33). Aside from being metabolized in target tissues, skeletal muscle BCAAs activate components in the sestrins/gator/RAG/ragulator pathway leading to activation of mammalian/mechanistic target of rapamycin complex 1 (mTORC1), a master regulator of protein synthesis (25). Full activation of mTORC1 is dependent on insulin and growth factor stimulation of the insulin receptor substrate-1(IRS-1)/phosphatidylinositol-3 kinase (PI3K)/protein kinase B (AKT) pathway, which allows RHEB, an mTORC1 activator to remain GTP loaded (24, 25). However, in cachexia, these anabolic pathways are downregulated, while catabolic pathways, such as autophagy/lysosomal and ubiquitin proteasome pathways (UPP) are elevated (495).

Animal studies have begun to show that the BCAAs have some positive effects on reversing cancer-induced cachexia (36, 337). Interestingly, these studies are conducted in young animals, although age and sex differences exist for BCAA metabolism. Males have higher BCAA concentrations (48) and leucine oxidation following endurance exercise (49). In addition, estrogen can decrease BCAA metabolism in females (603). Further, aged individuals (708) and animals (709) exhibit significantly lower amino acid concentrations and protein intake compared to their younger counterparts. However, the effect of chemotherapy on the activity and abundance of enzymes involved in BCAA metabolism, which can play a role in the alteration of plasma and tissue BCAA levels, have not been investigated in any tissue of aged animals. Therefore, one can speculate that the diminished effectiveness of BCAAs in fully reversing the symptoms of cachexia (38, 39), may be due to altered metabolism of these amino acids from chemotherapy. Herein, we present data on sex differences in cachexia outcomes and BCAA metabolism following chemotherapy in aged animals.

Materials and Methods

Ethics Statement

All animal experiments were approved by the York University Animal Care Committee in accordance with the recommendations of the Canadian Council on Animal Care and the requirements of the Government of Ontario's Animal Research Act (1980).

Reagents

Protease inhibitor (#P8340), phosphatase inhibitor (#P5726), dimethyl sulfoxide (DMSO) (#D5879-100ML), O-phthalaldehyde (OPA) (#P1378), puromycin (#P8833), 1,2-diamino-4,5-methylenedioxybenzene (DMB, #66807) and our chemotherapy drugs, CPT-11 (#I1406), 5FU (#F6627) and leucovorin (#F7878) were purchased from Sigma Aldrich (St. Louis, MO). Insulin was purchased over the counter from Shoppers Drugmart (Humulin R, #DIN00586714). Radioactive ^{14}C-L-valine (#NEC291EU050UC) was purchased from Perkin Elmer and DTT from MP Biomedicals (#2190D-A101X). Saline was purchased from Wisent (#311-010-CL).

Animals

Two-month-old CD2F1 male and female mice were purchased from Charles River Laboratories. Mice were acclimatized and housed in the vivarium with free access to food and water. Mice were aged to 18±2-months prior to receiving any treatment. According to the Jackson Lab, an 18-month-old mouse is equivalent to a 56-year-old human. Mice were separated into four groups: male vehicle, male drug, female vehicle, female drug (n=10 for all). Mice were administered intraperitoneally either the chemotherapy drug cocktail folfiri (50mg/kg 5FU, 90mg/kg Leucovorin and 24mg/kg CPT-11) (drug) or vehicle (10% DMSO in saline) for 6-weeks. Animal body weight and food consumption were recorded daily for the entirety of the treatment timeline (see appendix G for a weekly example). All animals were sacrificed via

cervical dislocation. Following sacrifice, several skeletal muscles and tissues were collected, weighed, frozen in liquid nitrogen and stored at -80°C for further analysis.

Insulin Tolerance Testing

Insulin tolerance tests (ITT) were performed in all animals at week 3 and 6 of treatment. Insulin (0.75units/kg) was administered subcutaneous after a 6h fast and blood glucose concentrations (AlphaTRAK Blood Glucose Monitoring System, #71675-01) measured on glucose strips (Alpha TRAK, #71681) were collected from the saphenous vein at 0, 5, 15, 30 and 120 minutes. Following each ITT, mice were rehydrated with a 750µL of saline.

BCKD Activity Assay

A homogenizer (Bio-Gen PRO200 Homogenizer) was used to crush frozen gastrocnemius or liver in 250µL of ice-cold buffer 1 (30mM KPI, 3mM EDTA, 5mM DTT, 1mM valine, 3% FBS (Gibco, #12483-020), 5% Triton X-100 (MP Biomedicals, LLC, #M2528), 1µm leupeptin). We then centrifuged the supernatant (10minutes at 10,000g, 4°C) and added 50µL of the supernatant into buffer 2 (300µL of 50mM HEPES, 30mM KPI, 0.4mM CoA, 3mM NAD+, 5% FBS, 2mM Thiamine, 2mM magnesium chloride and 7.8µM [^{14}C]valine). Valine was used as KIV, the keto acid of valine, is the preferred substrate for BCKD (33). Eppendorf tubes containing a raised 2M NAOH CO_2 wick served as a vessel for the reaction. The eppendorf tube was capped and then tape was used to create a tight seal to prevent any escaping of CO_2. Following 30 minutes in a non-shaking incubator set to 37°C, the radiolabeled $^{14}CO_2$ contained in the wick trap was counted in a liquid scintillation counter. To calculate BCKD activity, we divided each CPM by the amount of counts that is equal to 1µmol of the BCKD enzyme activity and corrected for total protein. See Appendix H for full procedure.

Western Blotting:

This procedure is similar to that of Chapter 5. Approximately 30-200mg of gastrocnemius muscle or liver tissue was weighed out and homogenized in 7X complete buffer: 20mM HEPES, 2mM EGTA, 50mM NaF, 100mM KCI, 0.2mM EDTA, 50mM B-Glycerospahte. This buffer was completed with protease inhibitor (10µL/mL), phosphatase inhibitor(10µL/mL), sodium vanadate (2.5µL/mL), DTT (1µL/mL) and benzamidine (5µL/mL). Homogenized samples were then centrifuged (1000g for 3 minutes, 4°C), and the resulting supernatant was centrifuged again (10000g for 30minutes, 4°C). Protein concentration was determined using the Pierce BCA Protein Assay Kit (Thermo Scientific #23225). Approximately 25µg of protein was then loaded and electrophoreses in 10 or 15% SDS-page gels. Gels were transferred overnight onto PVDF (0.2µM, BIO-RAD) membranes and quality of transfer was measured via ponceauS staining. Membranes were then incubated in milk to block non-specific antigen binding. Each membrane then underwent a 3x5 minute wash in TBST followed by overnight incubation at 4°C in the primary antibody of interest:

Primary Antibody	Dilution	Company	Secondary
MHC-1	1:500	Development Hybridoma #MF 20 – s	Mouse
Tropomyosin	1:400	Development Hybridoma #CH1 – s	Mouse
Troponin	1:400	Development Hybridoma #JLT12 – s	Mouse
p-FoxO3a^{ser253}	1:1000	Cell Signalling #9466	Rabbit
p-AKT^{ser473}	1:2000	Cell Signalling #4060	Rabbit
p-S6$^{ser235/236}$	1:1000	Cell Signalling #4858	Rabbit
p-S6K1^{thr389}	1:1000	Cell Signalling #9234	Rabbit
SNAT1	1:1000	Cell Signalling #36057	Rabbit
p-BCKD^{ser293}	1:1000	Cell Signalling #40368	Rabbit
BCKD	1:1000	Cell Signalling #90198	Rabbit
BCAT2	1:1000	Protein Tech #16417-1-AP	Rabbit
LAT1	1:500	Invitrogen #PA5-50485	Rabbit
MuRF1	1:1000	Protein Tech #55456-1-AP	Rabbit
BDK	1:1000	Invitrogen #PA5-31455	Rabbit
γ-tubulin	1:10000	Sigma Aldrich #T6557	Mouse

The following day, membranes were washed 3x5 minutes in TBST and incubated in either anti rabbit (Cell Signalling) or mouse (Cell Signalling) secondary antibodies for 3h. Membranes were washed again 3x5 minutes in TBST and HRP chemical luminescent was applied to each membrane and BioRad ChemiDoc XRS+ was used for signal visualization. Images were quantified using image lab software v7 (Bio-Rad).

High Pressure Liquid Chromatography

For BCAA concentrations, this procedure was similar to that of Chapter 5. During sample preparation of skeletal muscle and liver (see section *"Western Blotting"*), free amino acids were collected from the supernatant following the centrifugation step (10000g for 30 minutes). Amino acids (also from plasma) were diluted in a ratio of 1 (sample): 2 (potassium borate buffer): 1 (0.1N HCl): 8 (HPLC grade water). Diluted samples from skeletal muscle, liver and plasma were pre-column derivatized in a ratio of 1 (sample): 1 (OPA). Samples were then injected into a YMC-Triart C18 column (C18, 1.9µm, 75 x 3.0mm; YMC America, Allentown, PA, USA) fitted onto an ultra HPLC (Nexera X2, Shimadzu, Kyoto, Japan) system connected to a fluorescence detector (Shimadzu, Kyoto, Japan; excitation: 340nm; emission: 455nm). A gradient solution derived from 20mM potassium phosphate buffer (pH 6.5) (Mobile phase A) and a solution made from HPLC grade water (15%), acetonitrile (45%) and methanol (40%) (Mobile phase B) at a flow rate of 0.8mL/min was used to elude the amino acids. A gradient made up of 5%-100% mobile phase B was run over 21 minutes. Amino acid standard curves were used to help calculate amino acid concentrations and all samples from muscle and liver were normalized to total protein. See appendix C for full procedure.

For BCKA concentrations, homogenized muscle, liver and plasma samples, as well as standards were diluted in a 1:2:1:8 ratio (sample: potassium phosphate buffer: HPLC grade

water/homogenization buffer: HPLC grade water, respectively). Following dilution, samples were treated with DMB in 1:1 ratio. DMB solution was made by preparing 1.6mg of DMB of 1mL of solution containing: 4.9mg sodium sulfite, 70μL of 2-mercaptethanol, and 58μL of concentrated HCl in 870μL of ddH_2O. The sample + DMB solution was then heated (85°C, 45 minutes), cooled (on ice) and injected into a Inertsil ODS-4 (2 μm, 100 × 2.1 mm; GL Sciences, Torrance, CA, USA) fitted onto an ultra HPLC system (Nexera X2, Shimadzu, Kyoto, Japan) connected to a fluorescence detector (Shimadzu, Kyoto, Japan; excitation: 340nm; emission: 455nm). Using mobile phases A (30% water, 70% MeOH) and B (100% MeOH), flow rate was maintained at 0.2mL/min with stable column temperature (40°C). Full procedure in appendix C.

Protein Synthesis (SuNSET Analysis)

To avoid any nutrient effects on protein synthesis, mice were starved for 3h. Following starvation, mice were injected intraperitoneally with 0.040μmol/g bodyweight of puromycin in saline 30 minutes prior to euthanasia. Skeletal muscle samples were then immunoblotted against an anti-puromycin antibody (EMD Millipore, #MABE343) and corrected to their respective ponceauS staining.

Statistical Analysis

All immunoblot analyses were quantified and adjusted to their corresponding γ-tubulin values. Gamma tubulin was used as loading control as we noticed no significant effects of chemotherapy on it's abundance. In some cases, double bands are noticed in gamma tubulin blots. This is because when the membranes were previously blotted against anti-BCKD or p-BCKD^{ser293} antibodies before blotting with anti-gamma tubulin antibodies, the signals from BCKD or p-BCKD^{ser293} could still be seen. All graphs were drawn using Graph pad prism version 9. A two-way-ANOVA was used to measure treatment differences between all

conditions. The effect of chemotherapy within sex (male vehicle vs male drug OR female vehicle vs female drug) was identified as a *. Sex differences in chemotherapy's effect (male drug vs female drug) was identified as a $. Significance was determined when p-value < 0.05. P-values were considered a trend when they were equal to or less than 0.1. Results were expressed as standard error of the mean (SEM).

Results

Body and organ weights in aged animals treated with chemotherapy

Male (16%) and female (21%) aged mice lost weight following chemotherapy (Figure 6.1A). Body weight loss at each time point relative to control can be found in Appendix I. Weight loss was not due to differences in food intake (Figure 6.1B). Minimal effects of chemotherapy were found on heart, kidney and liver weights (Figure 6.1C – E). Males (p=0.06) and females (p=0.1) trended for increases in spleen weight (Figure 6.1F), while both sexes exhibited decreases in adipose tissue weight following chemotherapy (Figure 6.1G).

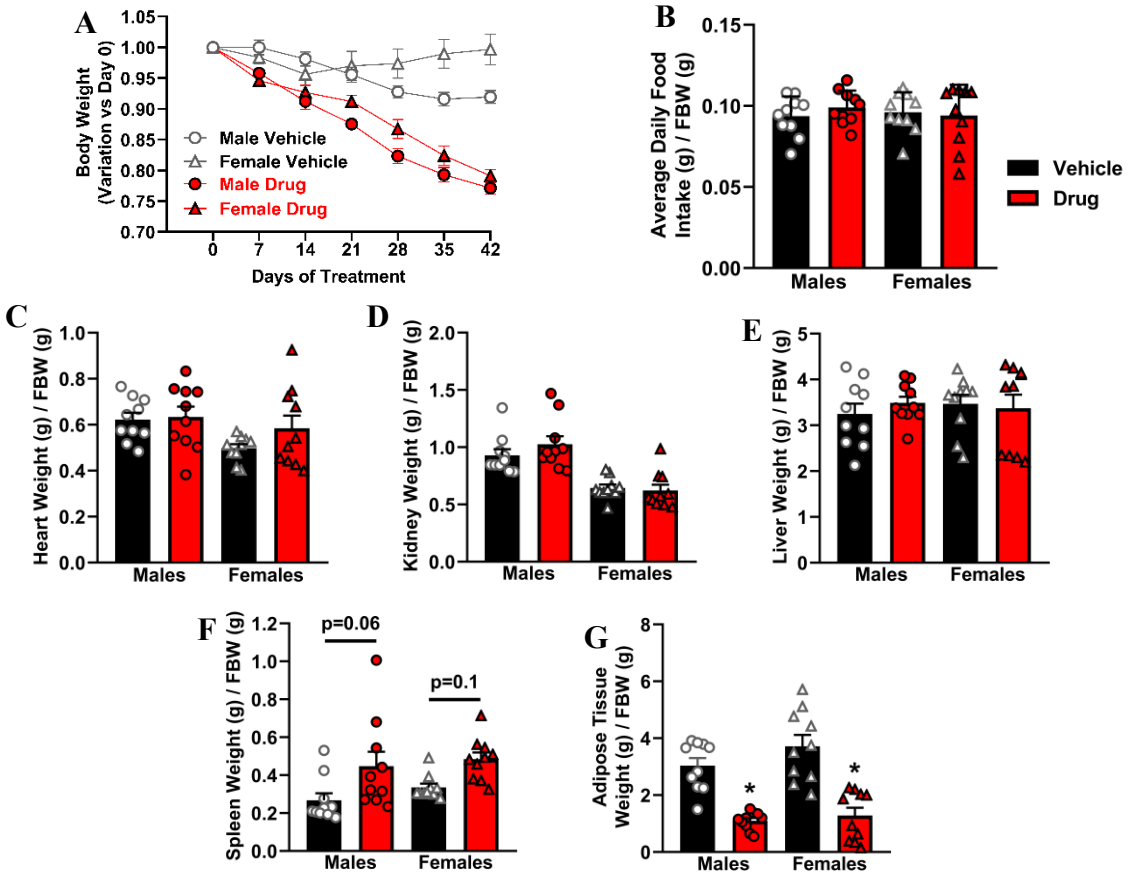

Fig 6.1 Body and organ weights in aged animals treated with chemotherapy. Male and female (18±2 months of age) CD2F1 mice were treated with either vehicle (10% DMSO in saline, black bars) or a chemotherapy drug cocktail (Drug: 50mg/kg 5-FLU, 90mg/kg Leucovorin, 24mg/kg CPT11, red bars) for 6 weeks. Body weight **(A)** and food intake **(B)** were recorded daily for 6 weeks. Weights of the organs: heart **(C)**, kidney **(D)**, liver **(E)**, spleen **(F)** and adipose tissue **(G)** are shown. Weights were normalized to final body weight (FBW). Bar graphs show mean ± SEM, n = 10, * $p < 0.05$ for the effect of chemotherapy. g, gram;

Skeletal muscle weights in aged animals treated with chemotherapy

Both sexes showed decreases in the skeletal muscle mass of the gastrocnemius and tibialis anterior following chemotherapy, with the loss of the gastrocnemius being worse in males (Figure 6.2A, B). Only males showed decreases in quadricep muscle weight (Figure 6.2C), while only females showed decreases in EDL weight (Figure 6.2D). No differences were found for soleus weight (Figure 6.2E). Myofibrillar proteins: MHC-1, troponin and tropomyosin were decreased following chemotherapy in both sexes (Figure 6.2F – I).

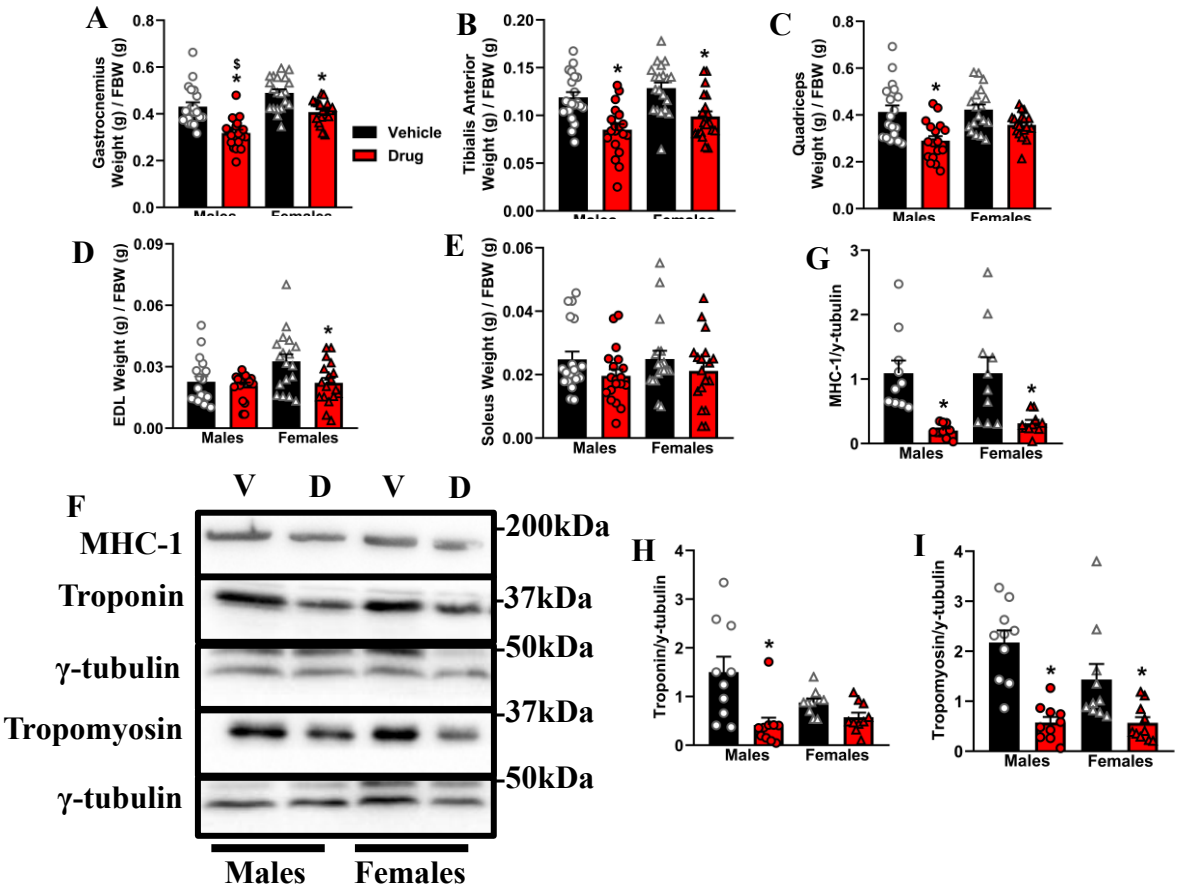

Fig 6.2 Skeletal muscle weights in aged animals treated with chemotherapy. Mice were treated as indicated in the legends to figure 1. Weights of the skeletal muscles: gastrocnemius **(A)**, tibialis anterior **(B)**, quadriceps **(C)**, EDL **(D)** and soleus **(E)** are shown. Weights were normalized to final body weight (FBW). Immunoblotting **(F)** and quantified data for MHC-1 **(G)**, troponin **(H)**, and tropomyosin **(I)** are shown. Bar graphs show mean ± SEM, n = 10, * $p < 0.05$ for the effect of chemotherapy, $ $p < 0.05$ for sex differences in chemotherapy's effect. V, Vehicle; D, Drug; g, gram; FBW, final body weight; MHC-1, myosin heavy chain-1.

Insulin tolerance, anabolic signalling and catabolic signalling following chemotherapy in aged animals

At week 3, chemotherapy had no effect on insulin tolerance in either sex, but drug-treated males had higher blood glucose (Figure 6.3A, B). By week 6, impaired insulin tolerance was observed in both sexes, with the impairment being more severe in males (Figure 6.3C, D). Chemotherapy decreased the phosphorylation of AKT^{ser473}, $S6K1^{thr389}$ and $S6^{ser235/236}$, corresponding with decreased protein synthesis (SuNSET analysis) in both sexes (Figure 6.3E – J). No effects of chemotherapy were found on the catabolic signals p-$FoxO3a^{ser253}$ or MuRF1 (Figure 6.3K – M). Lastly, chemotherapy treatment increased ubiquitination of proteins only in males (compared to male control and drug-treated females; Figure 6.3N, O).

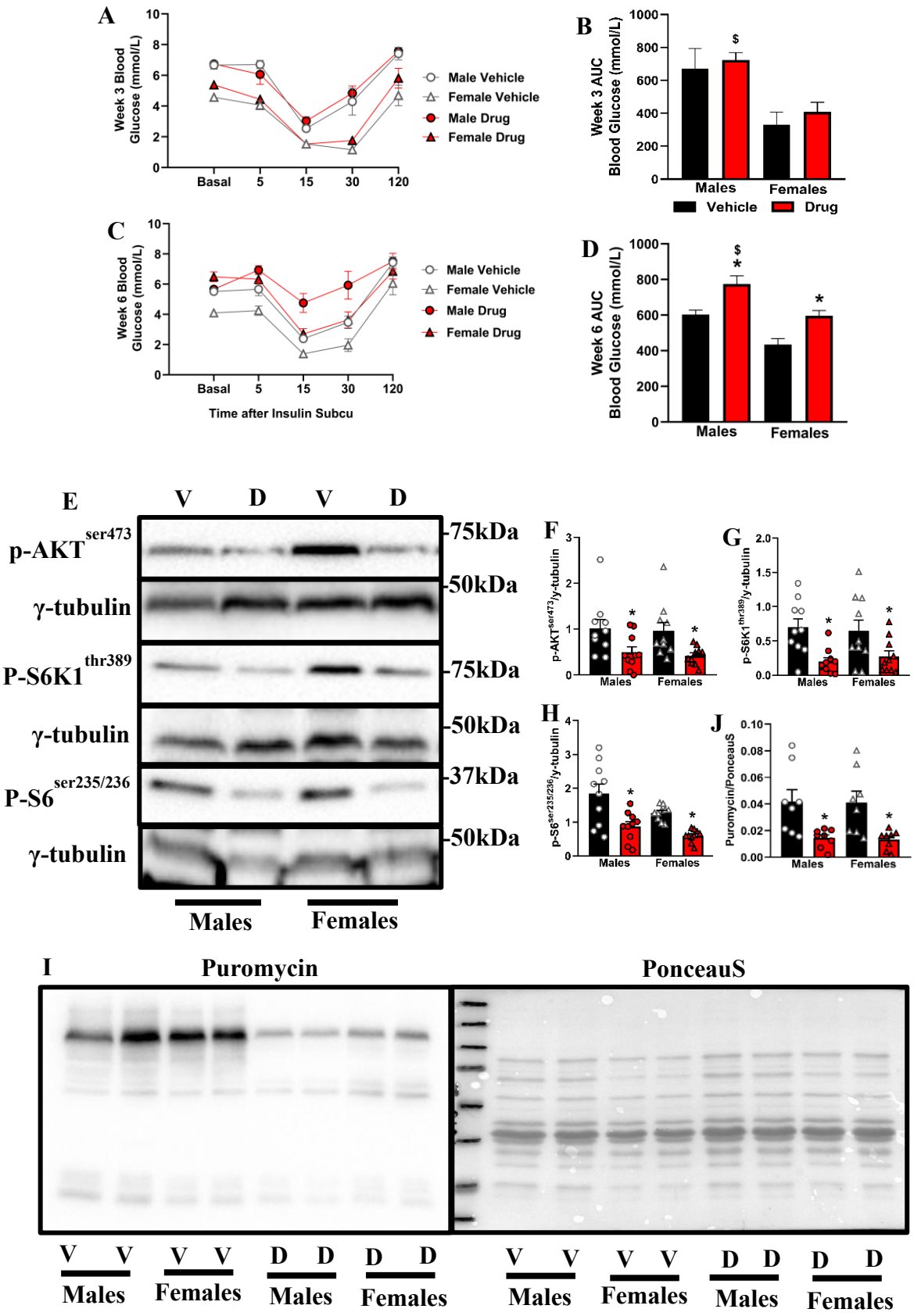
A
Week 3 Blood Glucose (mmol/L)
Male Vehicle
Female Vehicle
Male Drug
Female Drug
Basal
5
15
30
120
B
Week 3 AUC Blood Glucose (mmol/L)
Males
Females
Vehicle
Drug
C
Week 6 Blood Glucose (mmol/L)
Time after Insulin Subcu
D
Week 6 AUC Blood Glucose (mmol/L)
E
V
D
p-AKT ser473
γ-tubulin
P-S6K1 thr389
P-S6 ser235/236
75kDa
50kDa
37kDa
Males
Females
F
G
H
J
Puromycin/PonceauS
I
Puromycin
PonceauS

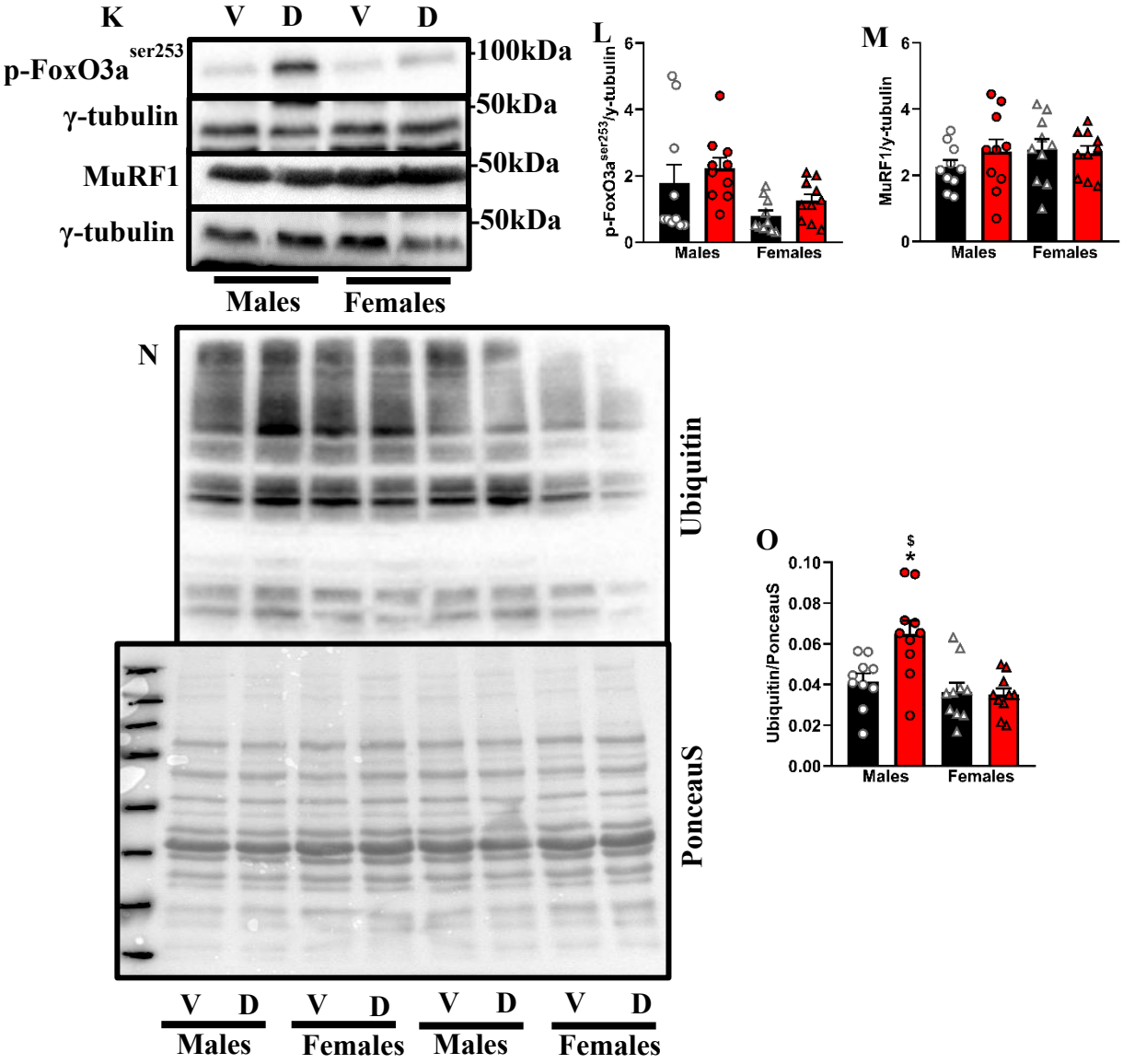

Fig 6.3 Insulin tolerance, anabolic signalling and catabolic signalling following chemotherapy in aged animals. Mice were treated as indicated in the legends to figure 1. At week 3 **(A, B)** and 6 **(C, D)** of treatment, all animals were starved for 6h and then underwent insulin tolerance testing. Immunoblotting **(E)** and quantified data for the phosphorylation of AKT^{ser473} **(F)**, S6K1^{thr389} **(G)** and S6$^{ser235/236}$ **(H)** are shown. Thirty minutes prior to euthanasia, mice were injected with 0.040µmol/g bodyweight of puromycin, euthanized and muscle protein samples were immunoblotted **(I)** against an anti-puromycin antibody and quantified/corrected to their respective ponceauS stain **(J)**. Immunoblotting **(K)** and quantified data for phosphorylated FoxO3a^{ser253} **(L)**, the skeletal muscle E3 ligase MuRF1 **(M)** and ubiquitinated proteins **(N, O)** are shown. Bar graphs show mean ± SEM, n = 8-10, * $p < 0.05$ for the effect of chemotherapy, $ $p < 0.05$ for sex differences in chemotherapy's effect. V, Vehicle; D, Drug; AUC, area under curve; p, phosphorylation.

Chemotherapy decreases skeletal muscle BCAA concentrations in aged male animals

Chemotherapy decreased AA concentrations of leucine, valine, total BCAAs and arginine only in males (Figure 6.4A – E). However, total BCAAs were higher in drug-treated males compared to drug-treated females. In both sexes, drug treatment had minimal effects on concentrations of alanine, phenylalanine, and serine (Figure 6.4F – H), while drug-treated males had higher glutamate concentrations compared to females (Figure 6.4I). Minimal effects were found on muscle BCKA concentrations (Figure 6.4J – L). Both sexes showed significant decreases in LAT1, but not SNAT1 following chemotherapy (Figure 6.4M – O).

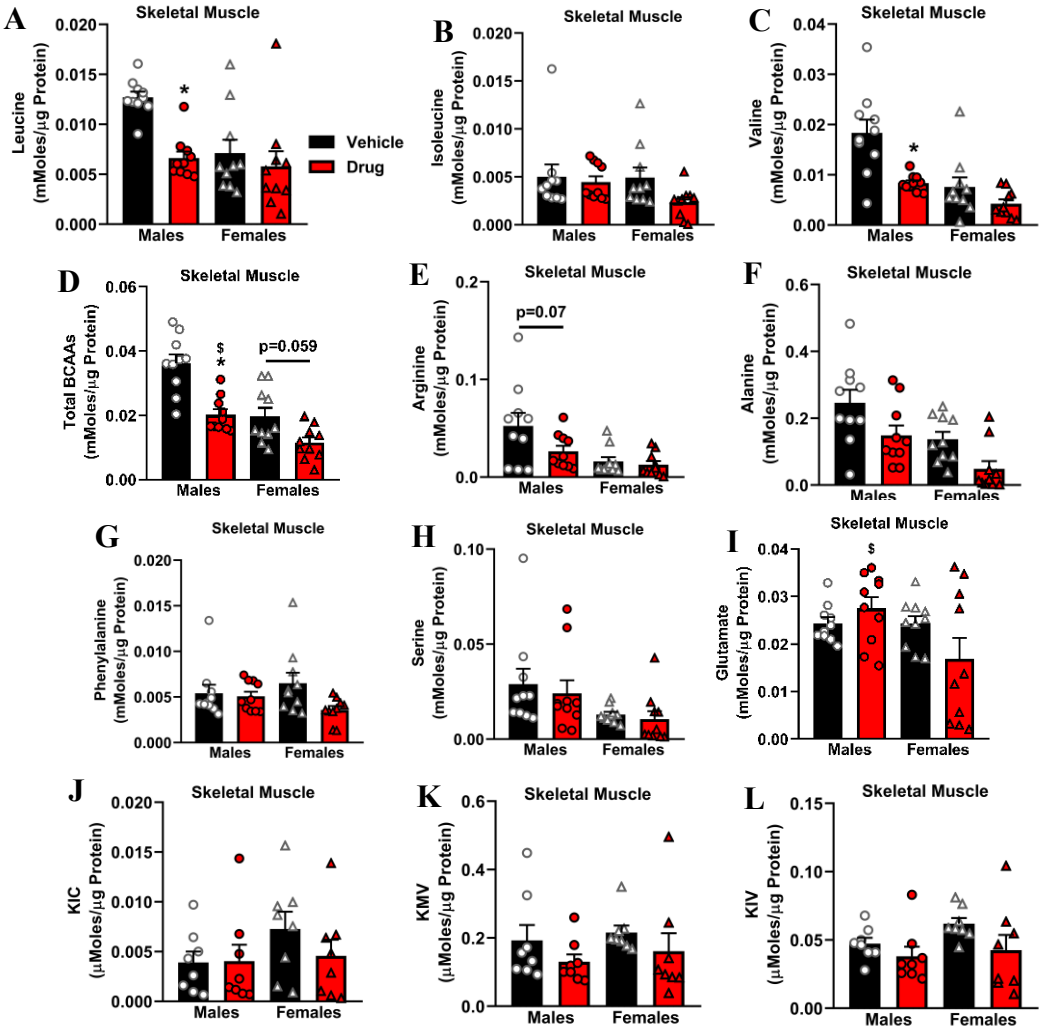

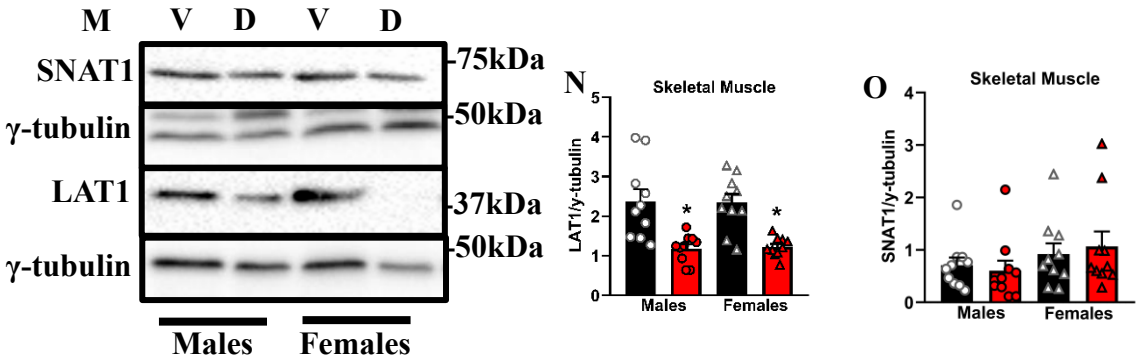

Figure 6.4 Chemotherapy decreases skeletal muscle BCAA concentrations in aged male animals. Mice were treated as indicated in the legends to figure 1. Concentrations of leucine **(A)**, isoleucine **(B)**, valine **(C)**, total BCAAs **(D)**, arginine **(E)**, alanine **(F)**, phenylalanine **(G)**, serine **(H)**, glutamate **(I)**, KIC **(J)**, KMV **(K)** and KIV **(L)** in the gastrocnemius muscle were detected via HPLC. Immunoblotting **(M)** and quantified data for LAT1 **(N)** and SNAT1 **(O)** are shown. Bar graphs show mean ± SEM, n = 8-10, * $p < 0.05$ for the effect of chemotherapy, $ $p < 0.05$ for sex differences in chemotherapy's effect. BCAAs, branched-chain amino acids; HPLC, high-pressure liquid chromatography. V, Vehicle; D, Drug.

In aged animals, chemotherapy increases skeletal muscle BCAA metabolism in males

Key enzymes involved in BCAA metabolism, BCAT2, BCKD and BDK were all unchanged following chemotherapy in both sexes (Figure 6.5A – D). Chemotherapy decreased p-BCKD^{ser293}, consistent with increased BCKD activity only in males following chemotherapy (Figure 6.5A, E, F).

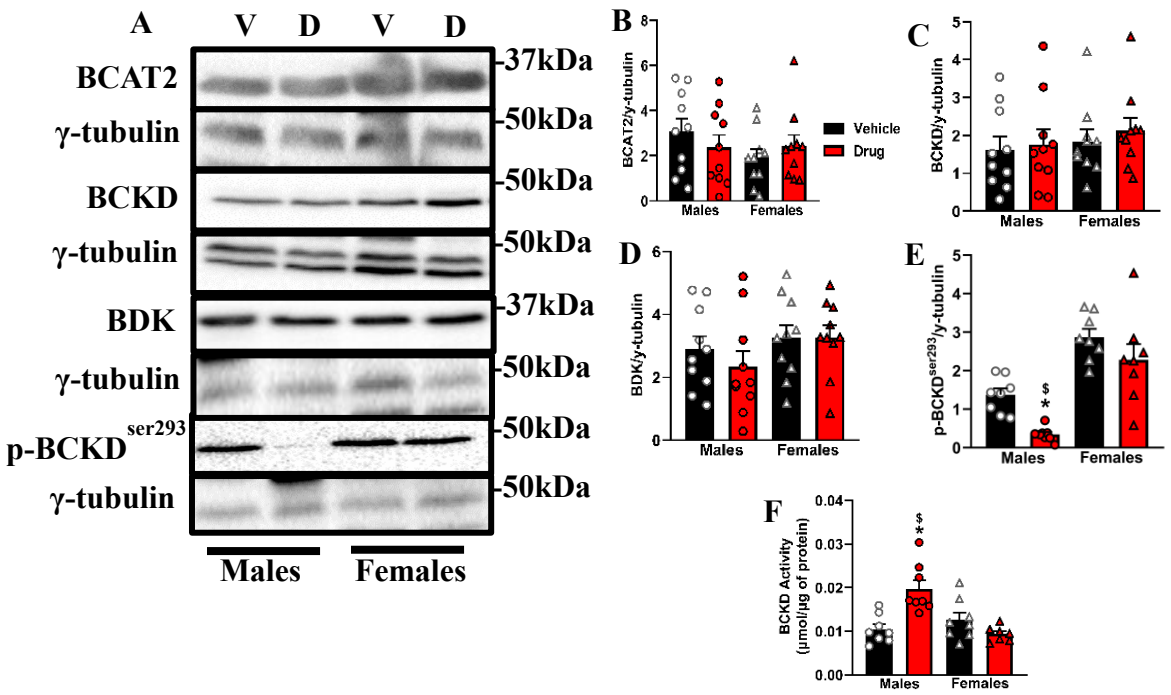

Figure 6.5 In aged animals, chemotherapy increases skeletal muscle BCAA metabolism in males. Mice were treated as indicated in the legends to figure 1. Key enzymes involved in BCAA metabolism were immunoblotted **(A)** and quantified against antibodies to BCAT2 **(B)**, BCKD **(C)**, BDK **(D)** and phosphorylated BCKD^{ser293} **(E)**. The enzymatic activity of BCKD was measured from the release of $^{14}CO_2$ (BCKD's decarboxylation) from ^{14}C labelled valine **(F)**. Bar graphs show mean ± SEM, n = 8-10, * $p < 0.05$ for the effect of chemotherapy, $ $p < 0.05$ for sex differences in chemotherapy's effect. V, Vehicle; D, Drug.

Chemotherapy leads to increased BCAAs in the plasma, but not the liver of aged animals

Chemotherapy increases plasma levels of leucine, but not isoleucine in both sexes (Figure 6.6A, B). Only males showed elevated levels of plasma valine and total BCAAs following chemotherapy (Figure 6.6C, D). No differences were found for plasma BCKAs (Figure 6.6E – G) or liver BCAA levels following chemotherapy (Figure 6.6H – K). However, drug-treated females exhibited decreases in liver KMV and KIV, but not KIC (Figure 6.6L – N). Minimal differences were found for protein expression of LAT1, BCKD and BDK in the liver of either sex (Figure 6.6O – R). Chemotherapy decreased p-BCKD^{ser293}, corresponding to elevations in liver BCKD activity in both sexes (Figure 6.6O, S, T).

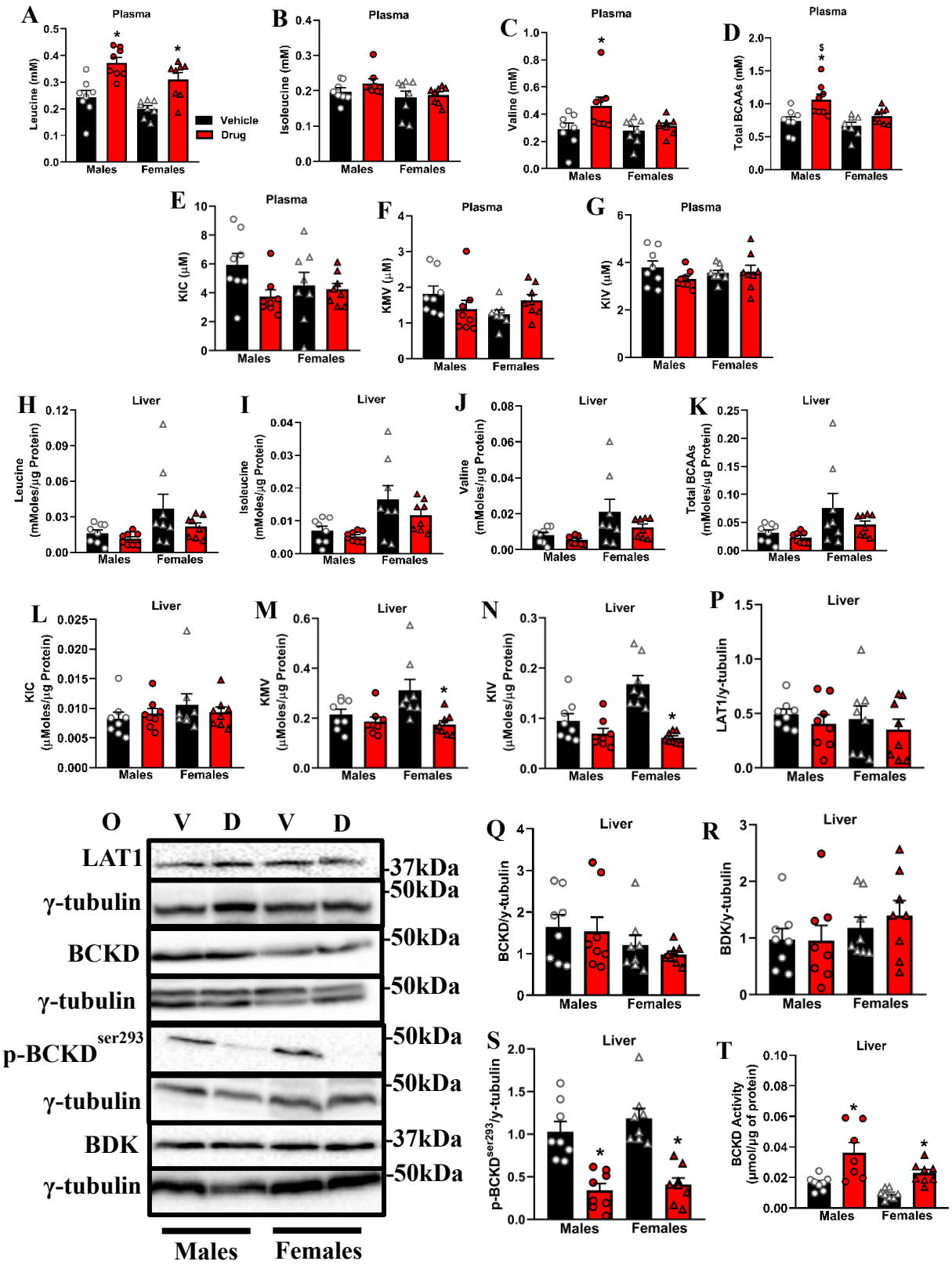
A
Plasma
Leucine (mM)
Vehicle
Drug
Males
Females
B
Plasma
Isoleucine (mM)
C
Plasma
Valine (mM)
D
Plasma
Total BCAAs (mM)
E
Plasma
KIC (μM)
F
Plasma
KMV (μM)
G
Plasma
KIV (μM)
H
Liver
Leucine (mMoles/μg Protein)
I
Liver
Isoleucine (mMoles/μg Protein)
J
Liver
Valine (mMoles/μg Protein)
K
Liver
Total BCAAs (mMoles/μg Protein)
L
Liver
KIC (μMoles/μg Protein)
M
Liver
KMV (μMoles/μg Protein)
N
Liver
KIV (μMoles/μg Protein)
P
Liver
LAT1/γ-tubulin
O
V
D
V
D
LAT1
γ-tubulin
BCKD
γ-tubulin
p-BCKD ser293
γ-tubulin
BDK
γ-tubulin
37kDa
50kDa
50kDa
50kDa
50kDa
50kDa
37kDa
50kDa
Males
Females
Q
Liver
BCKD/γ-tubulin
R
Liver
BDK/γ-tubulin
S
Liver
p-BCKDser293/γ-tubulin
T
Liver
BCKD Activity (μmol/μg of protein)

Figure 6.6 Chemotherapy treatment leads to increased BCAAs in the plasma, but not the liver of aged animals. Mice were treated as indicated in the legends to figure 1. Plasma leucine **(A)**, isoleucine **(B)**, valine **(C)**, total BCAAs **(D)**, KIC **(E)**, KMV **(F)** and KIV **(G)**, as well as liver leucine **(H)**, isoleucine **(I)**, valine **(J)**, total BCAAs **(K)**, KIC **(L)**, KMV **(M)**, KIV **(N)** were measured by HPLC. Immunoblotting **(O)** and quantified data for liver LAT1 **(P),** BCKD **(Q)**, BDK **(R)** and p-BCKD^{ser293} **(S)** are shown. BCKD activity in the liver **(T)**. Bar graphs show mean ± SEM, n = 8, * $p < 0.05$ for the effect of chemotherapy, $ $p < 0.05$ for sex differences in chemotherapy's effect. V, Vehicle; D, Drug; BCAAs, branched-chain amino acids; HPLC, high-pressure liquid chromatography.

BCAAs are positively correlated with muscle weight and LAT1, but not BCKD activity

Significant positive correlations were found between total BCAA and gastrocnemius muscle weight (Figure 6.7A) and LAT1 transporter expression (Figure 6.7B), but not BCKD activity (Figure 6.7C). However, gastrocnemius muscle weight was positively correlated with BCKD activity (Figure 6.7D) and LAT1 (6.7E).

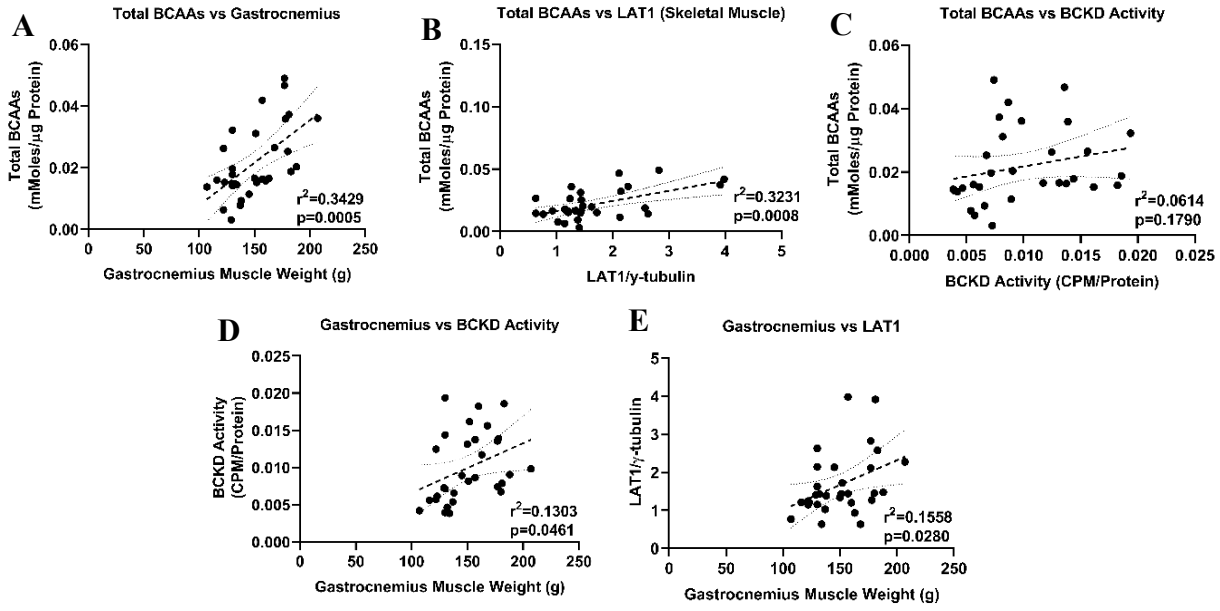

Fig 6.7 BCAAs are positively correlated with muscle weight and LAT1, but not BCKD activity. Correlations between total BCAAs and gastrocnemius **(A)**, LAT1 expression **(B)** and skeletal muscle BCKD activity **(C)**. Gastrocnemius muscle weight and LAT1 **(D)** and BCKD activity **(E)** correlations are also shown. Data were analyzed using linear regression and 95% confidence intervals are denoted. BCAAs, branched-chain amino acids; BCKD, branched-chain α-keto acid dehydrogenase complex.

Discussion

Herein, we report sex-related differences in cachexia and tissue-related BCAA metabolism/handling following chemotherapy in aged animals. We observed greater loss of gastrocnemius muscle weight, consistent with greater impairments in insulin tolerance and higher protein ubiquitination in males. Although LAT1, the canonical BCAA transporter, was decreased following chemotherapy in both sexes, only drug-treated males showed decreases in skeletal muscle BCAA concentrations. Further, only drug-treated males exhibited decreases in p-BCKD^{ser293}, corresponding to higher muscle BCKD activity. Findings from this study highlight sex-related differences in BCAA utilization/oxidation following chemotherapy in aged animals and are predictive of greater susceptibility to the damaging effects of chemotherapy in males.

Minimal sex differences were found for cachexia outcomes in aged animals. In addition, chemotherapy had no effect on food intake, as seen in a past study (8). This finding is likely due to the fact that we corrected food intake to final body weight, as this gives a better indication of food intake, rather than a result mediated by changes in overall body weight. Nonetheless, following chemotherapy, males lost more gastrocnemius and quadriceps skeletal muscle weight. This finding could be due to age-related decreases in testosterone (710). Although females also lose this hormone during aging (711), testosterone loss in males is predictably more detrimental, as testosterone is the prime anabolic hormone responsible for muscle mass regulation in males (690). This data is in opposition to our findings in young animals, as we have previously shown that chemotherapy causes more severe losses in female skeletal muscle following chemotherapy (Chapter 5, Study 2). Since, lean body mass is a determinant of chemotherapy dose (21), our data suggests that aged males are at a greater risk of decreased treatment effectiveness.

Insulin resistance is a common feature of cachexia (696). Consistent with worsened

cachexia outcomes, male aged animals exhibited greater impairments in insulin tolerance following chemotherapy. Prolonged increases in circulating plasma BCAA levels are associated with insulin resistance (702), an observation made only in males. In addition, as a measure of insulin action, we measured and found no differences for phosphorylation of AKT^{ser473}, but males were still less insulin tolerant compared to females. We previously found similar findings in young animals; whereby male mice were less insulin tolerant following chemotherapy (Chapter 5, Study 2). However, in young female mice, estrogen has protective effects against insulin resistance (697), an effect not seen in old females due to age-related decreases in estrogen. Therefore, investigating sex differences in other factors that are both increased by chemotherapy and induce insulin resistance warrants further research.

Consistent with previous reports (610), decreases in mTORC1 signalling and protein synthesis were independent of sex following chemotherapy. In addition, ubiquitin proteasome activity is reported to be higher in males (664), a finding in line with our observation of higher protein ubiquitination in males following chemotherapy. This observation could be related to the fact that testosterone, a hormone decreased in aging (710), can repress ubiquitin ligase expression (712). However, MuRF1, the E3 ligase responsible for the majority of protein ubiquitination in skeletal muscle (32), was not affected by chemotherapy treatment in either sex. It is possible that the catabolic effects of aging on MuRF1 expression was already significant (713) and therefore could not be worsened by chemotherapy. Nonetheless, chemotherapy-induced changes in other E3 ligases (not measured here) such as MAFbx/atrogin-1, parkin and Mind Bomb-1 (714), could account for the higher protein ubiquitination found in males. In addition, using MG132 to inhibit the proteasome may provide a more accurate picture of polyubiquitinated proteins, as sometimes antibody detection of ubiquitinated proteins is

inaccurate as some of the ubiquitinated proteins may have been degraded quickly (698).

Currently, interventions that prevent or attenuate muscle wasting are at the forefront of studies involving cachexia. Therefore, due to their anabolic properties (34), we were interested in the effects of chemotherapy on the BCAAs, as supplementation with these amino acids to do not delay the onset of cachexia. In healthy individuals, treatment with the BCAAs increases protein synthesis, while simultaneously decreasing protein breakdown (34). Therefore, in males, our observation of decreased skeletal muscle BCAAs is consistent with greater muscle weight loss and higher ubiquitination of proteins. Although reduced skeletal muscle BCAAs in males could be attributable to the effect of chemotherapy on reducing LAT1, females shared this decrease in the transporter, but did not show significant decreases in skeletal muscle BCAAs. Therefore, altered metabolism may account for the observed sex differences in skeletal muscle BCAA concentrations. Following chemotherapy in females, higher phosphorylation (inhibition) of $BCKD^{ser293}$ and decreased glutamate, suggests a sex-related compensatory mechanism, whereby BCAT2 can remove the amino group from glutamate and transfer it to the BCKAs (33), regenerating the BCAAs. This mechanism is further supported by no changes in plasma BCKAs and reduced BCKAs in the liver of females, as more BCKAs can build up in the skeletal muscle and be reconverted towards replenishing the BCAA pool to protect against atrophy. This compensatory mechanism seen in females, was not the case in males. Decreased p-$BCKD^{ser293}$ and increased skeletal muscle BCKD activity in males suggests greater breakdown of the BCAAs and their keto acids in the skeletal muscle, as males have been reported to oxidize more amino acids for energy during substrate deficits (699).

A limitation of this study is the clinical implication of treating healthy mice with chemotherapy. However, considering frailty and declines in regenerative processes with aging

(715), we can speculate that our aged mice would not be unable to survive invasive surgical procedures, such as tumour inoculation. In addition, since tumour-inoculated 6-week-old mice only survive ~14 days (7), it is likely that our aged animals would not survive long enough to observe any noticeable effects on body or muscle wasting. Therefore, we used clinically relevant anti-cancer drugs (216) to induce cachexia and probe sex differences in skeletal muscle BCAA metabolism, as metabolism of these amino acids are often only studied in tumours and overlooked in the skeletal muscle (40, 41). We also did not measure the total protein content of some of our phosphorylated proteins. However, we did measure and find no differences in total BCKD expression, while still finding differences in its phosphorylated form. In addition, we have previously shown no differences in the total levels of AKT, S6 and S6K1 following chemotherapy treatment with a similar cocktail in myotubes (chapter 4) and mice (chapter 5).

In summary, our data reveals that following chemotherapy in aged animals, males have worsened outcomes for gastrocnemius muscle weight, insulin tolerance and ubiquitination of proteins. In addition, aged male, but not aged female animals exhibit decreases in skeletal muscle BCAA concentrations, a finding related to sex differences in whole-body BCAA metabolism/utilization following chemotherapy. Our data suggests that in aged animals, males are most susceptible to muscle wasting during chemotherapy.

Author Contributions

SM and OAJA designed the experiments. SM performed all body weight, food intake and chemotherapy dosing measurements, dosing and calculations. SM performed euthanasia and tissue weight measurements, while GM dissected all tissues. All western blotting was performed by SM. For ITT, SM performed insulin calculations and injections, saphenous vein blood gathering onto glucose strips and insertion into glucometer, while GM recorded blood glucose values. For HPLC, SM formulated buffers and diluted and loaded all standards/samples, while GM made standards, inserted column and set machine parameters. SM analyzed the samples and drafted the initial version of the manuscript. OAJA reviewed and edited the manuscript. SM, GM and OAJA approve the final version of the manuscript.

Conflict of Interest

The authors declare no conflict of interest.

Acknowledgements

This study was funded by grants from the Natural Science and Engineering Research Council of Canada (NSERC) and from the Faculty of Health, York University, Toronto Canada to OAJA. Thank you to the Muscle Health Research Centre at York University for use of the HPLC. Thank you to the Paluzzi lab for the use of their imaging systems.

Funding

Work is supported by funds from the Natural Science and Engineering Research Council of Canada by the Faculty of Health, York University.

Chapter 7 Summary of Findings

7.1 General Conclusions

Age (1) and sex (2) are significant risk factors for cancer. Over 80% of cancer patients suffer from cachexia, a debilitating skeletal muscle wasting syndrome that significantly affects patient's quality of life (4). Chemotherapy, the most common form of cancer treatment, has also been reported as a major contributor to cachexia (6–8). The majority of previous reports investigating cancer and/or chemotherapy-induced cachexia are completed in young male animals (8, 18). There is currently no available cure for cachexia, and nutritional interventions, such as use of the BCAAs, have only showed some positive effects on cachectic symptoms (36, 37), but they do not fully reverse the syndrome. This could be related to the fact that previous reports investigate the effects of BCAAs and their metabolism only in tumours (40, 41) and how these amino acids are affected in the skeletal muscle are often overlooked. Therefore, altered metabolism of the BCAAs in the skeletal muscle following chemotherapy may help explain or rationalize the diminished effects of the BCAAs in attenuating cachexia.

In chapter 4, I investigated whether maintaining BCAA concentrations in chemotherapy-treated myotubes could attenuate atrophy. In support of my hypotheses, RNAi mediated deletion of NEdd4, the E3 protein ligase responsible for ubiquitin-dependent degradation of LAT1 (676), attenuated the effects of chemotherapy on LAT1 expression, intracellular BCAA concentrations, protein synthesis and myofibrillar protein abundance.

In chapter 5, I evaluated sex differences in cachexia outcomes and BCAA metabolism/availability in young mice following chemotherapy. Against my original hypotheses, we found that females exhibited more severe cachexia, associated with more severe increases and decreases in catabolic and anabolic signalling respectively.

In chapter 6, I explored sex differences in cachexia outcomes and BCAA

metabolism/availability in aged mice following chemotherapy. In support of my hypotheses, only males exhibited skeletal muscle loss of the BCAAs, associated with more severe cachexia.

7.2 Limitations and Future Directions

7.2.1 Chapter 4 (Study 1)

A main limitation of this study is that chemotherapy is not given in the absence of cancer. However, by using a clinically relevant chemotherapy cocktail, this *in-vitro* model allowed me to manipulate and explore the direct mechanistic effects of chemotherapy on skeletal muscle cell atrophy and amino acid metabolism.

Another potential limitation is that the link between myofibrillar protein content, anabolic signalling, BCAA concentrations and protein synthesis following NEdd4 depletion and LAT1 is indirect. Therefore, future experiments should consider overexpression to isolate the effects of LAT1. However, since transient overexpression of LAT1 does not increase intracellular amino acid concentrations nor protein synthesis in myotubes (675), I considered generating a cell line that specifically overexpresses LAT1. In fact, I originally planned to use the CRISPR/CAS9 method to generate this cell-specific line. Although I was able to successfully grow high yield DNA plasmids, I was unable to successfully transfect L6 myoblasts, as no cells survived treatment with antibiotic resistance. This could be due to the efficiency problems associated with transfections in L6 cells. Therefore, future studies using a more efficient cell line for transfections (such as C2C12) or using a transfection reagent (Sigma, #06366236001) may overcome these issues. After successfully establishing a cell line with overexpressed LAT1, I could assess the impact of chemotherapy on myotubes with elevated LAT1 compared to myotubes without LAT1 overexpression. My main question would revolve around determining whether LAT1 overexpression confers a protective effect against chemotherapy-induced atrophy.

I anticipate that myotubes overexpressing LAT1 will exhibit increased resistance to the effects of chemotherapy, given the sustained elevations of BCAA concentrations. This condition would potentially allow for the maintenance of mTORC1 activation and protein synthesis.

Lastly, studying *in-vitro* models poses other limitations. For example, I was unable to investigate the contributions of other tissues, such as the liver to the altered BCAA catabolism that was observed in chemotherapy-treated myotubes. In addition, although the novelty of my work may present the groundwork for future *in-vivo* studies that investigate amino acid transporters in cachexia, this work cannot be generalized to clinical settings unless they are replicated in pre-clinical models. Therefore, *in-vivo* studies investigating the effects of chemotherapy on similar measures as in my *in-vitro* study are warranted. Therefore, it is for this reason that I decided to pursue this in chapters 5 and 6.

7.2.2 Chapter 5 and 6 (Study 2 and 3)

I am aware of the clinical limitations associated with treating healthy mice with chemotherapy, as treatment with chemotherapy in the absence of cancer does not represent clinical settings. However, by using a clinically relevant chemotherapy drug cocktail, I was able to probe age and sex differences in cachexia and BCAA metabolism. In addition, my research does not strive to increase the effectiveness of chemotherapy as cancer treatment. Instead, I use chemotherapy as a model to induce skeletal muscle atrophy. *In-vivo*, this allows me to study the direct effects of chemotherapy on the mechanisms of skeletal muscle atrophy and amino acid metabolism. Nonetheless, in order to strengthen my conclusions, future experiments should include more groups in order to provide a better understanding of clinical settings. For example, tumour inoculation and chemotherapy lead to 10 – 15% decreases in body weight individually, but when tumour inoculation is combined with chemotherapy, greater than 20% body weight loss

can be observed (7). However, since humans who have cancer survive longer when they are treated with chemotherapy, chemotherapy still remains front line treatment for cancer. In addition to a vehicle and chemotherapy group, future experiments should include a tumour group and a tumour group treated with chemotherapy (total of 4 groups). Not only does this design provide a better clinical outlook, but it would also help to understand whether differences in BCAA metabolism between cancer alone and chemotherapy alone are aggregated when these conditions are combined. However, a limitation of this new design, which was also a limitation of study 5 and 6 is that the findings from these studies are purely descriptive in nature and interventions to attenuate the effects of chemotherapy-induced cachexia were not conducted. However, since an examination of age and sex effects on chemotherapy-induced cachexia has been rarely done, it was not clear what kind of interventions would be appropriate. In addition, the novel findings from these studies would be invaluable in designing future studies, as interventions that reduce the onset of cachexia in cancer patients is at the forefront of research today. Therefore, using the findings from chapter 4 (study 1) as the groundwork, generating mice that overexpress skeletal muscle LAT1 (potentially through the Cre/*loxP* system), would allow our lab to explore whether we can replicate my findings from cell culture *in-vivo*. Therefore, this new design would employ 6 groups: vehicle, chemotherapy, tumour, tumour plus chemotherapy, LAT1 overexpression and LAT1 overexpression plus tumour and chemotherapy treatment. Since I have shown that the inability for BCAAs to rescue myotube atrophy may be due to decreases in the transporter expression of LAT1, one could hypothesize that overexpression of skeletal muscle LAT1, may attenuate the loss of skeletal muscle mass from tumour and chemotherapy treatment in mice. However, since LAT1 is overexpressed in many cancers (26), site specific overexpression of LAT1 in the skeletal muscle would need to be confirmed.

Another limitation of these two studies is that I did not investigate the metabolism of the BCAAs in adipose tissue. Therefore, differences in tissue and circulating levels of the BCAAs following chemotherapy may be due to altered metabolism of the BCAAs in adipose tissue, especially when you consider differences in adipose tissue biology and distribution between the sexes (716). This is an area of future study that I am planning to explore.

Table 4 Young male and female percent change for each measured cachectic variable

Measured Variable	Male Percent Change (Vehicle vs Drug)	Female Percent Change (Vehicle vs Drug)	p-value of sex diff (α=0.05)
Body Weight Loss (Wk 6)	**10.9%***	**15%***	**<0.05#**
Skeletal Muscle			
Gastrocnemius	**17%***	**23%***	**<0.05#**
Quadricep	**17%***	**11%***	**0.83**
TA	**37%***	**33%***	**0.27**
Insulin Signalling			
p-AKT^{ser473}	**47%***	**44%***	**0.83**
Anabolic Signalling			
p-S6K1^{thr389}	**36%***	**61%***	**<0.05#**
p-S6$^{ser235/236}$	**50%***	**38%***	**0.29**
Protein Synthesis	**70%***	**83%***	**0.57**
Catabolic Signalling			
p-FoxO3a^{ser253}	**55%**	**46%***	**--**
MuRF1	**108%**	**582%***	**--**
SM BCAA Metabolism			
Total [BCAAs]	**70%***	**33%***	**<0.05#**
LAT1 Expression	**40%***	**50%***	**<0.05#**
BCKD Expression	**--**	**55%***	**--**
p-BCKD^{ser293} Expression	**125%***	**113%***	**0.21**
BCKD Activity	**68%***	**51%***	**0.39**
Plasma			
Total [BCAAs]	**40%***	**10%**	**--**
Liv BCAA Metabolism			
Total [BCAAs]	**99%***	**47%***	**0.11**
LAT1 Expression	**218%***	**201%***	**0.33**
p-BCKD^{ser293}	**150%***	**60%***	**0.08**
BCKD Activity	**81%***	**83%***	**0.32**

*** indicates significant decrease (red) or increase (green) within sex (i.e., male vehicle vs male drug, or female vehicle vs female drug).**

 # indicates significant sex differences in response to drug treatment.

SM: skeletal muscle; BCAA: Branched-chain amino acids; p: phosphorylated; Liv: liver

Table 5 Aged male and female percent change for each measured cachectic variable

Measured Variable	Male Percent Change (Vehicle vs Drug)	Female Percent Change (Vehicle vs Drug)	p-value of sex diff (α=0.05)
Body Weight Loss (Wk 6)	**22%***	**20%***	**0.18**
Skeletal Muscle			
Gastrocnemius	**26%***	**17%***	**<0.05#**
Quadricep	**30%***	**16%**	**0.12**
TA	**28%***	**23%***	**0.25**
Insulin Signalling			
p-AKT^{ser473}	**51%***	**56%***	**0.97**
Anabolic Signalling			
p-S6K1^{thr389}	**72%***	**57%***	**0.93**
p-S6$^{ser235/236}$	**52%***	**53%***	**0.65**
Protein Synthesis	**65%***	**67%***	**0.99**
Catabolic Signalling			
p-FoxO3a^{ser253}	**25%**	**55%**	**0.22**
MuRF1	**25%**	**5%**	**0.98**
SM BCAA Metabolism			
Total [BCAAs]	**44%***	**41%**	**<0.05#**
LAT1 Expression	**51%***	**48%***	**0.99**
BCKD Expression	**--**	**--**	**--**
p-BCKD^{ser293} Expression	**75%***	**20%**	**<0.05#**
BCKD Activity	**49%***	**21%**	**<0.05#**
Plasma			
Total [BCAAs]	**44%***	**22%**	**<0.05#**
Liv BCAA Metabolism			
Total [BCAAs]	**26%**	**38%**	**0.57**
LAT1 Expression	**17%**	**21%**	**0.97**
p-BCKD^{ser293}	**66%***	**65%***	**0.96**
BCKD Activity	**50%***	**98%***	**0.08**

*** indicates significant decrease (red) or increase (green) within sex (i.e., male vehicle vs male drug, or female vehicle vs female drug).**

 # indicates significant sex differences in response to drug treatment.

SM: skeletal muscle; BCAA: Branched-chain amino acids; p: phosphorylated; Liv: liver; Wk: week

7.3 Age Interactions in Chemotherapy's Effect on Cachexia and the BCAAs

The above studies only investigated the effects of chemotherapy on sex differences in young (table 4) and aged (table 5) mice, without comparing age. Therefore, to bridge this gap, I compared the effects of chemotherapy on differences across age (delta young male drug (study 2) vs delta aged male drug (study 3) ; delta young female drug (study 2) vs delta aged female drug (study 3). Body weight loss, food intake, skeletal muscle mass, anabolic signalling and BCAA metabolism were assessed (See Table 5).

Table 6 The effect of age on cachexia outcomes and skeletal muscle BCAA metabolism

Measured Variable	Young Male Drug	Aged Male Drug	p-value α=0.05	Young Female Drug	Aged Female Drug	p-value α=0.05
Body Weight Loss (Wk 6)	**10.9%**	**22%***	**<0.05**	**15%**	**20%***	**<0.05**
Food Intake (Intake (g) / FBW)	**0.1726**	**0.09902***	**<0.05**	**0.1706**	**0.09402***	**<0.05**
Skeletal Muscle						
Gastrocnemius	**-17%**	**-26%***	**<0.05**	**-23%**	**-17%**	**0.6611**
Quadriceps	**-17%**	**-30%**	**0.3876**	**-11%**	**-16%**	**0.8666**
Tibialis Anterior	**-37%**	**-28%**	**0.9419**	**-33%**	**-23%**	**0.9890**
Anabolic Signalling						
p-S6K1^{thr389}	**-36%**	**-72%***	**<0.05**	**-61%**	**-57%**	**0.9639**
Protein Synthesis	**-70%**	**-65%**	**0.9946**	**-83%**	**-67%**	**0.5517**
SM BCAA Metabolism						
Total [BCAAs]	**-70%**	**-44%**	**0.0782**	**-33%**	**-41%**	**0.9736**
LAT1 Expression	**-40%**	**-51%**	**0.5144**	**-50%**	**-48%**	**0.9850**

Red (decrease) or green (increase) indicates significant difference from each groups vehicle. Black represents non significance.

*** indicates significant difference across age with drug (young male vs aged male or young female vs aged female).**

g: gram; p: phosphorylated; SM: skeletal muscle; BCAA: Branched-chain amino acids; Wk: week.

Body Weight Loss and Food Intake

Aged male animals experienced significantly greater body weight loss compared to young males (aged: –22% vs young: –10.9%, $p < 0.05$). Similarly, body weight loss in aged females was also significantly greater compared to young females (aged: –20% vs young: –15%, $p < 0.05$), suggestive of greater body wasting in aged animals for both sexes. These findings are in line with previous work, whereby cisplatin-treated (425) and LLC tumour-bearing (717) old

animals also experienced exacerbated body weight loss in aging. However, much like my work, the cisplatin-treated mice did not include tumour inoculation and the LLC tumour-bearing animals were not treated with chemotherapy. Therefore, studies incorporating tumour-bearing animals treated with chemotherapy is an area of future work that should be considered in aging animals. In my study, greater body weight loss in aging drug-treated animals can partially be contributed to reductions in food intake, as both male and female drug-treated aged animals ate significantly less compared to their younger drug-treated counterparts (young male vs aged male, –42%, $p < 0.05$)(young female vs aged female, –45%, $p < 0.05$). These findings are consistent with reductions in food intake in aging, as ghrelin (hunger hormone) is decreased (592) and cholecystokinin (satiety hormone) is increased (593) during aging. Further contributing to greater body weight loss in aged animals, is the observation that only male and female drug-treated aged animals experienced adipose tissue wasting from chemotherapy (compared to controls), but young animals did not.

Skeletal Muscle Mass and Anabolic Signalling

The loss of gastrocnemius muscle weight was more profound in aged males compared to young males (aged: –26% vs young: –17%, $p < 0.05$) and is consistent with aged males experiencing significantly greater loss of p-S6K1^{thr389} compared to young males (aged: –72% vs young: –36%, $p < 0.05$). However, these findings did not translate to more severe decreases in protein synthesis of aged male animals (aged: –70% vs young: –65%, $p=0.9946$). Interestingly, the loss of skeletal muscle weight, anabolic signalling and protein synthesis was not exacerbated in aged female animals following chemotherapy. This female data is in opposition to a previous study, whereby older female animals did show exacerbated loss of lean mass and skeletal muscle size compared to their younger counterparts (425). However, this study referenced used a

different mouse strain (C57BL/6J), from a different vendor (Jackson Laboratory) treated with a different chemotherapy drug (cisplatin). Differences in findings between this study and my study may accurately represent variabilities in the impact that chemotherapy can have on cancer patients clinically. However, my data on the exacerbation of skeletal muscle weight loss in only aged drug-treated males (but not females), is supported by previous work, whereby males have a higher prevalence of cachectic outcomes compared to females (305).

BCAA Metabolism

An interesting finding of this analysis, is that young males experienced a near significant trend for greater decreases in skeletal muscle BCAA concentrations compared to aged males (young: –70% vs aged: –44%, $p=0.0782$). Since skeletal muscle BCAA concentrations are decreased in aging (708, 709), this finding may be explained by the simple fact that young male animals have more to lose. Moreover, skeletal muscle BCAA oxidation was decreased in young drug-treated males (–68%, $p < 0.05$, compared to young male control), while it was increased in aged drug-treated males animals (+49%, $p < 0.05$, compared to aged male control). This finding may suggest a compensatory mechanism to try and perverse the BCAA pool in young males to protect against muscle atrophy, whereas aged males oxidize more BCAAs to generate energy. This finding is supported by the fact that aged male animals suffered a greater loss of gastrocnemius muscle weight compared to young males (aged: –26% vs young: –17%, $p < 0.05$). However, since young drug-treated males still experienced greater losses of skeletal muscle BCAA concentrations compared to aged males, suggests, a least in part, that the BCAAs are being transported out of the skeletal muscle. These changes observed in males, were not found in females. In addition, decreases in the expression of skeletal muscle LAT1 was not exacerbated in aging for both sexes following chemotherapy.

Another interesting finding was that for liver BCAA metabolism, opposite findings were found between young and aged drug-treated animals. In young drug-treated animals (compared to their young vehicle counterparts), regardless of sex, total BCAA concentrations (male: +99%, female: +47%, $p < 0.05$), LAT1 expression (male: +218%, female: +201%, $p < 0.05$) and p-BCKD^{ser293} (male: +150%, female +60%, $p < 0.05$) were all increased following chemotherapy in the liver, corresponding with decreased BCKD activity (decreased BCAA oxidation). These findings suggest that the liver is the main receiver of muscle-derived BCAAs in young animals. However, in aged drug-treated animals, insignificant decreases were found for total liver BCAA concentrations and LAT1 expression. In addition, decreased p-BCKD^{ser293} (male: –66%, female: –65%, $p < 0.05$), corresponding to increased BCKD activity was found in aged animals (male: +50%, female: +98%, $p < 0.05$) with no sex differences. These findings suggest that the liver is either not the main receiver of muscle-derived BCAAs or that the BCAAs are immediately oxidized when they are transported to the liver of aged animals. It is also possible that the BCAAs may also be travelling to other areas such as the adipose tissue, which is a limitation of my study as I did not study it here, but may be useful for future investigations.

Taken together, findings from this analysis show that both male and female aged drug-treated animals experience exacerbated body weight loss and decreased food intake compared to their younger counterparts. However, since only aged drug-treated male animals showed more profound decreases in gastrocnemius muscle weight and anabolic signalling, it appears males may be more susceptible to chemotherapy-induced cachexia in aging. In addition, aged drug-treated male animals oxidize more skeletal muscle BCAAs during chemotherapy, potentially resulting in less signalling towards protein synthesis, a finding not seen in younger drug-treated males, as these animals exhibit decreased skeletal muscle BCAA oxidation. Since 18-month-old

mice represent ~56-year-old human, further studies using mice that are 24-month-old (equivalent to a 70-year-old human) could be employed. However, due to other physiological complications that can occur in old mice, especially sarcopenia (66), delineating the differences in muscle loss from sarcopenia, cancer and chemotherapy presents a further roadblock.

7.4 Conclusion

With no available cure, cachexia has been reported as a major contributor to the cause of death in many cancer patients. Therefore, interventions that attenuate muscle wasting is consistently at the forefront of cachexia research today. Findings from this thesis lay the foundation for studies to investigate the potential for increasing skeletal muscle amino acid concentrations and their transporters as a means for treating cachexia. In addition, I documented age- and sex-related differences in cachexia and tissue-specific BCAA metabolism following chemotherapy, suggesting that any successful treatment may need to consider patient age and sex as a means for better cachexia management.

Chapter 8 References

1. **U.S. Cancer Statistics Working Group**. US cancer statistics: 1999–2009 incidence and mortality web-based report. *CDC*: 2013.

2. **Kim HI**, **Lim H**, **Moon A**. Sex differences in cancer: Epidemiology, genetics and therapy. *Biomol Ther (Seoul)* 26: 335–342, 2018.

3. **Brenner DR**, **Weir HK**, **Demers AA**, **Ellison LF**, **Louzado C**, **Shaw A**, **Turner D**, **Woods RR**, **Smith LM**. Projected estimates of cancer in Canada in 2020. *CMAJ* 192: 199–205, 2020. doi: 10.1503/cmaj.191292.

4. **Melstrom LG**, **Melstrom KA**, **Ding XZ**, **Adrian TE**. Mechanisms of skeletal muscle degradation and its therapy in cancer cachexia. *Histol Histopathol* 22: 805–814, 2007.

5. **Douillard JY**, **Cunningham D**, **Roth AD**, **Navarro M**, **James RD**, **Karasek P**, **Jandik P**, **Iveson T**, **Carmichael J**, **Alakl M**, **Gruia G**, **Awad L**, **Rougier P**. Irinotecan combined with fluorouracil compared with fluorouracil alone. as first-line treatment for metastatic colorectal cancer: a multicentre randomised trial. *Lancet* 355: 1041–1047, 2000. doi: 10.1016/S0140-6736(00)02034-1.

6. **Pin F**, **Barreto R**, **Couch ME**, **Bonetto A**, **O'Connell TM**. Cachexia induced by cancer and chemotherapy yield distinct perturbations to energy metabolism. *J Cachexia Sarcopenia Muscle* 10: 140–154, 2019. doi: 10.1002/jcsm.12360.

7. **Ballarò R**, **Beltrà M**, **De Lucia S**, **Pin F**, **Ranjbar K**, **Hulmi JJ**, **Costelli P**, **Penna F**. Moderate exercise in mice improves cancer plus chemotherapy-induced muscle wasting and mitochondrial alterations. *FASEB Journal* 33: 5482–5494, 2019.

8. **Barreto R**, **Waning DL**, **Gao H**, **Liu Y**, **Zimmers TA**, **Bonetto A**. Chemotherapy-related cachexia is associated with mitochondrial depletion and the activation of ERK1/2 and p38 MAPKs. *Oncotarget* 7: 43442–60, 2016.

9. **de Matos-Neto EM**, **Lima JDCC**, **de Pereira WO**, **Figuerêdo RG**, **Riccardi DM dos R**, **Radloff K**, **das Neves RX**, **Camargo RG**, **Maximiano LF**, **Tokeshi F**, **Otoch JP**, **Goldszmid R**, **Câmara NOS**, **Trinchieri G**, **de Alcântara PSM**, **Seelaender M**. Systemic inflammation in cachexia - Is tumor cytokine expression profile the culprit? *Front Immunol* 6: 629-undefined, 2015.

10. **Asp ML**, **Tian M**, **Wendel AA**, **Belury MA**. Evidence for the contribution of insulin resistance to the development of cachexia in tumor-bearing mice. *Int J Cancer* 126: 756–763, 2010. doi: 10.1002/ijc.24784.

11. **Argilés JM**, **Fontes-Oliveira CC**, **Toledo M**, **López-Soriano FJ**, **Busquets S**. Cachexia: a problem of energetic inefficiency. *J Cachexia Sarcopenia Muscle* 5: 279–286, 2014.

12. **Aoyagi T**, **Terracina KP**, **Raza A**, **Matsubara H**, **Takabe K**. Cancer Cachexia, Mechanism and Treatment. *World J Gastrointest Oncol* 7: 17–29, 2015. doi: 10.4251/wjgo.v7.i4.17.

13. **Holden CM**. Anorexia in the terminally ill cancer patient: the emotional impact on the patient and the family. *Hosp J* 7: 73–84, 1991. doi: 10.1080/0742-969X.1991.11882706.

14. **Ramos EJB**, **Suzuki S**, **Marks D**, **Inui A**, **Asakawa A**, **Meguid MM**. Cancer anorexia-cachexia syndrome: Cytokines and neuropeptides. *Curr Opin Clin Nutr Metab Care* 7: 427–434, 2004.

15. **Stewart GD**, **Skipworth RJE**, **Fearon KCH**. Cancer cachexia and fatigue. *Clinical Medicine, Journal of the Royal College of Physicians of London* 6: 140–143, 2006.

16. **Dalise S**, **Tropea P**, **Galli L**, **Sbrana A**, **Chisari C**. Muscle function impairment in cancer patients in pre-cachexia stage. *Eur J Transl Myol* 30: 8931, 2020. doi: 10.4081/ejtm.2020.8931.

17. **Sakai H**, **Sagara A**, **Arakawa K**, **Sugiyama R**, **Hirosaki A**, **Takase K**, **Jo A**, **Sato K**, **Chiba Y**, **Yamazaki M**, **Matoba M**, **Narita M**. Mechanisms of cisplatin-induced muscle atrophy. *Toxicol Appl Pharmacol* 278: 190–199, 2014. doi: 10.1016/j.taap.2014.05.001.

18. **Barreto R**, **Mandili G**, **Witzmann FA**, **Novelli F**, **Zimmers TA**, **Bonetto A**. Cancer and chemotherapy contribute to muscle loss by activating common signaling pathways. *Front Physiol* 7: 472, 2016. doi: 10.3389/fphys.2016.00472.

19. **Takayama K**, **Atagi S**, **Imamura F**, **Tanaka H**, **Minato K**, **Harada T**, **Katakami N**, **Yokoyama T**, **Yoshimori K**, **Takiguchi Y**, **Hataji O**, **Takeda Y**, **Aoe K**, **Kim YH**, **Yokota S**, **Tabeta H**, **Tomii K**, **Ohashi Y**, **Eguchi K**, **Watanabe K**. Quality of life and survival survey of cancer cachexia in advanced non-small cell lung cancer patients—Japan nutrition and QOL survey in patients with advanced non-small cell lung cancer study. *Supportive Care in Cancer* 24: 3473–3480, 2016.

20. **von Haehling S**, **Anker MS**, **Anker SD**. Prevalence and clinical impact of cachexia in chronic illness in Europe, USA, and Japan: facts and numbers update 2016. *J Cachexia Sarcopenia Muscle* 7: 507–509, 2016.

21. **Ali R**, **Baracos VE**, **Sawyer MB**, **Bianchi L**, **Roberts S**, **Assenat E**, **Mollevi C**, **Senesse P**. Lean body mass as an independent determinant of dose-limiting toxicity and neuropathy in patients with colon cancer treated with FOLFOX regimens. *Cancer Med* 5: 607–616, 2016.

22. **Antoun S**, **Baracos VE**, **Birdsell L**, **Escudier B**, **Sawyer MB**. Low body mass index and sarcopenia associated with dose-limiting toxicity of sorafenib in patients with renal cell carcinoma. *Annals of Oncology* 21: 1594–1598, 2010.

23. **Jung HW**, **Kim JW**, **Kim JY**, **Kim SW**, **Yang HK**, **Lee JW**, **Lee KW**, **Kim DW**, **Kang SB**, **Kim K il**, **Kim CH**, **Kim JH**. Effect of muscle mass on toxicity and survival in patients with colon cancer undergoing adjuvant chemotherapy. *Supportive Care in Cancer* 23: 687–694, 2014. doi: 10.1007/s00520-014-2418-6.

24. **Bodine SC**, **Stitt TN**, **Gonzalez M**, **Kline WO**, **Stover GL**, **Bauerlein R**, **Zlotchenko E**, **Scrimgeour A**, **Lawrence JC**, **Glass DJ**, **Yancopoulos GD**. Akt/mTOR pathway is a crucial regulator of skeletal muscle hypertrophy and can prevent muscle atrophy in vivo. *Nat Cell Biol* 3: 1014–1019, 2001.

25. **Adegoke OAJ**, **Abdullahi A**, **Tavajohi-Fini P**. MTORC1 and the regulation of skeletal muscle anabolism and mass. *Applied Physiology, Nutrition and Metabolism* 37: 395–406, 2012.

26. **Zhao Y**, **Wang L**, **Pan J**. The role of L-type amino acid transporter 1 in human tumors. *Intractable Rare Dis Res* 4: 165–169, 2015.

27. **Chantranupong L**, **Wolfson RL**, **Orozco JM**, **Saxton RA**, **Scaria SM**, **Bar-Peled L**, **Spooner E**, **Isasa M**, **Gygi SP**, **Sabatini DM**. The sestrins interact with gator2 to negatively regulate the amino-acid-sensing pathway upstream of mTORC1. *Cell Rep* 9: 1–8, 2014.

28. **Nandagopal N**, **Roux PP**. Regulation of global and specific mRNA translation by the mTOR signaling pathway. *Translation* 3: e983402, 2015.

29. **Iadevaia V**, **Liu R**, **Proud CG**. MTORC1 signaling controls multiple steps in ribosome biogenesis. *Semin Cell Dev Biol* 36: 113–120, 2014.

30. **Hosokawa N**, **Hara T**, **Kaizuka T**, **Kishi C**, **Takamura A**, **Miura Y**, **Iemura SI**, **Natsume T**, **Takehana K**, **Yamada N**, **Guan JL**, **Oshiro N**, **Mizushima N**. Nutrient-dependent mTORCl association with the ULK1-Atg13-FIP200 complex required for autophagy. *Mol Biol Cell* 20: 1981–1991, 2009.

31. **Setiawan T**, **Sari IN**, **Wijaya YT**, **Julianto NM**, **Muhammad JA**, **Lee H**, **Chae JH**, **Kwon HY**. Cancer cachexia: molecular mechanisms and treatment strategies. *J Hematol Oncol* 16: 54, 2023.

32. **Bodine SC**, **Latres E**, **Baumhueter S**, **Lai VKM**, **Nunez L**, **Clarke BA**, **Poueymirou WT**, **Panaro FJ**, **Erqian Na**, **Dharmarajan K**, **Pan ZQ**, **Valenzuela DM**, **Dechiara TM**, **Stitt TN**, **Yancopoulos GD**, **Glass DJ**. Identification of ubiquitin ligases required for skeletal Muscle Atrophy. *Science (1979)* 294: 1704–1708, 2001.

33. **Mann G**, **Mora S**, **Madu G**, **Adegoke OAJ**. Branched-chain Amino Acids: Catabolism in Skeletal Muscle and Implications for Muscle and Whole-body Metabolism. *Front Physiol* 12: 2021.

34. **Blomstrand E**, **Eliasson J**, **Karlssonr HKR**, **Köhnke R**. Branched-chain amino acids activate key enzymes in protein synthesis after physical exercise. In: *Journal of Nutrition*. 2006, p. 269–273.

35. **Atherton PJ**, **Smith K**, **Etheridge T**, **Rankin D**, **Rennie MJ**. Distinct anabolic signalling responses to amino acids in C2C12 skeletal muscle cells. *Amino Acids* 38: 1533–1539, 2010.

36. **Gomes-Marcondes MCC**, **Ventrucci G**, **Toledo MT**, **Cury L**, **Cooper JC**. A leucine-supplemented diet improved protein content of skeletal muscle in young tumor-bearing rats. *Brazilian Journal of Medical and Biological Research* 36: 1589–1594, 2003. doi: 10.1590/S0100-879X2003001100017.

37. **Ventrucci G**, **Ramos Silva LG**, **Roston Mello MA**, **Gomes Marcondes MCC**. Effects of a Leucine-Rich Diet on Body Composition During Nutritional Recovery in Rats. *Nutrition* 20: 213–217, 2004. doi: 10.1016/j.nut.2003.10.014.

38. **Harima Y**, **Yamasaki T**, **Hamabe S**, **Saeki I**, **Okita K**, **Terai S**, **Sakaida I**. Effect of a late evening snack using branched-chain amino acid-enriched nutrients in patients undergoing hepatic arterial infusion chemotherapy for advanced hepatocellular carcinoma. *Hepatol Res* 40: 574–84, 2010.

39. **Poon RT-P**, **Yu W-C**, **Fan S-T**, **Wong J**. Long-term oral branched chain amino acids in patients undergoing chemoembolization for hepatocellular carcinoma: a randomized trial. *Aliment Pharmacol Ther* 19: 779–88, 2004.

40. **Ericksen RE**, **Lim SL**, **McDonnell E**, **Shuen WH**, **Vadiveloo M**, **White PJ**, **Ding Z**, **Kwok R**, **Lee P**, **Radda GK**, **Toh HC**, **Hirschey MD**, **Han W**. Loss of BCAA Catabolism during Carcinogenesis Enhances mTORC1 Activity and Promotes Tumor Development and Progression. *Cell Metab* 29: 1151–1165, 2019. doi: 10.1016/j.cmet.2018.12.020.

41. **Zhang L**, **Han J**. Branched-chain amino acid transaminase 1 (BCAT1) promotes the growth of breast cancer cells through improving mTOR-mediated mitochondrial biogenesis and function. *Biochem Biophys Res Commun* 486: 224–231, 2017.

42. **Mayers J**. Tissue of origin dictates branched-chain amino acid metabolism in mutant Kras-driven cancers. *Science (1979)* 353: 1161–1165, 2016.

43. **Rosa-Caldwell ME**, **Greene NP**. Muscle metabolism and atrophy: Let's talk about sex. *Biol Sex Differ* 10: 43, 2019.

44. **Hetzler KL**, **Hardee JP**, **Puppa MJ**, **Narsale AA**, **Sato S**, **Davis JM**, **Carson JA**. Sex differences in the relationship of IL-6 signaling to cancer cachexia progression. *Biochim Biophys Acta Mol Basis Dis* 1852: 139–148, 2015. doi: 10.1016/j.bbadis.2014.12.015.

45. **Siegel RL**, **Miller KD**, **Jemal A**. Cancer statistics, 2016. *CA Cancer J Clin* 66: 7–30, 2016. doi: 10.3322/caac.21332.

46. **Nattenmüller J**, **Wochner R**, **Muley T**, **Steins M**, **Hummler S**, **Teucher B**, **Wiskemann J**, **Kauczor HU**, **Wielputz MO**, **Heussel CP**. Prognostic impact of CT-quantified muscle and fat distribution before and after first-line-chemotherapy in lung cancer patients. *PLoS One* 12: 1–18, 2017. doi: 10.1371/journal.pone.0169136.

47. **Merz B**, **Frommherz L**, **Rist MJ**, **Kulling SE**, **Bub A**, **Watzl B**. Dietary pattern and plasma BCAA-variations in healthy men and women—results from the KarMeN study. *Nutrients* 10: 623, 2018. doi: 10.3390/nu10050623.

48. **Costanzo M**, **Caterino M**, **Sotgiu G**, **Ruoppolo M**, **Franconi F**, **Campesi I**. Sex differences in the human metabolome. *Biol Sex Differ* 13: 30, 2022. doi: 10.1186/s13293-022-00440-4.

49. **Mittendorfer B**, **Horowitz JF**, **Klein S**. Effect of gender on lipid kinetics during endurance exercise of moderate intensity in untrained subjects. *American Journal of Physiology-Endocrinology and Metabolism* 283: E58–E65, 2002. doi: 10.1152/ajpendo.00504.2001.

50. **Frontera WR**, **Ochala J**. Skeletal Muscle: A Brief Review of Structure and Function. *Behav Genet* 96 (3): 183–195, 2015.

51. **Zurlo F**, **Larson K**, **Bogardus C**, **Ravussin E**. Skeletal muscle metabolism is a major determinant of resting energy expenditure. *Journal of Clinical Investigation* 86: 1423–1427, 1990. doi: 10.1172/JCI114857.

52. **Argilés JM**, **Campos N**, **Lopez-Pedrosa JM**, **Rueda R**, **Rodriguez-Mañas L**. Skeletal Muscle Regulates Metabolism via Interorgan Crosstalk: Roles in Health and Disease. *J Am Med Dir Assoc* 17 (9): 789–796, 2016.

53. **Mukund K**, **Subramaniam S**. Skeletal muscle: A review of molecular structure and function, in health and disease. *Wiley Interdiscip Rev Syst Biol Med* 12: e1462-undefined, 2020.

54. **Otto Buczkowska E**, **Dworzecki T**. [The role of skeletal muscle in the regulation of glucose homeostasis]. *Endokrynol Diabetol Chor Przemiany Materii Wieku Rozw* 9: 93–7, 2003.

55. **Merz KE**, **Thurmond DC**. Role of Skeletal Muscle in Insulin Resistance and Glucose Uptake. In: *Comprehensive Physiology*. Wiley, 2020, p. 785–809.

56. **Jensen J**, **Rustad PI**, **Kolnes AJ**, **Lai YC**. The role of skeletal muscle glycogen breakdown for regulation of insulin sensitivity by exercise. *Front Physiol* 2 DEC: 112, 2011.

57. **Béchet D**, **Tassa A**, **Combaret L**, **Taillandier D**, **Attaix D**. Regulation of skeletal muscle proteolysis by amino acids. In: *Journal of Renal Nutrition*. 2005, p. 18–22.

58. **Jensen MD**. Fatty acid oxidation in human skeletal muscle. *Journal of Clinical Investigation* 110: 1607–1609, 2002.

59. **Atherton PJ**, **Greenhaff PL**, **Phillips SM**, **Bodine SC**, **Adams CM**, **Lang CH**. Control of skeletal muscle atrophy in response to disuse: Clinical/preclinical contentions and fallacies of evidence. *Am J Physiol Endocrinol Metab* 311 (3): 594–604, 2016.

60. **Derksen JWG**, **Kurk SA**, **Peeters PHM**, **Dorresteijn B**, **Jourdan M**, **van der Velden AMT**, **Nieboer P**, **de Jong RS**, **Honkoop AH**, **Punt CJA**, **Koopman M**, **May AM**. The association between changes in muscle mass and quality of life in patients with metastatic colorectal cancer. *J Cachexia Sarcopenia Muscle* 11, 2020. doi: 10.1002/jcsm.12562.

61. **Evans WJ**, **Lambert CP**. Physiological basis of fatigue. *Am J Phys Med Rehabil* 86: 29–46, 2007.

62. **Evans WJ**, **Morley JE**, **Argilés J**, **Bales C**, **Baracos V**, **Guttridge D**, **Jatoi A**, **Kalantar-Zadeh K**, **Lochs H**, **Mantovani G**, **Marks D**, **Mitch WE**, **Muscaritoli M**, **Najand A**, **Ponikowski P**, **Rossi Fanelli F**, **Schambelan M**, **Schols A**, **Schuster M**, **Thomas D**, **Wolfe R**, **Anker SD**. Cachexia: A new definition. *Clinical Nutrition* 27: 793–9, 2008.

63. **Morgan PT**, **Smeuninx B**, **Breen L**. Exploring the Impact of Obesity on Skeletal Muscle Function in Older Age. *Front Nutr* 7: 569904, 2020.

64. **Chen L-Y**, **Xia M-F**, **Wu L**, **Li Q**, **Hu Y**, **Ma H**, **Gao X**, **Lin H-D**. Skeletal muscle loss is associated with diabetes in middle-aged and older Chinese men without non-alcoholic fatty liver disease. *World J Diabetes* 12: 2119–2129, 2021. doi: 10.4239/wjd.v12.i12.2119.

65. **Kennel PJ**, **Mancini DM**, **Schulze PC**. Skeletal muscle changes in chronic cardiac disease and failure. *Compr Physiol* 5: 1947–1969, 2015. doi: 10.1002/cphy.c110003.

66. **Evans WJ**. What Is Sarcopenia? *J Gerontol A Biol Sci Med Sci* 50A: 5–8, 1995.

67. **Melton LJ**, **Khosla S**, **Crowson CS**, **O'Connor MK**, **O'Fallon WM**, **Riggs BL**. Epidemiology of sarcopenia. *J Am Geriatr Soc* 48: 625–30, 2000.

68. **Wilkinson DJ**, **Piasecki M**, **Atherton PJ**. The age-related loss of skeletal muscle mass and function: Measurement and physiology of muscle fibre atrophy and muscle fibre loss in humans. *Ageing Res Rev* 47: 123–132, 2018.

69. **Cuthbertson D**, **Smith K**, **Babraj J**, **Leese G**, **Waddell T**, **Atherton P**, **Wackerhage H**, **Taylor PM**, **Rennie MJ**. Anabolic signaling deficits underlie amino acid resistance of wasting, aging muscle. *FASEB J* 19: 422–4, 2005.

70. **Kumar V**, **Selby A**, **Rankin D**, **Patel R**, **Atherton P**, **Hildebrandt W**, **Williams J**, **Smith K**, **Seynnes O**, **Hiscock N**, **Rennie MJ**. Age-related differences in the dose-response relationship of muscle protein synthesis to resistance exercise in young and old men. *J Physiol* 587: 211–7, 2009.

71. **McPhee JS**, **French DP**, **Jackson D**, **Nazroo J**, **Pendleton N**, **Degens H**. Physical activity in older age: perspectives for healthy ageing and frailty. *Biogerontology* 17: 567–80, 2016.

72. **Kalinkovich A**, **Livshits G**. Sarcopenic obesity or obese sarcopenia: A cross talk between age-associated adipose tissue and skeletal muscle inflammation as a main mechanism of the pathogenesis. *Ageing Res Rev* 35: 200–221, 2017.

73. **Harman D**. Aging: a theory based on free radical and radiation chemistry. *J Gerontol* 11: 298–300, 1956.

74. **Guillet C**, **Prod'homme M**, **Balage M**, **Gachon P**, **Giraudet C**, **Morin L**, **Grizard J**, **Boirie Y**. Impaired anabolic response of muscle protein synthesis is associated with S6K1 dysregulation in elderly humans. *FASEB J* 18: 1586–7, 2004.

75. **Cuthbertson D**, **Smith K**, **Babraj J**, **Leese G**, **Waddell T**, **Atherton P**, **Wackerhage H**, **Taylor PM**, **Rennie MJ**. Anabolic signaling deficits underlie amino acid resistance of wasting, aging muscle. *FASEB J* 19: 422–4, 2005.

76. **Abe T**. Sex differences in whole body skeletal muscle mass measured by magnetic resonance imaging and its distribution in young Japanese adults. *Br J Sports Med* 37: 436–440, 2003.

77. **Janssen I**, **Heymsfield SB**, **Wang Z**, **Ross R**. Skeletal muscle mass and distribution in 468 men and women aged 18–88 yr. *J Appl Physiol* 89: 81–88, 2000.

78. **Neal A**, **Boldrin L**, **Morgan JE**. The satellite cell in male and female, developing and adult mouse muscle: distinct stem cells for growth and regeneration. *PLoS One* 7: e37950, 2012.

79. **Manzano R**, **Toivonen JM**, **Calvo AC**, **Miana-Mena FJ**, **Zaragoza P**, **Muñoz MJ**, **Montarras D**, **Osta R**. Sex, fiber-type, and age dependent in vitro proliferation of mouse muscle satellite cells. *J Cell Biochem* 112: 2825–36, 2011.

80. **De Lisio M**, **Farup J**. The role of satellite cells in activity-induced adaptations: breathing new life into the debate. *J Physiol* 595: 6225–6226, 2017. doi: 10.1113/JP274969.

81. **Nuzzo JL**. Sex differences in skeletal muscle fiber types: A meta-analysis. .

82. **Haizlip KM**, **Harrison BC**, **Leinwand LA**. Sex-Based Differences in Skeletal Muscle Kinetics and Fiber-Type Composition. *Physiology* 30: 30–39, 2015.

83. **Mauvais-Jarvis F**. Sex differences in metabolic homeostasis, diabetes, and obesity. *Biol Sex Differ* 6: 14, 2015.

84. **Gao Y**, **Arfat Y**, **Wang H**, **Goswami N**. Muscle Atrophy Induced by Mechanical Unloading: Mechanisms and Potential Countermeasures. *Front Physiol* 9: 235, 2018.

85. **Thomason DB**, **Herrick RE**, **Surdyka D**, **Baldwin KM**. Time course of soleus muscle myosin expression during hindlimb suspension and recovery. *J Appl Physiol (1985)* 63: 130–7, 1987.

86. **Brown JL**, **Rosa-Caldwell ME**, **Lee DE**, **Blackwell TA**, **Brown LA**, **Perry RA**, **Haynie WS**, **Hardee JP**, **Carson JA**, **Wiggs MP**, **Washington TA**, **Greene NP**. Mitochondrial

degeneration precedes the development of muscle atrophy in progression of cancer cachexia in tumour-bearing mice. *J Cachexia Sarcopenia Muscle* 8: 926–938, 2017.

87. **Delmonico MJ**, **Harris TB**, **Visser M**, **Park SW**, **Conroy MB**, **Velasquez-Mieyer P**, **Boudreau R**, **Manini TM**, **Nevitt M**, **Newman AB**, **Goodpaster BH**, **Health A and B**. Longitudinal study of muscle strength, quality, and adipose tissue infiltration. *Am J Clin Nutr* 90: 1579–85, 2009.

88. **Syverud BC**, **VanDusen KW**, **Larkin LM**. Growth Factors for Skeletal Muscle Tissue Engineering. *Cells Tissues Organs* 202: 169–179, 2016. doi: 10.1159/000444671.

89. **Srinivas-Shankar U**, **Roberts SA**, **Connolly MJ**, **O'Connell MDL**, **Adams JE**, **Oldham JA**, **Wu FCW**. Effects of testosterone on muscle strength, physical function, body composition, and quality of life in intermediate-frail and frail elderly men: A randomized, double-blind, placebo-controlled study. *Journal of Clinical Endocrinology and Metabolism* 95: 639–650, 2010. doi: 10.1210/jc.2009-1251.

90. **Velloso CP**. Regulation of muscle mass by growth hormone and IGF-I. *Br J Pharmacol* 154: 557–568, 2008.

91. **Burd NA**, **Tang JE**, **Moore DR**, **Phillips SM**. Exercise training and protein metabolism: Influences of contraction, protein intake, and sex-based differences. *J Appl Physiol* 106: 1692–1701, 2009.

92. **Dreyer HC**, **Fujita S**, **Cadenas JG**, **Chinkes DL**, **Volpi E**, **Rasmussen BB**. Resistance exercise increases AMPK activity and reduces 4E-BP1 phosphorylation and protein synthesis in human skeletal muscle. *Journal of Physiology* 576: 613–624, 2006. doi: 10.1113/jphysiol.2006.113175.

93. **Karakelides H**, **Irving BA**, **Short KR**, **O'Brien P**, **Nair KS**. Age, Obesity, and Sex Effects on Insulin Sensitivity and Skeletal Muscle Mitochondrial Function. *Diabetes* 59: 89–97, 2010. doi: 10.2337/db09-0591.

94. **Jones H**. Testosterone for the aging male; current evidence and recommended practice. *Clin Interv Aging* Volume 3: 25–44, 2008. doi: 10.2147/CIA.S190.

95. **Horstman AM**, **Dillon EL**, **Urban RJ**, **Sheffield-Moore M**. The Role of Androgens and Estrogens on Healthy Aging and Longevity. *J Gerontol A Biol Sci Med Sci* 67: 1140–1152, 2012. doi: 10.1093/gerona/gls068.

96. **Florini JR**. Growth Hormone and the Insulin-Like Growth Factor System in Myogenesis*. *Endocr Rev* 17: 481–517, 1996. doi: 10.1210/edrv-17-5-481.

97. **Díez JJ**, **Sangiao-Alvarellos S**, **Cordido F**. Treatment with growth hormone for adults with growth hormone deficiency syndrome: Benefits and risks. *Int J Mol Sci* 19: 893, 2018.

98. **van Bunderen CC**, **van Varsseveld NC**, **Erfurth EM**, **Ket JCF**, **Drent ML**. Efficacy and safety of growth hormone treatment in adults with growth hormone deficiency: A systematic review of studies on morbidity. *Clin Endocrinol (Oxf)* 81: 1–14, 2014.

99. **Sotiropoulos A**, **Ohanna M**, **Kedzia C**, **Menon RK**, **Kopchick JJ**, **Kelly PA**, **Pende M**. Growth hormone promotes skeletal muscle cell fusion independent of insulin-like growth factor 1 up-regulation. *Proc Natl Acad Sci U S A* 103: 7315–7320, 2006. doi: 10.1073/pnas.0510033103.

100. **Kim S-H**, **Park M-J**. Effects of growth hormone on glucose metabolism and insulin resistance in human. *Ann Pediatr Endocrinol Metab* 22: 145–152, 2017. doi: 10.6065/apem.2017.22.3.145.

101. **Goldstein J**, **Sites CK**, **Toth MJ**. Progesterone stimulates cardiac muscle protein synthesis via receptor-dependent pathway. *Fertil Steril* 82: 430–6, 2004.

102. **Schiaffino S**, **Dyar KA**, **Ciciliot S**, **Blaauw B**, **Sandri M**. Mechanisms regulating skeletal muscle growth and atrophy. *FEBS J* 280: 4294–314, 2013.

103. **Price TM**, **Dai Q**. The Role of a Mitochondrial Progesterone Receptor (PR-M) in Progesterone Action. *Semin Reprod Med* 33: 185–94, 2015.

104. **Dai Q**, **Shah AA**, **Garde R V**, **Yonish BA**, **Zhang L**, **Medvitz NA**, **Miller SE**, **Hansen EL**, **Dunn CN**, **Price TM**. A truncated progesterone receptor (PR-M) localizes to the mitochondrion and controls cellular respiration. *Mol Endocrinol* 27: 741–53, 2013.

105. **Sener A**, **Malaisse WJ**. L-leucine and a nonmetabolized analogue activate pancreatic islet glutamate dehydrogenase. *Nature* 288: 187–189, 1980. doi: 10.1038/288187a0.

106. **Fujita S**, **Rasmussen BB**, **Cadenas JG**, **Grady JJ**, **Volpi E**. Effect of insulin on human skeletal muscle protein synthesis is modulated by insulin-induced changes in muscle blood flow and amino acid availability. *Am J Physiol Endocrinol Metab* 291: 745–754, 2006. doi: 10.1152/ajpendo.00271.2005.

107. **Chow LS**, **Albright RC**, **Bigelow ML**, **Toffolo G**, **Cobelli C**, **Nair KS**. Mechanism of insulin's anabolic effect on muscle: Measurements of muscle protein synthesis and breakdown using aminoacyl-tRNA and other surrogate measures. *Am J Physiol Endocrinol Metab* 291: 729–736, 2006. doi: 10.1152/ajpendo.00003.2006.

108. **Proud CG**. Regulation of protein synthesis by insulin. In: *Biochemical Society Transactions*. 2006, p. 321–348.

109. **Garlick PJ**, **Grant I**. Amino acid infusion increases the sensitivity of muscle protein synthesis in vivo to insulin. Effect of branched-chain amino acids. *Biochemical Journal* 254: 579–584, 1988. doi: 10.1042/bj2540579.

110. **Larbaud D**, **Balage M**, **Taillandier D**, **Combaret L**, **Grizard J**, **Attaix D**. Differential regulation of the lysosomal, Ca2+-dependent and ubiquitin/proteasome-dependent

proteolytic pathways in fast-twitch and slow-twitch rat muscle following hyperinsulinaemia. *Clin Sci* 101: 551–558, 2001. doi: 10.1042/CS20010042.

111. **Nakhooda AF**, **Wei CN**, **Marliss EB**. Muscle protein catabolism in diabetes: 3-Methylhistidine excretion in the spontaneously diabetic "BB" rat. *Metabolism* 29: 1272–1277, 1980. doi: 10.1016/0026-0495(80)90158-4.

112. **Bennet WM**, **Connacher AA**, **Jung RT**, **Stehle P**, **Rennie MJ**. Effects of insulin and amino acids on leg protein turnover in IDDM patients. *Diabetes* 40: 499–508, 1991. doi: 10.2337/diab.40.4.499.

113. **Bennet WM**, **Connacher AA**, **Scrimgeour CM**, **Jung RT**, **Rennie MJ**. Euglycemic hyperinsulinemia augments amino acid uptake by human leg tissues during hyperaminoacidemia. *Am J Physiol Endocrinol Metab* 259: 85–94, 1990. doi: 10.1152/ajpendo.1990.259.2.e185.

114. **Hiipakka RA**, **Liao S**. Molecular mechanism of androgen action. *Trends Endocrinol Metab* 9: 317–24, 1998.

115. **Vingren JL**, **Kraemer WJ**, **Ratamess NA**, **Anderson JM**, **Volek JS**, **Maresh CM**. Testosterone physiology in resistance exercise and training: the up-stream regulatory elements. *Sports Med* 40: 1037–53, 2010.

116. **Mauras N**, **Hayes V**, **Welch S**, **Rini A**, **Helgeson K**, **Dokler M**, **Veldhuis JD**, **Urban RJ**. Testosterone deficiency in young men: marked alterations in whole body protein kinetics, strength, and adiposity. *J Clin Endocrinol Metab* 83: 1886–92, 1998.

117. **Demling RH**, **Orgill DP**. The anticatabolic and wound healing effects of the testosterone analog oxandrolone after severe burn injury. *J Crit Care* 15: 12–7, 2000.

118. **Hamilton KJ**, **Hewitt SC**, **Arao Y**, **Korach KS**. Estrogen Hormone Biology. *Curr Top Dev Biol* 125: 109–146, 2017.

119. **Carson JA**, **Manolagas SC**. Effects of sex steroids on bones and muscles: Similarities, parallels, and putative interactions in health and disease. *Bone* 80: 67–78, 2015.

120. **McClung JM**, **Davis JM**, **Wilson MA**, **Goldsmith EC**, **Carson JA**. Estrogen status and skeletal muscle recovery from disuse atrophy. *J Appl Physiol (1985)* 100: 2012–23, 2006.

121. **Teveroni E**, **Pellegrino M**, **Sacconi S**, **Calandra P**, **Cascino I**, **Farioli-Vecchioli S**, **Puma A**, **Garibaldi M**, **Morosetti R**, **Tasca G**, **Ricci E**, **Trevisan C Pietro**, **Galluzzi G**, **Pontecorvi A**, **Crescenzi M**, **Deidda G**, **Moretti F**. Estrogens enhance myoblast differentiation in facioscapulohumeral muscular dystrophy by antagonizing DUX4 activity. *J Clin Invest* 127: 1531–1545, 2017.

122. **Kamanga-Sollo E**, **White ME**, **Weber WJ**, **Dayton WR**. Role of estrogen receptor-α (ESR1) and the type 1 insulin-like growth factor receptor (IGFR1) in estradiol-stimulated proliferation of cultured bovine satellite cells. *Domest Anim Endocrinol* 44: 36–45, 2013.

123. **Symons TB**, **Sheffield-Moore M**, **Wolfe RR**, **Paddon-Jones D**. Moderating the portion size of a protein-rich meal improves anabolic efficiency in young and elderly. *J Am Diet Assoc* 109: 1582–1586, 2009.

124. **Pennings B**, **Boirie Y**, **Senden JMG**, **Gijsen AP**, **Kuipers H**, **van Loon LJC**. Whey protein stimulates postprandial muscle protein accretion more effectively than do casein and casein hydrolysate in older men. *American Journal of Clinical Nutrition* 93: 997–1005, 2011. doi: 10.3945/ajcn.110.008102.

125. **Hector AJ**, **Marcotte GR**, **Churchward-Venne TA**, **Murphy CH**, **Breen L**, **von Allmen M**, **Baker SK**, **Phillips SM**. Whey protein supplementation preserves postprandial myofibrillar protein synthesis during short-term energy restriction in overweight and obese adults. *Journal of Nutrition* 145: 246–252, 2015. doi: 10.3945/jn.114.200832.

126. **MacDougall JD**, **Gibala MJ**, **Tarnopolsky MA**, **MacDonald JR**, **Interisano SA**, **Yarasheski KE**. The time course for elevated muscle protein synthesis following heavy resistance exercise. *Canadian Journal of Applied Physiology* 20: 480–486, 1995. doi: 10.1139/h95-038.

127. **Phillips SM**, **Tipton KD**, **Aarsland A**, **Wolf SE**, **Wolfe RR**. Mixed muscle protein synthesis and breakdown after resistance exercise in humans. *Am J Physiol Endocrinol Metab* 273: 99–107, 1997. doi: 10.1152/ajpendo.1997.273.1.e99.

128. **Moore DR**, **Robinson MJ**, **Fry JL**, **Tang JE**, **Glover EI**, **Wilkinson SB**, **Prior T**, **Tarnopolsky MA**, **Phillips SM**. Ingested protein dose response of muscle and albumin protein synthesis after resistance exercise in young men. *American Journal of Clinical Nutrition* 89: 161–168, 2009. doi: 10.3945/ajcn.2008.26401.

129. **Churchward-Venne TA**, **Burd NA**, **Mitchell CJ**, **West DWD**, **Philp A**, **Marcotte GR**, **Baker SK**, **Baar K**, **Phillips SM**. Supplementation of a suboptimal protein dose with leucine or essential amino acids: Effects on myofibrillar protein synthesis at rest and following resistance exercise in men. *Journal of Physiology* 590: 2751–2765, 2012. doi: 10.1113/jphysiol.2012.228833.

130. **Areta JL**, **Burke LM**, **Ross ML**, **Camera DM**, **West DWD**, **Broad EM**, **Jeacocke NA**, **Moore DR**, **Stellingwerff T**, **Phillips SM**, **Hawley JA**, **Coffey VG**. Timing and distribution of protein ingestion during prolonged recovery from resistance exercise alters myofibrillar protein synthesis. *Journal of Physiology* 591: 2319–2331, 2013. doi: 10.1113/jphysiol.2012.244897.

131. **Macnaughton LS**, **Wardle SL**, **Witard OC**, **McGlory C**, **Hamilton DL**, **Jeromson S**, **Lawrence CE**, **Wallis GA**, **Tipton KD**. The response of muscle protein synthesis following whole-body resistance exercise is greater following 40 g than 20 g of ingested whey protein. *Physiol Rep* 4, 2016. doi: 10.14814/phy2.12893.

132. **Witard OC**, **Jackman SR**, **Breen L**, **Smith K**, **Selby A**, **Tipton KD**. Myofibrillar muscle protein synthesis rates subsequent to a meal in response to increasing doses of whey protein at rest and after resistance exercise. *American Journal of Clinical Nutrition* 99: 86–95, 2014. doi: 10.3945/ajcn.112.055517.

133. **Tipton KD**, **Elliott TA**, **Cree MG**, **Wolf SE**, **Sanford AP**, **Wolfe RR**. Ingestion of casein and whey prosteins result in muscle anabolism after resistance exercise. *Med Sci Sports Exerc* 36: 2073–2081, 2004. doi: 10.1249/01.MSS.0000147582.99810.C5.

134. **Reitelseder S**, **Agergaard J**, **Doessing S**, **Helmark IC**, **Lund P**, **Kristensen NB**, **Frystyk J**, **Flyvbjerg A**, **Schjerling P**, **van Hall G**, **Kjaer M**, **Holm L**. Whey and casein labeled with L-[1-13C]leucine and muscle protein synthesis: Effect of resistance exercise and protein ingestion. *Am J Physiol Endocrinol Metab* 300: 231–242, 2011. doi: 10.1152/ajpendo.00513.2010.

135. **Wilkinson SB**, **Tarnopolsky MA**, **MacDonald MJ**, **MacDonald JR**, **Armstrong D**, **Phillips SM**. Consumption of fluid skim milk promotes greater muscle protein accretion after resistance exercise than does consumption of an isonitrogenous and isoenergetic soy-protein beverage. *American Journal of Clinical Nutrition* 85: 1031–1040, 2007. doi: 10.1093/ajcn/85.4.1031.

136. **Tang JE**, **Moore DR**, **Kujbida GW**, **Tarnopolsky MA**, **Phillips SM**. Ingestion of whey hydrolysate, casein, or soy protein isolate: Effects on mixed muscle protein synthesis at rest and following resistance exercise in young men. *J Appl Physiol* 107: 987–992, 2009. doi: 10.1152/japplphysiol.00076.2009.

137. **Yang Y**, **Churchward-Venne TA**, **Burd NA**, **Breen L**, **Tarnopolsky MA**, **Phillips SM**. Myofibrillar protein synthesis following ingestion of soy protein isolate at rest and after resistance exercise in elderly men. *Nutr Metab (Lond)* 9: 57, 2012. doi: 10.1186/1743-7075-9-57.

138. **Poole C**, **Wilborn C**, **Taylor L**, **Kerksick C**. The role of post-exercise nutrient administration on muscle protein synthesis and glycogen synthesis. *J Sports Sci Med* 9: 354–363, 2010.

139. **Chandel NS**. Amino Acid Metabolism. *Cold Spring Harb Perspect Biol* 13: a040584, 2021. doi: 10.1101/cshperspect.a040584.

140. **Chantranupong L**, **Scaria SM**, **Saxton RA**, **Gygi MP**, **Shen K**, **Wyant GA**, **Wang T**, **Harper JW**, **Gygi SP**, **Sabatini DM**. The CASTOR Proteins Are Arginine Sensors for the mTORC1 Pathway. *Cell* 165: 153–164, 2016. doi: 10.1016/j.cell.2016.02.035.

141. **Yoshizawa F**. Regulation of protein synthesis by branched-chain amino acids in vivo. In: *Biochemical and Biophysical Research Communications*. 2004, p. 417–422.

142. **Norton LE**, **Layman DK**. Leucine regulates translation initiation of protein synthesis in skeletal muscle after exercise. In: *Journal of Nutrition*. 2006, p. 533–537.

143. **Kamei Y**, **Hatazawa Y**, **Uchitomi R**, **Yoshimura R**, **Miura S**. Regulation of skeletal muscle function by amino acids. *Nutrients* 12: 261, 2020.

144. **Kim D-H**, **Kim S-H**, **Jeong W-S**, **Lee H-Y**. Effect of BCAA intake during endurance exercises on fatigue substances, muscle damage substances, and energy metabolism substances. *J Exerc Nutrition Biochem* 17: 169–180, 2013. doi: 10.5717/jenb.2013.17.4.169.

145. **Siddik MAB**, **Shin AC**. Recent progress on branched-chain amino acids in obesity, diabetes, and beyond. *Endocrinology and Metabolism* 34: 234–246, 2019.

146. **Nishitani S**, **Takehana K**, **Fujitani S**, **Sonaka I**. Branched-chain amino acids improve glucose metabolism in rats with liver cirrhosis. *Am J Physiol Gastrointest Liver Physiol* 288, 2005. doi: 10.1152/ajpgi.00510.2003.

147. **Yoon MS**. The emerging role of branched-chain amino acids in insulin resistance and metabolism. *Nutrients* 8: 405, 2016.

148. **Zhang Y**, **Guo K**, **LeBlanc RE**, **Loh D**, **Schwartz GJ**, **Yu YH**. Increasing dietary leucine intake reduces diet-induced obesity and improves glucose and cholesterol metabolism in mice via multimechanisms. *Diabetes* 56: 1647–54, 2007. doi: 10.2337/db07-0123.

149. **Weber MG**, **Dias SS**, **de Angelis TR**, **Fernandes EV**, **Bernardes AG**, **Milanez VF**, **Jussiani EI**, **de Paula Ramos S**. The use of BCAA to decrease delayed-onset muscle soreness after a single bout of exercise: a systematic review and meta-analysis. *Amino Acids* 53: 1663–1678, 2021. doi: 10.1007/s00726-021-03089-2.

150. **Martinho D V.**, **Nobari H**, **Faria A**, **Field A**, **Duarte D**, **Sarmento H**. Oral Branched-Chain Amino Acids Supplementation in Athletes: A Systematic Review. *Nutrients* 14: 4002, 2022. doi: 10.3390/nu14194002.

151. **Newgard CB**, **An J**, **Bain JR**, **Muehlbauer MJ**, **Stevens RD**, **Lien LF**, **Haqq AM**, **Shah SH**, **Arlotto M**, **Slentz CA**, **Rochon J**, **Gallup D**, **Ilkayeva O**, **Wenner BR**, **Yancy WS**, **Eisenson H**, **Musante G**, **Surwit RS**, **Millington DS**, **Butler MD**, **Svetkey LP**. A Branched-Chain Amino Acid-Related Metabolic Signature that Differentiates Obese and Lean Humans and Contributes to Insulin Resistance. *Cell Metab* 9: 311–326, 2009. doi: 10.1016/j.cmet.2009.02.002.

152. **Flores-Guerrero J**, **Osté M**, **Kieneker L**, **Gruppen E**, **Wolak-Dinsmore J**, **Otvos J**, **Connelly M**, **Bakker S**, **Dullaart R**. Plasma Branched-Chain Amino Acids and Risk of Incident Type 2 Diabetes: Results from the PREVEND Prospective Cohort Study. *J Clin Med* 7: 513, 2018. doi: 10.3390/jcm7120513.

153. **Dickinson JM**, **Rasmussen BB**. Amino acid transporters in the regulation of human skeletal muscle protein metabolism. *Curr Opin Clin Nutr Metab Care* 16: 638–644, 2013.

154. **Verrey F**, **Closs EI**, **Wagner CA**, **Palacin M**, **Endou H**, **Kanai Y**. CATs and HATs: The SLC7 family of amino acid transporters. *Pflugers Arch* 447: 532–542, 2004.

155. **Verrey F**, **Closs EI**, **Wagner CA**, **Palacin M**, **Endou H**, **Kanai Y**. CATs and HATs: the SLC7 family of amino acid transporters. *Pfl*[illegible]*gers Archiv European Journal of Physiology* 447: 532–542, 2004. doi: 10.1007/s00424-003-1086-z.

156. **Bodoy S**, **Martín L**, **Zorzano A**, **Palacín M**, **Estévez R**, **Bertran J**. Identification of LAT4, a Novel Amino Acid Transporter with System L Activity. *Journal of Biological Chemistry* 280: 12002–12011, 2005. doi: 10.1074/jbc.M408638200.

157. **Poncet N**, **Mitchell FE**, **Ibrahim AFM**, **McGuire VA**, **English G**, **Arthur JSC**, **Shi YB**, **Taylor PM**. The catalytic subunit of the system L1 amino acid transporter (Slc7a5) facilitates nutrient signalling in mouse skeletal muscle. *PLoS One* 9: e89547, 2014. doi: 10.1371/journal.pone.0089547.

158. **Yanagida O**, **Kanai Y**, **Chairoungdua A**, **Kim DK**, **Segawa H**, **Nii T**, **Cha SH**, **Matsuo H**, **Fukushima J ichi**, **Fukasawa Y**, **Tani Y**, **Taketani Y**, **Uchino H**, **Kim JY**, **Inatomi J**, **Okayasu I**, **Miyamoto K ichi**, **Takeda E**, **Goya T**, **Endou H**. Human L-type amino acid transporter 1 (LAT1): Characterization of function and expression in tumor cell lines. *Biochim Biophys Acta Biomembr* 1514: 291–302, 2001. doi: 10.1016/S0005-2736(01)00384-4.

159. **Taylor PM**. Role of amino acid transporters in amino acid sensing. *American Journal of Clinical Nutrition* 99: 223–230, 2014. doi: 10.3945/ajcn.113.070086.

160. **Goto M**, **Miyahara I**, **Hirotsu K**, **Conway M**, **Yennawar N**, **Islam MM**, **Hutson SM**. Structural Determinants for Branched-chain Aminotransferase Isozyme-specific Inhibition by the Anticonvulsant Drug Gabapentin. *Journal of Biological Chemistry* 280: 37246–37256, 2005. doi: 10.1074/jbc.M506486200.

161. **Bledsoe RK**, **Dawson PA**, **Hutson SM**. Cloning of the rat and human mitochondrial branched chain aminotransferases (BCAT(m)). *Biochimica et Biophysica Acta - Protein Structure and Molecular Enzymology* 1339: 9–13, 1997. doi: 10.1016/S0167-4838(97)00044-7.

162. **Suryawan A**, **Hawes JW**, **Harris RA**, **Shimomura Y**, **Jenkins AE**, **Hutson SM**. A molecular model of human branched-chain amino acid metabolism. *American Journal of Clinical Nutrition* 68: 72–81, 1998.

163. **Sivanand S**, **Vander Heiden MG**. Emerging Roles for Branched-Chain Amino Acid Metabolism in Cancer. *Cancer Cell* 37: 147–156, 2020. doi: 10.1016/j.ccell.2019.12.011.

164. **Kainulainen H**, **Hulmi JJ**, **Kujala UM**. Potential role of branched-chain amino acid catabolism in regulating fat oxidation. *Exerc Sport Sci Rev* 41: 194–200, 2013. doi: 10.1097/JES.0b013e3182a4e6b6.

165. **Van Koevering M**, **Nissen S**. Oxidation of leucine and alpha-ketoisocaproate to beta-hydroxy-beta-methylbutyrate in vivo. *American Journal of Physiology-Endocrinology and Metabolism* 262: E27–E31, 1992. doi: 10.1152/ajpendo.1992.262.1.E27.

166. **Wilkinson DJ**, **Hossain T**, **Hill DS**, **Phillips BE**, **Crossland H**, **Williams J**, **Loughna P**, **Churchward-Venne TA**, **Breen L**, **Phillips SM**, **Etheridge T**, **Rathmacher JA**, **Smith K**, **Szewczyk NJ**, **Atherton PJ**. Effects of leucine and its metabolite β-hydroxy-β-methylbutyrate on human skeletal muscle protein metabolism. *J Physiol* 591: 2911–2923, 2013. doi: 10.1113/jphysiol.2013.253203.

167. **Kimura K**, **Cheng XW**, **Inoue A**, **Hu L**, **Koike T**, **Kuzuya M**. β-Hydroxy-β-methylbutyrate facilitates PI3K/Akt-dependent mammalian target of rapamycin and FoxO1/3a phosphorylations and alleviates tumor necrosis factor α/interferon γ–induced MuRF-1 expression in C2C12 cells. *Nutrition Research* 34: 368–374, 2014. doi: 10.1016/j.nutres.2014.02.003.

168. **Adeva-Andany MM**, **López-Maside L**, **Donapetry-García C**, **Fernández-Fernández C**, **Sixto-Leal C**. Enzymes involved in branched-chain amino acid metabolism in humans. *Amino Acids* 49: 1005–1028, 2017. doi: 10.1007/s00726-017-2412-7.

169. **Nobukuni Y**, **Mitsubuchi H**, **Endo F**, **Matsuda I**. Complete Primary Strcture of the Transacylase (E2b) Subunit of the Human Branched Chain a-keto acid dehydrogenase complex. 161: 1035–1041, 1989.

170. **Wynn RM**, **Chuang JL**, **Cote CD**, **Chuang DT**. Tetrameric assembly and conservation in the ATP-binding domain of rat branched-chain α-ketoacid dehydrogenase kinase. *Journal of Biological Chemistry* 275: 30512–30519, 2000. doi: 10.1074/jbc.M005075200.

171. **Damuni Z**, **Reed LJ**. Purification and properties of the catalytic subunit of the branched-chain alpha-keto acid dehydrogenase phosphatase from bovine kidney mitochondria. *Journal of Biological Chemistry* 262: 5129–5132, 1987.

172. **Suryawan A**, **Hawes JW**, **Harris RA**, **Shimomura Y**, **Jenkins AE**, **Hutson SM**. A molecular model of human branched-chain amino acid metabolism. *Am J Clin Nutr* 68: 72–81, 1998. doi: 10.1093/ajcn/68.1.72.

173. **McCarthy JJ**, **Esser KA**. Anabolic and catabolic pathways regulating skeletal muscle mass. *Curr Opin Clin Nutr Metab Care* 13: 230–235, 2010. doi: 10.1097/MCO.0b013e32833781b5.

174. **Winbanks CE**, **Chen JL**, **Qian H**, **Liu Y**, **Bernardo BC**, **Beyer C**, **Watt KI**, **Thomson RE**, **Connor T**, **Turner BJ**, **McMullen JR**, **Larsson L**, **McGee SL**, **Harrison CA**, **Gregorevic P**. The bone morphogenetic protein axis is a positive regulator of skeletal muscle mass. *J Cell Biol* 203: 345–57, 2013.

175. **Moberg M**, **Apró W**, **Ekblom B**, **Van Hall G**, **Holmberg HC**, **Blomstrand E**. Activation of mTORC1 by leucine is potentiated by branched-chain amino acids and even

more so by essential amino acids following resistance exercise. *Am J Physiol Cell Physiol* 310: C874–C884, 2016.

176. **Dangelmaier C**, **Manne BK**, **Liverani E**, **Jin J**, **Bray P**, **Kunapuli SP**. PDK1 selectively phosphorylates Thr(308) on Akt and contributes to human platelet functional responses. *Thromb Haemost* 111: 508–517, 2013. doi: 10.1160/TH13-06-0484.

177. **Lai K-M v.**, **Gonzalez M**, **Poueymirou WT**, **Kline WO**, **Na E**, **Zlotchenko E**, **Stitt TN**, **Economides AN**, **Yancopoulos GD**, **Glass DJ**. Conditional Activation of Akt in Adult Skeletal Muscle Induces Rapid Hypertrophy. *Mol Cell Biol* 24: 9295–9304, 2004. doi: 10.1128/mcb.24.21.9295-9304.2004.

178. **Sugita H**, **Kaneki M**, **Sugita M**, **Yasukawa T**, **Yasuhara S**, **Martyn JAJ**. Burn injury impairs insulin-stimulated Akt/PKB activation in skeletal muscle. *Am J Physiol Endocrinol Metab* 288: 585–591, 2005. doi: 10.1152/ajpendo.00321.2004.

179. **Zhang X**, **Tang N**, **Hadden TJ**, **Rishi AK**. Akt, FoxO and regulation of apoptosis. *Biochim Biophys Acta Mol Cell Res* 1813: 1978–1986, 2011.

180. **Beurel E**, **Grieco SF**, **Jope RS**. Glycogen synthase kinase-3 (GSK3): Regulation, actions, and diseases. *Pharmacol Ther* 148: 114–131, 2015.

181. **Lee SW**, **Dai G**, **Hu Z**, **Wang X**, **Du J**, **Mitch WE**. Regulation of muscle protein degradation: Coordinated control of apoptotic and ubiquitin-proteasome systems by phosphatidylinositol 3 kinase. *Journal of the American Society of Nephrology* 15: 1537–1545, 2004. doi: 10.1097/01.ASN.0000127211.86206.E1.

182. **Wang Q**, **Somwar R**, **Bilan PJ**, **Liu Z**, **Jin J**, **Woodgett JR**, **Klip A**. Protein Kinase B/Akt Participates in GLUT4 Translocation by Insulin in L6 Myoblasts. *Mol Cell Biol* 19: 4008–4018, 1999. doi: 10.1128/mcb.19.6.4008.

183. **Wang HY**, **Ducommun S**, **Quan C**, **Xie B**, **Li M**, **Wasserman DH**, **Sakamoto K**, **Mackintosh C**, **Chen S**. AS160 deficiency causes whole-body insulin resistance via composite effects in multiple tissues. *Biochemical Journal* 449: 479–489, 2013. doi: 10.1042/BJ20120702.

184. **Farese R v.** Function and dysfunction of aPKC isoforms for glucose transport in insulin-sensitive and insulin-resistant states. *Am J Physiol Endocrinol Metab* 283: 1–11, 2002.

185. **Sakamoto K**, **Holman GD**. Emerging role for AS160/TBC1D4 and TBC1D1 in the regulation of GLUT4 traffic. *Am J Physiol Endocrinol Metab* 295: 29–37, 2008.

186. **Mann G**, **Riddell MC**, **Adegoke OAJ**. Effects of Acute Muscle Contraction on the Key Molecules in Insulin and Akt Signaling in Skeletal Muscle in Health and in Insulin Resistant States. *Diabetology* 3: 423–446, 2022. doi: 10.3390/diabetology3030032.

187. **Inoki K**, **Li Y**, **Zhu T**, **Wu J**, **Guan KL**. TSC2 is phosphorylated and inhibited by Akt and suppresses mTOR signalling. *Nat Cell Biol* 4: 648–57, 2002. doi: 10.1038/ncb839.

188. **Ghosh J**, **Kapur R**. Role of mTORC1–S6K1 signaling pathway in regulation of hematopoietic stem cell and acute myeloid leukemia. *Exp Hematol* 50: 13–21, 2017.

189. **Burd NA**, **Holwerda AM**, **Selby KC**, **West DWD**, **Staples AW**, **Cain NE**, **Cashaback JGA**, **Potvin JR**, **Baker SK**, **Phillips SM**. Resistance exercise volume affects myofibrillar protein synthesis and anabolic signalling molecule phosphorylation in young men. *Journal of Physiology* 588: 3119–3130, 2010. doi: 10.1113/jphysiol.2010.192856.

190. **Marabita M**, **Baraldo M**, **Solagna F**, **Ceelen JJM**, **Sartori R**, **Nolte H**, **Nemazanyy I**, **Pyronnet S**, **Kruger M**, **Pende M**, **Blaauw B**. S6K1 Is Required for Increasing Skeletal Muscle Force during Hypertrophy. *Cell Rep* 17: 501–513, 2016. doi: 10.1016/j.celrep.2016.09.020.

191. **Nao Hosokawa**, **Taichi Hara**, **Takeshi Kaizuka CK**, **Akito Takamura YMSI**, **Natsume T**, **Kenji Takehana NY**, **Guan J-L**, **Noriko Oshiro and NM**. Nutrient-dependent mTORC1 Association with the ULK1–Atg13–FIP200 Complex Required for Autophagy. *Mol Biol Cell* 20: 1981–1991, 2009.

192. **Wykes LJ**, **Fiorotto M**, **Burrin DG**, **del Rosario M**, **Frazer ME**, **Pond WG**, **Jahoor F**. Chronic low protein intake reduces tissue protein synthesis in a pig model of protein malnutrition. *Journal of Nutrition* 126: 1481–1488, 1996. doi: 10.1093/jn/126.5.1481.

193. **Kilroe SP**, **Fulford J**, **Holwerda AM**, **Jackman SR**, **Lee BP**, **Gijsen AP**, **van Loon LJC**, **Wall BT**. Short-term muscle disuse induces a rapid and sustained decline in daily myofibrillar protein synthesis rates. *Am J Physiol Endocrinol Metab* 318: 117–130, 2020. doi: 10.1152/ajpendo.00360.2019.

194. **Dolly A**, **Dumas J**, **Servais S**. Cancer cachexia and skeletal muscle atrophy in clinical studies: what do we really know? *J Cachexia Sarcopenia Muscle* 11: 1413–1428, 2020. doi: 10.1002/jcsm.12633.

195. **Mueller C**. Disease-Related Malnutrition: An Evidence-Based Approach to Treatment. *Nutrition in Clinical Practice* 18: 1128–1129, 2003. doi: 10.1177/0115426503018006527.

196. **Cederholm T**, **Barazzoni R**, **Austin P**, **Ballmer P**, **Biolo G**, **Bischoff SC**, **Compher C**, **Correia I**, **Higashiguchi T**, **Holst M**, **Jensen GL**, **Malone A**, **Muscaritoli M**, **Nyulasi I**, **Pirlich M**, **Rothenberg E**, **Schindler K**, **Schneider SM**, **de van der Schueren MAE**, **Sieber C**, **Valentini L**, **Yu JC**, **van Gossum A**, **Singer P**. ESPEN guidelines on definitions and terminology of clinical nutrition. *Clinical Nutrition* 36: 49–64, 2017. doi: 10.1016/j.clnu.2016.09.004.

197. **Viart P**. Hemodynamic findings in severe protein calorie malnutrition. *American Journal of Clinical Nutrition* 30: 334–348, 1977.

198. **Putti R**, **Sica R**, **Migliaccio V**, **Lionetti L**. Diet impact on Mitochondrial Bioenergetics and Dynamics. *Front Physiol* 6: 109, 2015. doi: 10.3389/fphys.2015.00109.

199. **Rao RH**, **Menon RK**. Chronic malnutrition impairs insulin sensitivity through both receptor and postreceptor defects in rats with mild streptozocin diabetes. *Metabolism* 42: 772–779, 1993. doi: 10.1016/0026-0495(93)90248-M.

200. **Landi F**, **Camprubi-Robles M**, **Bear DE**, **Cederholm T**, **Malafarina V**, **Welch AA**, **Cruz-Jentoft AJ**. Muscle loss: The new malnutrition challenge in clinical practice. *Clinical Nutrition* 38: 2113–2120, 2019. doi: 10.1016/j.clnu.2018.11.021.

201. **Medzhitov R**. Inflammation 2010: new adventures of an old flame. *Cell* 140: 771–6, 2010.

202. **Haddad F**, **Zaldivar F**, **Cooper DM**, **Adams GR**. IL-6-induced skeletal muscle atrophy. *J Appl Physiol (1985)* 98: 911–7, 2005.

203. **Nathan C**, **Ding A**. Nonresolving inflammation. *Cell* 140: 871–82, 2010.

204. **Park BS**, **Yoon JS**. Relative skeletal muscle mass is associated with development of metabolic syndrome. *Diabetes Metab J* 37: 458–64, 2013. doi: 10.4093/dmj.2013.37.6.458.

205. **Freeman AM**, **Pennings N**. Insulin Resistance - StatPearls - NCBI Bookshelf. .

206. **Bano G**. Glucose homeostasis, obesity and diabetes. *Best Pract Res Clin Obstet Gynaecol* 17: 112–35, 2013. doi: 10.1016/j.bpobgyn.2013.02.007.

207. **Ali M**, **Bukhari SA**, **Ali M**, **Lee H-W**. Upstream signalling of mTORC1 and its hyperactivation in type 2 diabetes (T2D). *BMB Rep* 50: 601–609, 2017.

208. **Dibble CC**, **Manning BD**. Signal integration by mTORC1 coordinates nutrient input with biosynthetic output. *Nat Cell Biol* 15: 555–64, 2013.

209. **Lynch CJ**. Role of leucine in the regulation of mTOR by amino acids: revelations from structure-activity studies. *J Nutr* 131: 861S-865S, 2001.

210. **Lian K**, **Du C**, **Liu Y**, **Zhu D**, **Yan W**, **Zhang H**, **Hong Z**, **Liu P**, **Zhang L**, **Pei H**, **Zhang J**, **Gao C**, **Xin C**, **Cheng H**, **Xiong L**, **Tao L**. Impaired Adiponectin Signaling Contributes to Disturbed Catabolism of Branched-Chain Amino Acids in Diabetic Mice. *Diabetes* 64: 49–59, 2015.

211. **Hernández-Alvarez MI**, **Díaz-Ramos A**, **Berdasco M**, **Cobb J**, **Planet E**, **Cooper D**, **Pazderska A**, **Wanic K**, **O'Hanlon D**, **Gomez A**, **de La Ballina LR**, **Esteller M**, **Palacin M**, **O'Gorman DJ**, **Nolan JJ**, **Zorzano A**. Early-onset and classical forms of type 2 diabetes show impaired expression of genes involved in muscle branched-chain amino acids metabolism. *Sci Rep* 7: 1–12, 2017. doi: 10.1038/s41598-017-14120-6.

212. **Zhou M**, **Shao J**, **Wu CY**, **Shu L**, **Dong W**, **Liu Y**, **Chen M**, **Wynn RM**, **Wang J**, **Wang J**, **Gui WJ**, **Qi X**, **Lusis AJ**, **Li Z**, **Wang W**, **Ning G**, **Yang X**, **Chuang DT**, **Wang Y**, **Sun H**. Targeting BCAA catabolism to treat obesity-associated insulin resistance. *Diabetes* 68: 1730–1746, 2019. doi: 10.2337/db18-0927.

213. **Mccormack SE**, **Shaham O**, **Mccarthy MA**, **Deik AA**, **Wang TJ**, **Gerszten RE**, **Clish CB**, **Mootha VK**, **Grinspoon SK**, **Fleischman A**. Circulating branched-chain amino acid concentrations are associated with obesity and future insulin resistance in children and adolescents. *Pediatr Obes* 8: 52–61, 2013. doi: 10.1111/j.2047-6310.2012.00087.x.

214. **Yoshida T**, **Delafontaine P**. Mechanisms of cachexia in chronic disease states. *American Journal of the Medical Sciences* 350: 250–256, 2015. doi: 10.1097/MAJ.0000000000000511.

215. **Bonetto A**, **Rupert JE**, **Barreto R**, **Zimmers TA**. The Colon-26 Carcinoma Tumor-bearing Mouse as a Model for the Study of Cancer Cachexia. *J Vis Exp* : 54893-undefined, 2016. doi: 10.3791/54893.

216. **Tabernero J**, **Yoshino T**, **Cohn AL**, **Obermannova R**, **Bodoky G**, **Garcia-Carbonero R**, **Ciuleanu T-E**, **Portnoy DC**, **Van Cutsem E**, **Grothey A**, **Prausová J**, **Garcia-Alfonso P**, **Yamazaki K**, **Clingan PR**, **Lonardi S**, **Kim TW**, **Simms L**, **Chang S-C**, **Nasroulah F**. Ramucirumab versus placebo in combination with second-line FOLFIRI in patients with metastatic colorectal carcinoma that progressed during or after first-line therapy with bevacizumab, oxaliplatin, and a fluoropyrimidine (RAISE): a randomised, double-blind, multicentre, phase 3 study. *Lancet Oncol* 16: 499–508, 2015.

217. **Pomerantz MM**, **Freedman ML**. The genetics of cancer risk. *Cancer Journal* 17: 416–422, 2011.

218. **Parsa N**. Environmental factors inducing human cancers. *Iran J Public Health* 41: 1–9, 2012.

219. **Anand P**, **Kunnumakara AB**, **Sundaram C**, **Harikumar KB**, **Tharakan ST**, **Lai OS**, **Sung B**, **Aggarwal BB**. Cancer is a preventable disease that requires major lifestyle changes. *Pharm Res* 25: 2097–2116, 2008.

220. **Sarkar S**, **Horn G**, **Moulton K**, **Oza A**, **Byler S**, **Kokolus S**, **Longacre M**. Cancer development, progression, and therapy: an epigenetic overview. *Int J Mol Sci* 14: 21087–113, 2013.

221. **Scheel BI**, **Holtedahl K**. Symptoms, signs, and tests: The general practitioner's comprehensive approach towards a cancer diagnosis. *Scand J Prim Health Care* 33: 170–7, 2015. doi: 10.3109/02813432.2015.1067512.

222. **de Oliveira C**, **Weir S**, **Rangrej J**, **Krahn MD**, **Mittmann N**, **Hoch JS**, **Chan KKW**, **Peacock S**. The economic burden of cancer care in Canada: a population-based cost study. *CMAJ Open* 6: 1–10, 2018. doi: 10.9778/cmajo.20170144.

223. **White MC**, **Holman DM**, **Boehm JE**, **Peipins LA**, **Grossman M**, **Henley SJ**. Age and cancer risk: a potentially modifiable relationship. *Am J Prev Med* 46: S7-15, 2014.

224. **Belpomme D**, **Irigaray P**, **Hardell L**, **Clapp R**, **Montagnier L**, **Epstein S**, **Sasco AJ**. The multitude and diversity of environmental carcinogens. *Environ Res* 105: 414–29, 2007.

225. **Belpomme D**, **Irigaray P**, **Sasco AJ**, **Newby JA**, **Howard V**, **Clapp R**, **Hardell L**. The growing incidence of cancer: role of lifestyle and screening detection (Review). *Int J Oncol* 30: 1037–49, 2007.

226. **Dennis LK**, **Vanbeek MJ**, **Beane Freeman LE**, **Smith BJ**, **Dawson D V**, **Coughlin JA**. Sunburns and risk of cutaneous melanoma: does age matter? A comprehensive meta-analysis. *Ann Epidemiol* 18: 614–27, 2008.

227. **Hanahan D**, **Weinberg RA**. Hallmarks of cancer: the next generation. *Cell* 144: 646–74, 2011.

228. **López-Otín C**, **Blasco MA**, **Partridge L**, **Serrano M**, **Kroemer G**. The hallmarks of aging. *Cell* 153: 1194–217, 2013.

229. **Siegel RL**, **Miller KD**, **Jemal A**. Cancer statistics, 2017. *CA Cancer J Clin* 67: 7–30, 2017. doi: 10.3322/caac.21387.

230. **Arnold M**, **Sierra MS**, **Laversanne M**, **Soerjomataram I**, **Jemal A**, **Bray F**. Global patterns and trends in colorectal cancer incidence and mortality. *Gut* 66: 683–691, 2017. doi: 10.1136/gutjnl-2015-310912.

231. **Global Burden of Disease Cancer Collaboration**. Erratum: Global, regional, and national cancer incidence, mortality, years of life lost, years lived with disability, and disability-adjusted life-years for 32 cancer groups, 1990 to 2015: A systematic analysis for the global burden of disease study (JAMA Oncology (2016) DOI: 10.1001/jamaoncol.2016.5688). *JAMA Oncol* 3: 524–548, 2017.

232. **Tevfik Dorak M**, **Karpuzoglu E**. Gender differences in cancer susceptibility: An inadequately addressed issue. *Front Genet* 3: 268, 2012. doi: 10.3389/fgene.2012.00268.

233. **Crocetti E**, **Mallone S**, **Robsahm TE**, **Gavin A**, **Agius D**, **Ardanaz E**, **Lopez MDC**, **Innos K**, **Minicozzi P**, **Borgognoni L**, **Pierannunzio D**, **Eisemann N**. Survival of patients with skin melanoma in Europe increases further: Results of the EUROCARE-5 study. *Eur J Cancer* 51: 2179–2190, 2015. doi: 10.1016/j.ejca.2015.07.039.

234. **Wang H**, **Naghavi M**. Global, regional, and national life expectancy, all-cause mortality, and cause-specific mortality for 249 causes of death, 1980–2015: a systematic analysis for the Global Burden of Disease Study 2015. *The Lancet* 388: 1459–544, 2016. doi: 10.1016/S0140-6736(16)31012-1.

235. **Zheng L**, **Wang Y**, **Schabath MB**, **Grossman HB**, **Wu X**. Sulfotransferase 1A1 (SULT1A1) polymorphism and bladder cancer risk: A case-control study. *Cancer Lett* 202: 61–69, 2003. doi: 10.1016/j.canlet.2003.08.007.

236. **Bolufer P**, **Collado M**, **Barragán E**, **Cervera J**, **Calasanz MJ**, **Colomer D**, **Roman-Gómez J**, **Sanz MA**. The potential effect of gender in combination with common genetic polymorphisms of drug-metabolizing enzymes on the risk of developing acute leukemia. *Haematologica* 92: 308–314, 2007. doi: 10.3324/haematol.10752.

237. **Bond GL**, **Hirshfield KM**, **Kirchhoff T**, **Alexe G**, **Bond EE**, **Robins H**, **Bartel F**, **Taubert H**, **Wuerl P**, **Hait W**, **Toppmeyer D**, **Offit K**, **Levine AJ**. MDM2 SNP309 accelerates tumor formation in a gender-specific and hormone-dependent manner. *Cancer Res* 66: 5104–5110, 2006. doi: 10.1158/0008-5472.CAN-06-0180.

238. **Pierorazio PM**, **Ferrucci L**, **Kettermann A**, **Longo DL**, **Metter EJ**, **Carter HB**. Serum testosterone is associated with aggressive prostate cancer in older men: Results from the Baltimore Longitudinal Study of Aging. *BJU Int* 105: 824–829, 2010. doi: 10.1111/j.1464-410X.2009.08853.x.

239. **Do TN**, **Ucisik-Akkaya E**, **Davis CF**, **Morrison BA**, **Dorak MT**. An intronic polymorphism of IRF4 gene influences gene transcription in vitro and shows a risk association with childhood acute lymphoblastic leukemia in males. *Biochim Biophys Acta Mol Basis Dis* 1802: 292–300, 2010. doi: 10.1016/j.bbadis.2009.10.015.

240. **Lee ML**, **Chen GG**, **Vlantis AC**, **Tse GMK**, **Leung BCH**, **van Hasselt CA**. Induction of thyroid papillary carcinoma cell proliferation by estrogen is associated with an altered expression of Bcl-xL. *Cancer Journal* 11: 113–121, 2005. doi: 10.1097/00130404-200503000-00006.

241. **Yue W**, **Wang JP**, **Li Y**, **Fan P**, **Liu G**, **Zhang N**, **Conaway M**, **Wang H**, **Korach KS**, **Bocchinfuso W**, **Santen R**. Effects of estrogen on breast cancer development: Role of estrogen receptor independent mechanisms. *Int J Cancer* 127: 1748–1757, 2010. doi: 10.1002/ijc.25207.

242. **Hagan C**. WHEN ARE MICE CONSIDERED OLD? *The Jackson Laboratory*: 2017.

243. **Jackson SJ**, **Andrews N**, **Ball D**, **Bellantuono I**, **Gray J**, **Hachoumi L**, **Holmes A**, **Latcham J**, **Petrie A**, **Potter P**, **Rice A**, **Ritchie A**, **Stewart M**, **Strepka C**, **Yeoman M**, **Chapman K**. Does age matter? The impact of rodent age on study outcomes. *Lab Anim* 51: 160–169, 2017. doi: 10.1177/0023677216653984.

244. **Langille MGI**, **Meehan CJ**, **Koenig JE**, **Dhanani AS**, **Rose RA**, **Howlett SE**, **Beiko RG**. Microbial shifts in the aging mouse gut. *Microbiome* 2: 50, 2014. doi: 10.1186/s40168-014-0050-9.

245. **Pibiri M**, **Sulas P**, **Leoni VP**, **Perra A**, **Kowalik MA**, **Cordella A**, **Saggese P**, **Nassa G**, **Ravo M**. Global gene expression profile of normal and regenerating liver in young and old mice. *Age (Omaha)* 37: 9796, 2015. doi: 10.1007/s11357-015-9796-7.

246. **Greaves LC**, **Barron MJ**, **Campbell-Shiel G**, **Kirkwood TBL**, **Turnbull DM**. Differences in the accumulation of mitochondrial defects with age in mice and humans. *Mech Ageing Dev* 132: 588–591, 2011. doi: 10.1016/j.mad.2011.10.004.

247. **Busquets S**, **Toledo M**, **Marmonti E**, **Orpí M**, **Capdevila E**, **Betancourt A**, **López-Soriano FJ**, **Argilés JM**. Formoterol treatment downregulates the myostatin system in skeletal muscle of cachectic tumour-bearing rats. *Oncol Lett* 3: 185–189, 2012. doi: 10.3892/ol.2011.442.

248. **Costelli P**, **Carbó N**, **Tessitore L**, **Bagby GJ**, **Lopez-Soriano FJ**, **Argilés JM**, **Baccino FM**. Tumor necrosis factor-α mediates changes in tissue protein turnover in a rat cancer cachexia model. *Journal of Clinical Investigation* 92: 2783–2789, 1993. doi: 10.1172/JCI116897.

249. **Costelli P**, **Muscaritoli M**, **Bossola M**, **Moore-Carrasco R**, **Crepaldi S**, **Grieco G**, **Autelli R**, **Bonelli G**, **Pacelli F**, **Lopez-Soriano FJ**, **Argilés JM**, **Doglietto GB**, **Baccino FM**, **Rossi Fanelli F**. Skeletal muscle wasting in tumor-bearing rats is associated with MyoD down-regulation. *Int J Oncol* 26: 1663–1668, 2005. doi: 10.3892/ijo.26.6.1663.

250. **López-Soriano J**, **Argilés JM**, **López-Soriano FJ**. Lipid metabolism in rats bearing the Yoshida AH-130 ascites hepatoma. *Mol Cell Biochem* 165: 17–23, 1996. doi: 10.1007/bf00229741.

251. **Muscaritoli M**, **Costelli P**, **Bossola M**, **Grieco G**, **Bonelli G**, **Bellantone R**, **Doglietto GB**, **Rossi-Fanelli F**, **Baccino FM**. Effects of simvastatin administration in an experimental model of cancer cachexia. *Nutrition* 19: 936–939, 2003. doi: 10.1016/j.nut.2003.08.004.

252. **Penna F**, **Costamagna D**, **Pin F**, **Camperi A**, **Fanzani A**, **Chiarpotto EM**, **Cavallini G**, **Bonelli G**, **Baccino FM**, **Costelli P**. Autophagic degradation contributes to muscle wasting in cancer cachexia. *American Journal of Pathology* 182: 1367–1378, 2013. doi: 10.1016/j.ajpath.2012.12.023.

253. **Damrauer JS**, **Stadler ME**, **Acharyya S**, **Baldwin AS**, **Couch ME**, **Guttridge DC**. Chemotherapy-induced muscle wasting: association with NF-κB and cancer cachexia. *Eur J Transl Myol* 18: 139–148, 2018. doi: 10.4081/ejtm.2018.7590.

254. **Inaba S**, **Hinohara A**, **Tachibana M**, **Tsujikawa K**, **Fukada S**. Muscle regeneration is disrupted by cancer cachexia without loss of muscle stem cell potential. *PLoS One* 13: e0205467, 2018. doi: 10.1371/journal.pone.0205467.

255. **Joppa MA**, **Gogas KR**, **Foster AC**, **Markison S**. Central infusion of the melanocortin receptor antagonist agouti-related peptide (AgRP(83-132)) prevents cachexia-related symptoms induced by radiation and colon-26 tumors in mice. .

256. **Penna F**, **Costamagna D**, **Fanzani A**, **Bonelli G**, **Baccino FM**, **Costelli P**. Muscle wasting and impaired Myogenesis in tumor bearing mice are prevented by ERK inhibition. *PLoS One* 5: 13604-undefined, 2010. doi: 10.1371/journal.pone.0013604.

257. **Pin F**, **Busquets S**, **Toledo M**, **Camperi A**, **Lopez-Soriano FJ**, **Costelli P**, **Argilés JM**, **Penna F**. Combination of exercise training and erythropoietin prevents cancer-induced muscle alterations. *Oncotarget* 6: 43202–43215, 2015. doi: 10.18632/oncotarget.6439.

258. **Weyermann P**, **Dallmann R**, **Magyar J**, **Anklin C**, **Hufschmid M**, **Dubach-Powell J**, **Courdier-Fruh I**, **Henneböhle M**, **Nordhoff S**, **Mondadori C**. Orally available selective melanocortin-4 receptor antagonists stimulate food intake and reduce cancer-induced cachexia in mice. *PLoS One* 4: e4774, 2009. doi: 10.1371/journal.pone.0004774.

259. **Alves CRR**, **Neves W das**, **de Almeida NR**, **Eichelberger EJ**, **Jannig PR**, **Voltarelli VA**, **Tobias GC**, **Bechara LRG**, **de Paula Faria D**, **Alves MJN**, **Hagen L**, **Sharma A**, **Slupphaug G**, **Moreira JBN**, **Wisloff U**, **Hirshman MF**, **Negrão CE**, **de Castro G**, **Chammas R**, **Swoboda KJ**, **Ruas JL**, **Goodyear LJ**, **Brum PC**. Exercise training reverses cancer-induced oxidative stress and decrease in muscle COPS2/TRIP15/ALIEN. *Mol Metab* 39: 101012, 2020. doi: 10.1016/j.molmet.2020.101012.

260. **Lima C**, **Alves LE**, **Iagher F**, **Machado AF**, **Bonatto SJ**, **Kuczera D**, **Souza CF**, **Pequito DC**, **Muritiba AL**, **Nunes EA**, **Fernandes LC**. Anaerobic exercise reduces tumor growth, cancer cachexia and increases macrophage and lymphocyte response in Walker 256 tumor-bearing rats. *Eur J Appl Physiol* 104: 957–64, 2008. doi: 10.1007/s00421-008-0849-9.

261. **Nunes EA**, **Kuczera D**, **Brito GAP**, **Bonatto SJR**, **Yamazaki RK**, **Tanhoffer RA**, **Mund RC**, **Kryczyk M**, **Fernandes LC**. β-Hydroxy-β-methylbutyrate supplementation reduces tumor growth and tumor cell proliferation ex vivo and prevents cachexia in Walker 256 tumor-bearing rats by modifying nuclear factor-κB expression. *Nutrition Research* 28: 487–493, 2008. doi: 10.1016/j.nutres.2008.04.006.

262. **Piffar PM**, **Fernandez R**, **Tchaikovski O**, **Hirabara SM**, **Folador A**, **Pinto GJ**, **Jakobi S**, **Gobbo-Bordon D**, **Rohn T v.**, **Fabrício VEB**, **Moretto KD**, **Tosta E**, **Curi R**, **Fernandes LC**. Naproxen, clenbuterol and insulin administration ameliorates cancer cachexia and reduce tumor growth in Walker 256 tumor-bearing rats. *Cancer Lett* 201: 139–148, 2003. doi: 10.1016/S0304-3835(03)00472-5.

263. **Pizato N**, **Bonatto S**, **Yamazaki RK**, **Aikawa J**, **Nogata C**, **Mund RC**, **Nunes EA**, **Piconcelli M**, **Naliwaiko K**, **Curi R**, **Calder PC**, **Fernandes LC**. Ratio of 116 to n-3 fatty acids in the diet affects tumor growth and cachexia in Walker 256 tumor-bearing rats. *Nutr Cancer* 53: 194–201, 2005. doi: 10.1207/s15327914nc5302_8.

264. **Brown JL**, **Rosa-Caldwell ME**, **Lee DE**, **Blackwell TA**, **Brown LA**, **Perry RA**, **Haynie WS**, **Hardee JP**, **Carson JA**, **Wiggs MP**, **Washington TA**, **Greene NP**. Mitochondrial degeneration precedes the development of muscle atrophy in progression of cancer cachexia in tumour-bearing mice. *J Cachexia Sarcopenia Muscle* 8: 926–938, 2017. doi: 10.1002/jcsm.12232.

265. **Chen JA**, **Splenser A**, **Guillory B**, **Luo J**, **Mendiratta M**, **Belinova B**, **Halder T**, **Zhang G**, **Li YP**, **Garcia JM**. Ghrelin prevents tumour- and cisplatin-induced muscle wasting: characterization of multiple mechanisms involved. *J Cachexia Sarcopenia Muscle* 6: 132–143, 2015. doi: 10.1002/jcsm.12023.

266. **Das SK**, **Eder S**, **Schauer S**, **Diwoky C**, **Temmel H**, **Guertl B**, **Gorkiewicz G**, **Tamilarasan KP**, **Kumari P**, **Trauner M**, **Zimmermann R**, **Vesely P**, **Haemmerle G**, **Zechner R**, **Hoefler G**. Adipose triglyceride lipase contributes to cancer-associated cachexia. *Science (1979)* 333, 2011. doi: 10.1126/science.1198973.

267. **Iwata Y**, **Suzuki N**, **Ohtake H**, **Kamauchi S**, **Hashimoto N**, **Kiyono T**, **Wakabayashi S**. Cancer cachexia causes skeletal muscle damage via transient receptor potential vanilloid 2-independent mechanisms, unlike muscular dystrophy. .

268. **Liu H**, **Li L**, **Zou J**, **Zhou T**, **Wang B**, **Sun H**, **Yu S**. Coix seed oil ameliorates cancer cachexia by counteracting muscle loss and fat lipolysis. *BMC Complement Altern Med* 19: 267, 2019. doi: 10.1186/s12906-019-2684-4.

269. **Liu H**, **Luo J**, **Guillory B**, **Chen J**, **Zang P**, **Yoeli JK**, **Hernandez Y**, **Lee I (In-gi)**, **Anderson B**, **Storie M**, **Tewnion A**, **Garcia JM**. Ghrelin ameliorates tumor-induced adipose tissue atrophy and inflammation via Ghrelin receptor-dependent and -independent pathways. *Oncotarget* 11: 32863302, 2020. doi: 10.18632/oncotarget.27705.

270. **Markison S**, **Foster AC**, **Chen C**, **Brookhart GB**, **Hesse A**, **Hoare SRJ**, **Fleck BA**, **Brown BT**, **Marks DL**. The regulation of feeding and metabolic rate and the prevention of murine cancer cachexia with a small-molecule melanocortin-4 receptor antagonist. *Endocrinology* 146: 2766–2773, 2005. doi: 10.1210/en.2005-0142.

271. **Nicholson JR**, **Kohler G**, **Schaerer F**, **Senn C**, **Weyermann P**, **Hofbauer KG**. Peripheral administration of a melanocortin 4-receptor inverse agonist prevents loss of lean body mass in tumor-bearing mice. *Journal of Pharmacology and Experimental Therapeutics* 317: 771–777, 2006. doi: 10.1124/jpet.105.097725.

272. **Sin TK**, **Zhu JZ**, **Zhang G**, **Li YP**. P300 Mediates Muscle Wasting in Lewis Lung Carcinoma. *Cancer Res* 79: 1331–1342, 2019. doi: 10.1158/0008-5472.CAN-18-1653.

273. **Zhang G**, **Liu Z**, **Ding H**, **Miao H**, **Garcia JM**, **Li YP**. Toll-like receptor 4 mediates Lewis lung carcinoma-induced muscle wasting via coordinate activation of protein degradation pathways. *Sci Rep* 7: 2273, 2017. doi: 10.1038/s41598-017-02347-2.

274. **Hanada T**, **Toshinai K**, **Kajimura N**, **Nara-Ashizawa N**, **Tsukada T**, **Hayashi Y**, **Osuye K**, **Kangawa K**, **Matsukura S**, **Nakazato M**. Anti-cachectic effect of ghrelin in nude mice bearing human melanoma cells. *Biochem Biophys Res Commun* 301: 275–279, 2003. doi: 10.1016/S0006-291X(02)03028-0.

275. **Hanada T**, **Toshinai K**, **Date Y**, **Kajimura N**, **Tsukada T**, **Hayashi Y**, **Kangawa K**, **Nakazato M**. Upregulation of ghrelin expression in cachectic nude mice bearing human melanoma cells. *Metabolism* 53: 84–88, 2004. doi: 10.1016/j.metabol.2003.06.004.

276. **Van Norren K**, **Kegler D**, **Argilés JM**, **Luiking Y**, **Gorselink M**, **Laviano A**, **Arts K**, **Faber J**, **Jansen H**, **Van Der Beek EM**, **Van Helvoort A**. Dietary supplementation with a specific combination of high protein, leucine, and fish oil improves muscle function and daily activity in tumour-bearing cachectic mice. *Br J Cancer* 100: 713–722, 2009.

277. **Hiroux C**, **Dalle S**, **Koppo K**, **Hespel P**. Voluntary exercise does not improve muscular properties or functional capacity during C26-induced cancer cachexia in mice. *J Muscle Res Cell Motil* 42: 169–181, 2021. doi: 10.1007/s10974-021-09599-6.

278. **Weyermann P**, **Dallmann R**, **Magyar J**, **Anklin C**, **Hufschmid M**, **Dubach-Powell J**, **Courdier-Fruh I**, **Henneböhle M**, **Nordhoff S**, **Mondadori C**. Orally available selective melanocortin-4 receptor antagonists stimulate food intake and reduce cancer-induced cachexia in mice. *PLoS One* 4: 4774, 2009. doi: 10.1371/journal.pone.0004774.

279. **Kandarian SC**, **Nosacka RL**, **Delitto AE**, **Judge AR**, **Judge SM**, **Ganey JD**, **Moreira JD**, **Jackman RW**. Tumour-derived leukaemia inhibitory factor is a major driver of cancer cachexia and morbidity in C26 tumour-bearing mice. *J Cachexia Sarcopenia Muscle* 9: 1109–1120, 2018. doi: 10.1002/jcsm.12346.

280. **Inaba S**, **Hinohara A**, **Tachibana M**, **Tsujikawa K**, **Fukada S**. Muscle regeneration is disrupted by cancer cachexia without loss of muscle stem cell potential. *PLoS One* 13: 0205467, 2018. doi: 10.1371/journal.pone.0205467.

281. **de Lima EA**, **de Sousa LGO**, **Alexandre AA**, **Marshall AG**, **Zanchi NE**, **Neto JCR**. Aerobic exercise, but not metformin, prevents reduction of muscular performance by AMPk activation in mice on doxorubicin chemotherapy. *J Cell Physiol* 233: 9652–9662, 2018. doi: 10.1002/jcp.26880.

282. **Nunes EA**, **Kuczera D**, **Brito GAP**, **Bonatto SJR**, **Yamazaki RK**, **Tanhoffer RA**, **Mund RC**, **Kryczyk M**, **Fernandes LC**. β-Hydroxy-β-methylbutyrate supplementation reduces tumor growth and tumor cell proliferation ex vivo and prevents cachexia in Walker 256 tumor-bearing rats by modifying nuclear factor-κB expression. *Nutrition Research* 28: 487–493, 2008. doi: 10.1016/j.nutres.2008.04.006.

283. **Jensen S**, **Bloch Z**, **Quist M**, **Hansen TTD**, **Johansen C**, **Pappot H**, **Suetta C**, **Skjødt Rafn B**. Sarcopenia and loss of muscle mass in patients with lung cancer undergoing chemotherapy treatment: a systematic review and meta-analysis. *Acta Oncol (Madr)* 62: 318–328, 2023. doi: 10.1080/0284186X.2023.2180660.

284. **Naito T**, **Okayama T**, **Aoyama T**, **Ohashi T**, **Masuda Y**, **Kimura M**, **Shiozaki H**, **Murakami H**, **Kenmotsu H**, **Taira T**, **Ono A**, **Wakuda K**, **Imai H**, **Oyakawa T**, **Ishii T**, **Omori S**, **Nakashima K**, **Endo M**, **Omae K**, **Mori K**, **Yamamoto N**, **Tanuma A**, **Takahashi T**. Skeletal muscle depletion during chemotherapy has a large impact on physical function in elderly Japanese patients with advanced non–small-cell lung cancer. *BMC Cancer* 17: 571, 2017. doi: 10.1186/s12885-017-3562-4.

285. **Kakinuma K**, **Tsuruoka H**, **Morikawa K**, **Furuya N**, **Inoue T**, **Miyazawa T**, **Mineshita M**. Differences in skeletal muscle loss caused by cytotoxic chemotherapy and molecular targeted therapy in patients with advanced non-small cell lung cancer. *Thorac Cancer* 9: 99–104, 2018. doi: 10.1111/1759-7714.12545.

286. **Kimura M**, **Naito T**, **Kenmotsu H**, **Taira T**, **Wakuda K**, **Oyakawa T**, **Hisamatsu Y**, **Tokito T**, **Imai H**, **Akamatsu H**, **Ono A**, **Kaira K**, **Murakami H**, **Endo M**, **Mori K**, **Takahashi T**, **Yamamoto N**. Prognostic impact of cancer cachexia in patients with advanced non-small cell lung cancer. *Supportive Care in Cancer* 23: 1699–1708, 2015. doi: 10.1007/s00520-014-2534-3.

287. **Stene GB**, **Helbostad JL**, **Amundsen T**, **Sørhaug S**, **Hjelde H**, **Kaasa S**, **Grønberg BH**. Changes in skeletal muscle mass during palliative chemotherapy in patients with advanced lung cancer. *Acta Oncol (Madr)* 54: 340–348, 2015. doi: 10.3109/0284186X.2014.953259.

288. **Park SE**, **Choi JH**, **Park JY**, **Kim BJ**, **Kim JG**, **Kim JW**, **Park J-M**, **Chi K-C**, **Hwang IG**. Loss of skeletal muscle mass during palliative chemotherapy is a poor prognostic factor in patients with advanced gastric cancer. *Sci Rep* 10: 17683, 2020. doi: 10.1038/s41598-020-74765-8.

289. **Best TD**, **Roeland EJ**, **Horick NK**, **Van Seventer EE**, **El-Jawahri A**, **Troschel AS**, **Johnson PC**, **Kanter KN**, **Fish MG**, **Marquardt JP**, **Bridge CP**, **Temel JS**, **Corcoran RB**, **Nipp RD**, **Fintelmann FJ**. Muscle Loss Is Associated with Overall Survival in Patients with Metastatic Colorectal Cancer Independent of Tumor Mutational Status and Weight Loss. *Oncologist* 26, 2021. doi: 10.1002/onco.13774.

290. **Blauwhoff-Buskermolen S**, **Versteeg KS**, **de van der Schueren MAE**, **den Braver NR**, **Berkhof J**, **Langius JAE**, **Verheul HMW**. Loss of Muscle Mass During Chemotherapy Is Predictive for Poor Survival of Patients With Metastatic Colorectal Cancer. *Journal of Clinical Oncology* 34: 1339–1344, 2016. doi: 10.1200/JCO.2015.63.6043.

291. **Basile D**, **Parnofiello A**, **Vitale MG**, **Cortiula F**, **Gerratana L**, **Fanotto V**, **Lisanti C**, **Pelizzari G**, **Ongaro E**, **Bartoletti M**, **Garattini SK**, **Andreotti VJ**, **Bacco A**, **Iacono D**, **Bonotto M**, **Casagrande M**, **Ermacora P**, **Puglisi F**, **Pella N**, **Fasola G**, **Aprile G**, **Cardellino GG**. The <scp>IMPACT</scp> study: early loss of skeletal muscle mass in advanced pancreatic cancer patients. *J Cachexia Sarcopenia Muscle* 10: 368–377, 2019. doi: 10.1002/jcsm.12368.

292. **Babic A**, **Rosenthal MH**, **Sundaresan TK**, **Khalaf N**, **Lee V**, **Brais LK**, **Loftus M**, **Caplan L**, **Denning S**, **Gurung A**, **Harrod J**, **Schawkat K**, **Yuan C**, **Wang Q-L**, **Lee AA**, **Biller LH**, **Yurgelun MB**, **Ng K**, **Nowak JA**, **Aguirre AJ**, **Bhatia SN**, **Vander Heiden MG**, **Van Den Eeden SK**, **Caan BJ**, **Wolpin BM**. Adipose tissue and skeletal muscle wasting precede clinical diagnosis of pancreatic cancer. *Nat Commun* 14: 4317, 2023. doi: 10.1038/s41467-023-40024-3.

293. **Miki M**, **Lee L**, **Hisano T**, **Sugimoto R**, **Furukawa M**. Loss of adipose tissue or skeletal muscle during first-line gemcitabine/nab-paclitaxel therapy is associated with worse survival after second-line therapy of advanced pancreatic cancer. *Asia Pac J Clin Oncol* 18, 2022. doi: 10.1111/ajco.13669.

294. **Cabrera AR**, **Deaver JW**, **Lim S**, **Morena da Silva F**, **Schrems ER**, **Saling LW**, **Tsitkanou S**, **Rosa-Caldwell ME**, **Wiggs MP**, **Washington TA**, **Greene NP**. Females display relatively preserved muscle quality compared with males during the onset and early stages of C26-induced cancer cachexia. *J Appl Physiol* 135: 655–672, 2023. doi: 10.1152/japplphysiol.00196.2023.

295. **Baracos VE**, **Reiman T**, **Mourtzakis M**, **Gioulbasanis I**, **Antoun S**. Body composition in patients with non-small cell lung cancer: a contemporary view of cancer cachexia with the use of computed tomography image analysis. *Am J Clin Nutr* 91: 1133S-1137S, 2010.

296. **Cosper PF**, **Leinwand LA**. Cancer causes cardiac atrophy and autophagy in a sexually dimorphic manner. *Cancer Res* 71: 1710–20, 2011.

297. **Hendifar A**, **Yang D**, **Lenz F**, **Lurje G**, **Pohl A**, **Lenz C**, **Ning Y**, **Zhang W**, **Lenz H-J**. Gender disparities in metastatic colorectal cancer survival. *Clin Cancer Res* 15: 6391–7, 2009.

298. **Wallengren O**, **Iresjö B-M**, **Lundholm K**, **Bosaeus I**. Loss of muscle mass in the end of life in patients with advanced cancer. *Support Care Cancer* 23: 79–86, 2015.

299. **Picard M**, **Ritchie D**, **Thomas MM**, **Wright KJ**, **Hepple RT**. Alterations in intrinsic mitochondrial function with aging are fiber type-specific and do not explain differential atrophy between muscles. *Aging Cell* 10: 1047–55, 2011.

300. **Norman K**, **Stobäus N**, **Reiß J**, **Schulzke J**, **Valentini L**, **Pirlich M**. Effect of sexual dimorphism on muscle strength in cachexia. *J Cachexia Sarcopenia Muscle* 3: 111–116, 2012. doi: 10.1007/s13539-012-0060-z.

301. **Kilgour RD**, **Vigano A**, **Trutschnigg B**, **Hornby L**, **Lucar E**, **Bacon SL**, **Morais JA**. Cancer-related fatigue: the impact of skeletal muscle mass and strength in patients with advanced cancer. *J Cachexia Sarcopenia Muscle* 1: 177–185, 2010. doi: 10.1007/s13539-010-0016-0.

302. **Burkart M**, **Schieber M**, **Basu S**, **Shah P**, **Venugopal P**, **Borgia JA**, **Gordon L**, **Karmali R**. Evaluation of the impact of cachexia on clinical outcomes in aggressive lymphoma. *Br J Haematol* 186: 45–53, 2019. doi: 10.1111/bjh.15889.

303. **Burney BO**, **Garcia JM**. Hypogonadism in male cancer patients. *J Cachexia Sarcopenia Muscle* 3: 149–55, 2012.

304. **Naugler WE**, **Sakurai T**, **Kim S**, **Maeda S**, **Kim K**, **Elsharkawy AM**, **Karin M**. Gender disparity in liver cancer due to sex differences in MyD88-dependent IL-6 production. *Science* 317: 121–4, 2007.

305. **Zhong X**, **Zimmers TA**. Sex Differences in Cancer Cachexia. *Curr Osteoporos Rep* 18: 646–654, 2020.

306. **Yang L**, **Venneti S**, **Nagrath D**. Glutaminolysis: A Hallmark of Cancer Metabolism. *Annu Rev Biomed Eng* 19, 2017. doi: 10.1146/annurev-bioeng-071516-044546.

307. **Keenan MM**, **Chi JT**. Alternative fuels for cancer cells. *Cancer Journal (United States)* 21 Lippincott Williams and Wilkins: 49–55, 2015.

308. **Dang C V**. MYC on the path to cancer. *Cell* 149: 22–35, 2012. doi: 10.1016/j.cell.2012.03.003.

309. **Dong Y**, **Tu R**, **Liu H**, **Qing G**. Regulation of cancer cell metabolism: oncogenic MYC in the driver's seat. *Signal Transduct Target Ther* 5: 124, 2020. doi: 10.1038/s41392-020-00235-2.

310. **Elbadawy M**, **Usui T**, **Yamawaki H**, **Sasaki K**. Emerging Roles of C-Myc in Cancer Stem Cell-Related Signaling and Resistance to Cancer Chemotherapy: A Potential Therapeutic Target Against Colorectal Cancer. *Int J Mol Sci* 20, 2019. doi: 10.3390/ijms20092340.

311. **Sieghart W**, **Fuereder T**, **Schmid K**, **Cejka D**, **Werzowa J**, **Wrba F**, **Wang X**, **Gruber D**, **Rasoul-Rockenschaub S**, **Peck-Radosavljevic M**, **Wacheck V**. Mammalian target of rapamycin pathway activity in hepatocellular carcinomas of patients undergoing liver transplantation. *Transplantation* 83: 425–32, 2007. doi: 10.1097/01.tp.0000252780.42104.95.

312. **Villanueva A**, **Chiang DY**, **Newell P**, **Peix J**, **Thung S**, **Alsinet C**, **Tovar V**, **Roayaie S**, **Minguez B**, **Sole M**, **Battiston C**, **van Laarhoven S**, **Fiel MI**, **Di Feo A**, **Hoshida Y**, **Yea S**, **Toffanin S**, **Ramos A**, **Martignetti JA**, **Mazzaferro V**, **Bruix J**, **Waxman S**, **Schwartz M**, **Meyerson M**, **Friedman SL**, **Llovet JM**. Pivotal Role of mTOR Signaling in Hepatocellular Carcinoma. *Gastroenterology* 135: 1972–1983, 2008. doi: 10.1053/j.gastro.2008.08.008.

313. **Sahin F**, **Kannangai R**, **Adegbola O**, **Wang J**, **Su G**, **Torbenson M**. mTOR and P70 S6 kinase expression in primary liver neoplasms. *Clinical Cancer Research* 10: 8421–8425, 2004. doi: 10.1158/1078-0432.CCR-04-0941.

314. **Zeleznik OA**, **Balasubramanian R**, **Ren Y**, **Tobias DK**, **Rosner BA**, **Peng C**, **Bever AM**, **Frueh L**, **Jeanfavre S**, **Avila-Pacheco J**, **Clish CB**, **Mora S**, **Hu FB**, **Eliassen AH**. Branched-Chain Amino Acids and Risk of Breast Cancer. *JNCI Cancer Spectr* 5: pkab059, 2021. doi: 10.1093/jncics/pkab059.

315. **Lecuyer L**, **Dalle C**, **Lyan B**, **Demidem A**, **Rossary A**, **Vasson MP**, **Petera M**, **Lagree M**, **Ferreira T**, **Centeno D**, **Galan P**, **Hercberg S**, **Deschasaux M**, **Partula V**, **Srour B**, **Latino-Martel P**, **Kesse-Guyot E**, **Druesne-Pecollo N**, **Durand S**, **Pujos-Guillot E**, **Touvier M**. Plasma metabolomic signatures associated with long-term breast cancer risk in the SU.VI.MAX prospective cohort. *Cancer Epidemiology Biomarkers and Prevention* 28: 1300–1307, 2019. doi: 10.1158/1055-9965.EPI-19-0154.

316. **Mayers JR**, **Wu C**, **Clish CB**, **Kraft P**, **Torrence ME**, **Fiske BP**, **Yuan C**, **Bao Y**, **Townsend MK**, **Tworoger SS**, **Davidson SM**, **Papagiannakopoulos T**, **Yang A**, **Dayton TL**, **Ogino S**, **Stampfer MJ**, **Giovannucci EL**, **Qian ZR**, **Rubinson DA**, **Ma J**,

Sesso HD, **Gaziano JM**, **Cochrane BB**, **Liu S**, **Wactawski-Wende J**, **Manson JE**, **Pollak MN**, **Kimmelman AC**, **Souza A**, **Pierce K**, **Wang TJ**, **Gerszten RE**, **Fuchs CS**, **Vander Heiden MG**, **Wolpin BM**. Elevation of circulating branched-chain amino acids is an early event in human pancreatic adenocarcinoma development. *Nat Med* 20: 1193–1198, 2014. doi: 10.1038/nm.3686.

317. **Mayers JR**, **Torrence ME**, **Danai L V.**, **Papagiannakopoulos T**, **Davidson SM**, **Bauer MR**, **Lau AN**, **Ji BW**, **Dixit PD**, **Hosios AM**, **Muir A**, **Chin CR**, **Freinkman E**, **Jacks T**, **Wolpin BM**, **Vitkup D**, **Vander Heiden MG**. Tissue of origin dictates branched-chain amino acid metabolism in mutant Kras-driven cancers. *Science (1979)* 353: 1161–1165, 2016. doi: 10.1126/science.aaf5171.

318. **Lee JH**, **Cho Y ra**, **Kim JH**, **Kim J**, **Nam HY**, **Kim SW**, **Son J**. Branched-chain amino acids sustain pancreatic cancer growth by regulating lipid metabolism. *Exp Mol Med* 51: 1–11, 2019. doi: 10.1038/s12276-019-0350-z.

319. **Lieu EL**, **Nguyen T**, **Rhyne S**, **Kim J**. Amino acids in cancer. *Exp Mol Med* 52 Springer Nature: 15–30, 2020.

320. **Li JT**, **Yin M**, **Wang D**, **Wang J**, **Lei MZ**, **Zhang Y**, **Liu Y**, **Zhang L**, **Zou SW**, **Hu LP**, **Zhang ZG**, **Wang YP**, **Wen WY**, **Lu HJ**, **Chen ZJ**, **Su D**, **Lei QY**. BCAT2-mediated BCAA catabolism is critical for development of pancreatic ductal adenocarcinoma. *Nat Cell Biol* 22 Nature Research: 167–174, 2020.

321. **Zhu Z**, **Achreja A**, **Meurs N**, **Animasahun O**, **Owen S**, **Mittal A**, **Parikh P**, **Lo TW**, **Franco-Barraza J**, **Shi J**, **Gunchick V**, **Sherman MH**, **Cukierman E**, **Pickering AM**, **Maitra A**, **Sahai V**, **Morgan MA**, **Nagrath S**, **Lawrence TS**, **Nagrath D**. Tumour-reprogrammed stromal BCAT1 fuels branched-chain ketoacid dependency in stromal-rich PDAC tumours. *Nat Metab* 2: 775–792, 2020. doi: 10.1038/s42255-020-0226-5.

322. **Wang Y**, **Xiao J**, **Jiang W**, **Zuo D**, **Wang X**, **Jin Y**, **Qiao L**, **An H**, **Yang L**, **Dumoulin DW**, **Dempke WCM**, **Best SA**, **Ren L**. BCKDK alters the metabolism of non-small cell lung cancer. *Transl Lung Cancer Res* 10: 4459–4476, 2021. doi: 10.21037/tlcr-21-885.

323. **Costelli P**, **Llovera M**, **García-Martínez C**, **Carbó N**, **López-Soriano FJ**, **Argilés JM**. Enhanced leucine oxidation in rats bearing an ascites hepatoma (Yoshida AH-130) and its reversal by clenbuterol. *Cancer Lett* 91: 73–8, 1995.

324. **Argilés JM**, **López-Soriano FJ**. The energy state of tumor-bearing rats. *J Biol Chem* 266: 2978–82, 1991.

325. **Norton JA**, **Gorschboth CM**, **Wesley RA**, **Burt ME**, **Brennan MF**. Fasting plasma amino acid levels in cancer patients. *Cancer* 56: 1181–1186, 1985. doi: 10.1002/1097-0142(19850901)56:5<1181::AID-CNCR2820560535>3.0.CO;2-8.

326. **Zheng YH**, **Hu WJ**, **Chen BC**, **Grahn THM**, **Zhao YR**, **Bao HL**, **Zhu YF**, **Zhang QY**. BCAT1, a key prognostic predictor of hepatocellular carcinoma, promotes cell

proliferation and induces chemoresistance to cisplatin. *Liver International* 36: 1836–1847, 2016. doi: 10.1111/liv.13178.

327. **Siddiqui RA**, **Williams JF**. The regulation of fatty acid and branched-chain amino acid oxidation in cancer cachectic rats: A proposed role for a cytokine, eicosanoid, and hormone trilogy. *Biochem Med Metab Biol* 42: 71–86, 1989. doi: 10.1016/0885-4505(89)90043-1.

328. **Wang P**, **Wu S**, **Zeng X**, **Zhang Y**, **Zhou Y**, **Su L**, **Lin W**. BCAT1 promotes proliferation of endometrial cancer cells through reprogrammed BCAA metabolism. *Int J Clin Exp Pathol* 11: 5536–5546, 2018.

329. **Hattori A**, **Tsunoda M**, **Konuma T**, **Kobayashi M**, **Nagy T**, **Glushka J**, **Tayyari F**, **McSkimming D**, **Kannan N**, **Tojo A**, **Edison AS**, **Ito T**. Cancer progression by reprogrammed BCAA metabolism in myeloid leukaemia. *Nature* 545: 500–504, 2017. doi: 10.1038/nature22314.

330. **Eley HL**, **Russell ST**, **Tisdale MJ**. Effect of branched-chain amino acids on muscle atrophy in cancer cachexia. *Biochemical Journal* 407: 113–120, 2007.

331. **Peters SJ**, **Van Helvoort A**, **Kegler D**, **Argilès JM**, **Luiking YC**, **Laviano A**, **Van Bergenhenegouwen J**, **Deutz NEP**, **Haagsman HP**, **Gorselink M**, **Van Norren K**. Dose-dependent effects of leucine supplementation on preservation of muscle mass in cancer cachectic mice. *Oncol Rep* 26: 247–254, 2011.

332. **Ham DJ**, **Murphy KT**, **Chee A**, **Lynch GS**, **Koopman R**. Glycine administration attenuates skeletal muscle wasting in a mouse model of cancer cachexia. *Clinical Nutrition* 33: 448–458, 2014.

333. **Vicentini GE**, **Martins HA**, **Fracaro L**, **de Souza SRG**, **da Silva Zanoni KP**, **Silva TNX**, **Blegniski FP**, **Guarnier FA**, **Zanoni JN**. Does l-glutamine-supplemented diet extenuate NO-mediated damage on myenteric plexus of Walker 256 tumor-bearing rats? *Food Res Int* 101: 24–34, 2017.

334. **Martins HA**, **Sehaber CC**, **Hermes-Uliana C**, **Mariani FA**, **Guarnier FA**, **Vicentini GE**, **Bossolani GDP**, **Jussani LA**, **Lima MM**, **Bazotte RB**, **Zanoni JN**. Supplementation with L-glutamine prevents tumor growth and cancer-induced cachexia as well as restores cell proliferation of intestinal mucosa of Walker-256 tumor-bearing rats. *Amino Acids* 48: 2773–2784, 2016.

335. **Viana LR**, **E Chiocchetti G de M**, **Oroy L**, **Vieira WF**, **Busanello ENB**, **Marques AC**, **Salgado C de M**, **de Oliveira ALR**, **Vieira AS**, **Suarez PS**, **de Sousa LM**, **Castelucci BG**, **Vercesi AE**, **Consonni SR**, **Gomes-Marcondes MCC**. Leucine-rich diet improved muscle function in cachectic walker 256 tumour-bearing wistar rats. *Cells* 10: 3272, 2021. doi: 10.3390/cells10123272.

336. **Ventrucci G**, **Mello MAR**, **Gomes-Marcondes MCC**. Effect of a leucine-supplemented diet on body composition changes in pregnant rats bearing Walker 256 tumor. *Brazilian*

Journal of Medical and Biological Research 34: 333–338, 2001. doi: 10.1590/S0100-879X2001000300006.

337. **Ventrucci G**, **Mello MAR**, **Gomes-Marcondes MCC**. Proteasome activity is altered in skeletal muscle tissue of tumour-bearing rats fed a leucine-rich diet. *Endocr Relat Cancer* 11: 887–895, 2004.

338. **Viana LR**, **Tobar N**, **Busanello ENB**, **Marques AC**, **de Oliveira AG**, **Lima TI**, **Machado G**, **Castelucci BG**, **Ramos CD**, **Brunetto SQ**, **Silveira LR**, **Vercesi AE**, **Consonni SR**, **Gomes-Marcondes MCC**. Leucine-rich diet induces a shift in tumour metabolism from glycolytic towards oxidative phosphorylation, reducing glucose consumption and metastasis in Walker-256 tumour-bearing rats. *Sci Rep* 9: 15529, 2019. doi: 10.1038/s41598-019-52112-w.

339. **Smith HJ**, **Mukerji P**, **Tisdale MJ**. Attenuation of proteasome-induced proteolysis in skeletal muscle by {beta}-hydroxy-{beta}-methylbutyrate in cancer-induced muscle loss. *Cancer Res* 65: 277–83, 2005.

340. **Mirza KA**, **Pereira SL**, **Voss AC**, **Tisdale MJ**. Comparison of the anticatabolic effects of leucine and Ca-β-hydroxy-β-methylbutyrate in experimental models of cancer cachexia. *Nutrition* 30: 807–13, 2014.

341. **Aversa Z**, **Bonetto A**, **Costelli P**, **Minero VG**, **Penna F**, **Baccino FM**, **Lucia S**, **Rossi Fanelli F**, **Muscaritoli M**. β-hydroxy-β-methylbutyrate (HMB) attenuates muscle and body weight loss in experimental cancer cachexia. *Int J Oncol* 38: 713–20, 2011.

342. **Hunter DC**, **Weintraub M**, **Blackburn GL**, **Bistrian BR**. Branched chain amino acids as the protein component of parenteral nutrition in cancer cachexia. *British Journal of Surgery* 76: 149–153, 2005. doi: 10.1002/bjs.1800760215.

343. **Tayek JA**, **Bistrian BR**, **Hehir DJ**, **Martin R**, **Moldawer LL**, **Blackburn GL**. Improved protein kinetics and albumin synthesis by branched chain amino acid-enriched total parenteral nutrition in cancer cachexia. A prospective randomized crossover trial. *Cancer* 58: 147–57, 1986. doi: 10.1002/1097-0142(19860701)58:1<147::aid-cncr2820580126>3.0.co;2-i.

344. **No Authours Listed**. Long-term oral administration of branched chain amino acids after curative resection of hepatocellular carcinoma: a prospective randomized trial. The San-in Group of Liver Surgery. *Br J Surg* 84: 1525–31, 1997. doi: 10.1002/bjs.1800841109.

345. **Soares JDP**, **Siqueira JM**, **Oliveira ICL**, **Laviano A**, **Pimentel GD**. A high-protein diet, not isolated BCAA, is associated with skeletal muscle mass index in patients with gastrointestinal cancer. *Nutrition* 72: 110698, 2020. doi: 10.1016/j.nut.2019.110698.

346. **Pimentel GD**, **Pichard C**, **Laviano A**, **Fernandes RC**. High protein diet improves the overall survival in older adults with advanced gastrointestinal cancer. *Clin Nutr* 40: 1376–1380, 2021. doi: 10.1016/j.clnu.2020.08.028.

347. **May PE**, **Barber A**, **D'Olimpio JT**, **Hourihane A**, **Abumrad NN**. Reversal of cancer-related wasting using oral supplementation with a combination of beta-hydroxy-beta-methylbutyrate, arginine, and glutamine. *Am J Surg* 183: 471–9, 2002. doi: 10.1016/s0002-9610(02)00823-1.

348. **Wada N**, **Kurokawa Y**, **Tanaka K**, **Miyazaki Y**, **Makino T**, **Takahashi T**, **Wada H**, **Yamasaki M**, **Yamasaki M**, **Nakajima K**, **Eguchi H**, **Takiguchi S**, **Mori M**, **Doki Y**. Perioperative Nutritional Support With Beta-hydroxy-beta-methylbutyrate, Arginine, and Glutamine in Surgery for Abdominal Malignancies. *Wounds* 30: 251–256, 2018.

349. **Berk L**, **James J**, **Schwartz A**, **Hug E**, **Mahadevan A**, **Samuels M**, **Kachnic L**, **RTOG**. A randomized, double-blind, placebo-controlled trial of a beta-hydroxyl beta-methyl butyrate, glutamine, and arginine mixture for the treatment of cancer cachexia (RTOG 0122). *Support Care Cancer* 16: 1179–88, 2008. doi: 10.1007/s00520-008-0403-7.

350. **Barber MD**, **Ross JA**, **Voss AC**, **Tisdale MJ**, **Fearon KC**. The effect of an oral nutritional supplement enriched with fish oil on weight-loss in patients with pancreatic cancer. *Br J Cancer* 81: 80–6, 1999.

351. **Barber MD**, **Fearon KC**, **Tisdale MJ**, **McMillan DC**, **Ross JA**. Effect of a fish oil-enriched nutritional supplement on metabolic mediators in patients with pancreatic cancer cachexia. *Nutr Cancer* 40: 118–24, 2001.

352. **Wijler LA**, **Raats DAE**, **Elias SG**, **Dijk FJ**, **Quirindongo H**, **May AM**, **Furber MJW**, **Dorresteijn B**, **van Dijk M**, **Kranenburg O**. Specialized nutrition improves muscle function and physical activity without affecting chemotherapy efficacy in C26 tumour-bearing mice. *J Cachexia Sarcopenia Muscle* 12: 796–810, 2021.

353. **Wyart E**, **Hsu MY**, **Sartori R**, **Mina E**, **Rausch V**, **Pierobon ES**, **Mezzanotte M**, **Pezzini C**, **Bindels LB**, **Lauria A**, **Penna F**, **Hirsch E**, **Martini M**, **Mazzone M**, **Roetto A**, **Geninatti Crich S**, **Prenen H**, **Sandri M**, **Menga A**, **Porporato PE**. Iron supplementation is sufficient to rescue skeletal muscle mass and function in cancer cachexia. *EMBO Rep* 23: e53746, 2022.

354. **Beltrà M**, **Pöllänen N**, **Fornelli C**, **Tonttila K**, **Hsu MY**, **Zampieri S**, **Moletta L**, **Corrà S**, **Porporato PE**, **Kivelä R**, **Viscomi C**, **Sandri M**, **Hulmi JJ**, **Sartori R**, **Pirinen E**, **Penna F**. NAD+ repletion with niacin counteracts cancer cachexia. *Nat Commun* 14: 1849, 2023.

355. **Liu S**, **Wu H-J**, **Zhang Z-Q**, **Chen Q**, **Liu B**, **Wu J-P**, **Zhu L**. L-carnitine ameliorates cancer cachexia in mice by regulating the expression and activity of carnitine palmityl transferase. *Cancer Biol Ther* 12: 125–30, 2011.

356. **Busquets S**, **Serpe R**, **Toledo M**, **Betancourt A**, **Marmonti E**, **Orpí M**, **Pin F**, **Capdevila E**, **Madeddu C**, **López-Soriano FJ**, **Mantovani G**, **Macciò A**, **Argilés JM**. L-Carnitine: an adequate supplement for a multi-targeted anti-wasting therapy in cancer. *Clin Nutr* 31: 889–95, 2012.

357. **Liu H**, **Li L**, **Zou J**, **Zhou T**, **Wang B**, **Sun H**, **Yu S**. Coix seed oil ameliorates cancer cachexia by counteracting muscle loss and fat lipolysis. *BMC Complement Altern Med* 19: 267, 2019.

358. **Chen MC**, **Hsu WL**, **Hwang PA**, **Chen YL**, **Chou TC**. Combined administration of fucoidan ameliorates tumor and chemotherapy-induced skeletal muscle atrophy in bladder cancer-bearing mice. *Oncotarget* 7: 51608–51618, 2016. doi: 10.18632/oncotarget.9958.

359. **Campos-Ferraz PL**, **Gualano B**, **das Neves W**, **Andrade IT**, **Hangai I**, **Pereira RTS**, **Bezerra RN**, **Deminice R**, **Seelaender M**, **Lancha AH**. Exploratory studies of the potential anti-cancer effects of creatine. *Amino Acids* 48: 1993–2001, 2016.

360. **Argilés JM**, **Busquets S**, **Toledo M**, **López-Soriano FJ**. The role of cytokines in cancer cachexia. *Curr Opin Support Palliat Care* 3: 263–268, 2009. doi: 10.1097/SPC.0b013e3283311d09.

361. **Wang DT**, **Yin Y**, **Yang YJ**, **Lv PJ**, **Shi Y**, **Lu L**, **Wei LB**. Resveratrol prevents TNF-α-induced muscle atrophy via regulation of Akt/mTOR/FoxO1 signaling in C2C12 myotubes. *Int Immunopharmacol* 19: 206–213, 2014. doi: 10.1016/j.intimp.2014.02.002.

362. **Tolosa L**, **Morlá M**, **Iglesias A**, **Busquets X**, **Lladó J**, **Olmos G**. IFN-γ prevents TNF-α-induced apoptosis in C2C12 myotubes through down-regulation of TNF-R2 and increased NF-κB activity. *Cell Signal* 17: 1333–1342, 2005. doi: 10.1016/j.cellsig.2005.02.001.

363. **Scheede-Bergdahl C**, **Watt HL**, **Trutschnigg B**, **Kilgour RD**, **Haggarty A**, **Lucar E**, **Vigano A**. Is IL-6 the best pro-inflammatory biomarker of clinical outcomes of cancer cachexia? *Clinical Nutrition* 31: 85–88, 2012. doi: 10.1016/j.clnu.2011.07.010.

364. **Kuroda K**, **Nakashima J**, **Kanao K**, **Kikuchi E**, **Miyajima A**, **Horiguchi Y**, **Nakagawa K**, **Oya M**, **Ohigashi T**, **Murai M**. Interleukin 6 Is Associated with Cachexia in Patients with Prostate Cancer. *Urology* 69: 113–117, 2007. doi: 10.1016/j.urology.2006.09.039.

365. **Laine A**, **Iyengar P**, **Pandita TK**. The role of inflammatory pathways in cancer-associated cachexia and radiation resistance. *Molecular Cancer Research* 11: 967–972, 2013.

366. **Banks WA**. Anorectic effects of circulating cytokines: Role of the vascular blood-brain barrier. In: *Nutrition*. 2001, p. 434–437.

367. **Shinsyu A**, **Bamba S**, **Kurihara M**, **Matsumoto H**, **Sonoda A**, **Inatomi O**, **Andoh A**, **Takebayashi K**, **Kojima M**, **Iida H**, **Tani M**, **Sasaki M**. Inflammatory cytokines, appetite-regulating hormones, and energy metabolism in patients with gastrointestinal cancer. *Oncol Lett* 20: 1469–1479, 2020. doi: 10.3892/ol.2020.11662.

368. **Li Y-P**, **Chen Y**, **John J**, **Moylan J**, **Jin B**, **Mann DL**, **Reid MB**. TNF-α acts via p38 MAPK to stimulate expression of the ubiquitin ligase atrogin1/MAFbx in skeletal muscle. *The FASEB Journal* 19: 362–70, 2005. doi: 10.1096/fj.04-2364com.

369. **Wu C**, **Zhu M**, **Lu Z**, **Zhang Y**, **Li L**, **Li N**, **Yin L**, **Wang H**, **Song W**, **Xu H**. L-carnitine ameliorates the muscle wasting of cancer cachexia through the AKT/FOXO3a/MaFbx axis. *Nutr Metab (Lond)* 18: 98, 2021. doi: 10.1186/s12986-021-00623-7.

370. **Tisdale MJ**. Biology of cachexia. *J Natl Cancer Inst* 89: 1763–1773, 1997.

371. **Busquets S**, **Almendro V**, **Barreiro E**, **Figueras M**, **Argilés JM**, **López-Soriano FJ**. Activation of UCPs gene expression in skeletal muscle can be independent on both circulating fatty acids and food intake: Involvement of ROS in a model of mouse cancer cachexia. *FEBS Lett* 579: 717–722, 2005. doi: 10.1016/j.febslet.2004.12.050.

372. **Collins P**, **Bing C**, **McCulloch P**, **Williams G**. Muscle UCP-3 mRNA levels are elevated in weight loss associated with gastrointestinal adenocarcinoma in humans. *Br J Cancer* 86: 372–375, 2002. doi: 10.1038/sj.bjc.6600074.

373. **Sanchís D**, **Busquets S**, **Alvarez B**, **Ricquier D**, **López-Soriano FJ**, **Argilés JM**. Skeletal muscle UCP2 and UCP3 gene expression in a rat cancer cachexia model. *FEBS Lett* 436: 415–418, 1998. doi: 10.1016/S0014-5793(98)01178-8.

374. **Li Y**, **Jiang C**, **Xu G**, **Wang N**, **Zhu Y**, **Tang C**, **Wang X**. Homocysteine upregulates resistin production from adipocytes in vivo and in vitro. *Diabetes* 57: 817–827, 2008. doi: 10.2337/db07-0617.

375. **Aguirre V**, **Uchida T**, **Yenush L**, **Davis R**, **White MF**. The c-Jun NH2-terminal kinase promotes insulin resistance during association with insulin receptor substrate-1 and phosphorylation of Ser307. *Journal of Biological Chemistry* 275: 9047–9054, 2000. doi: 10.1074/jbc.275.12.9047.

376. **Hotamisligil G k. S**, **Peraldi P**, **Budavari A**, **Ellis R**, **White MF**, **Spiegelman BM**. IRS-1-Mediated Inhibition of Insulin Receptor Tyrosine Kinase Activity in TNF-alpha- and Obesity-Induced Insulin Resistance. *Science (1979)* 271: 665–8, 1996. doi: 10.1126/science.271.5249.665.

377. **Ye H**, **Adane B**, **Khan N**, **Alexeev E**, **Nusbacher N**, **Minhajuddin M**, **Stevens BM**, **Winters AC**, **Lin X**, **Ashton JM**, **Purev E**, **Xing L**, **Pollyea DA**, **Lozupone CA**, **Serkova NJ**, **Colgan SP**, **Jordan CT**. Subversion of Systemic Glucose Metabolism as a Mechanism to Support the Growth of Leukemia Cells. *Cancer Cell* 34: 659–673, 2018. doi: 10.1016/j.ccell.2018.08.016.

378. **Thackeray JT**, **Pietzsch S**, **Stapel B**, **Ricke-Hoch M**, **Lee CW**, **Bankstahl JP**, **Scherr M**, **Heineke J**, **Scharf G**, **Haghikia A**, **Bengel FM**, **Hilfiker-Kleiner D**. Insulin supplementation attenuates cancer-induced cardiomyopathy and slows tumor disease progression. *JCI Insight* 2: e93098, 2017. doi: 10.1172/jci.insight.93098.

379. **Lin X**, **Xiao Z**, **Chen T**, **Liang SH**, **Guo H**. Glucose Metabolism on Tumor Plasticity, Diagnosis, and Treatment. *Front Oncol* 10: 317, 2020.

380. **Arruebo M**, **Vilaboa N**, **Sáez-Gutierrez B**, **Lambea J**, **Tres A**, **Valladares M**, **González-Fernández Á**. Assessment of the evolution of cancer treatment therapies. *Cancers (Basel)* 3: 3279–3330, 2011.

381. **Altun İ**, **Sonkaya A**. The most common side effects experienced by patients were receiving first cycle of chemotherapy. *Iran J Public Health* 47: 1218–1219, 2018.

382. **Dasari S**, **Bernard Tchounwou P**. Cisplatin in cancer therapy: Molecular mechanisms of action. *Eur J Pharmacol* 740: 364–378, 2014.

383. **Wagstaff AJ**, **Ward A**, **Benfield P**, **Heel RC**. Carboplatin: A Preliminary Review of its Pharmacodynamic and Pharmacokinetic Properties and Therapeutic Efficacy in the Treatment of Cancer. *Drugs* 37: 162–190, 1989. doi: 10.2165/00003495-198937020-00005.

384. **Armand JP**, **Ducreux M**, **Mahjoubi M**, **Abigerges D**, **Bugat R**, **Chabot G**, **Herait P**, **de Forni M**, **Rougier P**. CPT-11 (Irinotecan) in the treatment of colorectal cancer. *Eur J Cancer* 31: 1283–1287, 1995. doi: 10.1016/0959-8049(95)00212-2.

385. **Zhang N**, **Yin Y**, **Xu SJ**, **Chen WS**. 5-Fluorouracil: Mechanisms of resistance and reversal strategies. *Molecules* 13: 1551–1569, 2008.

386. **Grem JL**. 5-Fluorouracil: Forty-plus and still ticking. A review of its preclinical and clinical development. *Invest New Drugs* 18: 299–313, 2000.

387. **Loadman PM**, **Bibby MC**. Pharmacokinetic Drug Interactions with Anticancer Drugs. *Clin Pharmacokinet* 26: 486–500, 1994.

388. **Mihich E**, **Grindey GB**. Multiple basis of combination chemotherapy. *Cancer* 40: 534–43, 1977. doi: 10.1002/1097-0142(197707)40:1+<534::AID-CNCR2820400720>3.0.CO;2-3.

389. **Perazella MA**, **Rosner MH**. Acute Kidney Injury in Patients With Cancer. *Oncology (Williston Park)* 32: 1770–1781, 2018. doi: 10.1056/nejmra1613984.

390. **Santos MLC**, **Brito BB de**, **Silva FAF da**, **Botelho AC dos S**, **Melo FF de**. Nephrotoxicity in cancer treatment: An overview. *World J Clin Oncol* 11: 190–204, 2020. doi: 10.5306/wjco.v11.i4.190.

391. **Grigorian A**, **O'brien CB**. Hepatotoxicity secondary to chemotherapy. *J Clin Transl Hepatol* 2: 95–102, 2014.

392. **Chan KK**, **Bateman JR**, **Tong M**, **Chlebowski RT**, **Chen HSG**, **Gross JF**, **Bateman JR**. Clinical Pharmacokinetics of Adriamycin in Hepatoma Patients with Cirrhosis. *Cancer Res* 40: 1263–1268, 1980.

393. **Săftescu S**, **Popovici D**, **Oprean C**, **Negru A**, **Croitoru A**, **Zemba M**, **Yasar I**, **Preda M**, **Negru Șerban**. Endurance of erythrocyte series in chemotherapy. *Exp Ther Med* 20: 214, 2020. doi: 10.3892/etm.2020.9344.

394. **Mandal M**, **Gardner CR**, **Sun R**, **Choi H**, **Lad S**, **Mishin V**, **Laskin JD**, **Laskin DL**. The spleen as an extramedullary source of inflammatory cells responding to acetaminophen-induced liver injury. *Toxicol Appl Pharmacol* 304: 110–120, 2016. doi: 10.1016/j.taap.2016.04.019.

395. **Panth N**, **Paudel KR**, **Parajuli K**. Reactive Oxygen Species: A Key Hallmark of Cardiovascular Disease. *Adv Med* 2016: 9152732, 2016. doi: 10.1155/2016/9152732.

396. **Moris D**, **Spartalis M**, **Spartalis E**, **Karachaliou GS**, **Karaolanis GI**, **Tsourouflis G**, **Tsilimigras DI**, **Tzatzaki E**, **Theocharis S**. The role of reactive oxygen species in the pathophysiology of cardiovascular diseases and the clinical significance of myocardial redox. *Ann Transl Med* 5(16): 326, 2017.

397. **Nitiss JL**, **Soans E**, **Rogojina A**, **Seth A**, **Mishina M**. Topoisomerase assays. *Curr Protoc Pharmacol* Chapter 3: Unit 3.3., 2012.

398. **Takagi T**, **Saotome T**. Chemotherapy with irinotecan (CPT-11), a topoisomerase-I inhibitor, for refractory and relapsed non-Hodgkin's lymphoma. *Leuk Lymphoma* 42: 577–86, 2001.

399. **Mathijssen RHJ**, **Loos WJ**, **Verweij J**, **Sparreboom A**. Pharmacology of topoisomerase I inhibitors irinotecan (CPT-11) and topotecan. *Curr Cancer Drug Targets* 2: 103–23, 2002.

400. **Armand JP**. CPT-11: clinical experience in phase I studies. *Semin Oncol* 23: 27–33, 1996.

401. **Merrouche Y**, **Extra JM**, **Abigerges D**, **Bugat R**, **Catimel G**, **Suc E**, **Marty M**, **Hérait P**, **Mahjoubi M**, **Armand JP**. High dose-intensity of irinotecan administered every 3 weeks in advanced cancer patients: a feasibility study. *J Clin Oncol* 15: 1080–6, 1997.

402. **Yue B**, **Gao R**, **Lv C**, **Yu Z**, **Wang H**, **Geng X**, **Wang Z**, **Dou W**. Berberine Improves Irinotecan-Induced Intestinal Mucositis Without Impairing the Anti-colorectal Cancer Efficacy of Irinotecan by Inhibiting Bacterial β-glucuronidase. *Front Pharmacol* 12: 774560, 2021.

403. **Domin BA**, **Mahony WB**, **Zimmerman TP**. Transport of 5-fluorouracil and uracil into human erythrocytes. *Biochem Pharmacol* 46: 503–10, 1993.

404. **Sobrero AF**, **Aschele C**, **Bertino JR**. Fluorouracil in colorectal cancer--a tale of two drugs: implications for biochemical modulation. *J Clin Oncol* 15: 368–81, 1997.

405. **Rose MG**, **Farrell MP**, **Schmitz JC**. Thymidylate synthase: a critical target for cancer chemotherapy. *Clin Colorectal Cancer* 1: 220–9, 2002.

406. **Ikram Burney**. Cancer Chemotherapy and Biotherapy. *Sultan Qaboos Univ Med J* 11: 424–425, 2011.

407. **Chu E**, **Koeller DM**, **Casey JL**, **Drake JC**, **Chabner BA**, **Elwood PC**, **Zinn S**, **Allegra CJ**. Autoregulation of human thymidylate synthase messenger RNA translation by thymidylate synthase. *Proc Natl Acad Sci U S A* 88: 8977–81, 1991.

408. **Berger SH**, **Jenh CH**, **Johnson LF**, **Berger FG**. Thymidylate synthase overproduction and gene amplification in fluorodeoxyuridine-resistant human cells. *Mol Pharmacol* 28: 461–7, 1985.

409. **Hegde VS**, **Nagalli S**. *Leucovorin*. 2023.

410. **Rustum YM**. Biochemical rationale for the 5-fluorouracil leucovorin combination and update of clinical experience. *J Chemother* 2 Suppl 1: 5–11, 1990.

411. **Zhang X**, **Duan R**, **Wang Y**, **Liu X**, **Zhang W**, **Zhu X**, **Chen Z**, **Shen W**, **He Y**, **Wang HQ**, **Huang M**, **Wang C**, **Zhang Z**, **Zhao X**, **Qiu L**, **Luo J**, **Sheng X**, **Guo W**. FOLFIRI (folinic acid, fluorouracil, and irinotecan) increases not efficacy but toxicity compared with single-agent irinotecan as a second-line treatment in metastatic colorectal cancer patients: a randomized clinical trial. *Ther Adv Med Oncol* 14: 17588359211068736, 2022.

412. **Sotos GA**, **Grogan L**, **Allegra CJ**. Preclinical and clinical aspects of biomodulation of 5-fluorouracil. *Cancer Treat Rev* 20: 11–49, 1994.

413. **Buyse M**, **Thirion P**, **Carlson RW**, **Burzykowski T**, **Molenberghs G**, **Piedbois P**. Relation between tumour response to first-line chemotherapy and survival in advanced colorectal cancer: a meta-analysis. Meta-Analysis Group in Cancer. *Lancet* 356: 373–8, 2000.

414. **Fanzani A**, **Zanola A**, **Rovetta F**, **Rossi S**, **Aleo MF**. Cisplatin triggers atrophy of skeletal C2C12 myotubes via impairment of Akt signalling pathway and subsequent increment activity of proteasome and autophagy systems. *Toxicol Appl Pharmacol* 250: 312–21, 2011.

415. **Guigni BA**, **Fix DK**, **Bivona JJ**, **Palmer BM**, **Carson JA**, **Toth MJ**. Electrical stimulation prevents doxorubicin-induced atrophy and mitochondrial loss in cultured myotubes. *Am J Physiol Cell Physiol* 317: 1213–1228, 2019. doi: 10.1152/ajpcell.00148.2019.

416. **Hain BA**, **Xu H**, **Waning DL**. Loss of REDD1 prevents chemotherapy-induced muscle atrophy and weakness in mice. *J Cachexia Sarcopenia Muscle* 12: 1597–1612, 2021.

417. **Mora S**, **Adegoke OAJ**. The effect of a chemotherapy drug cocktail on myotube morphology, myofibrillar protein abundance, and substrate availability. *Physiol Rep* 9, 2021.

418. **D'Lugos AC**, **Fry CS**, **Ormsby JC**, **Sweeney KR**, **Brightwell CR**, **Hale TM**, **Gonzales RJ**, **Angadi SS**, **Carroll CC**, **Dickinson JM**. Chronic doxorubicin administration impacts satellite cell and capillary abundance in a muscle-specific manner. *Physiol Rep* 7: e14052, 2019. doi: 10.14814/phy2.14052.

419. **Braun TP**, **Szumowski M**, **Levasseur PR**, **Grossberg AJ**, **Zhu X**, **Agarwal A**, **Marks DL**. Muscle atrophy in response to cytotoxic chemotherapy is dependent on intact glucocorticoid signaling in skeletal muscle. *PLoS One* 9: 3106489, 2014. doi: 10.1371/journal.pone.0106489.

420. **Buffart LM**, **Sweegers MG**, **de Ruijter CJ**, **Konings IR**, **Verheul HMW**, **van Zweeden AA**, **Grootscholten C**, **Chinapaw MJ**, **Altenburg TM**. Muscle contractile properties of cancer patients receiving chemotherapy: Assessment of feasibility and exercise effects. *Scand J Med Sci Sports* 30: 1918–1929, 2020. doi: 10.1111/sms.13758.

421. **Guigni BA**, **Callahan DM**, **Tourville TW**, **Miller MS**, **Fiske B**, **Voigt T**, **Korwin-Mihavics B**, **Anathy V**, **Dittus K**, **Toth MJ**. Skeletal muscle atrophy and dysfunction in breast cancer patients: Role for chemotherapy-derived oxidant stress. *Am J Physiol Cell Physiol* 315: C744–C756, 2018. doi: 10.1152/ajpcell.00002.2018.

422. **Nissinen TA**, **Degerman J**, **Räsänen M**, **Poikonen AR**, **Koskinen S**, **Mervaala E**, **Pasternack A**, **Ritvos O**, **Kivelä R**, **Hulmi JJ**. Systemic blockade of ACVR2B ligands prevents chemotherapy-induced muscle wasting by restoring muscle protein synthesis without affecting oxidative capacity or atrogenes. *Sci Rep* 6: 32695, 2016. doi: 10.1038/srep32695.

423. **Quinn CJ**, **Hydock DS**. Effects of endurance exercise and doxorubicin on skeletal muscle myogenic regulatory factor expression. *Muscles Ligaments Tendons J* 7: 418–425, 2017. doi: 10.11138/mltj/2017.7.3.418.

424. **de Lima Junior EA**, **Yamashita AS**, **Pimentel GD**, **De Sousa LGO**, **Santos RVT**, **Gonçalves CL**, **Streck EL**, **de Lira FS**, **Rosa Neto JC**. Doxorubicin caused severe hyperglycaemia and insulin resistance, mediated by inhibition in AMPk signalling in skeletal muscle. *J Cachexia Sarcopenia Muscle* 7: 615–625, 2016. doi: 10.1002/jcsm.12104.

425. **Huot JR**, **Pin F**, **Chatterjee R**, **Bonetto A**. PGC1α overexpression preserves muscle mass and function in cisplatin-induced cachexia. *J Cachexia Sarcopenia Muscle* 13: 2480–2491, 2022. doi: 10.1002/jcsm.13035.

426. **Matsuura N**, **Motoori M**, **Fujitani K**, **Nishizawa Y**, **Komatsu H**, **Miyazaki Y**, **Miyazaki S**, **Tomokuni A**, **Komori T**, **Iwase K**. Correlation between Skeletal Muscle Mass and Adverse Events of Neoadjuvant Chemotherapy in Patients with Gastric Cancer. *Oncology* 98: 29–34, 2020. doi: 10.1159/000502613.

427. **Okuno M**, **Goumard C**, **Kopetz S**, **Vega EA**, **Joechle K**, **Mizuno T**, **Tzeng C-WD**, **Chun YS**, **Lee JE**, **Vauthey J-N**, **Aloia TA**, **Conrad C**. Loss of muscle mass during preoperative chemotherapy as a prognosticator for poor survival in patients with colorectal liver metastases. *Surgery* 165: 329–336, 2019. doi: 10.1016/j.surg.2018.07.031.

428. **Degens JHRJ**, **Sanders KJC**, **de Jong EEC**, **Groen HJM**, **Smit EF**, **Aerts JG**, **Schols AMWJ**, **Dingemans A-MC**. The prognostic value of early onset, CT derived loss of

muscle and adipose tissue during chemotherapy in metastatic non-small cell lung cancer. *Lung Cancer* 133: 130–135, 2019. doi: 10.1016/j.lungcan.2019.05.021.

429. **Griffin OM**, **Duggan SN**, **Ryan R**, **McDermott R**, **Geoghegan J**, **Conlon KC**. Characterising the impact of body composition change during neoadjuvant chemotherapy for pancreatic cancer. *Pancreatology* 19: 850–857, 2019. doi: 10.1016/j.pan.2019.07.039.

430. **Kays JK**, **Shahda S**, **Stanley M**, **Bell TM**, **O'Neill BH**, **Kohli MD**, **Couch ME**, **Koniaris LG**, **Zimmers TA**. Three cachexia phenotypes and the impact of fat-only loss on survival in FOLFIRINOX therapy for pancreatic cancer. *J Cachexia Sarcopenia Muscle* 9: 673–684, 2018. doi: 10.1002/jcsm.12307.

431. **Paireder M**, **Asari R**, **Kristo I**, **Rieder E**, **Tamandl D**, **Ba-Ssalamah A**, **Schoppmann SF**. Impact of sarcopenia on outcome in patients with esophageal resection following neoadjuvant chemotherapy for esophageal cancer. *Eur J Surg Oncol* 43: 478–484, 2017. doi: 10.1016/j.ejso.2016.11.015.

432. **Yoon HG**, **Oh D**, **Ahn YC**, **Noh JM**, **Pyo H**, **Cho WK**, **Song YM**, **Park M**, **Hwang NY**, **Sun J-M**, **Kim HK**, **Zo JI**, **Shim YM**. Prognostic Impact of Sarcopenia and Skeletal Muscle Loss During Neoadjuvant Chemoradiotherapy in Esophageal Cancer. *Cancers (Basel)* 12, 2020. doi: 10.3390/cancers12040925.

433. **Unger JM**, **Vaidya R**, **Albain KS**, **Leblanc M**, **Minasian LM**, **Gotay CC**, **Henry NL**, **Fisch MJ**, **Lee SM**, **Blanke CD**, **Hershman DL**. Sex Differences in Risk of Severe Adverse Events in Patients Receiving Immunotherapy, Targeted Therapy, or Chemotherapy in Cancer Clinical Trials. *Journal of Clinical Oncology* 40: 1474–1486, 2022. doi: 10.1200/JCO.21.02377.

434. **Zucker I**, **Prendergast BJ**. Sex differences in pharmacokinetics predict adverse drug reactions in women. *Biol Sex Differ* 11: 32, 2020. doi: 10.1186/s13293-020-00308-5.

435. **Yamada Y**, **Koizumi W**, **Nishikawa K**, **Gotoh M**, **Fuse N**, **Sugimoto N**, **Nishina T**, **Amagai K**, **Chin K**, **Niwa Y**, **Tsuji A**, **Imamura H**, **Tsuda M**, **Yasui H**, **Fujii H**, **Yamaguchi K**, **Yasui H**, **Hironaka S**, **Shimada K**, **Hyodo I**. Sex differences in the safety of S-1 plus oxaliplatin and S-1 plus cisplatin for patients with metastatic gastric cancer. *Cancer Sci* 110: 2875–2883, 2019. doi: 10.1111/cas.14117.

436. **Steinberg JR**, **Turner BE**, **Weeks BT**, **Magnani CJ**, **Wong BO**, **Rodriguez F**, **Yee LM**, **Cullen MR**, **Steinberg JR**. Analysis of Female Enrollment and Participant Sex by Burden of Disease in US Clinical Trials between 2000 and 2020. *JAMA Netw Open* 4: e2113749, 2021. doi: 10.1001/jamanetworkopen.2021.13749.

437. **Jenei K**, **Meyers DE**, **Prasad V**. The Inclusion of Women in Global Oncology Drug Trials over the Past 20 Years. *JAMA Oncol* 7: 1569–1570, 2021.

438. **Özdemir BC**, **Gerard CL**, **Espinosa da Silva C**. Sex and Gender Differences in Anticancer Treatment Toxicity: A Call for Revisiting Drug Dosing in Oncology. *Endocrinology* 163: bqac058, 2022. doi: 10.1210/endocr/bqac058.

439. **Wagner AD**, **Oertelt-Prigione S**, **Adjei A**, **Buclin T**, **Cristina V**, **Csajka C**, **Coukos G**, **Dafni U**, **Dotto GP**, **Ducreux M**, **Fellay J**, **Haanen J**, **Hocquelet A**, **Klinge I**, **Lemmens V**, **Letsch A**, **Mauer M**, **Moehler M**, **Peters S**, **Özdemir BC**. Gender medicine and oncology: Report and consensus of an ESMO workshop. *Annals of Oncology* 30: 1914–1924, 2019.

440. **Joerger M**, **Huitema ADR**, **Van Den Bongard DHJG**, **Schellens JHM**, **Beijnen JH**. Quantitative effect of gender, age, liver function, and body size on the population pharmacokinetics of paclitaxel in patients with solid tumors. *Clinical Cancer Research* 12: 2150–2157, 2006. doi: 10.1158/1078-0432.CCR-05-2069.

441. **Gusella M**, **Crepaldi G**, **Barile C**, **Bononi A**, **Menon D**, **Toso S**, **Scapoli D**, **Stievano L**, **Ferrazzi E**, **Grigoletto F**, **Ferrari M**, **Padrini R**. Pharmacokinetic and demographic markers of 5-fluorouracil toxicity in 181 patients on adjuvant therapy for colorectal cancer. *Annals of Oncology* 17: 1656–1660, 2006. doi: 10.1093/annonc/mdl284.

442. **Dobbs NA**, **Twelves CJ**, **Gillies H**, **James CA**, **Harper PG**, **Rubens RD**. Gender affects doxorubicin pharmacokinetics in patients with normal liver biochemistry. *Cancer Chemother Pharmacol* 36: 473–476, 1995. doi: 10.1007/BF00685796.

443. **Nicolson TJ**, **Mellor HR**, **Roberts RRA**. Gender differences in drug toxicity. *Trends Pharmacol Sci* 31: 108–114, 2010. doi: 10.1016/j.tips.2009.12.001.

444. **Schrijvers D**. Role of red blood cells in pharmacokinetics of chemotherapeutic agents. *Clin Pharmacokinet* 42: 147–153, 2003.

445. **Soldin OP**, **Mattison DR**. Sex differences in pharmacokinetics and pharmacodynamics. *Clin Pharmacokinet* 48: 143–157, 2009.

446. **Silvaggio T**, **Mattison DR**. Setting occupational health standards: Toxicokinetic differences among and between men and women. *Journal of Occupational Medicine* 36: 849–854, 1994.

447. **Chansky K**, **Benedetti J**, **Macdonald JS**. Differences in toxicity between men and women treated with 5-fluorouracil therapy for colorectal carcinoma. *Cancer* 103: 1165–1171, 2005. doi: 10.1002/cncr.20878.

448. **Országhová Z**, **Mego M**, **Chovanec M**. Long-Term Cognitive Dysfunction in Cancer Survivors. *Front Mol Biosci* 8: 770413, 2021.

449. **Liaw CC**, **Wang CH**, **Chang HK**, **Liau CT**, **Yeh KY**, **Huang JS**, **Lin YC**. Gender discrepancy observed between chemotherapy-induced emesis and hiccups. *Supportive Care in Cancer* 9: 435–441, 2001. doi: 10.1007/s005200000231.

450. **Fabris S**, **MacLean DA**. Doxorubicin chemotherapy affects the intracellular and interstitial free amino acid pools in skeletal muscle. *PLoS One* 13: e0195330, 2018.

451. **Aggarwal BB**, **Sung B**. NF-κB in Cancer: A Matter of Life and Death. *Cancer Discov* 1: 469–471, 2011.

452. **Sultani M**, **Stringer AM**, **Bowen JM**, **Gibson RJ**. Anti-inflammatory cytokines: important immunoregulatory factors contributing to chemotherapy-induced gastrointestinal mucositis. *Chemother Res Pract* 2012: 490804, 2012.

453. **Ferrà C**, **de Sanjosé S**, **Gallardo D**, **Berlanga JJ**, **Rueda F**, **Marìn D**, **de la Banda E**, **Ancìn I**, **Peris J**, **Garcìa J**, **Grañena A**. IL-6 and IL-8 levels in plasma during hematopoietic progenitor transplantation. *Haematologica* 83: 1082–7, 1998.

454. **Hall PD**, **Benko H**, **Hogan KR**, **Stuart RK**. The influence of serum tumor necrosis factor-alpha and interleukin-6 concentrations on nonhematologic toxicity and hematologic recovery in patients with acute myelogenous leukemia. *Exp Hematol* 23: 1256–60, 1995.

455. **Arjumand W**, **Seth A**, **Sultana S**. Rutin attenuates cisplatin induced renal inflammation and apoptosis by reducing NFκB, TNF-α and caspase-3 expression in wistar rats. *Food and Chemical Toxicology* 49: 2013–2021, 2011. doi: 10.1016/j.fct.2011.05.012.

456. **Domitrović R**, **Cvijanović O**, **Pugel EP**, **Zagorac GB**, **Mahmutefendić H**, **Škoda M**. Luteolin ameliorates cisplatin-induced nephrotoxicity in mice through inhibition of platinum accumulation, inflammation and apoptosis in the kidney. *Toxicology* 310: 115–123, 2013. doi: 10.1016/j.tox.2013.05.015.

457. **Niiya M**, **Niiya K**, **Kiguchi T**, **Shibakura M**, **Asaumi N**, **Shinagawa K**, **Ishimaru F**, **Kiura K**, **Ikeda K**, **Ueoka H**, **Tanimoto M**. Induction of TNF-α, uPA, IL-8 and MCP-1 by doxorubicin in human lung carcinoma cells. *Cancer Chemother Pharmacol* 52: 391–398, 2003. doi: 10.1007/s00280-003-0665-1.

458. **Conklin KA**. Chemotherapy-associated oxidative stress: Impact on chemotherapeutic effectiveness. *Integr Cancer Ther* 3: 294–300, 2004.

459. **Mizutani H**, **Tada-Oikawa S**, **Hiraku Y**, **Kojima M**, **Kawanishi S**. Mechanism of apoptosis induced by doxorubicin through the generation of hydrogen peroxide. *Life Sci* 76: 1439–1453, 2005. doi: 10.1016/j.lfs.2004.05.040.

460. **Hershey DS**, **Bryant AL**, **Olausson J**, **Davis ED**, **Brady VJ**, **Hammer M**. Hyperglycemic-inducing neoadjuvant agents used in treatment of solid tumors: A review of the literature. *Oncol Nurs Forum* 41: 343–54, 2014. doi: 10.1188/14.ONF.E343-E354.

461. **Palmieri G**, **Lotrecchiano G**, **Ricci G**, **Spiezia R**, **Lombardi G**, **Bianco AR**, **Torino G**. Gonadal function after multimodality treatment in men with testicular germ cell cancer. *Eur J Endocrinol* 134: 431–6, 1996.

462. **Stuart NS**, **Woodroffe CM**, **Grundy R**, **Cullen MH**. Long-term toxicity of chemotherapy for testicular cancer--the cost of cure. *Br J Cancer* 61: 479–84, 1990.

463. **Howell SJ**, **Radford JA**, **Ryder WD**, **Shalet SM**. Testicular function after cytotoxic chemotherapy: evidence of Leydig cell insufficiency. *J Clin Oncol* 17: 1493–8, 1999.

464. **Sarfraz M**, **Ashraf Y**, **Sajid S**, **Ashraf MA**. Testosterone Level in Testicular Cancer Patients after Chemotherapy. *West Indian Med J* 64: 487–494, 2015.

465. **Kilarkaje N**. Effects of combined treatment of α-tocopherol, L-ascorbic acid, selenium and zinc on bleomycin, etoposide and cisplatin-induced alterations in testosterone synthesis pathway in rats. *Cancer Chemother Pharmacol* 74: 1175–89, 2014.

466. **Soewoto W**, **Agustriani N**. Estradiol Levels and Chemotherapy in Breast Cancer Patients: A Prospective Clinical Study. *World J Oncol* 14: 60–66, 2023.

467. **Pribylova O**, **Springer D**, **Svobodnik A**, **Kyr M**, **Zima T**, **Petruzelka L**. Influence of chemotherapy to hormonal levels in postmenopausal breast cancer patients. *Neoplasma* 55: 294–8, 2008.

468. **Bahmanpour S**, **Moradiyan E**, **Dehghani F**, **Zarei-Fard N**. Chemoprotective effects of plasma derived from mice of different ages and genders on ovarian failure after cyclophosphamide treatment. *J Ovarian Res* 13: 138, 2020.

469. **Morgan S**, **Anderson RA**, **Gourley C**, **Wallace WH**, **Spears N**. How do chemotherapeutic agents damage the ovary? *Hum Reprod Update* 18: 525–35, 2012.

470. **Meirow D**, **Dor J**, **Kaufman B**, **Shrim A**, **Rabinovici J**, **Schiff E**, **Raanani H**, **Levron J**, **Fridman E**. Cortical fibrosis and blood-vessels damage in human ovaries exposed to chemotherapy. Potential mechanisms of ovarian injury. *Hum Reprod* 22: 1626–33, 2007.

471. **Chang Y-W**, **Singh KP**. Long-term exposure to estrogen enhances chemotherapeutic efficacy potentially through epigenetic mechanism in human breast cancer cells. *PLoS One* 12: e0174227, 2017.

472. **Molina JR**, **Barton DL**, **Loprinzi CL**. Chemotherapy-induced ovarian failure: manifestations and management. *Drug Saf* 28: 401–16, 2005.

473. **Liem GS**, **Mo FKF**, **Pang E**, **Suen JJS**, **Tang NLS**, **Lee KM**, **Yip CHW**, **Tam WH**, **Ng R**, **Koh J**, **Yip CCH**, **Kong GWS**, **Yeo W**. Chemotherapy-Related Amenorrhea and Menopause in Young Chinese Breast Cancer Patients: Analysis on Incidence, Risk Factors and Serum Hormone Profiles. *PLoS One* 10: e0140842, 2015.

474. **Brand MD**, **Orr AL**, **Perevoshchikova IV**, **Quinlan CL**. The role of mitochondrial function and cellular bioenergetics in ageing and disease. *British Journal of Dermatology* 169: 1–8, 2013. doi: 10.1111/bjd.12208.

475. **Willingham TB**, **Ajayi PT**, **Glancy B**. Subcellular Specialization of Mitochondrial Form and Function in Skeletal Muscle Cells. *Front Cell Dev Biol* 9, 2021. doi: 10.3389/fcell.2021.757305.

476. **Kim JA**, **Wei Y**, **Sowers JR**. Role of mitochondrial dysfunction in insulin resistance. *Circ Res* 102: 401–414, 2008.

477. **Drake JC**, **Wilson RJ**, **Yan Z**. Molecular mechanisms for mitochondrial adaptation to exercise training in skeletal muscle. *The FASEB Journal* 30: 13–22, 2016. doi: 10.1096/fj.15-276337.

478. **Von Bank H**, **Hurtado-Thiele M**, **Oshimura N**, **Simcox J**. Mitochondrial Lipid Signaling and Adaptive Thermogenesis. *Metabolites* 11: 124, 2021. doi: 10.3390/metabo11020124.

479. **White JP**, **Puppa MJ**, **Sato S**, **Gao S**, **Price RL**, **Baynes JW**, **Kostek MC**, **Matesic LE**, **Carson JA**. IL-6 regulation on skeletal muscle mitochondrial remodeling during cancer cachexia in the Apc Min/+ mouse. *Skelet Muscle* 2: 14, 2012. doi: 10.1186/2044-5040-2-14.

480. **White JP**, **Baltgalvis KA**, **Puppa MJ**, **Sato S**, **Baynes JW**, **Carson JA**. Muscle oxidative capacity during IL-6-dependent cancer cachexia. *American Journal of Physiology-Regulatory, Integrative and Comparative Physiology* 300: R201–R211, 2011. doi: 10.1152/ajpregu.00300.2010.

481. **Antunes D**, **Padrão AI**, **Maciel E**, **Santinha D**, **Oliveira P**, **Vitorino R**, **Moreira-Gonçalves D**, **Colaço B**, **Pires MJ**, **Nunes C**, **Santos LL**, **Amado F**, **Duarte JA**, **Domingues MR**, **Ferreira R**. Molecular insights into mitochondrial dysfunction in cancer-related muscle wasting. *Biochimica et Biophysica Acta (BBA) - Molecular and Cell Biology of Lipids* 1841: 896–905, 2014. doi: 10.1016/j.bbalip.2014.03.004.

482. **Fontes-Oliveira CC**, **Busquets S**, **Toledo M**, **Penna F**, **Aylwin MP**, **Sirisi S**, **Silva AP**, **Orpí M**, **García A**, **Sette A**, **Genovese MI**, **Olivan M**, **López-Soriano FJ**, **Argilés JM**. Mitochondrial and sarcoplasmic reticulum abnormalities in cancer cachexia: Altered energetic efficiency? *Biochimica et Biophysica Acta (BBA) - General Subjects* 1830: 2770–2778, 2013. doi: 10.1016/j.bbagen.2012.11.009.

483. **van der Ende M**, **Grefte S**, **Plas R**, **Meijerink J**, **Witkamp RF**, **Keijer J**, **van Norren K**. Mitochondrial dynamics in cancer-induced cachexia. *Biochimica et Biophysica Acta (BBA) - Reviews on Cancer* 1870: 137–150, 2018. doi: 10.1016/j.bbcan.2018.07.008.

484. **de Castro GS**, **Simoes E**, **Lima JDCC**, **Ortiz-Silva M**, **Festuccia WT**, **Tokeshi F**, **Alcântara PS**, **Otoch JP**, **Coletti D**, **Seelaender M**. Human Cachexia Induces Changes in Mitochondria, Autophagy and Apoptosis in the Skeletal Muscle. *Cancers (Basel)* 11, 2019. doi: 10.3390/cancers11091264.

485. **Assi M**, **Rébillard A**. The Janus-Faced Role of Antioxidants in Cancer Cachexia: New Insights on the Established Concepts. *Oxid Med Cell Longev* 2016: 1–19, 2016. doi: 10.1155/2016/9579868.

486. **Gilliam LAA**, **Lark DS**, **Reese LR**, **Torres MJ**, **Ryan TE**, **Lin C-T**, **Cathey BL**, **Neufer PD**. Targeted overexpression of mitochondrial catalase protects against cancer chemotherapy-induced skeletal muscle dysfunction. *Am J Physiol Endocrinol Metab* 311: E293-301, 2016. doi: 10.1152/ajpendo.00540.2015.

487. **Sorensen JC**, **Cheregi BD**, **Timpani CA**, **Nurgali K**, **Hayes A**, **Rybalka E**. Mitochondria: Inadvertent targets in chemotherapy-induced skeletal muscle toxicity and

wasting? *Cancer Chemother Pharmacol* 78: 673–83, 2016. doi: 10.1007/s00280-016-3045-3.

488. **Hanna AD**, **Lam A**, **Tham S**, **Dulhunty AF**, **Beard NA**. Adverse effects of doxorubicin and its metabolic product on cardiac RyR2 and SERCA2A. *Mol Pharmacol* 86: 438–49, 2014. doi: 10.1124/mol.114.093849.

489. **Mallard J**, **Hucteau E**, **Charles A-L**, **Bender L**, **Baeza C**, **Pélissie M**, **Trensz P**, **Pflumio C**, **Kalish-Weindling M**, **Gény B**, **Schott R**, **Favret F**, **Pivot X**, **Hureau TJ**, **Pagano AF**. Chemotherapy impairs skeletal muscle mitochondrial homeostasis in early breast cancer patients. *J Cachexia Sarcopenia Muscle* 13: 1896–1907, 2022. doi: 10.1002/jcsm.12991.

490. **Ballarò R**, **Lopalco P**, **Audrito V**, **Beltrà M**, **Pin F**, **Angelini R**, **Costelli P**, **Corcelli A**, **Bonetto A**, **Szeto HH**, **O'Connell TM**, **Penna F**. Targeting Mitochondria by SS-31 Ameliorates the Whole Body Energy Status in Cancer- and Chemotherapy-Induced Cachexia. *Cancers (Basel)* 13, 2021. doi: 10.3390/cancers13040850.

491. **Neel BA**, **Lin Y**, **Pessin JE**. Skeletal muscle autophagy: a new metabolic regulator. *Trends in Endocrinology & Metabolism* 24: 635–643, 2013. doi: 10.1016/j.tem.2013.09.004.

492. **Sandri M**. Protein breakdown in muscle wasting: Role of autophagy-lysosome and ubiquitin-proteasome. *International Journal of Biochemistry and Cell Biology* 45: 2121–2129, 2013.

493. **Lach-Trifilieff E**, **Minetti GC**, **Sheppard K**, **Ibebunjo C**, **Feige JN**, **Hartmann S**, **Brachat S**, **Rivet H**, **Koelbing C**, **Morvan F**, **Hatakeyama S**, **Glass DJ**. An antibody blocking activin type II receptors induces strong skeletal muscle hypertrophy and protects from atrophy. *Mol Cell Biol* 34: 606–18, 2014.

494. **Huang J**, **Forsberg NE**. Role of calpain in skeletal-muscle protein degradation. *Proc Natl Acad Sci U S A* 95: 12100–5, 1998.

495. **Tisdale MJ**. Molecular pathways leading to cancer cachexia. *Physiology* 20: 340–349, 2005.

496. **Burger AM**, **Seth AK**. The ubiquitin-mediated protein degradation pathway in cancer: therapeutic implications. *Eur J Cancer* 40: 2217–2229, 2004. doi: 10.1016/j.ejca.2004.07.006.

497. **Bonaldo P**, **Sandri M**. Cellular and molecular mechanisms of muscle atrophy. *Dis Model Mech* 6: 25–39, 2013. doi: 10.1242/dmm.010389.

498. **Collins GA**, **Goldberg AL**. The Logic of the 26S Proteasome. *Cell* 169: 792–806, 2017.

499. **Lee D**, **Goldberg A**. Atrogin1/MAFbx: What atrophy, hypertrophy, and cardiac failure have in common. *Circ Res* 109: 123–126, 2011.

500. **Tintignac LA**, **Lagirand J**, **Batonnet S**, **Sirri V**, **Leibovitch MP**, **Leibovitch SA**. Degradation of MyoD mediated by the SCF (MAFbx) ubiquitin ligase. *Journal of Biological Chemistry* 280: 2847–2856, 2005. doi: 10.1074/jbc.M411346200.

501. **Csibi A**, **Cornille K**, **Leibovitch MP**, **Poupon A**, **Tintignac LA**, **Sanchez AMJ**, **Leibovitch SA**. The translation regulatory subunit eiF3f controls the kinase-dependent mTOR signaling required for muscle differentiation and hypertrophy in mouse. *PLoS One* 5: e8994, 2010. doi: 10.1371/journal.pone.0008994.

502. **Kedar V**, **McDonough H**, **Arya R**, **Li HH**, **Rockman HA**, **Patterson C**. Muscle-specific RING finger 1 is a bona fide ubiquitin ligase that degrades cardiac troponin I. *Proc Natl Acad Sci U S A* 101: 18135–18140, 2004. doi: 10.1073/pnas.0404341102.

503. **Clarke BA**, **Drujan D**, **Willis MS**, **Murphy LO**, **Corpina RA**, **Burova E**, **Rakhilin S V.**, **Stitt TN**, **Patterson C**, **Latres E**, **Glass DJ**. The E3 Ligase MuRF1 Degrades Myosin Heavy Chain Protein in Dexamethasone-Treated Skeletal Muscle. *Cell Metab* 6: 376–385, 2007. doi: 10.1016/j.cmet.2007.09.009.

504. **Cohen S**, **Zhai B**, **Gygi SP**, **Goldberg AL**. Ubiquitylation by Trim32 causes coupled loss of desmin, Z-bands, and thin filaments in muscle atrophy. *Journal of Cell Biology* 198: 575–589, 2012. doi: 10.1083/jcb.201110067.

505. **Lecker SH**, **Jagoe RT**, **Gilbert A**, **Gomes M**, **Baracos V**, **Bailey J**, **Price SR**, **Mitch WE**, **Goldberg AL**. Multiple types of skeletal muscle atrophy involve a common program of changes in gene expression. *FASEB Journal* 18: 39–51, 2004. doi: 10.1096/fj.03-0610com.

506. **Cong H**, **Sun L**, **Liu C**, **Tien P**. Inhibition of atrogin-1/MAFbx expression by adenovirus-delivered small hairpin RNAs attenuates muscle atrophy in fasting mice. *Hum Gene Ther* 22: 313–324, 2011. doi: 10.1089/hum.2010.057.

507. **Baehr LM**, **Furlow JD**, **Bodine SC**. Muscle sparing in muscle RING finger 1 null mice: Response to synthetic glucocorticoids. *Journal of Physiology* 589: 4759–4776, 2011. doi: 10.1113/jphysiol.2011.212845.

508. **Khal J**, **Hine A V.**, **Fearon KCH**, **Dejong CHC**, **Tisdale MJ**. Increased expression of proteasome subunits in skeletal muscle of cancer patients with weight loss. *International Journal of Biochemistry and Cell Biology* 37: 2196–2206, 2005. doi: 10.1016/j.biocel.2004.10.017.

509. **Khal J**, **Wyke SM**, **Russell ST**, **Hine A V.**, **Tisdale MJ**. Expression of the ubiquitin-proteasome pathway and muscle loss in experimental cancer cachexia. *Br J Cancer* 93: 774–780, 2005. doi: 10.1038/sj.bjc.6602780.

510. **Yuan L**, **Han J**, **Meng Q**, **Xi Q**, **Zhuang Q**, **Jiang Y**, **Han Y**, **Zhang B**, **Fang J**, **Wu G**. Muscle-specific E3 ubiquitin ligases are involved in muscle atrophy of cancer cachexia: An in vitro and in vivo study. *Oncol Rep* 33: 2261–8, 2015. doi: 10.3892/or.2015.3845.

511. **Adams V**, **Gußen V**, **Zozulya S**, **Cruz A**, **Moriscot A**, **Linke A**, **Labeit S**. Small-Molecule Chemical Knockdown of MuRF1 in Melanoma Bearing Mice Attenuates Tumor Cachexia Associated Myopathy. *Cells* 9: 2272, 2020. doi: 10.3390/cells9102272.

512. **Bossola M**, **Muscaritoli M**, **Costelli P**, **Bellantone R**, **Pacelli F**, **Busquets S**, **Argilès J**, **Lopez-Soriano FJ**, **Civello IM**, **Baccino FM**, **Rossi Fanelli F**, **Doglietto GB**. Increased muscle ubiquitin mRNA levels in gastric cancer patients. *Am J Physiol Regul Integr Comp Physiol* 280: R1518-23, 2001. doi: 10.1152/ajpregu.2001.280.5.R1518.

513. **Bossola M**, **Muscaritoli M**, **Costelli P**, **Grieco G**, **Bonelli G**, **Pacelli F**, **Rossi Fanelli F**, **Doglietto GB**, **Baccino FM**. Increased muscle proteasome activity correlates with disease severity in gastric cancer patients. *Ann Surg* 237: 384–9, 2003. doi: 10.1097/01.SLA.0000055225.96357.71.

514. **Williams A**, **Sun X**, **Fischer JE**, **Hasselgren PO**. The expression of genes in the ubiquitin-proteasome proteolytic pathway is increased in skeletal muscle from patients with cancer. *Surgery* 126: 744–9; discussion 749-50, 1999.

515. **Yamamoto Y**, **Hoshino Y**, **Ito T**, **Nariai T**, **Mohri T**, **Obana M**, **Hayata N**, **Uozumi Y**, **Maeda M**, **Fujio Y**, **Azuma J**. Atrogin-1 ubiquitin ligase is upregulated by doxorubicin via p38-MAP kinase in cardiac myocytes. *Cardiovasc Res* 79: 89–96, 2008.

516. **Feather CE**, **Lees JG**, **Makker PGS**, **Goldstein D**, **Kwok JB**, **Moalem-Taylor G**, **Polly P**. Oxaliplatin induces muscle loss and muscle-specific molecular changes in Mice. *Muscle Nerve* 57: 650–658, 2018.

517. **Wesselborg S**, **Stork B**. Autophagy signal transduction by ATG proteins: from hierarchies to networks. *Cell Mol Life Sci* 72: 4721–57, 2015.

518. **Brooks NE**, **Myburgh KH**. Skeletal muscle wasting with disuse atrophy is multi-dimensional: the response and interaction of myonuclei, satellite cells and signaling pathways. *Front Physiol* 5: 99, 2014.

519. **Ding W-X**, **Yin X-M**. Mitophagy: mechanisms, pathophysiological roles, and analysis. *Biol Chem* 393: 547–64, 2012.

520. **Parzych KR**, **Klionsky DJ**. An overview of autophagy: morphology, mechanism, and regulation. *Antioxid Redox Signal* 20: 460–73, 2014.

521. **Wirawan E**, **Vanden Berghe T**, **Lippens S**, **Agostinis P**, **Vandenabeele P**. Autophagy: for better or for worse. *Cell Res* 22: 43–61, 2012.

522. **Aversa Z**, **Pin F**, **Lucia S**, **Penna F**, **Verzaro R**, **Fazi M**, **Colasante G**, **Tirone A**, **Rossi Fanelli F**, **Ramaccini C**, **Costelli P**, **Muscaritoli M**. Autophagy is induced in the skeletal muscle of cachectic cancer patients. *Sci Rep* 6: 30340, 2016.

523. **Pigna E**, **Berardi E**, **Aulino P**, **Rizzuto E**, **Zampieri S**, **Carraro U**, **Kern H**, **Merigliano S**, **Gruppo M**, **Mericskay M**, **Li Z**, **Rocchi M**, **Barone R**, **Macaluso F**, **Di Felice V**, **Adamo S**, **Coletti D**, **Moresi V**. Aerobic Exercise and Pharmacological

Treatments Counteract Cachexia by Modulating Autophagy in Colon Cancer. *Sci Rep* 6: 26991, 2016.

524. **Puig-Vilanova E**, **Rodriguez DA**, **Lloreta J**, **Ausin P**, **Pascual-Guardia S**, **Broquetas J**, **Roca J**, **Gea J**, **Barreiro E**. Oxidative stress, redox signaling pathways, and autophagy in cachectic muscles of male patients with advanced COPD and lung cancer. *Free Radic Biol Med* 79: 91–108, 2015.

525. **Tardif N**, **Klaude M**, **Lundell L**, **Thorell A**, **Rooyackers O**. Autophagic-lysosomal pathway is the main proteolytic system modified in the skeletal muscle of esophageal cancer patients. *Am J Clin Nutr* 98: 1485–92, 2013.

526. **Barber MD**. Cancer cachexia and its treatment with fish-oil-enriched nutritional supplementation. *Nutrition* 17: 751–5, 2001.

527. **Springer J**, **Tschirner A**, **Haghikia A**, **von Haehling S**, **Lal H**, **Grzesiak A**, **Kaschina E**, **Palus S**, **Pötsch M**, **von Websky K**, **Hocher B**, **Latouche C**, **Jaisser F**, **Morawietz L**, **Coats AJS**, **Beadle J**, **Argiles JM**, **Thum T**, **Földes G**, **Doehner W**, **Hilfiker-Kleiner D**, **Force T**, **Anker SD**. Prevention of liver cancer cachexia-induced cardiac wasting and heart failure. *Eur Heart J* 35: 932–41, 2014. doi: 10.1093/eurheartj/eht302.

528. **Sanders PM**, **Russell ST**, **Tisdale MJ**. Angiotensin II directly induces muscle protein catabolism through the ubiquitin-proteasome proteolytic pathway and may play a role in cancer cachexia. *Br J Cancer* 93: 425–34, 2005. doi: 10.1038/sj.bjc.6602725.

529. **Kanzaki M**, **Soda K**, **Gin PT**, **Kai T**, **Konishi F**, **Kawakami M**. Erythropoietin attenuates cachectic events and decreases production of interleukin-6, a cachexia-inducing cytokine. *Cytokine* 32: 234–9, 2005. doi: 10.1016/j.cyto.2005.10.002.

530. **van Halteren HK**, **Bongaerts GPA**, **Verhagen CAM**, **Kamm YJL**, **Willems JL**, **Grutters GJ**, **Koopman JP**, **Wagener DJT**. Recombinant human erythropoietin attenuates weight loss in a murine cancer cachexia model. *J Cancer Res Clin Oncol* 130: 211–6, 2004. doi: 10.1007/s00432-003-0526-7.

531. **Penna F**, **Busquets S**, **Toledo M**, **Pin F**, **Massa D**, **López-Soriano FJ**, **Costelli P**, **Argilés JM**. Erythropoietin administration partially prevents adipose tissue loss in experimental cancer cachexia models. *J Lipid Res* 54: 3045–51, 2013. doi: 10.1194/jlr.M038406.

532. **Rowland KM**, **Loprinzi CL**, **Shaw EG**, **Maksymiuk AW**, **Kuross SA**, **Jung SH**, **Kugler JW**, **Tschetter LK**, **Ghosh C**, **Schaefer PL**, **Owen D**, **Washburn JH**, **Webb TA**, **Mailliard JA**, **Jett JR**. Randomized double-blind placebo-controlled trial of cisplatin and etoposide plus megestrol acetate/placebo in extensive-stage small-cell lung cancer: a North Central Cancer Treatment Group study. *J Clin Oncol* 14: 135–41, 1996. doi: 10.1200/JCO.1996.14.1.135.

533. **Neri B**, **Garosi VL**, **Intini C**. Effect of medroxyprogesterone acetate on the quality of life of the oncologic patient: a multicentric cooperative study. *Anticancer Drugs* 8: 459–65, 1997. doi: 10.1097/00001813-199706000-00007.

534. **Loprinzi CL**, **Michalak JC**, **Schaid DJ**, **Mailliard JA**, **Athmann LM**, **Goldberg RM**, **Tschetter LK**, **Hatfield AK**, **Morton RF**. Phase III evaluation of four doses of megestrol acetate as therapy for patients with cancer anorexia and/or cachexia. *J Clin Oncol* 11: 762–7, 1993. doi: 10.1200/JCO.1993.11.4.762.

535. **Bruera E**, **Macmillan K**, **Kuehn N**, **Hanson J**, **MacDonald RN**. A controlled trial of megestrol acetate on appetite, caloric intake, nutritional status, and other symptoms in patients with advanced cancer. *Cancer* 66: 1279–82, 1990. doi: 10.1002/1097-0142(19900915)66:6<1279::aid-cncr2820660630>3.0.co;2-r.

536. **Feliu J**, **González-Barón M**, **Berrocal A**, **Ordóñez A**, **Barón-Saura JM**. Treatment of cancer anorexia with megestrol acetate: which is the optimal dose? *J Natl Cancer Inst* 83: 449–50, 1991. doi: 10.1093/jnci/83.6.449.

537. **Mantovani G**, **Macciò A**, **Massa E**, **Madeddu C**. Managing cancer-related anorexia/cachexia. *Drugs* 61: 499–514, 2001.

538. **Willox JC**, **Corr J**, **Shaw J**, **Richardson M**, **Calman KC**, **Drennan M**. Prednisolone as an appetite stimulant in patients with cancer. *Br Med J (Clin Res Ed)* 288: 27, 1984.

539. **Loprinzi CL**, **Kugler JW**, **Sloan JA**, **Mailliard JA**, **Krook JE**, **Wilwerding MB**, **Rowland KM**, **Camoriano JK**, **Novotny PJ**, **Christensen BJ**. Randomized comparison of megestrol acetate versus dexamethasone versus fluoxymesterone for the treatment of cancer anorexia/cachexia. *J Clin Oncol* 17: 3299–306, 1999.

540. **Strasser F**, **Lutz TA**, **Maeder MT**, **Thuerlimann B**, **Bueche D**, **Tschöp M**, **Kaufmann K**, **Holst B**, **Brändle M**, **von Moos R**, **Demmer R**, **Cerny T**. Safety, tolerability and pharmacokinetics of intravenous ghrelin for cancer-related anorexia/cachexia: a randomised, placebo-controlled, double-blind, double-crossover study. *Br J Cancer* 98: 300–8, 2008.

541. **DeBoer MD**. Emergence of ghrelin as a treatment for cachexia syndromes. *Nutrition* 24: 806–14, 2008.

542. **Lai V**, **George J**, **Richey L**, **Kim HJ**, **Cannon T**, **Shores C**, **Couch M**. Results of a pilot study of the effects of celecoxib on cancer cachexia in patients with cancer of the head, neck, and gastrointestinal tract. *Head Neck* 30: 67–74, 2008.

543. **Jatoi A**, **Rowland K**, **Loprinzi CL**, **Sloan JA**, **Dakhil SR**, **MacDonald N**, **Gagnon B**, **Novotny PJ**, **Mailliard JA**, **Bushey TIL**, **Nair S**, **Christensen B**, **North Central Cancer Treatment Group**. An eicosapentaenoic acid supplement versus megestrol acetate versus both for patients with cancer-associated wasting: a North Central Cancer Treatment Group and National Cancer Institute of Canada collaborative effort. *J Clin Oncol* 22: 2469–76, 2004.

544. **Fearon KCH**. Effect of a protein and energy dense n-3 fatty acid enriched oral supplement on loss of weight and lean tissue in cancer cachexia: a randomised double blind trial. *Gut* 52: 1479–1486, 2003. doi: 10.1136/gut.52.10.1479.

545. **Jatoi A**, **Alberts SR**, **Foster N**, **Morton R**, **Burch P**, **Block M**, **Nguyen PL**, **Kugler J**, **North Central Cancer Treatment Group**. Is bortezomib, a proteasome inhibitor, effective in treating cancer-associated weight loss? Preliminary results from the North Central Cancer Treatment Group. *Support Care Cancer* 13: 381–6, 2005.

546. **Cannabis-In-Cachexia-Study-Group**, **Strasser F**, **Luftner D**, **Possinger K**, **Ernst G**, **Ruhstaller T**, **Meissner W**, **Ko Y-D**, **Schnelle M**, **Reif M**, **Cerny T**. Comparison of orally administered cannabis extract and delta-9-tetrahydrocannabinol in treating patients with cancer-related anorexia-cachexia syndrome: a multicenter, phase III, randomized, double-blind, placebo-controlled clinical trial from the Cannabis-In-Cachexia-Study-Group. *J Clin Oncol* 24: 3394–400, 2006.

547. **Jatoi A**, **Windschitl HE**, **Loprinzi CL**, **Sloan JA**, **Dakhil SR**, **Mailliard JA**, **Pundaleeka S**, **Kardinal CG**, **Fitch TR**, **Krook JE**, **Novotny PJ**, **Christensen B**. Dronabinol versus megestrol acetate versus combination therapy for cancer-associated anorexia: a North Central Cancer Treatment Group study. *J Clin Oncol* 20: 567–73, 2002.

548. **Lundholm K**, **Körner U**, **Gunnebo L**, **Sixt-Ammilon P**, **Fouladiun M**, **Daneryd P**, **Bosaeus I**. Insulin treatment in cancer cachexia: effects on survival, metabolism, and physical functioning. *Clin Cancer Res* 13: 2699–706, 2007.

549. **Chang AM**, **Halter JB**. Aging and insulin secretion. *American Journal of Physiology-Endocrinology and Metabolism* 284: E7–E12, 2003.

550. **Muller DC**, **Elahi D**, **Tobin JD**, **Andres R**. The effect of age on insulin resistance and secretion: a review. *Semin Nephrol* 16: 289–98, 1996.

551. **Guo X**, **Asthana P**, **Gurung S**, **Zhang S**, **Wong SKK**, **Fallah S**, **Chow CFW**, **Che S**, **Zhai L**, **Wang Z**, **Ge X**, **Jiang Z**, **Wu J**, **Zhang Y**, **Wu X**, **Xu K**, **Lin CY**, **Kwan HY**, **Lyu A**, **Zhou Z**, **Bian Z-X**, **Wong HLX**. Regulation of age-associated insulin resistance by MT1-MMP-mediated cleavage of insulin receptor. *Nat Commun* 13: 3749, 2022. doi: 10.1038/s41467-022-31563-2.

552. **Mittendorfer B**, **Horowitz JF**, **Klein S**. Gender differences in lipid and glucose kinetics during short-term fasting. *Am J Physiol Endocrinol Metab* 281: E1333-9, 2001.

553. **Kautzky-Willer A**, **Brazzale AR**, **Moro E**, **Vrbíková J**, **Bendlova B**, **Sbrignadello S**, **Tura A**, **Pacini G**. Influence of Increasing BMI on Insulin Sensitivity and Secretion in Normotolerant Men and Women of a Wide Age Span. *Obesity* 20: 1966–1973, 2012. doi: 10.1038/oby.2011.384.

554. **Broussard JL**, **Perreault L**, **Macias E**, **Newsom SA**, **Harrison K**, **Bui HH**, **Milligan P**, **Roth KD**, **Nemkov T**, **D'Alessandro A**, **Brozinick JT**, **Bergman BC**. Sex Differences in

Insulin Sensitivity are Related to Muscle Tissue Acylcarnitine But Not Subcellular Lipid Distribution. *Obesity* 29: 550–561, 2021. doi: 10.1002/oby.23106.

555. **Mauvais-Jarvis F**. Gender differences in glucose homeostasis and diabetes. *Physiol Behav* 187: 20–23, 2018. doi: 10.1016/j.physbeh.2017.08.016.

556. **Woodhouse LJ**, **Reisz-Porszasz S**, **Javanbakht M**, **Storer TW**, **Lee M**, **Zerounian H**, **Bhasin S**. Development of models to predict anabolic response to testosterone administration in healthy young men. *Am J Physiol Endocrinol Metab* 284: 1009–1017, 2003. doi: 10.1152/ajpendo.00536.2002.

557. **Kong A**, **Edmonds P**. Testosterone therapy in HIV wasting syndrome: Systematic review and meta-analysis. *Lancet Infectious Diseases* 2: 692–699, 2002.

558. **Wittert GA**, **Chapman IM**, **Haren MT**, **Mackintosh S**, **Coates P**, **Morley JE**. Oral testosterone supplementation increases muscle and decreases fat mass in healthy elderly males with low-normal gonadal status. *Journals of Gerontology - Series A Biological Sciences and Medical Sciences* 58: 618–625, 2003. doi: 10.1093/gerona/58.7.m618.

559. **Bhasin S**, **Woodhouse L**, **Storer TW**. Androgen effects on body composition. *Growth Hormone and IGF Research* 13: 63–71, 2003. doi: 10.1016/S1096-6374(03)00058-3.

560. **Schroeder ET**, **Singh A**, **Bhasin S**, **Storer TW**, **Azen C**, **Davidson T**, **Martinez C**, **Sinha-Hikim I**, **Jaque SV**, **Terk M**, **Sattler FR**. Effects of an oral androgen on muscle and metabolism in older, community-dwelling men. *Am J Physiol Endocrinol Metab* 284: 120–128, 2003. doi: 10.1152/ajpendo.00363.2002.

561. **Szulc P**, **Claustrat B**, **Marchand F**, **Delmas PD**. Increased Risk of Falls and Increased Bone Resorption in Elderly Men with Partial Androgen Deficiency: The MINOS Study. *Journal of Clinical Endocrinology and Metabolism* 88: 5240–5247, 2003. doi: 10.1210/jc.2003-030200.

562. **van den Beld AW**, **de Jong FH**, **Grobbee DE**, **Pols HAP**, **Lamberts SWJ**. Measures of Bioavailable Serum Testosterone and Estradiol and Their Relationships with Muscle Strength, Bone Density, and Body Composition in Elderly Men*. *J Clin Endocrinol Metab* 85: 3276–3282, 2000. doi: 10.1210/jcem.85.9.6825.

563. **Tenover JS**. Declining testicular function in aging men. *Int J Impot Res* 15 Suppl 4: S3-8, 2003.

564. **Chakravarti S**, **Collins WP**, **Forecast JD**, **Newton JR**, **Oram DH**, **Studd JW**. Hormonal profiles after the menopause. *Br Med J* 2: 784–7, 1976.

565. **Feldman HA**, **Longcope C**, **Derby CA**, **Johannes CB**, **Araujo AB**, **Coviello AD**, **Bremner WJ**, **McKinlay JB**. Age trends in the level of serum testosterone and other hormones in middle-aged men: longitudinal results from the Massachusetts male aging study. *J Clin Endocrinol Metab* 87: 589–98, 2002.

566. **Davis SR**, **Bell RJ**, **Robinson PJ**, **Handelsman DJ**, **Gilbert T**, **Phung J**, **Desai R**, **Lockery JE**, **Woods RL**, **Wolfe RS**, **Reid CM**, **Nelson MR**, **Murray AM**, **McNeil JJ**, **ASPREE Investigator Group**. Testosterone and Estrone Increase From the Age of 70 Years: Findings From the Sex Hormones in Older Women Study. *J Clin Endocrinol Metab* 104: 6291–6300, 2019.

567. **Vingren JL**, **Kraemer WJ**, **Ratamess NA**, **Anderson JM**, **Volek JS**, **Maresh CM**. Testosterone physiology in resistance exercise and training: the up-stream regulatory elements. *Sports Med* 40: 1037–53, 2010.

568. **Marouliss GB**, **Triantafillidis IK**. Polycystic ovarian disease: the adrenal connection. *Pediatr Endocrinol Rev* 3 Suppl 1: 205–7, 2006.

569. **Nuzzo JL**. Narrative Review of Sex Differences in Muscle Strength, Endurance, Activation, Size, Fiber Type, and Strength Training Participation Rates, Preferences, Motivations, Injuries, and Neuromuscular Adaptations. *J Strength Cond Res* 37: 494–536, 2023. doi: 10.1519/JSC.0000000000004329.

570. **Camilleri G**, **Kiani AK**, **Herbst KL**, **Kaftalli J**, **Bernini A**, **Dhuli K**, **Manara E**, **Bonetti G**, **Stuppia L**, **Paolacci S**, **Dautaj A**, **Bertelli M**. Genetics of fat deposition. *Eur Rev Med Pharmacol Sci* 25: 14–22, 2021. doi: 10.26355/eurrev_202112_27329.

571. **Avdagić S**, **Barić I**, **Keser I**, **Cecić I**, **Šatalić Z**, **Bobić J**, **Gomzi M**. Differences in Peak Bone Density Between Male and Female Students. *Archives of Industrial Hygiene and Toxicology* 60: 79–86, 2009. doi: 10.2478/10004-1254-60-2009-1886.

572. **Lee D-M**, **Bajracharya P**, **Lee EJ**, **Kim J-E**, **Lee H-J**, **Chun T**, **Kim J**, **Cho KH**, **Chang J**, **Hong S**, **Choi I**. Effects of gender-specific adult bovine serum on myogenic satellite cell proliferation, differentiation and lipid accumulation. *In Vitro Cell Dev Biol Anim* 47: 438–44, 2011.

573. **Swift-Gallant A**, **Monks DA**. Androgen receptor expression in satellite cells of the neonatal levator ani of the rat. *Dev Neurobiol* 73: 448–54, 2013.

574. **Bauman WA**, **Cirnigliaro CM**, **La Fountaine MF**, **Jensen AM**, **Wecht JM**, **Kirshblum SC**, **Spungen AM**. A small-scale clinical trial to determine the safety and efficacy of testosterone replacement therapy in hypogonadal men with spinal cord injury. *Horm Metab Res* 43: 574–9, 2011.

575. **Zhao W**, **Pan J**, **Zhao Z**, **Wu Y**, **Bauman WA**, **Cardozo CP**. Testosterone protects against dexamethasone-induced muscle atrophy, protein degradation and MAFbx upregulation. *J Steroid Biochem Mol Biol* 110: 125–9, 2008. doi: 10.1016/j.jsbmb.2008.03.024.

576. **Vandenput L**, **Ohlsson C**. Estrogens as regulators of bone health in men. *Nat Rev Endocrinol* 5: 437–43, 2009.

577. **Calmels P**, **Vico L**, **Alexandre C**, **Minaire P**. Cross-sectional study of muscle strength and bone mineral density in a population of 106 women between the ages of 44 and 87 years: relationship with age and menopause. *Eur J Appl Physiol Occup Physiol* 70: 180–6, 1995.

578. **Sipilä S**. Body composition and muscle performance during menopause and hormone replacement therapy. *J Endocrinol Invest* 26: 893–901, 2003.

579. **Syed F**, **Khosla S**. Mechanisms of sex steroid effects on bone. *Biochem Biophys Res Commun* 328: 688–96, 2005.

580. **Clarkson PM**, **Hubal MJ**. Are women less susceptible to exercise-induced muscle damage? *Curr Opin Clin Nutr Metab Care* 4: 527–31, 2001.

581. **Viña J**, **Borrás C**, **Gambini J**, **Sastre J**, **Pallardó F V**. Why females live longer than males: control of longevity by sex hormones. *Sci Aging Knowledge Environ* 2005: pe17, 2005.

582. **Viña J**, **Sastre J**, **Pallardó F V**, **Gambini J**, **Borrás C**. Role of mitochondrial oxidative stress to explain the different longevity between genders: protective effect of estrogens. *Free Radic Res* 40: 1359–65, 2006.

583. **Horstman AM**, **Dillon EL**, **Urban RJ**, **Sheffield-Moore M**. The role of androgens and estrogens on healthy aging and longevity. *J Gerontol A Biol Sci Med Sci* 67: 1140–52, 2012.

584. **Trachootham D**, **Lu W**, **Ogasawara MA**, **Nilsa R-DV**, **Huang P**. Redox regulation of cell survival. *Antioxid Redox Signal* 10: 1343–74, 2008.

585. **Tiidus PM**, **Lowe DA**, **Brown M**. Estrogen replacement and skeletal muscle: mechanisms and population health. *J Appl Physiol (1985)* 115: 569–78, 2013. doi: 10.1152/japplphysiol.00629.2013.

586. **Butcher RL**, **Collins WE**, **Fugo NW**. Plasma concentration of LH, FSH, prolactin, progesterone and estradiol-17beta throughout the 4-day estrous cycle of the rat. *Endocrinology* 94: 1704–8, 1974. doi: 10.1210/endo-94-6-1704.

587. **Sugiura T**, **Ito N**, **Goto K**, **Naito H**, **Yoshioka T**, **Powers SK**. Estrogen administration attenuates immobilization-induced skeletal muscle atrophy in male rats. *J Physiol Sci* 56: 393–9, 2006. doi: 10.2170/physiolsci.RP006906.

588. **Kawano S**, **Kanda K**, **Ohmori S**, **Izumi R**, **Yasukawa K**, **Murata Y**, **Seo H**. Effect of estrogen on the development of disuse atrophy of bone and muscle induced by tail-supension in rats. *Environ Med* 41: 89–92, 1997.

589. **Velarde MC**. Pleiotropic actions of estrogen: a mitochondrial matter. *Physiol Genomics* 45: 106–9, 2013. doi: 10.1152/physiolgenomics.00155.2012.

590. **Pitkänen HT**, **Oja SS**, **Kemppainen K**, **Seppä JM**, **Mero AA**. Serum amino acid concentrations in aging men and women. *Amino Acids* 24: 413–421, 2003. doi: 10.1007/s00726-002-0338-0.

591. **Rémond D**, **Shahar DR**, **Gille D**, **Pinto P**, **Kachal J**, **Peyron M-A**, **Dos Santos CN**, **Walther B**, **Bordoni A**, **Dupont D**, **Tomás-Cobos L**, **Vergères G**. Understanding the gastrointestinal tract of the elderly to develop dietary solutions that prevent malnutrition. *Oncotarget* 6: 13858–98, 2015.

592. **Akamizu T**, **Murayama T**, **Teramukai S**, **Miura K**, **Bando I**, **Irako T**, **Iwakura H**, **Ariyasu H**, **Hosoda H**, **Tada H**, **Matsuyama A**, **Kojima S**, **Wada T**, **Wakatsuki Y**, **Matsubayashi K**, **Kawakita T**, **Shimizu A**, **Fukushima M**, **Yokode M**, **Kangawa K**. Plasma ghrelin levels in healthy elderly volunteers: the levels of acylated ghrelin in elderly females correlate positively with serum IGF-I levels and bowel movement frequency and negatively with systolic blood pressure. *J Endocrinol* 188: 333–44, 2006.

593. **Little TJ**, **Horowitz M**, **Feinle-Bisset C**. Role of cholecystokinin in appetite control and body weight regulation. *Obes Rev* 6: 297–306, 2005.

594. **Cavill NA**, **Foster CEM**. Enablers and barriers to older people's participation in strength and balance activities: A review of reviews. *J Frailty Sarcopenia Falls* 3: 105–113, 2018.

595. **Bennett E**, **Peters SAE**, **Woodward M**. Sex differences in macronutrient intake and adherence to dietary recommendations: findings from the UK Biobank. *BMJ Open* 8: e020017, 2018.

596. **Nuzzo JL**. Sex Difference in Participation in Muscle-Strengthening Activities. *J Lifestyle Med* 10: 110–115, 2020.

597. **Lee CC**, **Watkins SM**, **Lorenzo C**, **Wagenknecht LE**, **Il'yasova D**, **Chen Y-DI**, **Haffner SM**, **Hanley AJ**. Branched-Chain Amino Acids and Insulin Metabolism: The Insulin Resistance Atherosclerosis Study (IRAS). *Diabetes Care* 39: 582–8, 2016.

598. **Drummond MJ**, **Glynn EL**, **Fry CS**, **Timmerman KL**, **Volpi E**, **Rasmussen BB**. An increase in essential amino acid availability upregulates amino acid transporter expression in human skeletal muscle. *Am J Physiol Endocrinol Metab* 298: 1011–1018, 2010. doi: 10.1152/ajpendo.00690.2009.

599. **Drummond MJ**, **Dickinson JM**, **Fry CS**, **Walker DK**, **Gundermann DM**, **Reidy PT**, **Timmerman KL**, **Markofski MM**, **Paddon-Jones D**, **Rasmussen BB**, **Volpi E**. Bed rest impairs skeletal muscle amino acid transporter expression, mTORC1 signaling, and protein synthesis in response to essential amino acids in older adults. *Am J Physiol Endocrinol Metab* 302: 1113–1122, 2012. doi: 10.1152/ajpendo.00603.2011.

600. **Dickinson JM**, **Drummond MJ**, **Coben JR**, **Volpi E**, **Rasmussen BB**. Aging differentially affects human skeletal muscle amino acid transporter expression when essential amino acids are ingested after exercise. *Clinical Nutrition* 32: 273–280, 2013. doi: 10.1016/j.clnu.2012.07.009.

601. **Drummond MJ**, **Fry CS**, **Glynn EL**, **Timmerman KL**, **Dickinson JM**, **Walker DK**, **Gundermann DM**, **Volpi E**, **Rasmussen BB**. Skeletal muscle amino acid transporter expression is increased in young and older adults following resistance exercise. *J Appl Physiol* 111: 135–142, 2011. doi: 10.1152/japplphysiol.01408.2010.

602. **Lamont LS**, **McCullough AJ**, **Kalhan SC**. Gender differences in the regulation of amino acid metabolism. *J Appl Physiol (1985)* 95: 1259–65, 2003.

603. **Obayashi M**, **Shimomura Y**, **Nakai N**, **Jeoung NH**, **Nagasaki M**, **Murakami T**, **Sato Y**, **Harris RA**. Estrogen controls branched-chain amino acid catabolism in female rats. *J Nutr* 134: 2628–33, 2004.

604. **KOBAYASHI R**, **SHIMOMURA Y**, **MURAKAMI T**, **NAKAI N**, **OTSUKA M**, **ARAKAWA N**, **SHIMIZU K**, **HARRIS RA**. Hepatic Branched-Chain .ALPHA.-Keto Acid Dehydrogenase Complex in Female Rats: Activation by Exercise and Starvation. *J Nutr Sci Vitaminol (Tokyo)* 45: 303–309, 1999. doi: 10.3177/jnsv.45.303.

605. **Markofski MM**, **Dickinson JM**, **Drummond MJ**, **Fry CS**, **Fujita S**, **Gundermann DM**, **Glynn EL**, **Jennings K**, **Paddon-Jones D**, **Reidy PT**, **Sheffield-Moore M**, **Timmerman KL**, **Rasmussen BB**, **Volpi E**. Effect of age on basal muscle protein synthesis and mTORC1 signaling in a large cohort of young and older men and women. *Exp Gerontol* 65: 1–7, 2015.

606. **Drummond MJ**, **Fry CS**, **Glynn EL**, **Timmerman KL**, **Dickinson JM**, **Walker DK**, **Gundermann DM**, **Volpi E**, **Rasmussen BB**. Skeletal muscle amino acid transporter expression is increased in young and older adults following resistance exercise. *J Appl Physiol (1985)* 111: 135–42, 2011.

607. **Drummond MJ**, **Dreyer HC**, **Pennings B**, **Fry CS**, **Dhanani S**, **Dillon EL**, **Sheffield-Moore M**, **Volpi E**, **Rasmussen BB**. Skeletal muscle protein anabolic response to resistance exercise and essential amino acids is delayed with aging. *J Appl Physiol (1985)* 104: 1452–61, 2008.

608. **Francaux M**, **Demeulder B**, **Naslain D**, **Fortin R**, **Lutz O**, **Caty G**, **Deldicque L**. Aging Reduces the Activation of the mTORC1 Pathway after Resistance Exercise and Protein Intake in Human Skeletal Muscle: Potential Role of REDD1 and Impaired Anabolic Sensitivity. *Nutrients* 8, 2016.

609. **Volpi E**, **Lucidi P**, **Bolli GB**, **Santeusanio F**, **De Feo P**. Gender Differences in Basal Protein Kinetics in Young Adults. *J Clin Endocrinol Metab* 83: 4363–4367, 1998.

610. **West DWD**, **Burd NA**, **Churchward-Venne TA**, **Camera DM**, **Mitchell CJ**, **Baker SK**, **Hawley JA**, **Coffey VG**, **Phillips SM**. Sex-based comparisons of myofibrillar protein synthesis after resistance exercise in the fed state. *J Appl Physiol* 112: 1805–1813, 2012.

611. **Dreyer HC**, **Fujita S**, **Glynn EL**, **Drummond MJ**, **Volpi E**, **Rasmussen BB**. Resistance exercise increases leg muscle protein synthesis and mTOR signalling independent of sex. *Acta Physiologica* 199: 71–81, 2010.

612. **Norman K**, **Pichard C**, **Lochs H**, **Pirlich M**. Prognostic impact of disease-related malnutrition. *Clinical Nutrition* 27: 5–15, 2008.

613. **Khalatbari-Soltani S**, **Marques-Vidal P**. The economic cost of hospital malnutrition in Europe; a narrative review. *Clin Nutr ESPEN* 10: e89–e94, 2015.

614. **Norman K**, **Haß U**, **Pirlich M**. Malnutrition in Older Adults-Recent Advances and Remaining Challenges. *Nutrients* 13, 2021.

615. **Hébuterne X**, **Bermon S**, **Schneider SM**. Ageing and muscle: the effects of malnutrition, re-nutrition, and physical exercise. *Curr Opin Clin Nutr Metab Care* 4: 295–300, 2001.

616. **Lengelé L**, **Bruyère O**, **Beaudart C**, **Reginster J-Y**, **Locquet M**. Impact of Malnutrition Status on Muscle Parameter Changes over a 5-Year Follow-Up of Community-Dwelling Older Adults from the SarcoPhAge Cohort. *Nutrients* 13, 2021.

617. **Inouye SK**, **Studenski S**, **Tinetti ME**, **Kuchel GA**. Geriatric syndromes: clinical, research, and policy implications of a core geriatric concept. *J Am Geriatr Soc* 55: 780–91, 2007.

618. **Bork KA**, **Diallo A**. Boys Are More Stunted than Girls from Early Infancy to 3 Years of Age in Rural Senegal. *J Nutr* 147: 940–947, 2017.

619. **Adair LS**, **Guilkey DK**. Age-specific determinants of stunting in Filipino children. *J Nutr* 127: 314–20, 1997.

620. **Thurstans S**, **Opondo C**, **Seal A**, **Wells JC**, **Khara T**, **Dolan C**, **Briend A**, **Myatt M**, **Garenne M**, **Mertens A**, **Sear R**, **Kerac M**. Understanding Sex Differences in Childhood Undernutrition: A Narrative Review. *Nutrients* 14, 2022.

621. **Thalacker-Mercer AE**, **Dell'Italia LJ**, **Cui X**, **Cross JM**, **Bamman MM**. Differential genomic responses in old vs. young humans despite similar levels of modest muscle damage after resistance loading. *Physiol Genomics* 40: 141–9, 2010.

622. **Bruunsgaard H**, **Skinhøj P**, **Pedersen AN**, **Schroll M**, **Pedersen BK**. Ageing, tumour necrosis factor-alpha (TNF-alpha) and atherosclerosis. *Clin Exp Immunol* 121: 255–60, 2000.

623. **Cesari M**, **Penninx BWJH**, **Pahor M**, **Lauretani F**, **Corsi AM**, **Rhys Williams G**, **Guralnik JM**, **Ferrucci L**. Inflammatory markers and physical performance in older persons: the InCHIANTI study. *J Gerontol A Biol Sci Med Sci* 59: 242–8, 2004.

624. **Reid MB**, **Lännergren J**, **Westerblad H**. Respiratory and limb muscle weakness induced by tumor necrosis factor-alpha: involvement of muscle myofilaments. *Am J Respir Crit Care Med* 166: 479–84, 2002.

625. **Sanada F**, **Taniyama Y**, **Muratsu J**, **Otsu R**, **Shimizu H**, **Rakugi H**, **Morishita R**. Source of Chronic Inflammation in Aging. *Front Cardiovasc Med* 5, 2018. doi: 10.3389/fcvm.2018.00012.

626. **Gheller BJF**, **Riddle ES**, **Lem MR**, **Thalacker-Mercer AE**. Understanding Age-Related Changes in Skeletal Muscle Metabolism: Differences Between Females and Males. *Annu Rev Nutr* 36: 129–56, 2016.

627. **Beyer I**, **Mets T**, **Bautmans I**. Chronic low-grade inflammation and age-related sarcopenia. *Curr Opin Clin Nutr Metab Care* 15: 12–22, 2012. doi: 10.1097/MCO.0b013e32834dd297.

628. **Llovera M**, **López-Soriano FJ**, **Argilés JM**. Effects of tumor necrosis factor-alpha on muscle-protein turnover in female Wistar rats. *J Natl Cancer Inst* 85: 1334–9, 1993.

629. **Remels AH V**, **Gosker HR**, **Schrauwen P**, **Hommelberg PPH**, **Sliwinski P**, **Polkey M**, **Galdiz J**, **Wouters EFM**, **Langen RCJ**, **Schols AMWJ**. TNF-alpha impairs regulation of muscle oxidative phenotype: implications for cachexia? *FASEB J* 24: 5052–62, 2010.

630. **Rosa-Caldwell ME**, **Greene NP**. Muscle metabolism and atrophy: let's talk about sex. *Biol Sex Differ* 10: 43, 2019.

631. **Hetzler KL**, **Hardee JP**, **LaVoie HA**, **Murphy EA**, **Carson JA**. Ovarian function's role during cancer cachexia progression in the female mouse. *Am J Physiol Endocrinol Metab* 312: E447–E459, 2017.

632. **Koopman RJ**, **Mainous AG**, **Diaz VA**, **Geesey ME**. Changes in age at diagnosis of type 2 diabetes mellitus in the United States, 1988 to 2000. *Ann Fam Med* 3: 60–3, 2005.

633. **Shou J**, **Chen P-J**, **Xiao W-H**. Mechanism of increased risk of insulin resistance in aging skeletal muscle. *Diabetol Metab Syndr* 12: 14, 2020.

634. **Cowie CC**, **Rust KF**, **Ford ES**, **Eberhardt MS**, **Byrd-Holt DD**, **Li C**, **Williams DE**, **Gregg EW**, **Bainbridge KE**, **Saydah SH**, **Geiss LS**. Full accounting of diabetes and pre-diabetes in the U.S. population in 1988-1994 and 2005-2006. *Diabetes Care* 32: 287–94, 2009.

635. **Møller AB**, **Kampmann U**, **Hedegaard J**, **Thorsen K**, **Nordentoft I**, **Vendelbo MH**, **Møller N**, **Jessen N**. Altered gene expression and repressed markers of autophagy in skeletal muscle of insulin resistant patients with type 2 diabetes. *Sci Rep* 7: 43775, 2017.

636. **Petersen KF**, **Morino K**, **Alves TC**, **Kibbey RG**, **Dufour S**, **Sono S**, **Yoo PS**, **Cline GW**, **Shulman GI**. Effect of aging on muscle mitochondrial substrate utilization in humans. *Proc Natl Acad Sci U S A* 112: 11330–4, 2015.

637. **Seo E**, **Kim S**, **Lee SJ**, **Oh B-C**, **Jun H-S**. Ginseng berry extract supplementation improves age-related decline of insulin signaling in mice. *Nutrients* 7: 3038–53, 2015.

638. **Geer EB**, **Shen W**. Gender differences in insulin resistance, body composition, and energy balance. *Gend Med* 6 Suppl 1: 60–75, 2009.

639. **Nishizawa H**, **Shimomura I**, **Kishida K**, **Maeda N**, **Kuriyama H**, **Nagaretani H**, **Matsuda M**, **Kondo H**, **Furuyama N**, **Kihara S**, **Nakamura T**, **Tochino Y**, **Funahashi**

T, **Matsuzawa Y**. Androgens decrease plasma adiponectin, an insulin-sensitizing adipocyte-derived protein. *Diabetes* 51: 2734–41, 2002.

640. **Geer EB**, **Shen W**. Gender differences in insulin resistance, body composition, and energy balance. *Gend Med* 6 Suppl 1: 60–75, 2009.

641. **Moreno M**, **Ordoñez P**, **Alonso A**, **Díaz F**, **Tolivia J**, **González C**. Chronic 17beta-estradiol treatment improves skeletal muscle insulin signaling pathway components in insulin resistance associated with aging. *Age (Dordr)* 32: 1–13, 2010.

642. **Deguchi M**, **Mochizuki M**, **Tojo S**. [Effect of human chorionic somatomammotropin on release of glucose by perfused rat liver (author's transl)]. *Acta Obstet Gynaecol Jpn* 32: 1889–906, 1980.

643. **Greenhill C**. Sex differences in insulin resistance. *Nat Rev Endocrinol* 14: 65–65, 2018.

644. **Amorim JA**, **Coppotelli G**, **Rolo AP**, **Palmeira CM**, **Ross JM**, **Sinclair DA**. Mitochondrial and metabolic dysfunction in ageing and age-related diseases. *Nat Rev Endocrinol* 18: 243–258, 2022. doi: 10.1038/s41574-021-00626-7.

645. **Guo Y**, **Guan T**, **Shafiq K**, **Yu Q**, **Jiao X**, **Na D**, **Li M**, **Zhang G**, **Kong J**. Mitochondrial dysfunction in aging. *Ageing Res Rev* 88: 101955, 2023. doi: 10.1016/j.arr.2023.101955.

646. **Srivastava S**. The Mitochondrial Basis of Aging and Age-Related Disorders. *Genes (Basel)* 8: 398, 2017. doi: 10.3390/genes8120398.

647. **Bellanti F**, **Lo Buglio A**, **Vendemiale G**. Mitochondrial Impairment in Sarcopenia. *Biology (Basel)* 10: 31, 2021. doi: 10.3390/biology10010031.

648. **Montero D**, **Madsen K**, **Meinild-Lundby A**, **Edin F**, **Lundby C**. Sexual dimorphism of substrate utilization: Differences in skeletal muscle mitochondrial volume density and function. *Exp Physiol* 103: 851–859, 2018. doi: 10.1113/EP087007.

649. **Chweih H**, **Castilho RF**, **Figueira TR**. Tissue and sex specificities in Ca^{2+} handling by isolated mitochondria in conditions avoiding the permeability transition. *Exp Physiol* 100: 1073–1092, 2015. doi: 10.1113/EP085248.

650. **Justo R**, **Boada J**, **Frontera M**, **Oliver J**, **Bermúdez J**, **Gianotti M**. Gender dimorphism in rat liver mitochondrial oxidative metabolism and biogenesis. *American Journal of Physiology-Cell Physiology* 289: C372–C378, 2005. doi: 10.1152/ajpcell.00035.2005.

651. **Cardinale DA**, **Larsen FJ**, **Schiffer TA**, **Morales-Alamo D**, **Ekblom B**, **Calbet JAL**, **Holmberg H-C**, **Boushel R**. Superior Intrinsic Mitochondrial Respiration in Women Than in Men. *Front Physiol* 9, 2018. doi: 10.3389/fphys.2018.01133.

652. **Colom B**, **Alcolea M**, **Valle A**, **Oliver J**, **Roca P**, **García-Palmer F**. Skeletal Muscle of Female Rats Exhibit Higher Mitochondrial Mass and Oxidative-Phosphorylative

Capacities Compared to Males. *Cellular Physiology and Biochemistry* 19: 205–212, 2007. doi: 10.1159/000099208.

653. **Straface E**, **Vona R**, **Campesi I**, **Franconi F**. Mitochondria can orchestrate sex differences in cell fate of vascular smooth muscle cells from rats. *Biol Sex Differ* 6: 34, 2015. doi: 10.1186/s13293-015-0051-9.

654. **Ventura-Clapier R**, **Piquereau J**, **Veksler V**, **Garnier A**. Estrogens, Estrogen Receptors Effects on Cardiac and Skeletal Muscle Mitochondria. *Front Endocrinol (Lausanne)* 10, 2019. doi: 10.3389/fendo.2019.00557.

655. **Miotto PM**, **McGlory C**, **Holloway TM**, **Phillips SM**, **Holloway GP**. Sex differences in mitochondrial respiratory function in human skeletal muscle. *American Journal of Physiology-Regulatory, Integrative and Comparative Physiology* 314: R909–R915, 2018. doi: 10.1152/ajpregu.00025.2018.

656. **Sharma J**, **Johnston M V**, **Hossain MA**. Sex differences in mitochondrial biogenesis determine neuronal death and survival in response to oxygen glucose deprivation and reoxygenation. *BMC Neurosci* 15: 9, 2014. doi: 10.1186/1471-2202-15-9.

657. **Husom AD**, **Peters EA**, **Kolling EA**, **Fugere NA**, **Thompson L V**, **Ferrington DA**. Altered proteasome function and subunit composition in aged muscle. *Arch Biochem Biophys* 421: 67–76, 2004.

658. **Lee CK**, **Klopp RG**, **Weindruch R**, **Prolla TA**. Gene expression profile of aging and its retardation by caloric restriction. *Science* 285: 1390–3, 1999.

659. **Ferrington DA**, **Husom AD**, **Thompson L V**. Altered proteasome structure, function, and oxidation in aged muscle. *FASEB J* 19: 644–6, 2005.

660. **Vernace VA**, **Arnaud L**, **Schmidt-Glenewinkel T**, **Figueiredo-Pereira ME**. Aging perturbs 26S proteasome assembly in Drosophila melanogaster. *FASEB J* 21: 2672–82, 2007.

661. **Clavel S**, **Coldefy A-S**, **Kurkdjian E**, **Salles J**, **Margaritis I**, **Derijard B**. Atrophy-related ubiquitin ligases, atrogin-1 and MuRF1 are up-regulated in aged rat Tibialis Anterior muscle. *Mech Ageing Dev* 127: 794–801, 2006.

662. **Saez I**, **Vilchez D**. The Mechanistic Links Between Proteasome Activity, Aging and Age-related Diseases. *Curr Genomics* 15: 38–51, 2014.

663. **Ogawa M**, **Kitakaze T**, **Harada N**, **Yamaji R**. Female-specific regulation of skeletal muscle mass by USP19 in young mice. *J Endocrinol* 225: 135–45, 2015.

664. **Ogawa M**, **Kitano T**, **Kawata N**, **Sugihira T**, **Kitakaze T**, **Harada N**, **Yamaji R**. Daidzein down-regulates ubiquitin-specific protease 19 expression through estrogen receptor β and increases skeletal muscle mass in young female mice. *J Nutr Biochem* 49: 63–70, 2017.

665. **Kroemer G**. Autophagy: a druggable process that is deregulated in aging and human disease. *J Clin Invest* 125: 1–4, 2015.

666. **Wohlgemuth SE**, **Seo AY**, **Marzetti E**, **Lees HA**, **Leeuwenburgh C**. Skeletal muscle autophagy and apoptosis during aging: effects of calorie restriction and life-long exercise. *Exp Gerontol* 45: 138–48, 2010.

667. **Piekarski A**, **Khaldi S**, **Greene E**, **Lassiter K**, **Mason JG**, **Anthony N**, **Bottje W**, **Dridi S**. Tissue distribution, gender- and genotype-dependent expression of autophagy-related genes in avian species. *PLoS One* 9: e112449, 2014.

668. **Oliván S**, **Calvo AC**, **Manzano R**, **Zaragoza P**, **Osta R**. Sex differences in constitutive autophagy. *Biomed Res Int* 2014: 652817, 2014.

669. **Loberg RD**, **Bradley DA**, **Tomlins SA**, **Chinnaiyan AM**, **Pienta KJ**. The Lethal Phenotype of Cancer: The Molecular Basis of Death Due to Malignancy. *CA Cancer J Clin* 57: 225–241, 2007.

670. **Holeček M**. Branched-chain amino acids in health and disease: Metabolism, alterations in blood plasma, and as supplements. *Nutr Metab (Lond)* 33: 15, 2018.

671. **Katayama T**, **Chigi Y**, **Okamura D**. The ensured proliferative capacity of myoblast in serum-reduced conditions with Methyl-β-cyclodextrin. *Front Cell Dev Biol* 11: 1193634, 2023. doi: 10.3389/fcell.2023.1193634.

672. **Holeček M**. Beta-hydroxy-beta-methylbutyrate supplementation and skeletal muscle in healthy and muscle-wasting conditions. *J Cachexia Sarcopenia Muscle* 8: 529–541, 2017.

673. **Holeček M**. Relation between glutamine, branched-chain amino acids, and protein metabolism 1 1Guest Editor: Gil Hardy, PhD. *Nutrition* 18: 130–133, 2002.

674. **Zhao C**, **Guo H**, **Hou Y**, **Lei T**, **Wei D**, **Zhao Y**. Multiple Roles of the Stress Sensor GCN2 in Immune Cells. *Int J Mol Sci* 24, 2023. doi: 10.3390/ijms24054285.

675. **Roberson PA**, **Mobley CB**, **Romero MA**, **Haun CT**, **Osburn SC**, **Mumford PW**, **Vann CG**, **Greer RA**, **Ferrando AA**, **Roberts MD**. LAT1 Protein Content Increases Following 12 Weeks of Resistance Exercise Training in Human Skeletal Muscle. *Front Nutr* 7: 628405, 2021.

676. **Barthelemy C**, **André B**. Ubiquitylation and endocytosis of the human LAT1/SLC7A5 amino acid transporter. *Sci Rep* 9: 16760, 2019.

677. **Meier C**, **Ristic Z**, **Klauser S**, **Verrey F**. Activation of system L heterodimeric amino acid exchangers by intracellular substrates. *EMBO J* 21: 580–9, 2002. doi: 10.1093/emboj/21.4.580.

678. **Liu X**, **Reyna S V.**, **Ensenat D**, **Peyton KJ**, **Wang H**, **Schafer AI**, **Durante W**. Platelet-derived growth factor stimulates LAT1 gene expression in vascular smooth muscle: Role in cell growth. *The FASEB Journal* 18: 768–770, 2004.

679. **Hodson N**, **Brown T**, **Joanisse S**, **Aguirre N**, **West D**, **Moore D**, **Baar K**, **Breen L**, **Philp A**. Characterisation of L-Type Amino Acid Transporter 1 (LAT1) Expression in Human Skeletal Muscle by Immunofluorescent Microscopy. *Nutrients* 10: 23, 2017.

680. **Nemati A**, **Alipanah-Moghadam R**, **Molazadeh L**, **Baghi AN**. The effect of glutamine supplementation on oxidative stress and matrix metalloproteinase 2 and 9 after exhaustive exercise. *Drug Des Devel Ther* 13: 4215–4223, 2019.

681. **Yao K**, **Yin YL**, **Chu W**, **Liu Z**, **Deng D**, **Li T**, **Huang R**, **Zhang J**, **Tan B**, **Wang W**, **Wu G**. Dietary arginine supplementation increases mTOR signaling activity in skeletal muscle of neonatal pigs. *Journal of Nutrition* 138: 867–872, 2008. doi: 10.1093/jn/138.5.867.

682. **Campbell BI**, **La Bounty PM**, **Roberts M**. The Ergogenic Potential of Arginine. *J Int Soc Sports Nutr* 1: 35–38, 2004.

683. **Hatazawa Y**, **Tadaishi M**, **Nagaike Y**, **Morita A**, **Ogawa Y**, **Ezaki O**, **Takai-Igarashi T**, **Kitaura Y**, **Shimomura Y**, **Kamei Y**, **Miura S**. PGC-1α-mediated branched-chain amino acid metabolism in the skeletal muscle. *PLoS One* 9: 1–10, 2014. doi: 10.1371/journal.pone.0091006.

684. **Sahlin K**. NADH in human skeletal muscle during short-term intense exercise. *Pflugers Arch* 403: 193–6, 1985. doi: 10.1007/BF00584099.

685. **Huang X**, **Chen J**, **Cao W**, **Yang L**, **Chen Q**, **He J**, **Yi Q**, **Huang H**, **Zhang E**, **Cai Z**. The many substrates and functions of NEDD4-1. *Cell Death Dis* 10: 904, 2019. doi: 10.1038/s41419-019-2142-8.

686. **Venkataraman S**, **Prasad BVLS**, **Selvarajan R**. RNA Dependent RNA Polymerases: Insights from Structure, Function and Evolution. *Viruses* 10, 2018. doi: 10.3390/v10020076.

687. **Collao N**, **Akohene-Mensah P**, **Nallabelli J**, **Binet ER**, **Askarian A**, **Lloyd J**, **Niemiro GM**, **Beals JW**, **van Vliet S**, **Rajgara R**, **Saleh A**, **Wiper-Bergeron N**, **Paluska SA**, **Burd NA**, **De Lisio M**. The role of L-type amino acid transporter 1 (Slc7a5) during in vitro myogenesis. *Am J Physiol Cell Physiol* 323: C595–C605, 2022. doi: 10.1152/ajpcell.00162.2021.

688. **Lim S**, **Brown JL**, **Washington TA**, **Greene NP**. Development and progression of cancer cachexia: Perspectives from bench to bedside. *Sports Medicine and Health Science* 2: 177–185, 2020.

689. **Byers SL**, **Wiles M V.**, **Dunn SL**, **Taft RA**. Mouse estrous cycle identification tool and images. *PLoS One* 7: e35538, 2012. doi: 10.1371/journal.pone.0035538.

690. **Bhasin S**, **Woodhouse L**, **Casaburi R**, **Singh AB**, **Bhasin D**, **Berman N**, **Chen X**, **Yarasheski KE**, **Magliano L**, **Dzekov C**, **Dzekov J**, **Bross R**, **Phillips J**, **Sinha-Hikim I**, **Shen R**, **Storer TW**. Testosterone dose-response relationships in healthy young men.

American Journal of Physiology-Endocrinology and Metabolism 281: E1172–E1181, 2001.

691. **Ebadi M**, **Field CJ**, **Lehner R**, **Mazurak VC**. Chemotherapy diminishes lipid storage capacity of adipose tissue in a preclinical model of colon cancer. *Lipids Health Dis* 16: 247, 2017.

692. **Karastergiou K**, **Smith SR**, **Greenberg AS**, **Fried SK**. Sex differences in human adipose tissues – the biology of pear shape. *Biol Sex Differ* 3: 13, 2012.

693. **Ponti F**, **Santoro A**, **Mercatelli D**, **Gasperini C**, **Conte M**, **Martucci M**, **Sangiorgi L**, **Franceschi C**, **Bazzocchi A**. Aging and Imaging Assessment of Body Composition: From Fat to Facts. *Front Endocrinol (Lausanne)* 10: 861, 2020.

694. **Marques VA**, **Ferreira-Junior JB**, **Lemos T V**, **Moraes RF**, **Junior JR de S**, **Alves RR**, **Silva MS**, **Freitas-Junior R de**, **Vieira CA**. Effects of Chemotherapy Treatment on Muscle Strength, Quality of Life, Fatigue, and Anxiety in Women with Breast Cancer. *Int J Environ Res Public Health* 17, 2020. doi: 10.3390/ijerph17197289.

695. **Prigerson HG**, **Bao Y**, **Shah MA**, **Paulk ME**, **LeBlanc TW**, **Schneider BJ**, **Garrido MM**, **Reid MC**, **Berlin DA**, **Adelson KB**, **Neugut AI**, **Maciejewski PK**. Chemotherapy Use, Performance Status, and Quality of Life at the End of Life. *JAMA Oncol* 1: 778–84, 2015. doi: 10.1001/jamaoncol.2015.2378.

696. **Honors MA**, **Kinzig KP**. The role of insulin resistance in the development of muscle wasting during cancer cachexia. *J Cachexia Sarcopenia Muscle* 3: 5–11, 2012. doi: 10.1007/s13539-011-0051-5.

697. **De Paoli M**, **Zakharia A**, **Werstuck GH**. The Role of Estrogen in Insulin Resistance. *Am J Pathol* 191: 1490–1498, 2021.

698. **Coll-Martínez B**, **Crosas B**. How the 26S Proteasome Degrades Ubiquitinated Proteins in the Cell. *Biomolecules* 9, 2019. doi: 10.3390/biom9090395.

699. **Lamont LS**, **McCullough AJ**, **Kalhan SC**. Gender differences in leucine, but not lysine, kinetics. *J Appl Physiol* 91: 357–362, 2001.

700. **Timmerman KL**, **Lee JL**, **Fujita S**, **Dhanani S**, **Dreyer HC**, **Fry CS**, **Drummond MJ**, **Sheffield-Moore M**, **Rasmussen BB**, **Volpi E**. Pharmacological Vasodilation Improves Insulin-Stimulated Muscle Protein Anabolism but Not Glucose Utilization in Older Adults. *Diabetes* 59: 2764–2771, 2010. doi: 10.2337/db10-0415.

701. **Kahlhofer J**, **Teis D**. The human LAT1–4F2hc (SLC7A5–SLC3A2) transporter complex: Physiological and pathophysiological implications. *Basic & Clinical Pharmacology & Toxicology133* 133: 459–472, 2022.

702. **White PJ**, **Newgard CB**. Branched-chain amino acids in disease. *Science (1979)* 363: 582–583, 2019.

703. **Li N**, **Cen Z**, **Zhao Z**, **Li Z**, **Chen S**. BCAA dysmetabolism in the host and gut microbiome, a key player in the development of obesity and T2DM. *Medicine in Microecology* 16: 100078, 2023.

704. **Wu AH**, **Vigen C**, **Tseng C**, **Garcia AA**, **Spicer D**. Effect of Chemotherapy on the Gut Microbiome of Breast Cancer Patients During the First Year of Treatment. *Breast Cancer: Targets and Therapy* Volume 14: 433–451, 2022.

705. **Gannon MC**, **Nuttall FQ**. Amino acid ingestion and glucose metabolism-A review. *IUBMB Life* 62: 660–668, 2010.

706. **von Haehling S**, **Anker SD**. Prevalence, incidence and clinical impact of cachexia: facts and numbers-update 2014. *J Cachexia Sarcopenia Muscle* 5: 261–263, 2014.

707. **Thoresen L**, **Frykholm G**, **Lydersen S**, **Ulveland H**, **Baracos V**, **Prado CMM**, **Birdsell L**, **Falkmer U**. Nutritional status, cachexia and survival in patients with advanced colorectal carcinoma. Different assessment criteria for nutritional status provide unequal results. *Clinical Nutrition* 32: 65–72, 2013. doi: 10.1016/j.clnu.2012.05.009.

708. **Ribeiro R V**, **Solon-Biet SM**, **Pulpitel T**, **Senior AM**, **Cogger VC**, **Clark X**, **O'Sullivan J**, **Koay YC**, **Hirani V**, **Blyth FM**, **Seibel MJ**, **Waite LM**, **Naganathan V**, **Cumming RG**, **Handelsman DJ**, **Simpson SJ**, **Le Couteur DG**. Of Older Mice and Men: Branched-Chain Amino Acids and Body Composition. *Nutrients* 11, 2019. doi: 10.3390/nu11081882.

709. **Sun YS**, **Zhao Z**, **Yang ZN**, **Xu F**, **Lu HJ**, **Zhu ZY**, **Shi W**, **Jiang J**, **Yao PP**, **Zhu HP**. Risk factors and preventions of breast cancer. *Int J Biol Sci* 13: 1387–1397, 2017.

710. **Barone B**, **Napolitano L**, **Abate M**, **Cirillo L**, **Reccia P**, **Passaro F**, **Turco C**, **Morra S**, **Mastrangelo F**, **Scarpato A**, **Amicuzi U**, **Morgera V**, **Romano L**, **Calace FP**, **Pandolfo SD**, **De Luca L**, **Aveta A**, **Sicignano E**, **Trivellato M**, **Spena G**, **D'Alterio C**, **Fusco GM**, **Vitale R**, **Arcaniolo D**, **Crocetto F**. The Role of Testosterone in the Elderly: What Do We Know? *Int J Mol Sci* 23: 3535, 2022. doi: 10.3390/ijms23073535.

711. **Pataky MW**, **Young WF**, **Nair KS**. Hormonal and Metabolic Changes of Aging and the Influence of Lifestyle Modifications. *Mayo Clin Proc* 96: 788–814, 2021.

712. **Pires-Oliveira M**, **Maragno ALGC**, **Parreiras-e-Silva LT**, **Chiavegatti T**, **Gomes MD**, **Godinho RO**. Testosterone represses ubiquitin ligases atrogin-1 and Murf-1 expression in an androgen-sensitive rat skeletal muscle in vivo. *J Appl Physiol* 108: 266–273, 2010.

713. **Gumucio JP**, **Mendias CL**. Atrogin-1, MuRF-1, and sarcopenia. *Endocrine* 43: 12–21, 2013.

714. **Hughes DC**, **Baehr LM**, **Waddell DS**, **Sharples AP**, **Bodine SC**. Ubiquitin Ligases in Longevity and Aging Skeletal Muscle. *Int J Mol Sci* 23: 7602, 2022.

715. **Jones DL**, **Rando TA**. Emerging models and paradigms for stem cell ageing. *Nat Cell Biol* 13: 506–512, 2011.

716. **Chang E**, **Varghese M**, **Singer K**. Gender and Sex Differences in Adipose Tissue. *Curr Diab Rep* 18: 69, 2018. doi: 10.1007/s11892-018-1031-3.

717. **Geppert J**, **Walth AA**, **Terrón Expósito R**, **Kaltenecker D**, **Morigny P**, **Machado J**, **Becker M**, **Simoes E**, **Lima JDCC**, **Daniel C**, **Berriel Diaz M**, **Herzig S**, **Seelaender M**, **Rohm M**. Aging Aggravates Cachexia in Tumor-Bearing Mice. *Cancers (Basel)* 14, 2021. doi: 10.3390/cancers14010090.

Chapter 9 Appendix

Appendix A – *In-vitro* and *In-vivo* Drug Dosages

In-vitro Dosing Calculations

Drug Stock Solutions:

- CPT-11 (Sigma, #I1406): 50mg dissolved in 1mL DMSO (Sigma, #D5879)
    - Weight 50mg of CPT-11 on thin filter paper
    - Dump the 50mg into a 1.5mL eppendorf tube
    - Add 1mL of DMSO, vortex to dissolve
    - Aliquot into 30µL amounts and store at -20 (not near door)

- 5FU (Sigma, #F6627): 50mg dissolved in 1mL DMSO
    - Weight 50mg of 5FU on thin filter paper
    - Dump the 50mg into a 1.5mL eppendorf tube
    - Add 1mL of DMSO, vortex to dissolve
    - Aliquot into 30µL amounts and store at -20 (not near door)

- Leucovorin (Sigma, #F7878): 20mg dissolved in 1mL ddH_2O
    - Weight 20mg of leucovorin on thin filter paper
    - Dump the 20mg into a 1.5mL eppendorf tube
    - Add 1mL of ddH_2O, vortex to dissolve
    - Aliquot into 30µL amounts and store at -20 (not near door)

Drug Dosages:

Sample Calculations shown for making 40mLs of cocktail in differentiation media.

- CPT-11: 20µg/mL
    - (20µg/mL (conc we want) x 40mLs (total volume)) / 50000µg/mL (stock) = 16µL
- 5FU: 50µg/mL
    - (50µg/mL (conc we want) x 40mLs (total volume)) / 50000µg/mL (stock) = 40µL
- Leucovorin: 10µg/mL
    - (10µg/mL (conc we want) x 40mLs (total volume)) / 20000µg/mL (stock) = 20µL

For vehicle: Add 1.4µL/mL of DMSO into differentiation media:

- 1.4µL x 40mLs = 56µL of DMSO into 40mLs of differentiation media

In-vivo Dosing Calculations

Drug Stock Solutions:

- CPT-11: 11.07mg/mL dissolved in 10% DMSO
    - Weight 11.07mg of CPT-11 on thin filter paper
    - Dump the 11.07mg into a 1.5mL eppendorf tube
    - Add 1mL of 10% DMSO, vortex to dissolve

- Aliquot into 100µL amounts and store at -20 (not near door)

- 5FU: 11.07mg/mL dissolved in 10% DMSO
  - Weight 11.07mg of 5-FU on thin filter paper
  - Dump the 11.07mg into a 1.5mL eppendorf tube
  - Add 1mL of 10% DMSO, vortex to dissolve
  - Aliquot into 150µL amounts and store at -20 (not near door)

- Leucovorin: 20mg/mL dissolved in ddH_2O
  - Weight 20mg of leucovorin on thin filter paper
  - Dump the 20mg into a 1.5mL eppendorf tube
  - Add 1mL of ddH_2O, vortex to dissolve
  - Aliquot into 150µL amounts and store at -20 (not near door)

Drug Doses:

- CPT-11: 24mg/kg
- 5-FU: 50mg/kg
- Leucovorin: 90mg/kg

For a mouse that weights 30g, total volume of injection a mouse can receive is 12x their body weight. Therefore, a mouse weighing 30g, can receive a max of 360uL.

- 5-FU 50mg / 1.50mg = 1000g / 30g | 11.07mg / 1.50mg = 1000uL / **135.5µL**

- Leucovorin 90mg / 2.7mg = 1000g / 30g | 11.07mg / 2.7mg = 1000uL / **135µL**

- CPT-11 24mg / 0.72mg = 1000g / 30g | 11.07mg / 0.72mg = 1000uL / **64.9µL**

Injection 1

Drug: 5-FU and leucovorin are given together. Therefore this cocktail is composed of 135.5µL of 5FU, 135µL of leucovorin and then 89.5µL of saline (these three total 360µL).

Vehicle: Because only the 5FU injection above has 10% DMSO, vehicle mice get this equivalent value (135.5µL of 10% DMSO) + the remaining as saline (224.5µL) to total 360µL.

Injection 2

Drug: CPT-11 is given by itself 2 hours after the above injection. Therefore this cocktail is composed of 64.9µL of CPT-11 and 295.1µL of saline (again totaling 360µL).

Vehicle: Because the above CPT-11 injection has 10% DMSO, vehicle mice get this equivalent value (64.9µL of 10% DMSO) + the remaining as saline (295.1µL) to total 360µL.

Appendix B – Transfection Procedure

Materials:

- NEdd4 siRNA (Sigma, #NM_001008300)
- Scrambled siRNA (Sigma, #SIC001)
- Lipofectamine RNAiMAX (Thermo Fisher, #100014472)
- Opti-MEM (Gibco, #31985-062)
- 6-well plates (Greiner Bio-One, #657165)
- Chemotherapy Drugs
    - CPT-11 (Sigma, #I1406)
    - 5FU (Sigma, #F6627)
    - Leucovorin (Sigma, #F7878)
- DMSO (Sigma, #D5879)
- Differentiation Medium: AMEM (Wisent, #310-010-CL) supplemented with horse serum (Gibco, #26050-088), with and w/o antibiotic (Wisent, #15240-062)
- Harvesting materials
    - PBS (Wisent, #311-010-CL)
    - Lysis Buffer + Phosphatase Inhibitor (Sigma, #P5726)
    - Scraping Tools

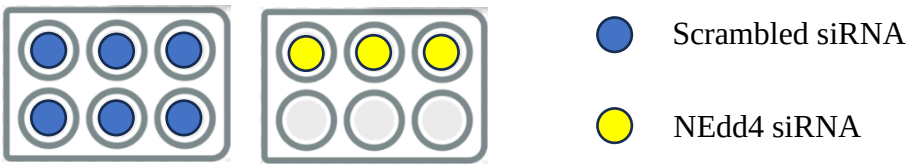

Protocol:

1. Seed, grow and differentiate myotubes until day 3 of differentiation

2. On day 3 of differentiation, in the sterile hood, prepare three 15mL tubes labelled A, B, C
    a. A: Lipofectamine + Opti-MEM (every well gets this)
    b. B: Scrambled siRNA (All the blue dot wells get this)
    c. C: NEdd4 siRNA (All the yellow dot well get this)

3. Into tube A add (all 9 wells will need this mixture):
    a. 1167µL of Opti-MEM
        i. For optimum, add 121.1µL/well. Since every well needs this mixture and we have a total of 9 wells (multiple by 9.5 for safety), we need 1150.45µL of optimum. Round this to 12mLs.
    b. 33µL of lipofectamine
        i. This is a 1:36 ratio of optimum to lipofectamine. So for 12mLs, 1:36 ratio is 33µL and then 1167µL of Opti-MEM

4. Into tube B add for scrambled wells (only 6 wells need this mixture):

a. 25.35µL of scrambled siRNA
    i. For scrambled siRNA, add 3.9µL/well, only 6 wells need this (do 6.5 for safety), so 3.9 x 6.5 = 25.35µL
b. 787.15µL of Opti-MEM
    i. Again for optimum, add 121.1µL/well, for 6 wells (do 6.5), so 121.1 x 6.5 = 787.15µL

5. Into tube C add for NEdd4 wells (only 3 wells need this mixture) add:
    a. 13.65µL of NEdd4 siRNA
        i. For NEdd4 siRNA, add 3.9µL/well, only 3 wells need this (do 3.5 for safety), so 3.9 x 3.5 = 13.65µL
    b. 423.85µL of Opti-MEM
        i. For optimum, add 121.1µL/well, for 3 wells (do 3.5), so 121.1 x 3.5 = 423.85µL

6. In tube A, you have a total of 1200µL. In a new 15mL tube labelled AB, add in a 1:1 ratio:
    a. 800µL of tube A
    b. 800µL of tube B
        i. This is your mixture that is going to be added into scrambled wells (6)

7. In a new 15mL tube labelled AC, add in a 1:1 ratio:
    a. 400µL of tube A
    b. 400µL of tube C
        i. This is your mixture that is going to be added into NEdd4 wells (3)

8. Let the new tubes, AB and AC sit for 5 minutes.

9. During the 5 minute wait, add 1mL of differentiation media w/o antibiotic into each well of your 6 wells with myotubes previously grown. Add into all 9wells.

10. Of the 6 scrambled wells that we have, 3 of the wells are going to be treated with vehicle and 3 of them are going to be treated with chemotherapy. Then the NEdd4 siRNA wells are also going to be treated with chemotherapy. Therefore, label the wells now as:
    a. Vehicle + scrambled (3)
    b. Chemotherapy + scrambled (3)
    c. Chemotherapy + NEdd4 (3)

Scrambled siRNA

NEdd4 siRNA

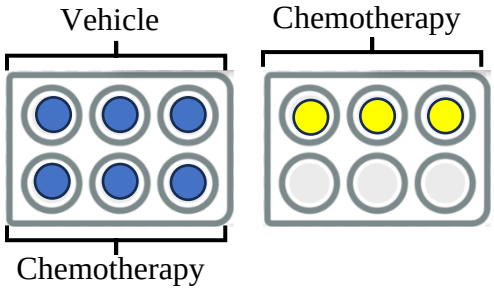

11. After the 5 minute wait period, add 250µL of tube AB into labelled scrambled and chemotherapy drug wells. Then add 250µL of tube AC into labelled NEdd4 + chemotherapy wells. Take note of the time that you added this 250µL.

12. Twenty-four hours after transfection (now day 4), add 1mL of differentiation media (with antibiotic) into each well for 6 hours.

13. After 6 hours, treat wells with respective vehicle or chemotherapy drug treatments. Remember, 3 wells treated with scrambled are going to get vehicle, 3 wells treated with scrambled are going to get chemotherapy and 3 wells treated with NEdd4 siRNA are going to get chemotherapy.

14. After 48 hours, harvest wells as needed for respective methods.

Appendix C – High Pressure Liquid Chromatography (HPLC) Protocol – BCAAs

Materials:

- Column (YMC-Triart 75mm x 3.0mmOD x 1.9um particle size)
- Metal Ferrule (IDEX health & science, #VHP-321,)
- Metal tubing (IDEX health & science, #U-154)
- Vials and lids (Supelco, #27080-U)
- Vial Inserts (Supelco, #24716)
- Phthalaldehyde solution (OPA) – keep on ice
    - Phthalaldehyde salt (Sigma, #P1378)
    - HPLC grade methanol (Fisher Chemical, #A-4524)
    - Brij 35 (Sigma, #B4184)
    - 2-mercaptoethanol (Sigma, #M6250)
    - 0.04M sodium borate buffer
- Micropipette (20-200µL) and tips (yellow/white: 20-200µL)
- Samples (on ice)
- Saturated Potassium Borate Buffer (30g of potassium borate into 800mL of ddH_2O, bring up to 1L, then add potassium borate until no more will dissolve)
- Standards (on ice, standard purchased from Sigma, #AAS18)
- Phosphate buffered saline (PBS)(Wisent, #311-010-CL)
- 10% Trichloroacetic Acid (TCA)(Millipore, #196057)
- 0.1N hydrochloric acid (HCl)
- Sodium hydroxide (NaOH)
- Buffer A (made in 1L glass bottles in lab)
    - K_2HPO_4 salt (salt bench)
        - (BioShop, #PPD555.1)
    - KH_2PO_4 salt (salt bench)
        - (BioShop, #PPM302.1)
    - ddH_2O
- Buffer B (made in 1L glass bottles in lab)
    - HPLC grade methanol (Fisher Chemical, #A-4524)
    - HPLC grade acetonitrile (Sigma-Aldrich, #34998)
    - ddH_2O

Making OPA Reagent (Light sensitive)

- To make 5mLs (in a 15mL test tube wrapped with aluminum foil)
    - Add 0.02g of OPA in 500µL of HPLC grade methanol
    - Add 120µL of Brij 35
    - Add 20mL of 2-mercaptoethanol
    - Add 4.48mL of 0.04M Sodium borate buffer (15.234g of sodium borate in 900mL of ddH_2O, and then adjust to pH 9.5 with sodium hydroxide (NaOH)/hydrochloric acid (HCl) with pH reading machine in the lab and bring up to 1L).

Making Buffer A: 20mmol/L (potassium) phosphate buffer (pH6.5)

Add 800mL of ddH_2O in a suitable container. Typically we used a 1L Erlenmeyer flask.

1. Add 1.175 g of K_2HPO_4 to the solution.
2. Add 1.804 g of KH_2PO_4 to the solution.
3. Add ddH_2O until volume is 1L.

Making Buffer B: HPLC-grade Acetonitrile/HPLC-grade Methanol/Water

Prepare 1L

1. 450mL of Acetonitrile
2. 400mL Methanol
3. 150ml of ddH_2O

Sample/Standard Preparation:

Cell Harvesting

1. Wash myotubes in 6-well plates twice with 2mL/well of PBS
2. Harvest cells with 250µL of 10% TCA
3. Mix up and down with micropipette to break down cell suspension

Sample Preparation

1. Centrifuge lysate at 2.3g for 15minutes in 4^oC
2. Next take lysate supernatant and dilute in another set of test tubes as shown below

Sample Dilution

Prepare sample by diluting in a ratio of 1:2:1:8:

1: Sample
2: Saturated Potassium Borate Buffer
1: 0.1N HCL
8: ddH_2O

Ensure that samples are filtered before ran through the column. They can be filtered using a 0.2µM 1ml syringe filter (83.1826.001 from Sarstedt). In the filtering process you lose a lot of sample so prepare for this.

Standard Preparation and Dilution

Dilute samples similarly to samples in a ratio of 1:2:1:8

1: Standard (Sigma, #AAS18) *See next step, making standard*
2: Saturated Potassium Borate Buffer
1: 0.1N TCA*
8: ddH_2O

***AA standard in HCl so add 0.1N TCA into standards, while samples are harvested with TCA, so add 0.1 HCl into samples**

Making Standards:
Make sure to have 4 standard curve points (0, 0.25, 0.5, 1.0)

- **For 0 standard curve point:**
  - **1:** ddH_2O
  - **2:** saturated potassium buffer
  - **1:** 0.1N TCA
  - **8:** ddH_2O

- **For 0.25 standard curve point**: first dilute amino acid standard 1-part amino acid standard, 3-part ddH_2O. Then:
  - **1:** diluted amino acid standard
  - **2:** saturated potassium buffer
  - **1:** 0.1N TCA
  - **8:** ddH_2O

- **For 0.5 standard curve point:** first dilute amino acid standard 1-part amino acid standard, 1-part ddH_2O. Then:
  - **1:** diluted amino acid standard
  - **2:** saturated potassium buffer
  - **1:** 0.1N TCA
  - **8:** ddH_2O

- **For 1.0 standard curve point:**
  - **1:** undiluted amino acid standard
  - **2:** saturated potassium buffer
  - **1:** 0.1N TCA
  - **8:**ddH_2O

Protocol Parameters:

- **Gradient Elution**
- **Flow rate:** 0.8mL/min
- **Column temperature:** 35 degrees Celsius
- **Cell Temp:** 4 degrees Celsius
- **Excitation-Emission:** 350-450
- **Maximum Pressure**: 18000psi
- **Injection volume:** 1mL
- **Preferred Column:** YMC-Triart 75mm x 3.0mmOD x 1.9um particle size
- **Pretreatment**: Go to Reagent and add 40mL (this is the OPA that'll be put into sample in each vial – 1:1 ratio of OPA to sample, so add 40mL into each sample vial as well)

Appendix C (cont.) – High Pressure Liquid Chromatography (HPLC) Protocol – BCKAs

Materials:

- Column (Intersil ODS-4 100mm x 2.1mmOD x 2um particle size)
- Metal Ferrule (IDEX health & science, #VHP-321)
- Metal tubing (IDEX health & science, #U-154)
- Vials and lids (Supelco, #27080-U)
- Vial Inserts (Supelco, #24716)
- 1,2-diamino-4,5-methylenedioxybenzene (DMB) (Sigma Aldrich, #66807) – keep on ice
    - Sodium sulfite (Biotech, #7757-83-7)
    - 2-mercaptoethanol (Sigma, #M6250)
    - Concentrated HCl (Sigma, Aldrich, #258148)
    - Double distilled water
- Micropipette (20-200µL) and tips (yellow: 20-200mL)
- Samples (on ice)
- 0.1N hydrochloric acid (HCl)
- Sodium hydroxide (NaOH)
- Buffer A (made in 1 L glass bottles in lab)
    - HPLC grade methanol (30%) (Fisher Chemical, #A-4524)
    - ddH_2O (70%)
- Buffer B (made in 1L glass bottles in lab)
    - 100 % HPLC grade methanol (Fisher Chemical, #A-4524)

DMB solution was prepared by adding 1.6mg of DMB to 1.0mL of solution, which contained 4.9 mg of sodium sulfite, 70mL of 2-mercaptethanol, and 58mL of concentrated HCl in 0.87mL of ddH_2O.

Sample Preparation/Dilution:
Prepare sample/standard in 1:2:1:8 ratio
1: Sample/Standard
2: Saturated Potassium Borate Buffer
1: ddH_2O/homogenization buffer*
8: ddH_2O

*Sample was tissue homogenized in homogenization buffer, so the standard receives 1 part homogenization buffer, while standard was made in ddH_2O, so sample receives 1 extra part ddH_2O instead of homogenization buffer

Standard Preparation/Dilution:
Standards are made using KIC, KIV and KMV salts in the lab:
Dissolved 25mg/mL. Then did a 1:10000 dilution (equivalent to about 19.2µM for KIC and KMV, and 21.53µM for KIV). If not diluted, then the peaks are oversaturated. After it is diluted (1.0), to create a standard curve, it is diluted 2-fold (0.5) and 4-fold (0.25). Just HPLC-grade water is used as the 0 point in the standard curve.

Ensure that samples are filtered before ran through the column. They can be filtered using a 0.2µM 1ml syringe filter (83.1826.001 from sarstedt). In the filtering process you lose a lot of sample, so prepare for this.

Protocol Parameters:
Gradient elution was performed as follows: 0 min 0% B, 3.33 min 0%B, 5 min 50%B, 17.34 min 50%B
Flow rate: 0.2mL/min
Column temperature: 40 degrees Celsius
Cell Temp: 4 degrees Celsius
Excitation-Emission: 367-446
Maximum Pressure: 18000psi
Injection volume: 5mL
Preferred Column: Intersil ODS-4 100mm x 2.1mmOD x 2um particle size
Pretreatment: 40mL of DMB solution is added to 40mL of standard/sample and then heated at 85^{o}C for 45 minutes then cooled on ice for at least 5 minutes.

Appendix D – Immunofluorescence Microscopy (*In-vitro)*

Materials:

- 12-well plates (Greiner Bio-One, #665165)
- Sterile autoclaved tweezers
- Cover Slips (Fisher Scientific, #12-54618CIR-2)
- PBS (Wisent, #311-010-CL)
- 4% Paraformaldehyde (Sigma, #6148)
- Triton X-100 (MP Biomedicals, LLC, #M2528)
- Bovine Serum Albumin (Biotech, #9048-46-9)
- Horse Serum (Gibco, #26050-088)
- MHC-1 primary antibody (Development Hybridoma, #MF 20 – s)
- Fluorochrome Secondary Antibody (Vector Labs, Vectashield, #TI-1000W0901)
- DAPI Mounting Medium (Vector Labs, Vectashield, #H-1200)

Protocol:

1. Sterilize cover slips by autoclaving them. Place a single cover slip into each well of a 12-well plate using sterile autoclaved tweezers.
2. Plate L6 myoblasts ($1x10^5$) in the 12-well plate on top of cover slips. Include sufficient number of well so you can have a negative control. Grow myoblasts according to regular procedure.
3. When cells are confluent, change to differentiation medium.
4. Change medium every 24-48 hours until day 4 or 5 when myotubes are ready for treatment. On day 4, treat cells with the chemotherapy drug cocktail according to regular protocol.
5. Remove medium and rinse each well 2X with 1mL of PBS.
6. FIXING: In fume hood, fix cells by incubating them in 1mL/well of paraformaldehyde (4% PFA in PBS) for 10minutes at room temperature. Use gentle swirling on a rocker. After 10minutes, remove paraformaldehyde and store in a container in hood.
    a. Sample Calculation for PFA
        i. 4% PFA was already made in the lab, so I did not have to make this. It is in the freezer -20 door. I just thawed and used. It is in 50mL test tubes (purple lid)
7. Do 3X quick rinse in PBS with 1mL/well.
8. PERMEABILIZATION: Permeabilize the cells by adding 1mL/well of 0.03% Triton X-100 in PBS. Incubate for 5 minutes.
    a. Sample Calculation for Triton X-100 (To make 12mLs). Can make this in a 15mL test tube.
        i. 11996.4mL of PBS
        ii. 3.6µL of Triton
            1. Triton is very syrup-like. Add into a small beaker and microwave for 30 seconds to turn it into a liquid.
9. WASHING: Remove Triton solution and wash 5X, 1mL/wash, 5minutes/wash.

10. BLOCKING: Incubate with 400µL/well of blocking solution: 10% horse serum in PBS. Block at 37°C for 1hour with periodic swirl.
    a. Sample Calculation for blocking solution (to make 5mLs)
        i. 480µL of horse serum
        ii. 4320µL of PBS
            1. Can be made in a 15mL test tube. Make sure to thaw horse serum prior to beginning.
11. PRIMARY ANTIBODY: Add sufficient amount of diluted antibody, ~500µL/well. (MHC-1 from Dev Hybridoma, 2.5µg/mL diluted in 1% BSA in PBS). Incubate overnight at 4°C with gentle rocking.
    a. Sample calculation for primary antibody (to make 3mLs)
        i. 2970µL of PBS
        ii. 30µL of 1% BSA
        iii. 230µL of MHC primary
            1. For MHC, 2.5µg/mL (conc we want) x 3mLs (total volume) / 32µg/mL (this value is conc on MHC tube) = 230µL
12. WASH: Decant and save primary antibody. Do one quick rinse in PBS and then 3X wash in PBS, 5minutes/wash with gentle rocking.
13. SECONDARY ANTIBODY: Dilute secondary antibody (Texas Red anti-mouse IgG, raised in horse). Dilute 1:100 with 1% BSA in PBS. After removing PBS from washing (step 12), add 500µL/well of the diluted secondary antibody and incubate for 2hour, room temperature on a rocker. Make sure to keep the wells covered and protected from light using aluminum foil. This is to ensure that no photo-damage takes place on the fluorochromes of the secondary antibody.
    a. Sample calculation for secondary antibody (to make 5.5mLs)
        i. 5445µL of PBS
        ii. 55µL of 1% BSA
        iii. 55µL of secondary (anti mouse, horse raised)
14. WASH: Remove secondary antibody and wash 5X, 10minutes/wash in PBS.
15. MOUNTING: Take appropriately labelled microscope slides. Put a drop of mounting medium on each slide. The mounting medium contains DAPI (to stain the nucleus) and anti-oxidants to prevent oxidation of the fluorochromes.
16. With a pair of tweezers, take the cover slip out and invert the slip on the mounting medium. Ensure the side on which the cells are face the DAPI mounting medium.
17. MICROSCOPY: Observe under the microscope.

Appendix E – *In-vitro* BCKD Activity Assay

Materials:

- Head Pad
- PBS (Wisent, #311-010-CL)
- 1mL Syringes (Becton, Dickinson and Company, #309597)
- Cell Scraper
- Eppendorf Tubes (Sarstedt, #72.690.300)
- 6-Well cell culture plates (Greiner Bio-One, #657165)
- Clear Scotch Tape
- Scintillation Vials (Perkin-Elmer, #6008118)
- Scintillation Fluid (Ecoscint A, National Diagnostics, #LS-273)
- Filter Paper Wicks (1.3cm x 2cm)
- 2M NaOH
- Heated incubator (non-shaking)
- Growth Media, made by supplementing AMEM (Wisent Inc, #310-010-CL) with 10% FBS (Gibco, #12483-020) and 1% antibiotic (Gibco, #15240-062)
- Krebs Ringer Buffer (KRB)
    - 856µL/well
- Thiamine Hydrochloride (Sigma, #T1270)
    - Working dilution: 1mg/856µL of KRB
- Valine (Sigma, #V0513)
- Radioactive Valine (Perkin Elmer, #NEC291EU050UC)
- Lysis Buffer
- Reaction Mixture
    - Working volume is 1mL
        - 936.65µL of PBS
        - 43.35µL of valine (Stock: 50mg/mL)
        - 20µL of Radiolabeled U-^{14}C-Valine (Perkin Elmer, #NEC291EU050UC)

Protocol:

1. L6 cells should be seeded into 6-well plates with 200,000 cells/well and grown to Day 0. Grow/differentiate cells and treat them respective to your experiment details.
2. Prepare taping and filtered paper wicks:
    a. You will need 4 pieces of tape per 6well (6 wicks total)
        i. One piece of tape for the long side of the six well with three filter paper wicks (1 per well)
        ii. 3 smaller pieces of tape for short side of 6well with 1 filer paper wick per piece of tape
3. Prepare KRB (856µL/well) supplemented with thiamine hydrochloride (1mg/856µL KRB)
4. Prepare 61µL/well of reaction mix

    a. Note, this is radioactive, so lab coats and radioactive bench must be worn
5. Inside sterile hood, suck the media from each 6well and replace with 200µL of GM (if day 0) or DM (days 1 through 5)
6. Move the 6well to radioactive bench in the lab
7. Add 856µL/well of KRB supplemented with a thiamine hydrochloride
8. Add 61µL/well of reaction mix
    a. This is 0.12µCi.
9. Prepare tape and filter papers wicks
    a. Add two filter paper wick with 60µL of 2M NaOH in the middle of well to serve as controls
    b. Place the tape with the filter paper wicks on its side so the wicks are parallel to the bench
    c. Add 60µL of 2M NaOH to each filter paper wick
    d. Note: Nothing should come in contact with the filter paper wick aside from the 2M NaOH as this can skew results heavily.
10. With the NaOH added to each wick, place the mounting slips across the 6wells so the filter paper wicks are in the center of each 6well. Mount the tape to the side of the 6well.
11. Once all the wells are covered, make sure to run your finger around the rim of each well, ensuring there are no bubbles or gaps compromising the seal. Example pictures are shown below (A – D).

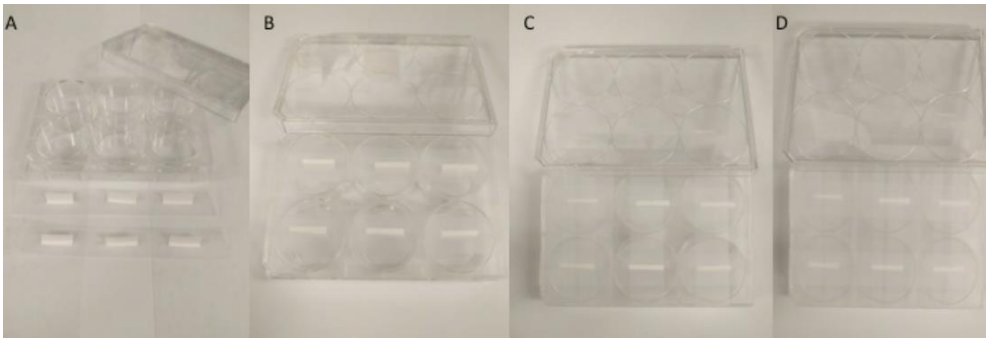

12. Place the 6-well lid over top of the newly taped plate and wrap a single piece of clear table around the entirety of the lid
    a. Make sure that as you place this tape, you do not tip the 6-well, as the liquid can splash and soak the filter paper wicks.
13. Label each well with the needed label and place inside incubator at:
    a. 37 degrees
    b. 0rpm (we do not want any liquid to splash onto the wicks)
    c. For denoted time (anywhere between 1h and 3h)
14. During this time period:
    a. Scintillation vials can be collected, labeled and filled with 3.5mLs of scintillation fluid
    b. Also prepare sample eppendorf tubes for harvesting and lysis buffer.
15. After the time period, grab the 6-well plate and bring to the radioactive bench

16. Using a small set of scissors, make an incision in the clear tape, along the inside perimeter of the plate and cut along the perimeter of the three slides
17. At this stage, peel back all the clear tape as a single unit, you will find it looks like a basket weave to which all the filter wicks should be secured. Sample pictures are shown below (A – D).

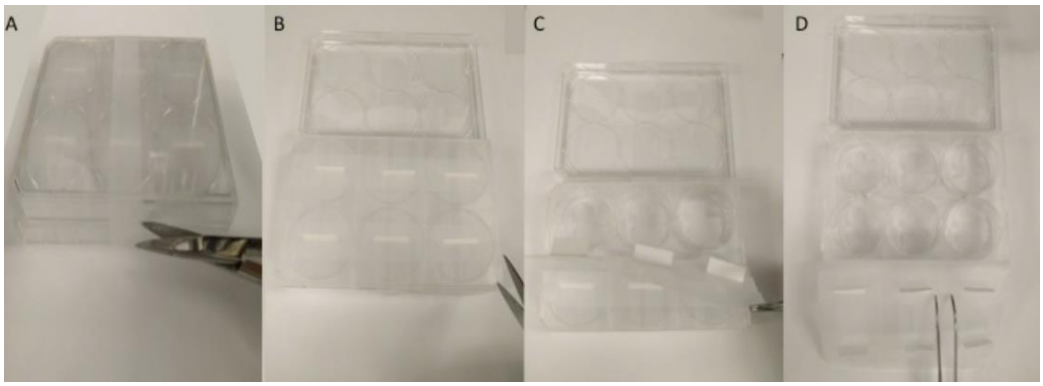

18. Using a cleaned set of forceps, remove the filter paper wicks and place them into their respective scintillation vials
19. Aspirate the remaining contents from the 6well and rinse twice with ice cold PBS
20. Following the second rinse, add 100µL of lysis buffer to each well
21. Harvest cells following our typical harvesting procedure.
    a. These samples are used for the protein assay, in order to correct for total protein content.

Sample BCKD activity assay pictures were obtained from a previous thesis in our lab by Brendan Beatty and accessed through YorkSpace.
Link: https://yorkspace.library.yorku.ca/items/e6486534-0c4a-459f-bd65-95f92957c152

Appendix F – Estrous Tracking in Female Mice

Materials Needed:

- 0.9% Saline in water (PBS, Wisent, #311-010-CL)
    - For 5mLs, 45µL PBS and 4955µL double distilled water
- Microscope (10x Objective Lens)
- Microscope Slide (Fisher Brand, #12-550-343) and Cover Slips (Fisher Scientific, #12-54618CIR-2)
- Q-Tips or cotton swabs (Grocery Store – Sobeys)
- 2-20µL Pipette (in the lab) and Tips

Steps:

1. Grab the female mouse by the base of the tail and place her on the lid of the cage so she grabs on with her hands. Make sure she is facing away from you and her front paws grip the cage
2. Lift the tail in order to expose the genitalia/vulva area
3. Dip the q-tip in 0.9% saline and wipe the vaginal area clean of any secretions.
4. Fill the pipette tip with 20µL of 0.9% saline. Insert the tip (1-2mm depth) into the vagina, ejecting the saline and then immediately redrawing the saline back up.
5. Eject the saline (now with vaginal cells) onto a clean microscope slide and cover with a cover slip
6. View the slide under the 10x objective lens and match the image you see with the corresponding estrous stages below. 40X objective can also be used.

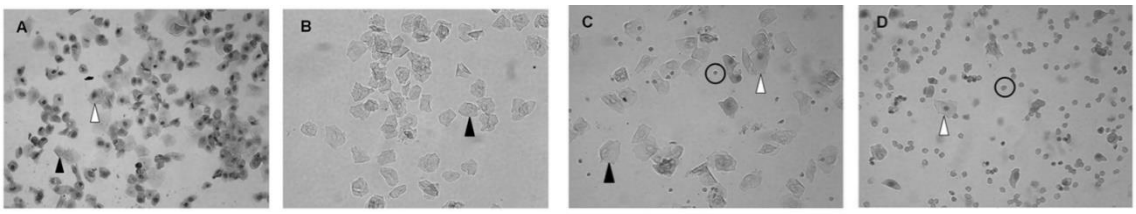

- A = Pro-estrus
    - Small nucleated, non-cornified epithelial cells. Lasts approximately 12-hours.
- B = Estrus
    - Large, cornified squamous epithelial cells in clusters. No visible nuclei and shape is irregular. Last approximately 12-hours.
- C = Metestrus
    - Presence of leukocytes (neutrophils) and some nucleated epithelial or cornified squamous epithelial cells. Lasts approximately 21-hours.
- D = Di-estrus
    - Predominantly leukocytes (neutrophils) and some nucleated non-cornified epithelial cells. This stage lasts approximately 48-72 hours.

Black arrows represent cornified epithelial, circles represent leukocytes, white arrows represent nucleated epithelial

Appendix G – Daily Animal Monitoring Log

For this example, 2 mice were housed in the same cage

Date	Activity	Food Intake (g)	Weight (g)
September 27 Monday Did we Inject today? _____Yes_____	Regular Activity	Weight of Food: ____64.3g_____ Amount Eaten: 23.4g/3 (over weekend) = 7.8g/2=3.9g_____	Animal Weight: _____23.2g____ Weight Change: ____-0.8g____
September 28 Tuesday Did we Inject today? _____No_____	Regular Activity	Weight of Food: ____56.3g_____ Amount Eaten: ___8g/2=4g_____	Animal Weight: ____23.4g_____ Weight Change: ____+0.2g____
September 29 Wednesday Did we Inject today? _____No_____	Regular Activity	Weight of Food: ____49.9g_____ Amount Eaten: __6.4g/2=3.2g_____	Animal Weight: ____23.4g_____ Weight Change: ___None_____
September 30 Thursday Did we Inject today? _____Yes_____	Regular Activity	Weight of Food: ____43.3g_____ Amount Eaten: ___6.6g/2=3.3g_____	Animal Weight: _____23.9g____ Weight Change: ____+0.5g____
October 1 Friday Did we Inject today? _____No_____	Regular Activity	Weight of Food: _____36.2g____ Amount Eaten: ____7.1g/2=3.55g____	Animal Weight: _____23.8g____ Weight Change: ____-0.1g____

Appendix H – *In-vivo* BCKD Activity Assay

Buffer 1

- Potassium Phosphate Buffer (KPi) (30mM, pH 7.5)
- EDTA (3mM)
- DTT (5mM)
    - (Research Organics, #2190D-A101X)
- Valine (1mM)
    - (Sigma, #V0513)
- FBS (3%)
    - (Gibco, #12483-020)
- Triton X-100 (5%)
    - (MP Biomedicals, LLC, #M2528)
- Leupeptin (1μM)
    - (Sigma, #L2884)

Buffer 2

- Hepes (50mM)
    - (BioShop, #HEP001)
- KPI (30mM)
- CoA (0.4mM)
    - (Sigma, #C4282)
- NAD+ (3mM)
    - (Sigma, #N0632)
- FBS (5%)
    - (Gibco, #12483-020)
- Thiamine (2mM)
    - (Sigma, #T1270)
- Magnesium Chloride$_2$ (2mM)
    - (Sigma, #7786-30-3)
- Radiolabeled U-^{14}C-Valine (7.8μM)
    - (Perkin Elmer, #NEC291EU050UC)

Protocol:

1. Make KPi Buffer (30mM)
    a. Buffer is made in KPI Buffer. Start by making a stock of 30mM KPI Buffer
        i. To make 100mLs
            1. KPi is made of potassium phosphate dibasic (K_2HPO_4 salt, BioShop #PPD555.1) and potassium phosphate monobasic (KH_2PO_4 salt, BioShop, #PPM302.1)
                a. Add 80mL of ddH_2O in a 200mL beaker
                b. Add 107.96mg of potassium phosphate monobasic
                c. Add 384.376mg of potassium phosphate dibasic

2. Make Buffer 1
    a. In order to make a 25mL solution of buffer 1, start by adding 15mL of your KPi buffer into a 50mL test tube. Next add the following:
        i. EDTA (3mM) = 150µL
        ii. DTT (5mM) = 125µL
        iii. Valine (1mM) = 147.92µL
            1. This is in the door of -20 freezer. There is a stock of 169014µM. Use this stock to add the 147.92µL.
        iv. FBS (3%) = 750µL
        v. Triton X-100 (5%) = 1250µL
        vi. Leupeptin (1uM) = 11.90µL
            1. There is a main stock of 10mM in the -20 freezer door and a more diluted stock of 2.1mM. Use the 2.1mM to add the 11.90µL.
        vii. After adding everything all the above steps, top of mixture to 25mLs using the 30mM KPi buffer you made.

3. Make Buffer 2
    a. Buffer is made in KPi Buffer again.
    b. In order to make a 30mL solution of buffer 2, start by adding 15mL of your KPi buffer into a 50mL test tube. Next add the following:
        i. HEPES (50mM) = 357.465mg
        ii. CoA (0.4mM) = 9.2mg
        iii. NAD+ (3mM) = 61.75mg
        iv. FBS (5%) = 1.5mLs
        v. Thiamine (2mM) = 20.24mg
        vi. Magnesium Clhoride$_2$ = 12.2mg
        vii. **NOTE**: Do not add the radioactive valine into this now. Will add later in step 5
        viii. After adding everything, top up the mixture to 30mLs using KPI buffer.

4. On ice, homogenize (PRO200) ~35mg of tissue sample at max speed in 250µL of ice-cold Buffer 1. Homogenize for 30 seconds in a 15mL homogenization tube (Sarstedt, #62.515.006). Take the full homogenate and transfer into a 1.5mL eppendorf tube.
    a. Note: Sometimes these homogenization tubes are too long. So may need to cut off the top a little bit.

5. Centrifuge the homogenized sample in each eppendorf tube for 10 minutes at 10,000g, 4°C

6. During the 10 minutes, calculate the total amount of buffer 2 you are going to need. This example is given for if you have 20 samples:
    a. For each sample, we need 300µL x 20 (samples) = 6000µL total. Per sample, we want to add 0.16µL of radioactive valine. That means in 6000µL add 3.2µL (20 x

0.16) of radioactive valine. After making this, add 300µL of buffer 2 with the radioactive valine into 20 separate eppendorf tubes (because you have 20 samples).

7. Grab the homogenate from the centrifuge, remove 50µL of the supernatant and add to 300µL of Buffer 2 in each 1.5mL eppendorf tube. During this time, BCKD is going to be active, so need to do the next couple of steps fast.

8. Add 60µL of 2M NaOH to a tape a raised wick trap over the lid of the eppendorf tube, cap the tube, and tape over to make sure there is a tight seal. Sample pictures are show below.
    a. We do not want any CO_2 from the BCKD reaction to escape

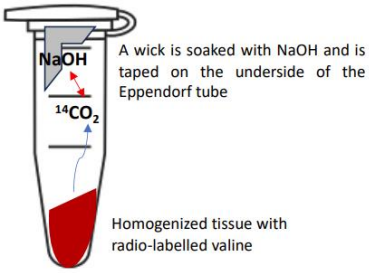

9. Place in a non-shaking incubator at 37°C for 30minutes. It is important that this is non-shaking because don't want any of the liquid to splash onto the wick.

10. After the 30 minutes, remove the wick from each eppendorf tube and place in a scintillation vial with 3.5mLs of scintillation fluid. Count this value in a liquid scintillation counter.

11. In order to all get a read of total radioactive in each tube, take 50µL of the liquid from each eppendorf tube and place in a separate scintillation vial with 3.5mLs of scintillation fluid. Count this value in a liquid scintillation counter as well.

12. The remaining liquid left in each eppendorf tube is then used to run a protein assay.

13. After you get the scintillation value for the wick, scintillation value for the total radioactivity and protein concentration in each sample, BCKD activity can be calculated by dividing CPM by the total radioactivity and then dividing that value by total protein concentration.

Appendix I – Relative Body Weight Loss Compared to Control at Each Time Point

These tables represent the percentage of body weight loss in chemotherapy drug-treated animals compared to control at each time point. Data is shown for chapter 5 (Figure 5.1) and chapter 6 (Figure 6.1).

Figure 5.1 Table

This table corresponds to figure 5.1, page 93

Time Point (Day)	Male	Female
0	--	--
7	2%	3%
14	4.9%	5.8%
21	4.9%	7.5%
28	6%	14%
35	11%	21%
42	15%	25%

Figure 6.1 Table

This table corresponds to figure 6.1, page 120

Time Point (Day)	Male	Female
0	--	--
7	3%	4.1%
14	7.1%	3%
21	8.3%	6.1%
28	11.8%	10.3%
35	14%	17%
42	16%	21%

Appendix J – Additional Contributions

Co-Author: Published

1. **Mora, S**., & Adegoke, O. A. J. (2021). The effect of a chemotherapy drug cocktail on myotube morphology, myofibrillar protein abundance and substrate availability. *Physiological Reports*, 9(13).

2. Mann, G., **Mora S.**, Madu G., and Adegoke O. A. J. (2021). Branched-Chain Amino Acids: Catabolism in Skeletal Muscle and Implications for Muscle and Whole-Body Metabolism. *Front. Physiol*. 12:702826.

3. Adegoke OAJ., Huang Y., Fu X., and **Mora S.** (2022). Editorial: Nutrition in the Regulation of Muscle Development and Repair. *Front. Physiol*. 13:853007.

4. **Mora, S**., and Adegoke, O. A. J. Maintenance of the Branched-Chain Amino Acid transporter LAT1 Counteracts Myotube Atrophy following Chemotherapy. Accepted at the *American Journal of Physiology – Cell* (Chapter 4, Study 1).

Co-Author: Accepted

1. **Mora, S**., Mann, G., and Adegoke, O. A. J. Sex Differences in Cachexia and BCAA Metabolism following Chemotherapy. Submitted to *Physiological Reports* (Chapter 5, Study 2).

Co-Author: In Submission

1. Mann, G., **Mora S.**, and Adegoke O. A. J. Insulin Signalling is Uncoupled from Whole-body Insulin Sensitivity in response to Leucine and Ketoisocaproic gavage. 2024.

2. Mann, G., **Mora S.**, and Adegoke O. A. J. Effect of Aging and Sex on BCAA Metabolism. 2024.

3. Logan Davari, **Stephen Mora**, Gagandeep Mann, Adegoke OAJ. Dietary micronutrient insufficiencies are secondary to dietary caloric insufficiencies in male and female varsity ice hockey players. *Journal of Physical Education and Sport* 2024.

Co-Author: In progress

1. **Mora, S**., and Adegoke, O. A. J. Sex-related Differences in Cachexia Outcomes and Branched-Chain Amino Acid Metabolism following Chemotherapy in Old Animals. *Journal of Applied Physiology*. 2024. (Chapter 6, Study 3)

2. **Stephen Mora**, Logan Davari, Termeh Ataie, Parsa N, and Adegoke OAJ. Myofibrillar protein anabolism and AKT activation in myotubes depleted of PDCD4. *Biochemical Journal* 2024.